

CONTENTS

1 Random notes to sort	7
2 Fabrication	8
2.1 No Category	8
2.2 Macroscopic parameters	8
2.3 Resonators	9
2.4 Materials parameters	10
2.4.1 Transition temperatures	10
2.5 Deposition	11
2.5.1 Depsition via parallel angles	11
2.5.2 Perpendicular deposition	12
2.5.3 Perpendicular deposition	12
2.6 Coupling-capacitance	13
2.7 Josephson parameters	14
2.8 Capacitance parameters	14
2.9 Summary	15
2.10 Autocad-Beamer Design	16
2.11 Typical exposure	17
3 Experiment	18
3.1 S-parameters	18
4 Dipole operator for coupling [3] [1]	19
4.1 Summary [3]	22
5 Emission from system	23
5.1 As derived in Oleg's papers [1][3]	24
5.2 Atom emission	24
5.3 Emission by the atom	25
5.4 Single drive configuration	26
5.5 Combining the sections above	27
5.6 Coherent and incoherent emission	30

6 Scattering by system [3]	32
6.1 Coherent dynamics and decoherence in a superconducting weak link [17]	33
7 Relaxation due to noise	33
7.1 Relaxation from the noise spectrum	33
8 Unitary transformations and the rotating frame	35
8.1 Example application	36
8.2 Example application 2	38
8.3 Qubit operations	40
9 Dissipation	41
9.1 Application to relaxation	42
9.2 Pure dephasing	44
9.3 Dynamics with Pauli Matrices	45
10 Linbalnd operators covered in depth	51
10.1 Pure dephasing	51
10.2 Pure dephasing from partial trace	54
10.3 General roundup	55
10.4 Relaxation in the Linbland Equation	56
11 Two level system evolution	59
12 Quantum Electrodynamics Formalism	63
12.1 Superconductors	63
12.2 Josephson junction	63
12.2.1 Inductance energy	65
12.2.2 Summary of energies	65
12.3 JJ Brief summary	66
12.4 Shapiro steps	66
12.5 Effective "ball" system	67
12.6 SQUID to control E_J [22]	68
12.7 Building blocks for quantum circuits.	70
12.7.1 Kinetic Inductance	70
13 Charge basis	74
13.1 Prooving the phase raising effect	74

14 Phase basis	76
15 Two Level System	77
16 Single cooper pair box system	78
16.1 Adding a parallel JJ	80
16.2 Transmon	81
16.2.1 Capacitance through parallel structures	82
16.2.2 Capacitances from JJ	83
16.3 The critical current and E_{J0}	83
16.4 Quantising the Hamiltonian	84
16.4.1 Charge energy dominates, $E_C/E_J \gg 1$	84
16.5 Deriving energy from geometry	86
16.5.1 Effect of N_{ext} is negligible in transmon	87
16.5.2 Using sufficient number of charge states for simulation	88
16.5.3 Maintaining anharmonicity	88
16.6 Charge dispersion	89
16.7 Summary for transmon	89
16.7.1 Choosing ratio	90
16.8 Transmon 2-level approximation	93
16.9 Charge energy dominates: E_C/E_J :	94
16.10 Flux energy dominates: $E_C/E_J \ll 1$	95
16.10.1 Numerical solution	95
16.10.2 Periodic analogy	97
17 Coupling transmon with resonator	99
17.0.1 Coupling strength	99
18 RF SQUID (Flux qubit). $E_J/E_C \sim 50$	102
18.1 Regimes of RF SQUIDs [15]	102
18.2 Hamiltonian	103
18.3 Numerical solution of Hamiltonian	105
18.4 Solution in the degenerate case	107
18.5 Question about fabrication	112
19 3 JJ qubit	113

20 4JJ-series Flux Qubit [20]	117
20.1 Derivation of the Hamiltonian	117
20.2 Bloat over	118
21 Flux qubit 4 JJ [13]	120
22 Phase qubit. $E_J/E_C \sim 10^6$	124
23 Transmon source	125
24 Resonators	126
24.1 Deriving resonator equations	126
24.2 The voltages at the gaps of the resonator	128
24.3 Resonator types	132
24.4 Resonator Emission	132
24.5 Resonator example [2]	132
24.6 Resonator Fabrication	133
25 Qubit-Resonator Interaction [4]	135
25.1 General solutions	137
25.2 Resontant case	138
25.3 Non-resonant case	139
25.4 Stark shift measurements	141
25.5 Resonant case = Dressed States	142
25.6 Actual simulations	144
25.7 Decay rates and quality factors	146
25.8 Second order effects	146
25.9 Driving qubit-resonator system	149
25.10 Dynamics using Linbalnd equation	149
26 Measurement with resonator	151
26.1 Choosing power	153
27 Creating a dark state in a 3-level system[21][1]	154
27.1 Driving the three level atom	154
27.2 Driving to the dark state	158

28 Coherent Quantum Phase Slip (CQPS) [14]	159
28.1 Literature	159
28.2 Cooper box duality	160
28.3 Mooij 2006 paper [14]	161
28.4 Derivation	161
28.5 Inverse shapiro steps	163
28.6 Plasma Frequency	163
28.7 What sets the energies	164
28.8 Standard of voltage	164
28.9 Coherent quantum phase slip 2012 [2]	165
28.9.1 Choosing material	166
28.9.2 Fitting of results	166
28.10 Evidence for coherent quantum phase-slips across a Josephson junction array [12]	167
28.11 Coherent flux tunneling through NbN nanowires [18]	168
28.12 Coherent dynamics and decoherence in a superconducting weak link [17]	168
29 Single Photon	170
29.1 What is spectral density	170
29.2 Making measurement	170
30 Simulating circuits	171
31 Properties of photons	173
31.1 Emission and line broadening	173
31.2 Classical vs Quantum pulses	173
31.3 More about photons	175
31.4 Photon bunching	176
31.5 Types of light	177
31.6 Photon antibunching	177
31.7 Creating antibunching	179
31.8 Squeezed light	179
31.9 Phase distribution	180
32 Interaction picture	181
33 Interaction between light and atom	182
33.1 Resonance	184

34 The dipole approximation	187
35 Background on quantum mechanics principles	188
35.1 The density matrix	188
36 Open quantum systems	192
36.1 How a mixed state arises	192
36.2 Superoperators	193
36.3 Deriving equation for open quantum system	194
36.4 Example application	196
36.5 Summary of method	198
37 Representing 2-level system as a spin	199
38 Rabi oscillations	202
39 Perturbation Theory	203
39.1 Fermi's golden rule	205
40 Changing the basis	206
41 Fluctuation dissipation theory from Brian Cowans Notes	208
41.1 Summary	208
41.2 Correltion function	209
41.3 Fluctuation dissipation theory	209
41.4 Responses	211
41.4.1 Sinusoidal Excitation	211
41.4.2 Frequency representation	213
41.4.3 Step excitation	215
41.4.4 Delta exciation	215
41.5 Summary	215
41.6 Energy	216
41.7 Onsager's hypothesis	217
41.8 Charge and current	218

CHAPTER 1

RANDOM NOTES TO SORT

- When in excited state, qubit emits a single photon - a Fock state, whose phase is undefined. Therefore this is an incoherent emission.

FABRICATION

Fabrication is not an easy thing, and yet it can be completed in the space of a single week

2.1 No Category

- Always ground the qubits directly - never through a capacitor;

2.2 Macroscopic parameters

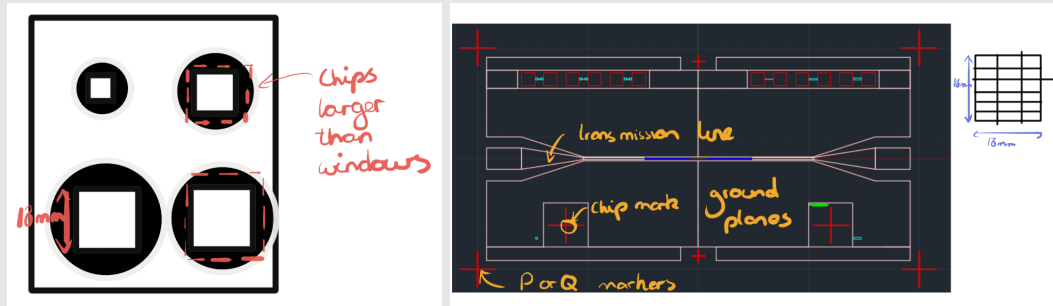


Figure 1: Big markers are the P,Q markers described below.

1. **Sample chips** are mounted in a cassette with windows. The available sizes are:

- 18 mm x 18 mm;
- 13 mm x 13 mm;
- 8 mm x 8 mm.

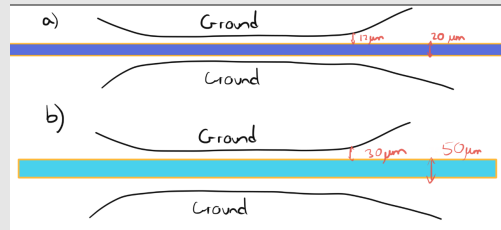
The chip must be larger than this window in order to be fixed in place.

2. **Qubit chip:** 5 mm x 3 mm. This means that a 18 mm chip will fit 3×7 of them.

3. **Transmission line:** is characterized by width and separation with the ground planes. **This defines the impedance of the line, which must be 50Ω .**

- **Narrow:** Width = $20\mu\text{m}$, Separation = $12\mu\text{m}$;
- **Wide:** Width = $55\mu\text{m}$, Separation = $30\mu\text{m}$;

- The width determines the speed of propagation - wider \equiv greater speed and higher frequencies.



2.3 Resonators

Resonators designed by Rais come in two lengths:

- 400 μm ;
- 200 μm .

The frequency of a resonator is given by:

$$f_j = \frac{v}{L_r}$$

$$\left\{ \begin{array}{l} v = \frac{1}{\sqrt{L*C}} \\ L = \text{inductance per unit length} \\ C = \text{capacitance per unit length} \\ L_r = \text{length of resonator} \end{array} \right.$$

2.4 Materials parameters

In a charge qubit, the only part that needs to be superconducting is the JJ superconducting-insulator-superconducting structure. **All other components can be made from normal metal, as there is no persistent current.**

2.4.1 Transition temperatures

- NbN 4.5 K;
 - Al 1.3 K;
 - Ti 0.63 K.

2.5 Deposition

2.5.1 Deposition via parallel angles

- **Ground planes and bonding contacts:** Ti (10 nm) - Au (80 nm)
- **Aluminum JJ:**
 - Copolymer 13% $T = 600\text{nm}$
 - Either ZEP520a:Anisol 1:2 or ARP6200 4% $t = 100\text{nm}$
 - **The undercut is 150 nm;**
 - Angle evaporation leads to:
 - * Shift in the pattern by $T \tan(\alpha)$;
 - * Shortening of the pattern by $t \tan(\alpha)$.
 - Meaning that in order to get an overlap between red and yellow we need to shift the deposition holes;

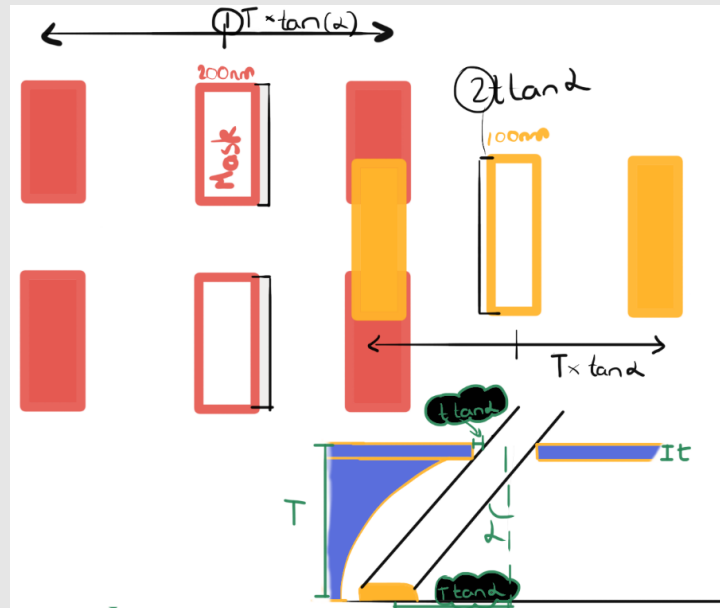


Figure 2: Angle α shifts the pattern by $T \tan(\alpha)$ and shortens it by $t \tan(\alpha)$. Thus the pattern needs to be made longer and shifted to get the desired structure.

- Shift the bottom layer and top layer in opposite directions by

$$\text{Shift} = T \tan(\alpha).$$

- Elongate the windows **on the inner sides** by

NO NEED TO DO THIS

$$\text{Elongate} = t \tan(\alpha),$$

For $T = 600 \text{ nm}$ and $t = 100 \text{ nm}$ and 12° :

Shift = 150 nm;

For $T = 600 \text{ nm}$ and $t = 100 \text{ nm}$ and 9° :

Shift = 110 nm;

The separation between neighbouring holes for the resist to be stable is 100 nm.

After the first deposition the mask gets smaller, so avoid vertical symmetry

2.5.2 Perpendicular deposition

A better deposition is the one that was proposed by Rais, where deposition is done at 0 and 30 degrees.

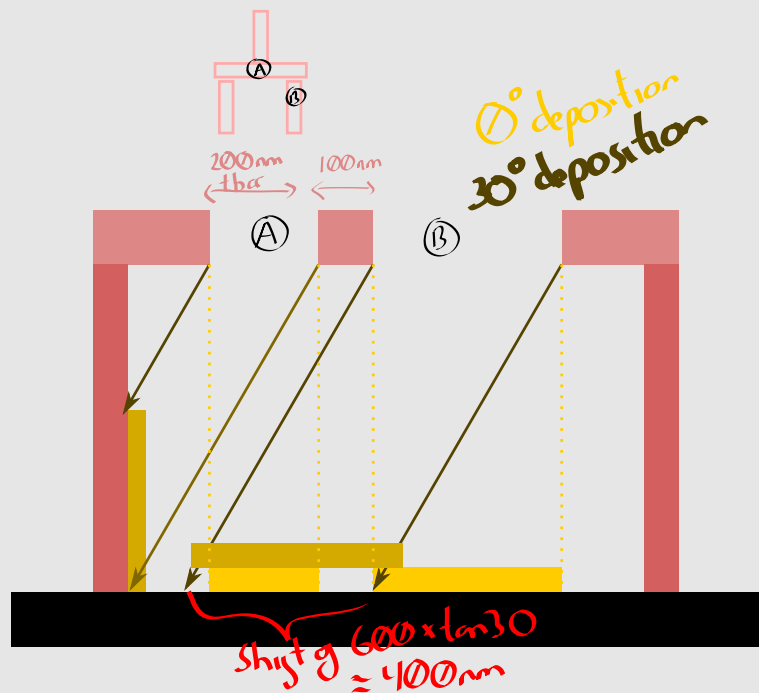


Figure 3: Perpendicular deposition followed by 30° angle deposition will remove the “shadow” of the tbar.

2.5.3 Perpendicular deposition

An even better way to deposit, is to perform two depositions at 90° to each other.

- First deposition deposits horizontal strips;

- Second deposition deposits vertical strips;
- The sharp angle ensures that one deposition is independent of the other;
- The **wall holes** ensure that there is no “cliffs” at the end of the strips;

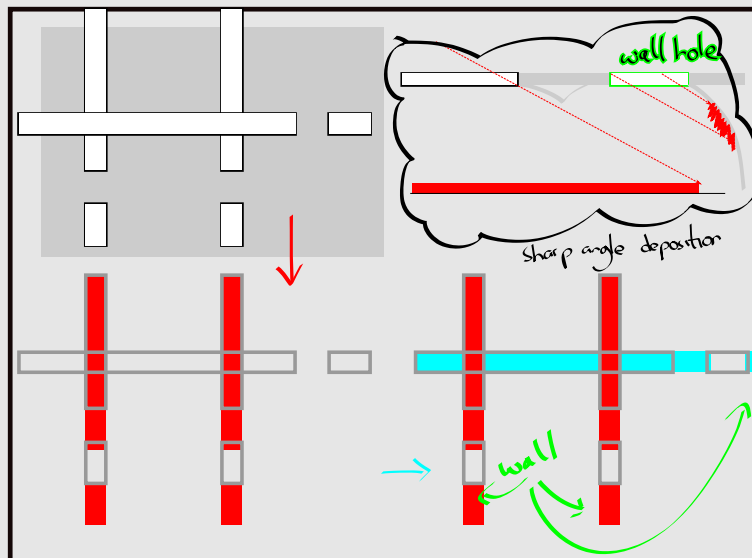
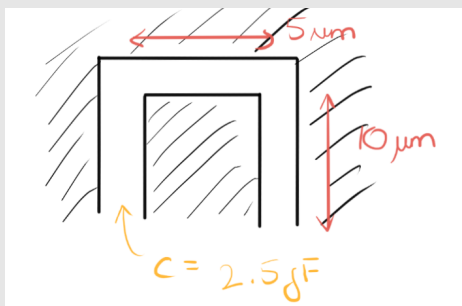


Figure 4: Sharp angle of deposition, means that perpendicular directions will only deposit certain strips. The holes ensure that there are no “cliffs” at the end of the strips that could impact fabrication quality. lines

2.6 Coupling-capacitance

- Separation of elements should be of the order of $2\ \mu\text{m}$;
- **Each $10\ \mu\text{m}$ of parallel structures adds on 1 fF of capacitance.**



Think of it as counting the length of the meander between structures.

Each $10\ \mu\text{m}$ of length adds 1 pA .

2.7 Josephson parameters

$$E = E_J(1 - \cos(\phi))$$

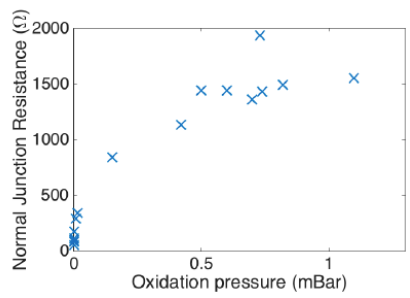
$$\begin{cases} E_J = \frac{\Phi_0 I_c}{2\pi} \\ I_c R_n = \frac{\pi \Delta(0)}{2e} \end{cases} \quad \text{critical current from BCS theory.}$$

A typical JJ will have an area of say $100 \times 200 \text{ nm}^2$

$$E_J = \frac{R_q}{R_n/N_{sq}} \frac{\Delta(0)}{2}$$

$$\begin{cases} R_n = 18.4 \text{ k}\Omega & \text{sheet resistance of } 100 \times 100 \text{ nm}^2 \\ R_q = \frac{h}{(2e)^2} \end{cases}$$

The wider the JJ is in squares, N_{sq} , the lower the resistance of the junction. The calibration graph for a $200 \times 800 \text{ nm}^2$ junctions is shown below:



JJ resistance increases by $\sim 10\%$ as one goes from room to cryogenic temperatures.

2.8 Capacitance parameters

$$E_c = \frac{(2e)^2}{2C},$$

we need the capacitance of the JJ. We can treat the two overlapping parts of the JJ acting a parallel plate capacitor with

$$C = \frac{\varepsilon \varepsilon_0 A}{d},$$

with the permittivity for Aluminum oxide being $\varepsilon \approx 10$ and thickness $d \approx 2 \text{ nm}$. This give s a junction $200 \times 800 \text{ nm}^2$ a charging frequency of $E_c/\hbar \approx 19 \text{ GHz}$.

2.9 Summary

Energy		Variable parameter	Energy ($N_{sq} = 10, N_{NbN} = 5$)
E_J	$\frac{R_q}{R_\square/N_{sq}} \frac{\Delta(0)}{2}$	$R_q = \frac{h}{(2e)^2} = 6.484 \text{ k}\Omega$, $\Delta = 1.73 * (k_b \times 1.3 \text{ K}) = 3.1 \times 10^{-23}$, $R_\square = 18.4 \text{ k}\Omega$	77.5 GHz
E_C	$\frac{(2e)^2}{2CN_{sq}}$	$\varepsilon = 10, d = 2 \text{ nm}$, $A = 100 \times 100 \text{ nm}^2$, $C = \frac{\varepsilon \varepsilon_0 A}{d} = 0.5 \text{ fF}$	17.4 GHz
E_L	$\frac{\Phi_0^2}{(2\pi)^2 2LN_{NbN}}$	$\Phi_0 = 2 \times 10^{-15} \text{ Wb}$, $L = 1.5 \text{ nH per NbN square}$	16.2 GHz

2.10 Autocad-Beamer Design

- All shapes **must** be polylines. They must be joined up in a single line, or they wont work;
- Units are in microns;
- **Place small markers in the corners of the pattern so that centering is correct;**
- Once design is finished, select all → Purge → All → type "none*" → Yes to all;
- **Decide on the P, Q markers that will be used to align the chip - note down their chip coordinates**

2.11 Typical exposure

- Depending on the current you'd like to use, you have to choose between:
 - High Throughput: EOS mode 3, 100 keV, lens 4, from 2nA and above
 - High Resolution: EOS mode 6, 100 keV, lens 5, 100-400 pA.
- 100 nA for the bulky regions;
- **Reading markers:**
 1. Select window to work with: A, B, C or D;
 2. Find global markers P,Q that are usually on the periphery of the chip (green)
 3. For each chip define a chip mark (blue) e.g. 490,490;
 4. Specify the center the central chip (-3500,2500) so that the chip pattern is tied to the global markers.

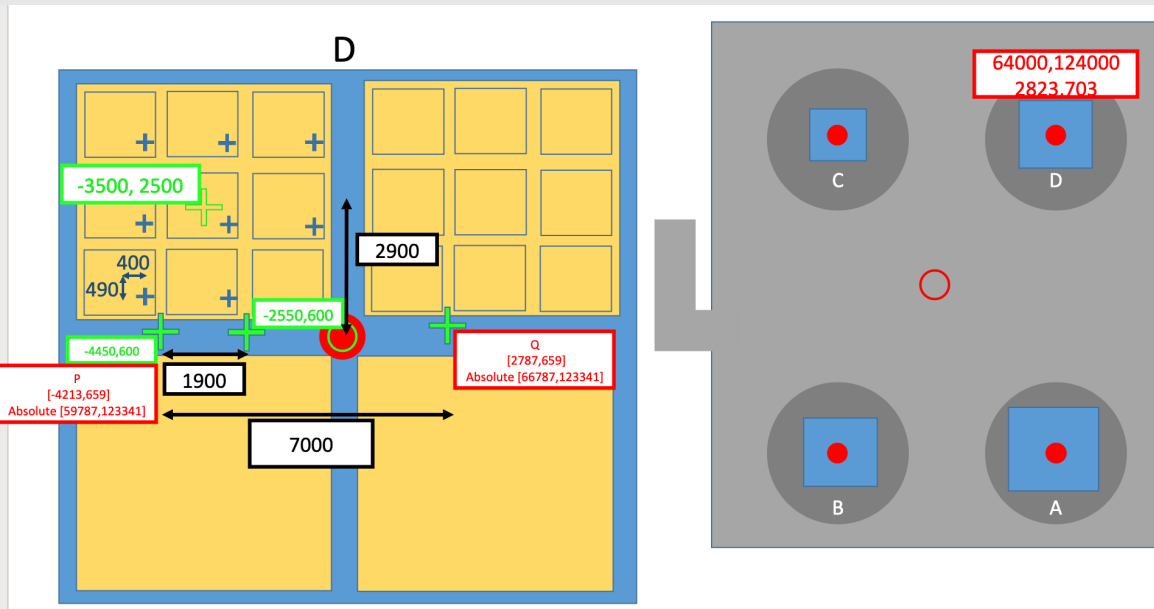


Figure 5: Red is the measured values of the P, Q markers. Green is the designed positions that are set as targets.

EXPERIMENT

3.1 S-parameters

$$\begin{pmatrix} b_1 \\ b_2 \end{pmatrix} = \begin{pmatrix} S_{11} & S_{12} \\ S_{21} & S_{22} \end{pmatrix} \begin{pmatrix} a_1 \\ a_2 \end{pmatrix}$$

- S_{11} , is the input port voltage reflection coefficient;
- S_{12} , is the reverse voltage gain;
- S_{21} , is the forward voltage gain;
- S_{22} , is the output port voltage reflection coefficient.

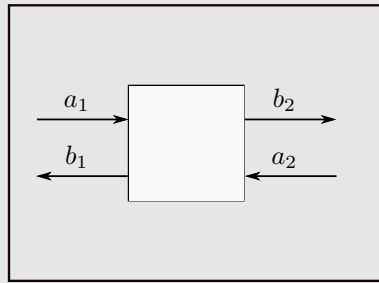


Figure 6: Measurement of transmission and reflection

CHAPTER 4

DIPOLE OPERATOR FOR COUPLING [3] [1]

Premise

We examine driving close to $|i\rangle \leftrightarrow |j\rangle$.

$$\hbar\Omega_{ij}\cos(\omega_{ij}t) = \vartheta_{ij} |V_{mw}| \cos(\omega_{ij}t)$$

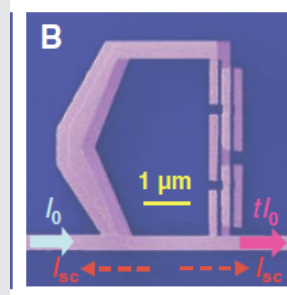
$$\vartheta_{ij} = C_{q-mw} V_{\text{qubit}} \zeta_{ij}$$

- $|V_{mw}|$: voltage amplitude in the transmission line;
- C_{q-mw} : mutual capacitance between the line and qubit;
- V_{qubit} : persistent voltage on the qubit;
- $\zeta = \begin{pmatrix} \langle 0 | \hat{A} | 0 \rangle & \langle 0 | \hat{A} | 1 \rangle & \dots \\ \langle 1 | \hat{A} | 0 \rangle & \langle 1 | \hat{A} | 1 \rangle & \dots \\ \vdots & \vdots & \ddots \end{pmatrix}$: normalised (to unity) matrix elements.

$$\hbar\Omega_{ij}\cos(\omega_{ij}t) = \vartheta_{ij} |I_{mw}| \cos(\omega_{ij}t)$$

$$\vartheta_{ij} = M I_p \zeta_{ij}$$

- $|I_{mw}|$: current amplitude in the transmission line;
- M : mutual inductance between the line and qubit;
- I_p : persistent current in the loop;
- $\zeta = \begin{pmatrix} \langle 0 | \hat{A} | 0 \rangle & \langle 0 | \hat{A} | 1 \rangle & \dots \\ \langle 1 | \hat{A} | 0 \rangle & \langle 1 | \hat{A} | 1 \rangle & \dots \\ \vdots & \vdots & \ddots \end{pmatrix}$: normalised (to unity) matrix elements.



1. Writing out the flux energy in the qubit, due to the qubits, Q_{qubit} , and induced, M_I magnetic fluxes:

1. Writing out the charging energy in the qubit, due to the qubits, Q_{qubit} , and induced capacitively charges:

$$\begin{aligned} E_C &= \frac{Q_{\text{total}}^2}{2C_{\text{total}}} \\ &= \frac{1}{2C_{\text{total}}} \left[Q_{\text{qubit}} + C_{\text{q-r}} V_{\text{mw}} \right]^2 \\ &= \frac{1}{2C_{\text{total}}} \left[Q_{\text{qubit}}^2 + 2Q_{\text{qubit}} C_{\text{q-mw}} V_{\text{mw}} + C_{\text{q-mw}}^2 V_{\text{mw}}^2 \right] \end{aligned}$$

Only the red terms are of interest for interaction, since they link the qubit and microwave systems. **Therefore only the red one is carried on.**

2.

$$\begin{aligned} E_c &= \frac{Q_{\text{qubit}}}{C_{\text{total}}} C_{\text{q-mw}} V_{\text{mw}} \\ &= V_{\text{qubit}} C_{\text{q-mw}} V_{\text{mw}}, \end{aligned}$$

where we have the residual voltage from the charge on the qubit V_{qubit} .

3. Now let us take the quantum mechanical operators and evaluate with the qubit states (which **do not** act on the microwave line operator \hat{V}_{mw}):

$$\begin{aligned} \mathcal{H}_{\text{int}} &= \hat{V}_{\text{qubit}} \hat{C}_{\text{q-r}} \hat{V}_{\text{mw}} \\ &= \sum_{i,j} |i\rangle \langle j| \langle i| \hat{C}_{\text{qr}} \hat{V}_{\text{qubit}} |j\rangle \hat{V}_{\text{mw}} \\ &= \sum_{i,j} |i\rangle \langle j| \vartheta_{ij} \hat{V}_{\text{mw}} \end{aligned}$$

1. Writing out the flux energy in the qubit, due to the qubits, Φ_{qubit} , and induced, M_I magnetic fluxes:

$$\begin{aligned} E_\Phi &= \frac{\Phi_{\text{total}}^2}{2L} \\ &= \frac{1}{2L_{\text{total}}} \left[\Phi_{\text{qubit}} + M I_{\text{mw}} \right]^2 \\ &= \frac{1}{2L_{\text{total}}} \left[\Phi_{\text{qubit}}^2 + 2\Phi_{\text{qubit}} M I_{\text{mw}} + M^2 I_{\text{mw}}^2 \right] \end{aligned}$$

Only the red terms are of interest for interaction, since they link the qubit and microwave systems. **Therefore only the red one is left.**

$$\begin{aligned} E_\Phi &= \frac{\Phi_{\text{qubit}}}{L_{\text{total}}} M I_{\text{mw}} \\ &= I_p M I_{\text{mw}} \end{aligned}$$

where we added the persistent current in the loop I_p .

3. Now let us take the quantum mechanical operators and evaluate the matrix elements [3]:

$$\begin{aligned} \mathcal{H}_{\text{int}} &= \hat{I}_{\text{mw}} \hat{M} \hat{I}_p \\ &= \sum_{i,j} |i\rangle \langle j| \langle i| \hat{M} \hat{I}_p |j\rangle \hat{I}_{\text{mw}} \\ &= \sum_{i,j} |i\rangle \langle j| \vartheta_{ij} \hat{I}_{\text{mw}} \end{aligned}$$

4.

$$\vartheta_{ij} = M I_p \zeta_{ij}.$$

Effectively the atom transitions from 1 persistent current state to another.

Adding a matrix element factor, so that only a change of state ($|0\rangle \leftrightarrow |1\rangle$) generates a change

$$|M I_p| \zeta_{ij}.$$

Dispelling common myths: so what is the difference between

$$\delta A = \langle e | \hat{A} | e \rangle - \langle g | \hat{A} | g \rangle \quad \text{and} \quad \langle e | \hat{A} | g \rangle$$

Well, it comes down to what elements you need from the interaction matrix:

$$\hat{A} \equiv \begin{pmatrix} \langle g | \hat{A} | g \rangle & \langle g | \hat{A} | e \rangle \\ \langle e | \hat{A} | g \rangle & \langle e | \hat{A} | e \rangle \end{pmatrix}$$

These cross terms can be used in perturbation theory

1. \hat{V}_{qubit} is the qubit voltage operator, which next to a transition reads

$$\hat{V}_{\text{qubit}} = \frac{2e}{C_{\text{total}}} \sigma_x.$$

2. \hat{V}_{mw} is the microwave field operator

$$\hat{V}_{\text{mw}} = |V_{\text{mw}}| \cos(\omega t) (a^\dagger + a)$$

3. Fully we have

$$\begin{aligned} H_{\text{int}} &= 2e \frac{\hat{C}_{\text{q-mw}}}{C_{\text{total}}} |V_{\text{mw}}| \cos(\omega t) \sigma_x \\ &= \hbar \Omega \cos(\omega t) \sigma_x. \end{aligned}$$

$$\mathcal{H}_{\text{int}} = g_0 (\sigma^+ + \sigma^-) (a + a^\dagger), \quad g_0 = V_{q0} C_{qr} V_{r0},$$

1. Now, to express the value $\hat{I}_{\text{mw}} = |I_{\text{mw}}| \cos(\omega_d t)$ as an operator, we follow these reasons:

- The current which supplied the energy couples the

to get

$$\hat{I}_{mw} = |I_{mw}| \cos(\omega_{ij}t) (a + a^\dagger).$$

So altogether, the operator on the qubit system is

$$\begin{aligned} \mathcal{H}_{int} &= \sum_{i,j} \left[|I_{mw}| \vartheta_{ij} \cos(\omega_{ij}t) \right] |i\rangle \langle j| \\ &= \sum_{i,j} \hbar \Omega_{ij} \cos(\omega_{ij}t) |i\rangle \langle j| \quad \hbar \Omega_{ij} = |I_{mw}| M I_p \zeta_{ij} \end{aligned}$$

4.1 Summary [3]

When a qubit system emits, the strength of emission depends on the dipole moment of the system, as we saw in Chapter 4:

$$\vartheta_{ij} = \begin{cases} C_{q-mw} V_{\text{qubit}} \zeta_{ij} & \text{capacitive coupling causes induced charge} \\ MI_p \zeta_{ij} & \text{inductive coupling causes induced flux} \end{cases}$$

adding some time dependence of ω , **since the system will respond at the rate of out driving**, and expanding out the matrix elements for a two level system

$$\zeta = \begin{pmatrix} \langle 0 | \hat{A} | 0 \rangle & \langle 0 | \hat{A} | 1 \rangle \\ \langle 1 | \hat{A} | 0 \rangle & \langle 1 | \hat{A} | 1 \rangle \end{pmatrix} \rightarrow \begin{pmatrix} 0 & \langle \sigma^- \rangle \\ \langle \sigma^+ \rangle & 0 \end{pmatrix}$$

we can concentrate on the **relaxation** matrix element to get

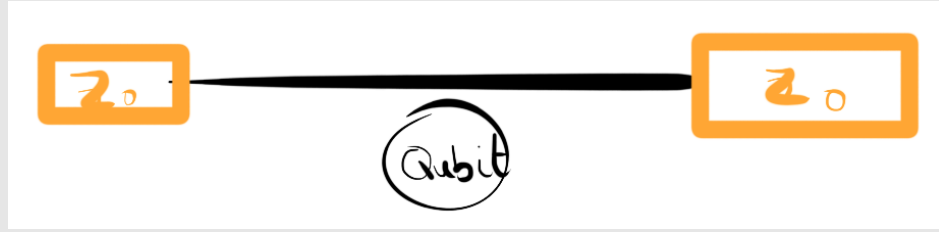
$$\vartheta_{ij}(t) = MI_p \langle \sigma^- \rangle e^{-i\omega t} \quad (1)$$

CHAPTER 5

EMISSION FROM SYSTEM

Before we begin, let us clarify certain assumptions:

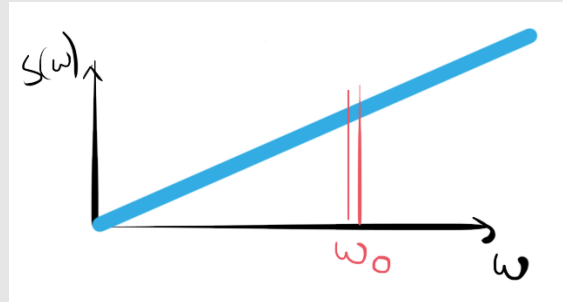
- [8] all the fields are reflected coherent or incoherently.
- An atom left to itself in an excited state **will never decay**;
- Decay only occurs due to quantum noise. The most trivial case, is having two Z_0 resistors somewhere on the transmission line:



- The quantum noise **which is the variation of current squared** is defined by

$$S(w) = \langle j^2 \rangle = \frac{1}{Z_0} \hbar \omega$$

but only a small part of it will be affecting relaxation of our ω_0 qubit.



- This mean square current, $\langle j^2 \rangle$ will interact with the flux being created by the switching state of the atom, $\vartheta = MI_p \langle \sigma^- \rangle e^{-i\omega t}$, to give an energy

$$E_{\text{interaction}}^2 = \langle j^2 \rangle \vartheta^2 = \hbar \omega_0 \frac{1}{Z_0} \vartheta^2$$

- The frequency associated with this energy (and hence the transition rate associated with this energy)

$$\Gamma = \sqrt{\frac{E_{\text{interaction}}^2}{\hbar^2}} = \dots \text{ (oleg promised to explain)}$$

5.1 As derived in Oleg's papers [1][3]

Here it is written, that relaxation occur due to quantum noise in the system:

$$\Gamma_{ij} = \hbar\omega_{ij} \frac{\vartheta_{ij}^2}{\hbar^2 Z_0},$$

which depends on

- The energy associated with the transition $\hbar\omega_{ij}$;
- The dipole matrix transition element $\vartheta_{ij} = \langle i | U | j \rangle \equiv MI_{\text{PC}}\zeta_{ij}$;
- The impedance of the line Z_0 ;

5.2 Atom emission

The atom will scatter waves according to

$$I_{\text{sc}}(x, t) = \left[i \frac{\hbar\Gamma_{21}}{\phi_{21}} \langle \sigma_{21} \rangle \right] e^{ik|x| - \omega_{21}t},$$

and $\langle \sigma_{21} \rangle$ is found from the stationary state of the Master equation $\dot{\rho} = 0$. The transmission coefficient is:

$$\begin{aligned} t &= \frac{\text{Input current + scattered current}}{\text{Input current}} \geq 1 \\ &= 1 + \left[i \frac{\hbar\Gamma_{21}}{\phi_{21}} \langle \sigma_{21} \rangle \right] e^{ik|x| - \omega_{21}t} / \frac{\hbar\Omega_{21}}{\phi_{21}} \quad \text{ignore} \\ &= 1 + i \frac{\Gamma_{21}}{\Omega_{21}} \langle \sigma_{21} \rangle \end{aligned}$$

The relaxation rate is caused by quantum noise in the 1D space:

$$\Gamma_{21} = \hbar\omega_{21} \left(\frac{MI_{\text{persistent}}}{\hbar} \right)^2 \frac{1}{Z}$$

5.3 Emission by the atom

The input-output theory shows that the average field emitted by an artificial atom to an open transmission line is

$$\langle V_{\text{sc}} \rangle = i \sqrt{\frac{\Gamma_{ij}}{2}} \langle \sigma_{ji} \rangle, \quad (2)$$

where $\langle \sigma_{ji} \rangle = \text{Tr} \{ |j\rangle \langle i| \rho \} = \rho_{ij}$, and Γ_{ij} is the $|i\rangle \leftrightarrow |j\rangle$ relaxation rate. The angular frequency of the emission is ω_{ij} .

- V_L^+ resonant input with the $|i\rangle \leftrightarrow |j\rangle$ transition and defined by;
- $V_L^- = V_L^+ + V_{\text{sc}}$ the transmitted field, which is a combination of the incident and emitted fields¹;
- $V_R^- = -V_{\text{sc}}$ the reflected field, only composed of emission by the artificial atom.

The transmission, t , and reflection, r , coefficients are defined as

$$\begin{aligned} t &= \frac{\langle V_L^- \rangle}{\langle V_L^+ \rangle} = 1 + \frac{i\Gamma_{ij}}{\langle V_L^+ \rangle \sqrt{2\Gamma_{ij}}} \rho_{ij}; \\ r &= \frac{\langle V_L^- \rangle}{\langle V_L^+ \rangle} = 1 - t; \end{aligned} \quad (3)$$

where $\langle V \rangle = \frac{1}{T} \int_0^T V(t) dt$ is the average voltage over a normalisation time T . Since the Rabi frequency, Ω , is related to the drive amplitude, $\langle V_L^+ \rangle$,

$$\Omega_{ij} = \langle V_L^+ \rangle \sqrt{2\Gamma_{ij}},$$

Equation (2), (3), reduce to

$$\begin{aligned} t &= 1 + i \frac{\Gamma_{ij}}{\Omega_{ij}} \rho_{ij}; \\ r &= 1 - t. \end{aligned} \quad (4)$$

The coefficients of Eq. (4) apply to coherent emission, when angular frequencies of the driving and emitted fields coincide, $\omega_{ij}^d \approx \omega_{ij}$, and interference between the onset and emitted waves occur.

¹The artificial atom, whose dynamics, Eq. (39), are determined by the incident field, is treated as a stand-alone quantum system that emits a field V_{sc} . This resultant field is a sum of the incident, V_L^+ , and emitted, V_{sc} , fields, created by two distinct objects in the quantum system.

5.4 Single drive configuration

When a single drive couples two levels $|i\rangle, |j\rangle$, the non-interacting third level can be traced out from Eq. (38). The procedure of solving the Master equation, and determining ρ , was done with **Mathematica**. The ρ_{21}, ρ_{31} coefficients obtained, for respective $|1\rangle \leftrightarrow |2\rangle, |1\rangle \leftrightarrow |3\rangle$, drives, upon substitution into Eq. (4) give

$$r_{21} = \frac{\Gamma_{21}}{2\gamma_{21}} \frac{1 + i\delta\omega_{21}/\gamma_{21}}{1 + (\delta\omega_{21}/\gamma_{21})^2 + \Omega_{21}^2/\Gamma_{21}\gamma_{21}}; \quad r_{31} = \frac{\Gamma_{31}}{2\gamma_{31}} \frac{1 + i\delta\omega_{31}/\gamma_{31}}{1 + (\delta\omega_{31}/\gamma_{31})^2 + \Omega_{31}^2/\Gamma_{31}\gamma_{31}}, \quad (5)$$

Figure 7 shows the real components of r_{ij} as function of the detuning of the driving field from the atomic transition, $\delta\omega_{ij} = \delta\omega_{ij}^d - \delta\omega_{ij}$. The reflectance peak corresponds to the case when the atom relaxes to the ground state, and emits a photons that is coherent² with the incident field, but shifted by a phase of π .³ Destructive interference occurs with the incident field and the wave is fully reflected.

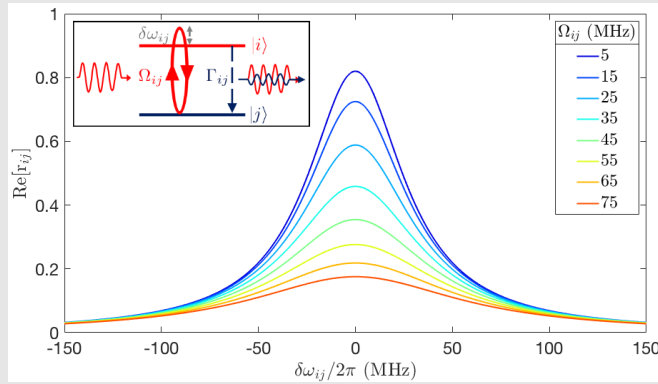


Figure 7: **Simulations of elastic scattering of an incident microwave in an arbitrary $|i\rangle, |j\rangle$, system.** Shown are the real part of the reflection coefficient, $\Re(r_{ij})$, evaluated with Eq. (5) for $\Gamma_{ij} = 50, \Gamma_{\phi,ij} = 5$, for a range of driving powers, Ω_{ij} . When the incident field is on resonance with the atomic transition, $\delta\omega_{ij} = 0$, the reflectance curve exhibits a peak, as emission from the artificial atom undergo destructive interference with the incident wave. The weaker the driving power, the stronger this interference becomes.

The sharpness of the central features diminishes for larger driving amplitudes, Ω . As the number of photons in the transmission line grows, the photon emitted by the atom cannot interfere with all the ones propagating down the transmission line. This photon overload causes t and r to become insensitive to atomic transitions. To saturate the peak, one applies weak drives, $\Omega_{ij} \ll \Gamma_{ij}\gamma_{ij}$ in which case Eq. (5) no longer depends on the driving amplitude

$$\Re[r_{21}] = \frac{\Gamma_{21}}{2\gamma_{21}} \frac{1}{1 + (\delta\omega_{21}/\gamma_{21})^2}; \quad \Re[r_{31}] = \frac{\Gamma_{31}}{2\gamma_{31}} \frac{1}{1 + (\delta\omega_{31}/\gamma_{31})^2},$$

allowing one to determine the decoherence rates γ_{ij}, Γ_{ij} from fittings to observed values.

²Of the same frequency.

³Signified by the i factor in Eq. (4).

The typical Lorentzian has the form

$$L(d\omega) = A \frac{\gamma}{d\omega^2 + \gamma^2}$$

which has a **Full-Width-At-Half-Maximum** of 2γ . Rewriting

$$\frac{\Gamma_{ij}}{2\gamma_{ij}} \frac{1}{1 + (\delta\omega_{ij}/\gamma_{ij})^2} \Rightarrow \left[\frac{\Gamma_{ij}}{2} \right] \frac{\gamma}{d\omega_{ij}^2 + \gamma_{ij}^2}$$

we see that

$$\gamma_{ij} = \frac{\text{Full width at half maximum}}{2}.$$

5.5 Combining the sections above

Emission from a system is linked to the voltage operator, V^+ .

- The voltage operator is defined as:

$$\hat{V}^+ = i \frac{\hbar \Gamma_1}{\phi} \sigma^-,$$

the ‘-’ coming from the fact that the atom must relax in order for voltage to be produced. The average produced field would be

$$\langle \hat{V}^+ \rangle = i \frac{\hbar \Gamma_1}{\phi} \langle \sigma^- \rangle,$$

- Now, the power resulting from this voltage, which is effectively noise as the atom relaxes spontaneously, can be found:

$$\begin{aligned} \langle V^2(\omega) \rangle &= \frac{1}{2\pi} \int_{-\infty}^{\infty} \langle \hat{V}^-(0) \hat{V}^+(\tau) \rangle e^{i\omega\tau} d\tau \\ &= \frac{\hbar^2 \Gamma_1^2}{\phi^2} \frac{1}{2\pi} \int_{-\infty}^{\infty} \langle \sigma_+(0) \sigma_-(\tau) \rangle e^{i\omega\tau} d\tau \end{aligned}$$

- Using a trick in Oleg's book, one can find that the term $\langle \sigma_+(0) \sigma_-(\tau) \rangle$ can be decomposed as:

– **Total sum is**

$$\frac{1 + \langle \sigma_z \rangle}{2}.$$

- The coherent part is

$$\langle \sigma_+ \rangle \langle \sigma_- \rangle.$$

- Therefore the incoherent part must be the difference between the two:

$$\frac{1 + \langle \sigma_z \rangle}{2} - \langle \sigma_+ \rangle \langle \sigma_- \rangle.$$

- Finding the total emitted power, by integrating over the full frequency range and assuming that we are dealing with stationary states (ss) that would form in the system when averaging:

$$\begin{aligned} \text{Power}_{\text{total}} &= \frac{1}{Z} \int \langle V^2(\omega) \rangle d\omega \\ &= \frac{1}{Z} \int \frac{\hbar^2 \Gamma_1^2}{\phi^2} \frac{1}{2\pi} \int_{-\infty}^{\infty} \frac{1 + \langle \sigma_z \rangle_{ss}}{2} e^{i\omega\tau} d\tau d\omega \\ &= \frac{\hbar^2 \Gamma_1^2}{Z\phi^2} \frac{1 + \langle \sigma_z \rangle_{ss}}{2} \int \frac{1}{2\pi} \int e^{i\omega\tau} d\tau d\omega \end{aligned}$$

Using the fact that the integral over the delta function is just 0 and $\Gamma_1 = \frac{\hbar\omega\phi^2 Z}{\hbar^2}$

$$= \hbar\omega\Gamma_1 \frac{1 + \langle \sigma_z \rangle_{ss}}{2}$$

Now, because we are driving continuously, decoherence will result in our rotation of the state from $|0\rangle$ to $|1\rangle$ to form an intermediate value when $\langle \sigma_z \rangle = 0$ and so the maximum emitted power from the atom will be:

$$\boxed{\text{Power}_{\text{total}} = \frac{\hbar\omega\Gamma_1}{2}}$$

- Now, redoing the same, but only considering the coherent contribution i.e. instead of $\frac{1 + \langle \sigma_z \rangle_{ss}}{2}$ use $\langle \sigma_+ \rangle \langle \sigma_- \rangle$ we round up at:

$$\begin{aligned} \text{Power}_{\text{coherent}} &= \hbar\omega\Gamma_1 \langle \sigma_+ \rangle_{ss} \langle \sigma_- \rangle_{ss} = \text{upon subbing in the obtained expectation values} \\ &= \hbar\omega\Gamma_1 \left(\frac{2\Gamma_1\Omega}{2\Gamma_1^2 + \Omega^2} \right) \\ &\Rightarrow \text{max value} = \frac{\hbar\omega\Gamma_1}{8} \end{aligned}$$

- You can measure this power with the SPA i.e. you measure 1/8 of a single photon power;
- Then, you can tune your VNA power to match this $8\times$ coherent signal power, and be supplying exactly one photon to the system. Then there will be no leakages, as the photon will be absorbed

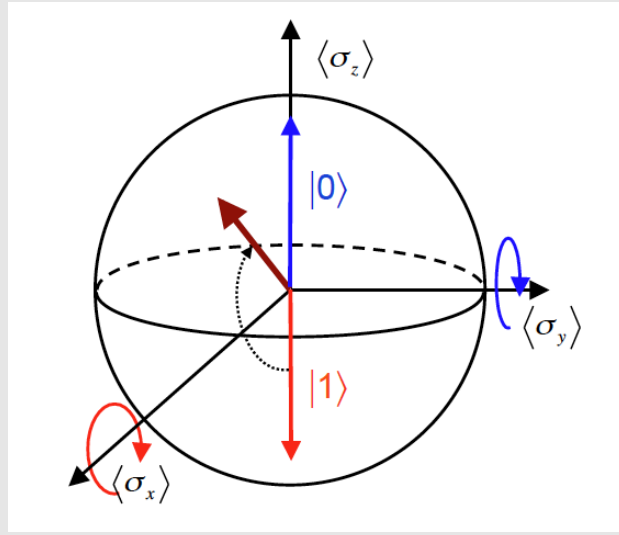
by the system, with no leftover for leaking;

- The total number of photons in the system can be found from

$$N = \frac{\Omega}{\Gamma_1}$$

5.6 Coherent and incoherent emission

1. **Coherent field**, means a fixed phase relation with the two input fields. For example, supplying $e^{i\omega_1 t}$ and $e^{i\omega_2 t} \rightarrow e^{i(\omega_1+\omega_2)t+\phi}$ where ϕ is a fixed value. This allow further entanglement procedures;
2. **Emission by qubit** can be characterised as coherent and incoherent emission. One needs to work with $\langle \sigma_i \rangle$ values and look at the corresponding bloch sphere.



Recalling that

$$\rho_{00} = \frac{\langle \sigma_z \rangle + 1}{2}; \quad \rho_{01} = \frac{\langle \sigma_x \rangle - i \langle \sigma_y \rangle}{2} = \langle \sigma_+ \rangle; \quad \rho_{10} = \frac{\langle \sigma_x \rangle + i \langle \sigma_y \rangle}{2} = \langle \sigma_- \rangle;$$

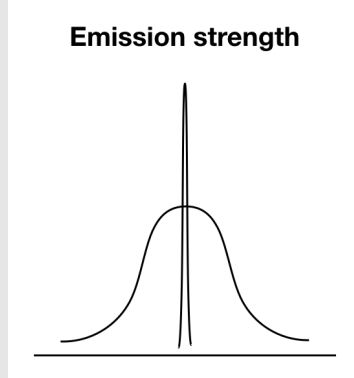
$$\langle \sigma_x \rangle = \rho_{01} + \rho_{10}; \quad \langle \sigma_y \rangle = i\rho_{01} - i\rho_{10}; \quad \langle \sigma_z \rangle = \rho_{00} - \rho_{11}$$

The more a state is on the equator, the more coherence it has since a superposition is formed. Recall that, so that when the “arrow” projects fully onto the equator, it means that the atom is in a superposed state e.g. $\frac{|0\rangle+|1\rangle}{\sqrt{2}} \rightarrow \begin{pmatrix} 1/2 & 1/2 \\ 1/2 & 1/2 \end{pmatrix} \rightarrow \langle \vec{\sigma} \rangle_z = 0, \langle \vec{\sigma} \rangle_x = 1$ (or some other rotation around y).

Coherent emissions $\propto \langle \sigma_x \rangle$

Incoherent $\propto \langle \sigma_z \rangle$.

Both emissions will occur at the frequency of the qubit ω_0 (i.e. energy level separation), but emission from $\langle \sigma_x \rangle$ will be sharp, while incoherent emission from $\langle \sigma_z \rangle$ will be broad as shown below



3. Now draw the parallels between:

- The field in a resonator

a and a^\dagger ;

- Qubit

$$\text{excitation } \sigma_+ = |1\rangle\langle 0| = \begin{pmatrix} 0 & 0 \\ 1 & 0 \end{pmatrix} = (\sigma_x - i\sigma_y)/2 \text{ and relaxation}$$

$$\sigma_- = |0\rangle\langle 1| = \begin{pmatrix} 0 & 1 \\ 0 & 0 \end{pmatrix} = (\sigma_x + i\sigma_y)/2$$

in the following way

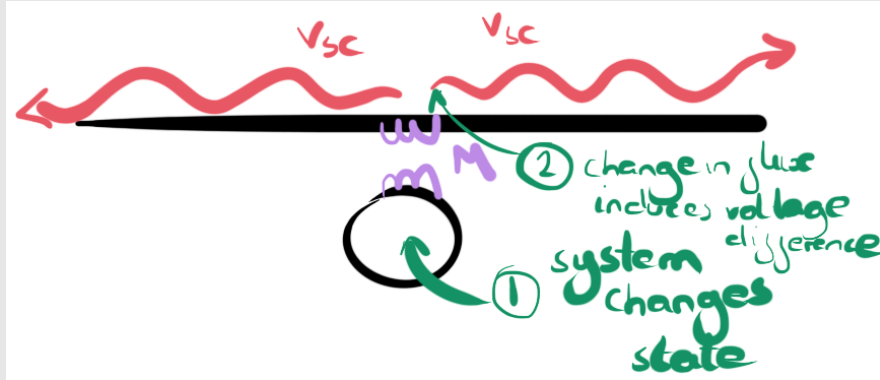
Coherent field	$(a + a^\dagger)$	$\langle \sigma_x \rangle$
Photon number	$aiadagger$	$\langle \sigma_z \rangle$

CHAPTER 6

SCATTERING BY SYSTEM [3]

Main result:

$$2ikV_{sc} = i\omega\phi_p \langle\sigma^-\rangle.$$



1. Beginning with the telegraph equations for the voltage difference at the position of the atom:

$$\begin{cases} \frac{d\Delta V}{dx} = l \frac{dI}{dt} \\ \Delta V = |V_{sc}| [e^{i(kx - \omega t)} - e^{i(-kx - \omega t)}] \end{cases} \Rightarrow \frac{d\Delta V}{dx} = 2ikV_{sc} \quad (6)$$

2. Now, the atom is situated specific point on the line, $x = 0$, **and only at this point is the voltage discontinuous.** Thus we incorporate delta function into Eq. (6)

$$\frac{d\Delta V}{dx} = 2ikV_{sc}\delta(x) \quad (7)$$

3. This voltage is caused by a change of the linked flux (dipole) during a transition (Eq. (1))

$$\text{small change in flux} = \vartheta_{ij}(t) = MI_p \langle\sigma^-\rangle e^{i\omega t}.$$

4. Let's evaluated the induced voltage due to this changing of flux

$$\Delta V = \dot{\Phi} = i\omega MI_p \langle\sigma^-\rangle e^{i\omega t} \quad (8)$$

5. Integrating Eq. (7) and subbing in Eq. (8) we arrive at

$$2ikV_{sc} = i\omega\phi_p \langle\sigma_-\rangle \quad \phi_p = MI_p e^{i\omega t}$$

6.1 Coherent dynamics and decoherence in a superconducting weak link [17]

Here authors say that dissipation is caused by resistance R_q parallel to the inductance:

$$S_i(\omega_q) = \frac{2\hbar\omega_q}{2\pi R_q}$$

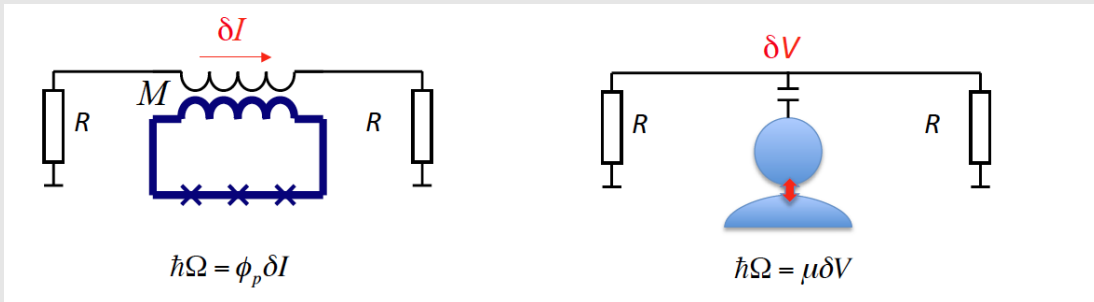
which causes a relaxation rate

$$\Gamma_1 = \frac{2\pi S_i(\omega_q)\varphi_p^2 \sin^2(\theta)}{\hbar^2}$$

where from $\Delta E = \sqrt{(2I_p\delta\Phi)^2 + E_s^2}$, $\tan(\theta) = \frac{E_s}{2I_p\delta\Phi}$ (see Sec. 28) we define θ and $\varphi_p = L_q I_p = \frac{1}{2}\Phi_0$ is the dipole moment of the loop coupled to the resistance (not clear at all).

RELAXATION DUE TO NOISE

7.1 Relaxation from the noise spectrum



In the systems above noise may come from current or voltage fluctuations. We shall analyse the latter case, in which the voltage fluctuation acts as an effective driving field

$$\mathcal{H} = -\frac{\hbar\omega}{2}\sigma_z + \frac{\mu\delta V(\omega)}{2}\sigma_x \cos(\omega t); \quad \delta V(\omega) = \frac{1}{T} \int_{-T/2}^{T/2} \delta V(te^{-i\omega t}) dt,$$

and after applying the RWA

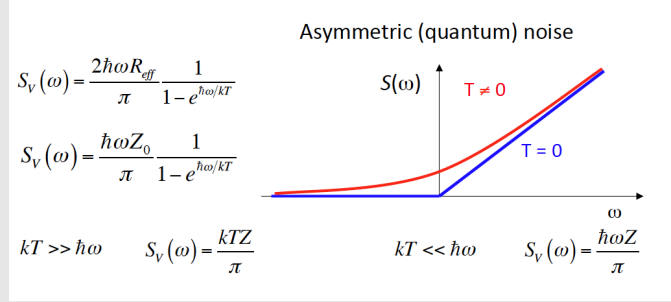
$$\mathcal{H} = \frac{\mu\delta V(\omega)}{2}\sigma_x,$$

the evolution of a system state

$$U(T)|0\rangle = |0\rangle - \frac{\mu\delta V(\omega)}{2}\frac{T}{\hbar}|1\rangle \quad \rightarrow \quad P_1 = \frac{\mu^2 T^2}{4\hbar^2} \langle \delta V^2 \rangle,$$

and incorporating the spectral noise density $S(\Omega)$ which we integrate over in the frequency range $\Delta\omega = 2\pi/T$ (longer acquisition time means narrower spectrum of noise since we average more and more, and only low frequency remains will remain in the system.)

$$\begin{aligned} \langle \delta V^2 \rangle &= S(\omega) \frac{2\pi}{T} \\ P_1 &= \frac{\mu^2 T^2}{4\hbar^2} \langle \delta V^2 \rangle \end{aligned} \Rightarrow P_1 = \frac{\pi\mu^2}{2\hbar^2} S(\omega) T \rightarrow \text{rate of excitation} \approx \Gamma = \frac{\pi\mu^2}{2\hbar^2} S(\omega).$$



CHAPTER 8

UNITARY TRANSFORMATIONS AND THE ROTATING FRAME

The Hermitian conjugate of an operator is defined as

$$U^\dagger = (U^*)^T,$$

and the operator can be classified under two types

- $U^\dagger \equiv U$ a Hermitian operator;
- $U^\dagger \equiv U^{-1}$ is a unitary operator.

The most important equation for unitary operators is

$$U^\dagger U = \mathbb{I},$$

examples of which are Pauli spin matrices $\sigma_x, \sigma_y, \sigma_z$.

Now we shall examine the rotation operator, which rotates the state of a two levels system by an angle 2α about the j axis of the Bloch sphere

$$\begin{aligned} U &= \exp \left[i\alpha \sigma_j \right] = \sum_k \frac{(i\alpha)^k}{k!} \sigma_j^k \\ &= \sum_{k=0} \frac{\alpha^{2k} (-1)^k}{2k} \mathbb{I} + i \sum_{k=0} \frac{\alpha^{2k+1} (-1)^k}{2k+1} \sigma_j \\ &= \cos(\alpha) \mathbb{I} + i \sin(\alpha) \sigma_j, \end{aligned}$$

where we utilise $\sigma_j \sigma_j = \mathbb{I}$. For the three Pauli spin matrices this will read

$$U(\sigma_x) = \begin{pmatrix} \cos \alpha & i \sin \alpha \\ i \sin \alpha & \cos \alpha \end{pmatrix}; \quad U(\sigma_u) = \begin{pmatrix} \cos \alpha & \sin \alpha \\ -\sin \alpha & \cos \alpha \end{pmatrix}; \quad U(\sigma_z) = \begin{pmatrix} e^{i\alpha} & 0 \\ 0 & e^{-i\alpha} \end{pmatrix}. \quad (9)$$

Furthermore, one can double check the unitarity of the matrix:

$$U^\dagger U = \left(\cos(\alpha)\mathbb{I} + i \sin(\alpha)\sigma_j \right) \left(\cos(\alpha)\mathbb{I} - i \sin(\alpha)\sigma_j \right) = \mathbb{I} \cos^2(\alpha) + \sigma_j \sigma_j \sin^2(\alpha) \equiv \mathbb{I}.$$

When a unitary transformation $\Psi' = U\Psi \leftrightarrow \Psi = U^\dagger\Psi'$ is applied, the Schrödinger equation will be modified as such

$$\begin{aligned} i\hbar \frac{dU^\dagger \Psi'}{dt} &= \mathcal{H} U^\dagger \Psi' \\ i\hbar U^\dagger \frac{d\Psi'}{dt} + i\hbar \dot{U}^\dagger \Psi' &= \mathcal{H} U^\dagger \Psi' \quad \text{no time dependance of } U \\ i\hbar \frac{d\Psi'}{dt} &= \left[U \mathcal{H} U^\dagger - i\hbar U \dot{U}^\dagger \right] \Psi' \end{aligned}$$

Expectation values are conserved in unitary transformations:

$$\begin{aligned} \langle \psi | A | \psi \rangle &\equiv (\langle \psi | U) U^\dagger A U (U^\dagger | \psi \rangle) \\ &\equiv \langle \psi' | A' | \psi' \rangle \end{aligned}$$

So expectation values of an operator remain unchanged. **This means that physical quantities can be equally well calculated in transformed frames e.g. enter the rotating frame to find $\langle \sigma_x \rangle$.**

Also important are commutation properties between the three Pauli Matrices

$$\sigma_i \sigma_j = -\sigma_j \sigma_i,$$

which results in the following relations involving the unitary operator of rotation about the y-axis

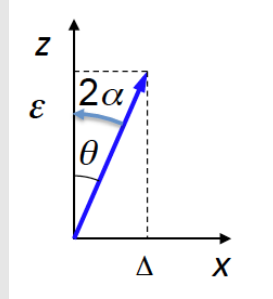
$$\begin{cases} U_y \sigma_z = \left(\cos(\alpha)\mathbb{I} + i \sin(\alpha)\sigma_y \right) \sigma_z = \sigma_z \left(\cos(\alpha)\mathbb{I} - i \sin(\alpha)\sigma_y \right) = \sigma_z U_y^\dagger \\ U_y \sigma_x = \sigma_x U_y^\dagger \\ U_y \sigma_y = \sigma_y U_y \end{cases} \quad (10)$$

8.1 Example application

A general two levels system with energy separation ε interaction between the two states of strength Δ can be written

$$\begin{aligned}
\mathcal{H} &= \begin{pmatrix} -\epsilon/2 & 0 \\ 0 & \epsilon/2 \end{pmatrix} + \begin{pmatrix} 0 & -\Delta/2 \\ -\Delta/2 & 0 \end{pmatrix} = -\frac{\epsilon}{2}\sigma_z - \frac{\Delta}{2}\sigma_x \\
&= -\frac{\sqrt{\epsilon^2 + \Delta^2}}{2} \left(\frac{\epsilon}{\sqrt{\epsilon^2 + \Delta^2}}\sigma_z + \frac{\Delta}{\sqrt{\epsilon^2 + \Delta^2}}\sigma_x \right) \\
&= -\frac{\Delta E}{2} (\cos(\theta)\sigma_z + \sin(\theta)\sigma_x)
\end{aligned}$$

$$\Rightarrow \begin{cases} \mathcal{H} = -\frac{\Delta E}{2}(\sigma_z \cos(\theta) + \sigma_x \sin(\theta)) \\ \Delta E = \sqrt{\epsilon^2 + \Delta^2} \\ \tan(\theta) = \frac{\Delta}{\epsilon} \end{cases}$$



Now we perform a transformation to rotate the state by $2\alpha = \theta$

$$\mathbf{U} = e^{i\frac{\theta}{2}\sigma_y} = \cos(\alpha)\mathbb{I} + i \sin(\alpha)\sigma_y$$

to rotate the basis in this plane. **Note that the transformation uses an angle HALF of the required turn.** The time independent Hamiltonian will be transformed, and evaluating using the commutation relations Eq.(10)

$$\begin{aligned}
\mathcal{H}' &= U\mathcal{H}U^\dagger = U \left[-\frac{\Delta E}{2}(\sigma_z \cos(\theta) + \sigma_x \sin(\theta)) \right] \left[\cos(\theta/2)\mathbb{I} - i \sin(\theta/2)\sigma_y \right] \\
&= U \left[\cos(\theta/2)\mathbb{I} + i \sin(\theta/2)\sigma_y \right] \left[-\frac{\Delta E}{2}(\sigma_z \cos(\theta) + \sigma_x \sin(\theta)) \right] \\
&= UU\mathcal{H} = -\frac{\Delta E}{2} \left[\cos(\theta)\mathbb{I} + i \sin(\theta)\sigma_y \right] \left[(\sigma_z \cos(\theta) + \sigma_x \sin(\theta)) \right] \\
&= -\frac{\Delta E}{2} \left[\cos^2(\theta)\sigma_z + \sin(\theta)\cos(\theta)\sigma_x + i \sin(\theta)\cos(\theta)\sigma_y\sigma_z + i \sin^2(\theta)\sigma_y\sigma_x \right] \\
&= -\frac{\Delta E}{2} \left[\cos^2(\theta)\sigma_z + \sin(\theta)\cos(\theta)\sigma_x + i \sin(\theta)\cos(\theta)i\sigma_x + i \sin^2(\theta)-i\sigma_z \right] \\
&= -\frac{\Delta E}{2}\sigma_z,
\end{aligned}$$

with eigenstates $|\tilde{0}\rangle, |\tilde{1}\rangle$ at energies $-\Delta E/2, +\Delta E/2$ respectively. Recalling that the transformation we

applied was

$$\tilde{\Psi} = U\Psi \quad \Rightarrow \quad \Psi = U^\dagger \tilde{\Psi},$$

in the initial eigenbasis, the two states will read

$$\begin{aligned} |0\rangle_{\text{initial}} &= U^\dagger |\tilde{0}\rangle = \left(\cos(\theta/2)\mathbb{I} + i \sin(\theta/2)\sigma_y \right) \begin{pmatrix} 1 \\ 0 \end{pmatrix} = \begin{pmatrix} \cos(\theta/2) \\ \sin(\theta/2) \end{pmatrix} \\ |1\rangle_{\text{initial}} &= U^\dagger |\tilde{1}\rangle = \begin{pmatrix} -\sin(\theta/2) \\ \cos(\theta/2) \end{pmatrix}. \end{aligned}$$

So ultimately, rotating by $\theta/2$ will rotate the basis so as to cancel the interaction term.

8.2 Example application 2

Now we have a qubit that is driven by a resonant external field, **this time it is not a Δ interactions as the strength varies with time**

$$\mathcal{H} = -\frac{\hbar\omega_0}{2}\sigma_z - \hbar\Omega \cos(\omega_0 t)\sigma_x$$

for which we shall try the unitary transformation

$$U(t) = \exp \left[-i \frac{\omega_0 t}{2} \sigma_z \right] \tag{11}$$

resulting in the Hamiltonian

$$\begin{aligned}
\mathcal{H}' &= U\mathcal{H}U^\dagger - i\hbar U\dot{U}^\dagger \\
&= -\frac{\hbar\omega}{2}e^{-i\omega_0 t/2\sigma_z}\sigma_z e^{+i\omega_0 t/2\sigma_z} - \hbar\Omega\frac{e^{i\omega t} + e^{-i\omega t}}{2}e^{-i\omega_0 t/2\sigma_z}\sigma_x e^{i\omega_0 t/2\sigma_z} - i\hbar e^{-i\omega_0 t/2\sigma_z}\left(i\frac{\omega}{2}\sigma_z\right)e^{i\omega_0 t/2\sigma_z} \\
&= -\frac{\hbar\Omega}{2}\left(e^{i\omega t} + e^{-i\omega t}\right)e^{-i\omega_0 t/2\sigma_z}e^{(-1)i\omega_0 t/2\sigma_z}\sigma_x \\
&= -\frac{\hbar\Omega}{2}\left(e^{i\omega t} + e^{-i\omega t}\right)e^{-i\omega_0 t\sigma_z}\sigma_x \\
&= -\frac{\hbar\Omega}{2}\left(e^{i\omega t} + e^{-i\omega t}\right)\begin{pmatrix} e^{-i\omega_0 t} & 0 \\ 0 & e^{+i\omega_0 t} \end{pmatrix}\begin{pmatrix} 0 & 1 \\ 1 & 0 \end{pmatrix} \\
&= -\frac{\hbar\Omega}{2}\left(e^{i\omega t} + e^{-i\omega t}\right)\begin{pmatrix} 0 & e^{i\omega_0 t} \\ e^{-i\omega_0 t} & 0 \end{pmatrix} \\
&= -\frac{\hbar\Omega}{2}\begin{pmatrix} 0 & 1 + e^{2i\omega_0 t} \\ 1 + e^{-2i\omega_0 t} & 0 \end{pmatrix} \\
&\approx -\frac{\hbar\Omega}{2}\begin{pmatrix} 0 & 1 \\ 1 & 0 \end{pmatrix} \\
&\approx -\frac{\hbar\Omega}{2}\sigma_x
\end{aligned}$$

where we have applied the RWA where we neglect fast rotating terms

which correspond to non conserved energy processes

qubit Hamiltonian ($\mathcal{H} = -\frac{\hbar\omega}{2}\sigma_z$), implicitly taking into account the raw evolution to concentrate only on the driving field contribution.

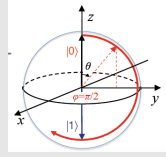
Coupling of levels via radiation = RWA.

Now the evolution of the state

$$U(t) = e^{-i\mathcal{H}'/\hbar t} = e^{i\Omega t/2\sigma_x}$$

gives according to Eq.(9)

$$|\Psi\rangle = U|0\rangle = \cos\left(\frac{\Omega t}{2}\right)|0\rangle + e^{i\pi/2}\sin\left(\frac{\Omega t}{2}\right)|1\rangle.$$



States $|0\rangle$, $|1\rangle$ of the same energy (due to the driving) interact with each other

It may be interesting to observe the case when the drive is changed

$$\hbar\Omega \cos(\omega t)\sigma_x \quad \rightarrow \quad \hbar\Omega \cos(\omega t + \phi)\sigma_x = \hbar\Omega \left[\cos(\omega t) \cos(\phi) - \sin(\omega t) \sin(\phi) \right] \sigma_x$$

for which the procedure for the cosine part using the same unitary transformation Eq.(11) gives

$$-\frac{\hbar\Omega}{2} \cos(\phi)\sigma_x,$$

while the $\sin(\omega t) = i(e^{i\omega t} - e^{-i\omega t})/2$ gets

$$-\frac{\hbar\Omega}{2} \sin(\phi)\sigma_y,$$

giving

$$\mathcal{H}' = -\frac{\hbar\Omega}{2} \left(\sigma_x \cos \phi + \sigma_y \sin \phi \right)$$

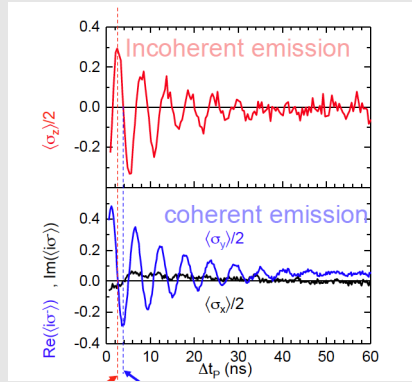
8.3 Qubit operations

In the previous section, the qubit system was subjected to a field that induced rotation about the x-axis. In a similar way, one can perform qubit operations about other axes

Axis	Field operator \mathcal{H}	Unitary evolution $U = \exp[i\mathcal{H}t/\hbar]$	$t = \frac{\pi}{\Omega}$	$t = \frac{\pi}{2\Omega}$
X	$-\frac{\hbar\Omega}{2}\sigma_x$	$\begin{pmatrix} \cos \Omega t/2 & -i \sin \Omega t/2 \\ -i \sin \Omega t/2 & \cos \Omega t/2 \end{pmatrix}$	$\text{NOT} = \begin{pmatrix} 0 & -i \\ -i & 0 \end{pmatrix}$	
Y	$-\frac{\hbar\Omega}{2}\sigma_y$	$\begin{pmatrix} \cos \Omega t/2 & -\sin \Omega t/2 \\ \sin \Omega t/2 & \cos \Omega t/2 \end{pmatrix}$	$\text{FLIP} = \begin{pmatrix} 0 & -1 \\ 1 & 0 \end{pmatrix}$	
Z	$-\frac{\hbar\Omega}{2}\sigma_z$	$\begin{pmatrix} e^{-i\Omega t/2} & 0 \\ 0 & e^{i\Omega t/2} \end{pmatrix}$	$\begin{pmatrix} -i & 0 \\ 0 & i \end{pmatrix}$	$H = \frac{1}{\sqrt{2}} \begin{pmatrix} 1 & -1 \\ 1 & 1 \end{pmatrix}$

DISSIPATION

In this chapter we will ultimately look to understand the image below, which describes the dissipation processes that can occur in a two levels system



In all of the calculation we shall use the density matrix representation in order to represent mixed states that form in a system. Important properties of density matrices are:

- **Diagonal - off diagonal connection for pure state**

$$\rho = |\psi\rangle \langle\psi| = \begin{pmatrix} \alpha \\ \beta \end{pmatrix} \begin{pmatrix} \alpha^* & \beta^* \end{pmatrix} = \begin{pmatrix} |\alpha|^2 & \alpha\beta^* \\ \alpha^*\beta & |\beta|^2 \end{pmatrix} \Rightarrow |\rho_{01}|^2 = \rho_{00}\rho_{11}$$

- **Sum** of the diagonal elements

$$\rho_{00} + \rho_{11} = 1$$

- **Some common expectation values**

$$\begin{aligned}\langle \sigma_z \rangle &= \text{Tr} \left\{ \begin{pmatrix} \rho_{00} & \rho_{01} \\ \rho_{10} & \rho_{11} \end{pmatrix} \begin{pmatrix} 1 & 0 \\ 0 & -1 \end{pmatrix} \right\} = \text{Tr} \left\{ \begin{pmatrix} \rho_{00} & -\rho_{01} \\ \rho_{10} & -\rho_{11} \end{pmatrix} \right\} = \rho_{00} - \rho_{11}; \\ \rho_{11} &= \frac{1 - \langle \sigma_z \rangle}{2}; \quad d\rho_{00} = \frac{1 + \langle \sigma_z \rangle}{2} \\ \langle \sigma_x \rangle &= \rho_{01} + \rho_{10} \end{aligned} \tag{12}$$

$$\begin{aligned}\langle \sigma_y \rangle &= i\rho_{01} - i\rho_{10} \\ \langle \sigma_+ \rangle &= \frac{\langle \sigma_x \rangle + i \langle \sigma_y \rangle}{2} = \rho_{10} \\ \langle \sigma_- \rangle &= \frac{\langle \sigma_x \rangle - i \langle \sigma_y \rangle}{2} = \rho_{01}\end{aligned}$$

- **Evolution** is governed by the Von-Neumann equation

$$i\hbar\dot{\rho} = [\mathcal{H}, \rho]$$

a simple two level system, $\mathcal{H} = -\hbar\omega\sigma_z/2$ giving rise to

$$\begin{aligned}i\hbar \begin{pmatrix} \rho_{00} & \rho_{01} \\ \rho_{10} & \rho_{11} \end{pmatrix} &= -\frac{\hbar\omega}{2} \begin{pmatrix} 1 & 0 \\ 0 & -1 \end{pmatrix} \begin{pmatrix} \rho_{00} & \rho_{01} \\ \rho_{10} & \rho_{11} \end{pmatrix} + \frac{\hbar\omega}{2} \begin{pmatrix} \rho_{00} & \rho_{01} \\ \rho_{10} & \rho_{11} \end{pmatrix} \begin{pmatrix} 1 & 0 \\ 0 & -1 \end{pmatrix} \\ &= -i\omega \begin{pmatrix} 0 & -\rho_{01} \\ -\rho_{10} & 0 \end{pmatrix}\end{aligned}$$

$$\rho_{00} = \rho_{00}(0); \quad \rho_{11}(t) = \rho_{11}(0); \quad \rho_{01}(t) = \rho_{01}(0)e^{i\omega t}; \quad \rho_{10}(t) = \rho_{10}(0)e^{i\omega t}$$

This is rotation about on the equator of the Bloch sphere.

9.1 Application to relaxation

Now, if we excite the system, we will inevitably observe a decay to the ground state - the probability of the system being in an excited states exponentially decreases

$$\frac{d\rho_{11}}{dt} = -\rho_{11} \frac{1}{T} = -\rho_{11} \Gamma_1 \Rightarrow \rho_{11} = \rho_{11}(0)e^{-t/T}. \tag{13}$$

Such a relaxation will eventually lead to the state of the system to change to a mixed state

$$\rho(0) = |1\rangle \langle 1| = \begin{pmatrix} 0 & 0 \\ 0 & 1 \end{pmatrix}_{\text{pure}} \rightarrow \rho(t = T \ln 2) = \begin{pmatrix} \frac{1}{2} & 0 \\ 0 & \frac{1}{2} \end{pmatrix}_{\text{mixed}}, \tag{14}$$

which in terms of probabilities has the **exact same properties** as

$$\rho = \begin{pmatrix} 1 & 1 \\ 1 & 1 \end{pmatrix}_{\text{pure}}.$$

The state in Eq.(14) has lost coherence as the system underwent relaxation. The system that was initially in a pure state when $|\rho_{01}(0)|^2 = \rho_{00}(0)\rho_{11}(0)$ to a mixed state when $|\rho_{01}(t)|^2 \leq \rho_{00}(t)\rho_{11}(t)$. The off diagonal terms loose information and tend to zero.

This is accounted for by writing the Lindblad term

$$\dot{\rho} = \frac{-i}{\hbar} [\mathcal{H}, \rho] + \mathcal{L}; \quad \mathcal{L} = \begin{pmatrix} \rho_{11}\Gamma_1 & -\Gamma_2\rho_{01} \\ -\Gamma_2\rho_{01} & -\Gamma_1\rho_{11} \end{pmatrix},$$

- **Relaxation** will cause ρ_{00} to increase and ρ_{11} to decrease
- **Pure dephasing** - it is well known that the diagonal elements of a density matrix **must** obey

$$|\rho_{01}|^2 \leq \rho_{00}\rho_{11},$$

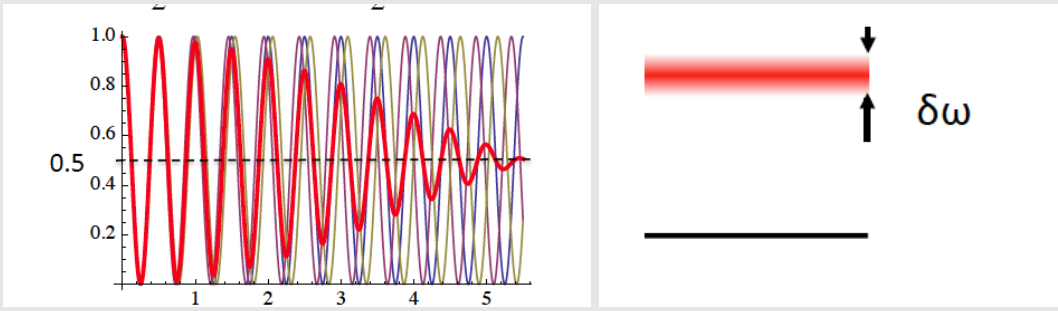
equality being achieved for a pure state. During relaxation ρ_{00} increases and ρ_{11} decreases, but as relaxation can only decrease coherence, it is only the latter term that will effect off diagonal elements

$$\begin{aligned} \delta|\rho_{01}| &\leq \sqrt{\rho_{00}\rho_{11}}\delta|\rho_{01}| && \leq \sqrt{\rho_{00}(\rho_{11} + \delta\rho_{11})} - \sqrt{\rho_{00}\rho_{11}}(\sqrt{1 - \Gamma_1 dt} - 1) \\ \rightarrow \delta\rho_{11} &= -\rho_{11}\Gamma_1 dt \quad \text{from Eq.(13)} && \approx \sqrt{\rho_{00}\rho_{11}}\left(-\frac{\Gamma_1}{2}dt\right) \\ &&& = -|\rho_{01}|\frac{\Gamma_1}{2}dt \end{aligned}$$

meaning that the decay of the off diagonal terms cannot be slower than $\frac{\Gamma_1}{2}$. Taking into account other ways of diagonal terms dephasing, Γ_ϕ , one assigns

$$\Gamma_2 = \frac{\Gamma_1}{2} + \Gamma_\phi; \quad T_2 = \frac{1}{\Gamma_2} \tag{15}$$

This is a very crude argument, and possibly a coincidence. Nevertheless, the required Γ_2 factors is distilled.



9.2 Pure dephasing

Attention will now be direct to the Γ_2 term introduced in Eq.(15), and more specifically its pure dephasing component Γ_ϕ . Pure dephasing is due to noise that affects the separation of the qubit energy levels. Recall from Sec. 8.2, that a qubit system that is subjected to a resonant driving field (whose frequency, ω , matches the energy separation, $\hbar\omega_0$, of the levels)

$$\mathcal{H} = -\frac{\hbar\omega_0}{2}\sigma_z - \hbar\Omega \cos(\omega_0 t)\sigma_x,$$

will, in the RWA, evolve from an initial state $|0\rangle$ according to

$$|\Psi\rangle = U|0\rangle = \cos\left(\frac{\Omega t}{2}\right)|0\rangle + e^{i\pi/2}\sin\left(\frac{\Omega t}{2}\right)|1\rangle.$$

Should the separation of the levels vary, $\hbar\omega_0 \rightarrow \hbar\omega'$, then the qubit will be in resonance with another component of the driving field, $\hbar\Omega' \cos(\omega't)\sigma_x$, meaning that the evolved state will be a superposition of the form

$$|\Psi\rangle = \sum_i \alpha_i \left[\cos\left(\frac{\Omega_i t}{2}\right)|0\rangle + i \sin\left(\frac{\Omega_i t}{2}\right)|1\rangle \right],$$

leading to a probability of observing the system in $|0\rangle$ of

$$P_0 = |\langle 0 | \Psi \rangle|^2 = \sum_i \alpha_i \cos^2\left(\frac{\Omega_i t}{2}\right) = \{ \text{equal weights for 3 states} \} = \frac{1}{3} \left(\cos^2\left(\frac{\Omega_1 t}{2}\right) + \cos^2\left(\frac{\Omega_2 t}{2}\right) + \cos^2\left(\frac{\Omega_3 t}{2}\right) \right),$$

which leads to a probability 'averaging' as one monitors the system for longer times t , the characteristic decay time being labelled as $T_\phi = 1/\Gamma_\phi$. The Rabi oscillations are 'washed out' due to this dephasing. The bigger the fluctuations of the energy levels the stronger the washing out. If one hopes to observe any oscillations, then the Rabi frequency $\Omega \gg 1/T_\phi = \Gamma_2$ to ensure that oscillation occur before dying off.

9.3 Dynamics with Pauli Matrices

Summarising up to this point, we have argued for the appearance of the Linblad term in the Master equation to account for decoherence and relaxation processes in the system

$$\mathcal{L} = \begin{pmatrix} \Gamma_1 \rho_{11} - \Gamma^{ex} \rho_{00} & -\Gamma_2 \rho_{01} \\ -\Gamma_2 \rho_{10} & \Gamma^{ex} \rho_{00} - \Gamma_1 \rho_{11} \end{pmatrix}; \quad \dot{\rho} = -\frac{i}{\hbar} [\mathcal{H}, \rho] + \mathcal{L},$$

and shown a few useful expectation values, that allow one to express the dynamics of the system via the expectation values of the Pauli matrices, Eq.(12)

$$\rho_{00} = \frac{\langle \sigma_z \rangle + 1}{2}; \quad \rho_{01} = \frac{\langle \sigma_x \rangle - i \langle \sigma_y \rangle}{2} = \langle \sigma_+ \rangle; \quad \rho_{10} = \frac{\langle \sigma_x \rangle + i \langle \sigma_y \rangle}{2} = \langle \sigma_- \rangle; \quad \rho_{11} = \frac{1 - \langle \sigma_z \rangle}{2}.$$

$$\langle \sigma_x \rangle = \rho_{01} + \rho_{10}; \quad \langle \sigma_y \rangle = i\rho_{01} - i\rho_{10}; \quad \langle \sigma_z \rangle = \rho_{00} - \rho_{11}$$

Lets compute the evolution of these expectation values

$$\frac{d\langle \sigma_j \rangle}{dt} = \text{Tr} \left\{ \sigma_j \frac{d\rho}{dt} \right\} = \text{Tr} \left\{ -\frac{i}{\hbar} \sigma_j (\mathcal{H}\rho - \rho\mathcal{H}) + \sigma_j \mathcal{L} \right\}$$

$$\mathcal{H} = \frac{\hbar\Omega}{2} \left(\sigma_x \cos(\phi) - \sigma_y \sin(\phi) \right),$$

and evaluating for all the matrices

$$\begin{aligned} \frac{d\langle \sigma_x \rangle}{dt} &= -i\frac{\Omega}{2} \text{Tr} \{ (\sigma_x \sigma_x \rho - \sigma_x \rho \sigma_x) \cos(\phi) + (\sigma_x \sigma_y \rho - \sigma_x \rho \sigma_y) \sin(\phi) \} + \text{Tr} \{ \sigma_x \mathcal{L} \} \\ &= \Omega \langle \sigma_z \rangle \sin(\phi) - \Gamma_2 \langle \sigma_x \rangle \\ \frac{d\langle \sigma_y \rangle}{dt} &= \Omega \langle \sigma_z \rangle \sin(\phi) - \Gamma_2 \langle \sigma_y \rangle \\ \frac{d\langle \sigma_y \rangle}{dt} &= -\Omega (\langle \sigma_x \rangle \cos(\phi) + \langle \sigma_y \rangle \sin(\phi)) - \Gamma_1 \langle \sigma_z \rangle + \Gamma_1 \end{aligned}$$

or in more compact form

$$\frac{d}{dt} \begin{pmatrix} \langle \sigma_x \rangle \\ \langle \sigma_y \rangle \\ \langle \sigma_z \rangle \end{pmatrix} = \begin{pmatrix} -\Gamma_2 & 0 & \Omega \sin(\phi) \\ 0 & -\Gamma_2 & \Omega \cos(\phi) \\ -\Omega \sin(\phi) & -\Omega \cos(\phi) & -\Gamma_1 \end{pmatrix} \begin{pmatrix} \langle \sigma_x \rangle \\ \langle \sigma_y \rangle \\ \langle \sigma_z \rangle \end{pmatrix} + \begin{pmatrix} 0 \\ 0 \\ \Gamma_1 \end{pmatrix} \rightarrow \frac{d\vec{\sigma}}{dt} = B\vec{\sigma} + \vec{b}. \quad (16)$$

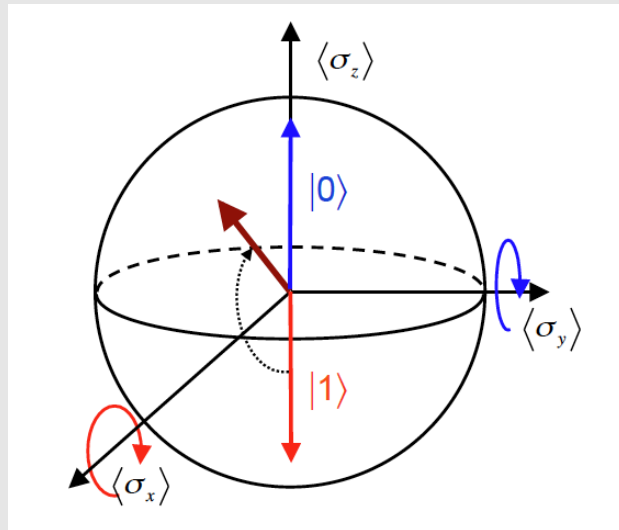
The dynamics of this system are the exact same as for a spin 1/2 particle in a magnetic field \mathbf{B} studied in

Chapter 37 Eq. (59). The different components of the vector $\langle \vec{\sigma} \rangle$ can be plotted on a sphere. Note that unlike the Bloch sphere used previously, these vectors do **not** have to be on the surface. The various states $\langle \vec{\sigma} \rangle$ correspond to

$$\rho_{00} = 1 \rightarrow \langle \vec{\sigma} \rangle = \begin{pmatrix} 0 \\ 0 \\ 1 \end{pmatrix}$$

$$\rho_{11} = 1 \rightarrow \langle \vec{\sigma} \rangle = \begin{pmatrix} 0 \\ 0 \\ -1 \end{pmatrix}$$

$$\rho_{00} = \rho_{11} \rightarrow \langle \vec{\sigma} \rangle = \begin{pmatrix} \cos(\phi) \\ \sin(\phi) \\ 0 \end{pmatrix}$$



Starting in the superposed state So now let us study some dynamics, where, unless specified, we take the initial state to be $\rho_{00} = 1/2$ i.e. on the equator where the atom has equal occupation in levels $|0\rangle$ and $|1\rangle$. A general state would be

$$\Psi = \frac{|0\rangle + e^{i\phi}|1\rangle}{\sqrt{2}} \rightarrow \rho = \frac{1}{2} \begin{pmatrix} 1 & e^{-i\phi} \\ e^{i\phi} & 1 \end{pmatrix}$$

- **No driving No decoherence** - the superposed state will remain superposed.

$$\begin{aligned} \mathcal{H} = -\frac{\hbar\omega}{2}\sigma_z &\Rightarrow U = \begin{pmatrix} e^{i\omega t} & 0 \\ 0 & e^{-i\omega t} \end{pmatrix} \\ &\Rightarrow \rho(t) = U\rho(0)U^\dagger = \frac{1}{2} \begin{pmatrix} e^{i\omega t} & e^{i(\omega t-\phi)} \\ e^{-i(\omega t-\phi)} & e^{-i\omega t} \end{pmatrix} \begin{pmatrix} e^{-i\omega t} & 0 \\ 0 & e^{+i\omega t} \end{pmatrix} \\ &= \frac{1}{2} \begin{pmatrix} 1 & e^{i(2\omega t-\phi)} \\ e^{-i(2\omega t-\phi)} & 1 \end{pmatrix} \end{aligned}$$

But when we consider the situation from by entering the rotating frame (the interaction picture), see Chapter 8 and Ch. 32

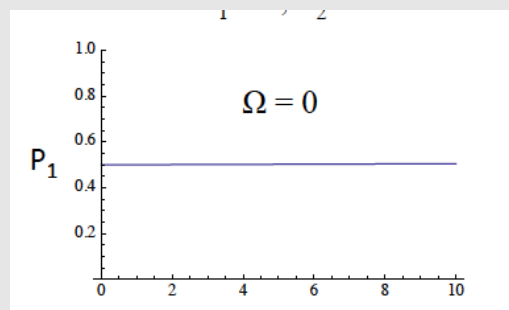
$$U_0(t) = e^{i\frac{\mathcal{H}_0}{\hbar}t},$$

the interaction picture Hamiltonian will be of the form Eq. (41)

$$\mathcal{H}_i = U_0(t)^\dagger [\mathcal{H} - \mathcal{H}_0] U_0(t) \equiv 0,$$

and so there will be no evolution in the system in this rotated frame that we work with. The expectation values, $\langle\sigma_x\rangle$, $\langle\sigma_z\rangle$ are the same as in the rotated and non-rotating frames:

$${}_I \langle \psi | \hat{O}_I | \psi \rangle_I = {}_S \langle \psi | U_0 U_0^\dagger \hat{O}_S U_0 U_0^\dagger | \psi \rangle_s \equiv {}_S \langle \psi | \hat{O}_S | \psi \rangle_s$$



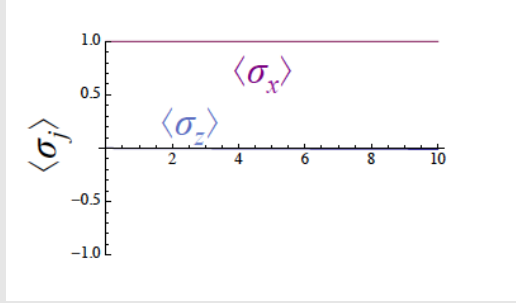
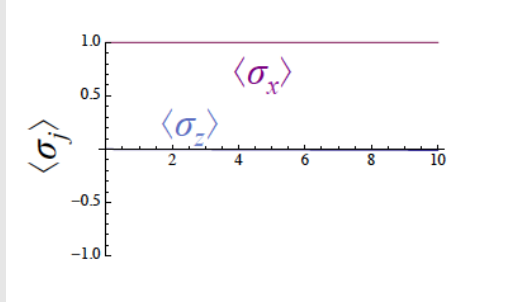


Figure 8:

Figure 9: On the equator the atom has equal weight in $|0\rangle$ and $|1\rangle$, so $\langle \sigma_z \rangle$ is 0. The $\langle \sigma_x \rangle$ is stationary.

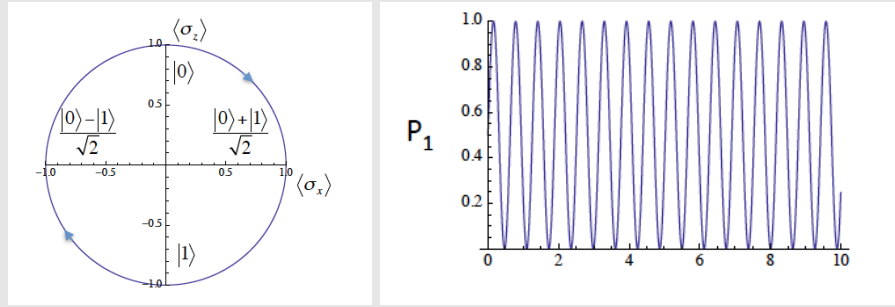
- **Driving No decoherence,** $\Gamma_1 = 0, \Gamma_2 = 0$

We evolution of the wavefunction is taken to be **under a drive from a resonant field**

$$|\Psi\rangle = \cos\left(\frac{\Omega t}{2}\right)|0\rangle + i \sin\left(\frac{\Omega t}{2}\right)|1\rangle; \quad \rho = |\Psi\rangle\langle\Psi|$$

$$\begin{aligned} \rho_{11} &= \sin^2(\Omega t/2) & \langle \sigma_x \rangle &= \rho_{01} + \rho_{10} = \sin(\Omega t) \\ \rho_{01} &= \sin(\Omega t/2) \sin(\Omega t/2) = \frac{\sin(\Omega t)}{2} & \langle \sigma_y \rangle &= i\rho_{01} - i\rho_{10} = 0 \\ \rho_{10} &= \sin(\Omega t/2) \sin(\Omega t/2) = \frac{\sin(\Omega t)}{2} & \langle \sigma_z \rangle &= 1 - 2\rho_{00} = \cos(\Omega t) \end{aligned}$$

and the point on the sphere simply rotates about the $\langle \sigma_y \rangle$ axis. If there was a phase shift in the driving field ϕ then the rotation would turn by that angle about the $\langle \sigma_z \rangle$ axis. Overall these are the Rabi oscillations

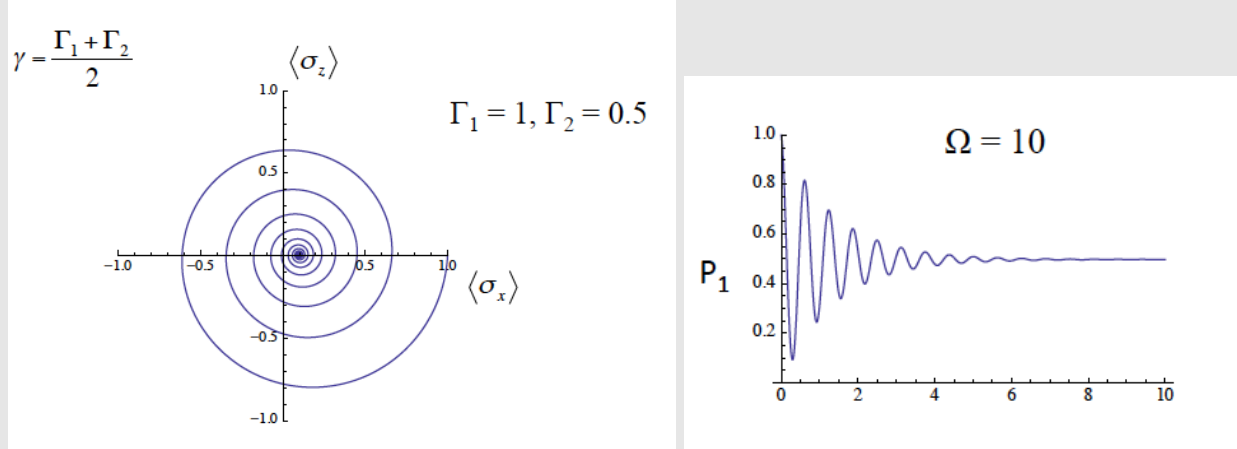


- **Driving With decoherence** $\Gamma_1 = 1, \Gamma_2 = 0.5, \gamma = \Gamma_1 + \Gamma_2/2$, it is simpler to solve the dynamics of Eq.(16) for $\langle \vec{\sigma} \rangle$

For the case when one starts off with state $\rho_{00} = 1$

$$\begin{aligned}\langle \sigma_x \rangle &\approx e^{-\gamma t} \sin(\Omega t) & \rho_{00} &= \frac{\langle \sigma_z \rangle + 1}{2} \approx \frac{1 + e^{-\gamma t} \cos(\Omega t)}{2} \\ \langle \sigma_y \rangle &= 0 & \rho_{01} &= \frac{\langle \sigma_x \rangle - i \langle \sigma_y \rangle}{2} = \frac{e^{-\gamma t} \sin(\Omega t)}{2} \\ \langle \sigma_z \rangle &\approx e^{-\gamma t} \cos(\Omega t) & \rho_{10} &= \frac{\langle \sigma_x \rangle + i \langle \sigma_y \rangle}{2} = \frac{e^{-\gamma t} \sin(\Omega t)}{2}\end{aligned}$$

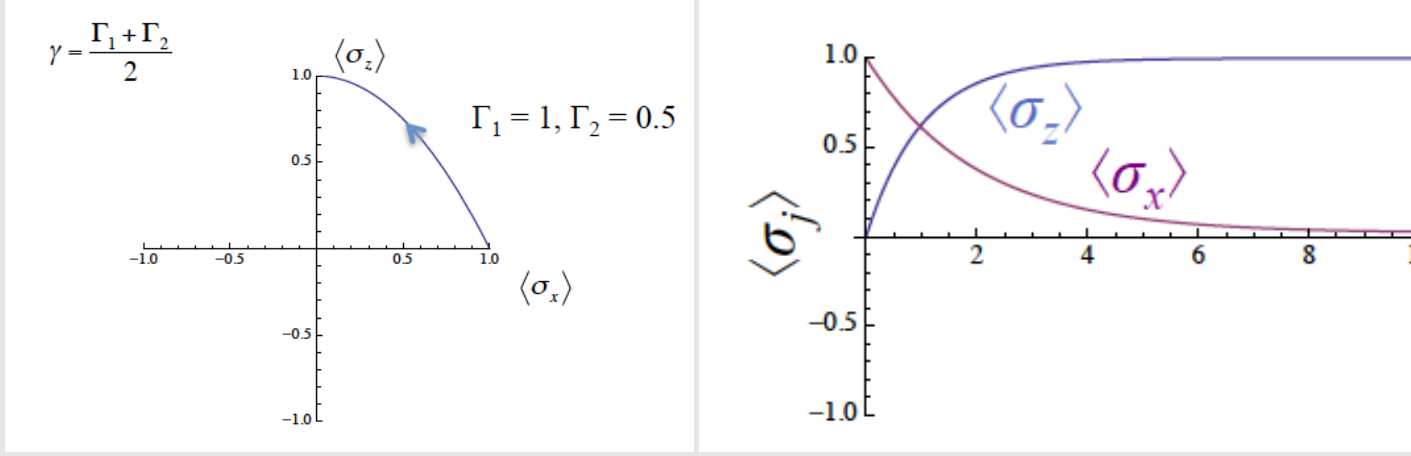
In this case the two components begin to spiral in as a result of the dephasing. The central point is the stationary condition in which both $\langle \sigma_x \rangle$ and $\langle \sigma_z \rangle$ take on a finite value - the stationary state value.



- **No driving with decoherence and relaxation** $\rho_{00} = \rho_{11} = 1/2$ then

$$\begin{aligned}\langle \sigma_x \rangle &= e^{-\Gamma_2 t} & \rho_{00} &= 1 - \frac{e^{-\Gamma_1 t}}{2} \\ \langle \sigma_y \rangle &= 0 & \rho_{01} &= \frac{e^{-\Gamma_2 t}}{2} \\ \langle \sigma_z \rangle &= 1 - e^{-\Gamma_1 t} & \rho_{10} &= \frac{e^{-\Gamma_2 t}}{2}\end{aligned}$$

The system, initially on the ‘equator’ of the sphere, transitions to the ground state

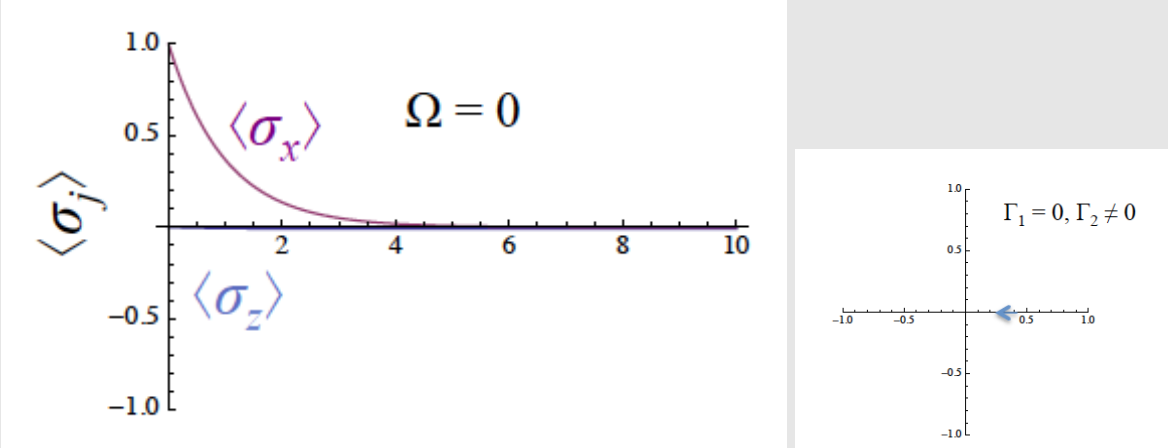


- **No driving Only dephasing** $\Gamma_1 = 0, \Gamma_2 \neq 0$ when we start off in a superposed state $\rho_{11} = 1/2 \rightarrow \langle \sigma_z \rangle = 0$

$$\begin{aligned}\langle \sigma_x \rangle &= e^{-\Gamma_2 t} & \rho_{00} &= \frac{1}{2} \\ \langle \sigma_y \rangle &= 0 & \rho_{01} &= \frac{e^{-\Gamma_2 t}}{2} \\ \langle \sigma_z \rangle &= 0 & \rho_{10} &= \frac{e^{-\Gamma_2 t}}{2}\end{aligned}$$

The expectation value simply moves towards the origin, where $\langle \sigma_z \rangle = 0$ and the system becomes equally likely to exist in the excited or ground state $\rho_{00} = \rho_{11}$. The off diagonal terms loose coherence.

Thus, relaxation will tend to shift $\langle \sigma_z \rangle$ to 1, and together with pure dephasing it shortens the expectation values of the $\langle \sigma_x \rangle$ and $\langle \sigma_y \rangle$ directions.



CHAPTER 10

LINBALND OPERATORS COVERED IN DEPTH

This section will cover how we derive these L_j operators which were used in Sec. 9.3.

10.1 Pure dephasing

Let us consider a two level system, whose Hamiltonian is undergoing a fluctuation in time due to **movement of the energy levels**

$$\mathcal{H} = \begin{pmatrix} \epsilon(t) & 0 \\ 0 & 0 \end{pmatrix} \xrightarrow{\text{eigenstates}} \begin{aligned} |0\rangle &= \begin{pmatrix} 0 \\ 1 \end{pmatrix} \\ |1\rangle &= \begin{pmatrix} 1 \\ 0 \end{pmatrix} \end{aligned}$$

Under free evolution an arbitrary state $|\Psi(0)\rangle = a|1\rangle + b|0\rangle$ will evolve to:

$$\begin{aligned}
|\Psi(t)\rangle &= \prod_i U(\Delta t_i) |\Psi(0)\rangle \\
&= \prod_i \exp \left[-i \frac{\epsilon(\Delta t_i)}{\hbar} \begin{pmatrix} 1 & 0 \\ 0 & 0 \end{pmatrix} \right] \begin{pmatrix} a \\ b \end{pmatrix} \\
&= \prod_i \left(\mathbb{I} \begin{pmatrix} a \\ b \end{pmatrix} + \sum_{N=1}^{\infty} \frac{\left[\frac{-i\epsilon(\Delta t_i)}{\hbar} \right]^N}{N!} \begin{pmatrix} 1 & 0 \\ 0 & 0 \end{pmatrix} \begin{pmatrix} a \\ b \end{pmatrix} \right) \\
&= \prod_i \left(\begin{pmatrix} a \\ b \end{pmatrix} + \exp \left[-i \frac{\epsilon(\Delta t_i)}{\hbar} \right] \begin{pmatrix} a \\ 0 \end{pmatrix} - \begin{pmatrix} a \\ 0 \end{pmatrix} \right) \\
&= \prod_i \begin{pmatrix} e^{-i \frac{\epsilon(\Delta t_i)}{\hbar}} a \\ b \end{pmatrix} = \begin{pmatrix} e^{-i \sum_i \frac{\epsilon(\Delta t_i)}{\hbar}} a \\ b \end{pmatrix} \\
&= \begin{pmatrix} ae^{i\varphi} \\ b \end{pmatrix} \quad \varphi = - \int_0^t \frac{\epsilon(t')}{\hbar} dt'
\end{aligned}$$

Thus, free evolution under a fluctuating energy will lead to a phase accumulation between the two states:

$$|\Psi\rangle = a e^{i\varphi} |1\rangle + b |0\rangle = \begin{pmatrix} ae^{i\varphi} \\ b \end{pmatrix}$$

which we can probe by measuring the $\langle \sigma_x \rangle$ component and see this integrated phase:

$$\langle \sigma_x \rangle = ab^* e^{i\varphi} + a^* b e^{-i\varphi} \xrightarrow{\text{a,b real}} 2ab \cos(\varphi). \quad (17)$$

Single run Each measurement of σ_x gives ± 1 with probabilities (projecting onto the respective eigensubspaces):

$$P(1) = \left| \langle \Psi | \left(\frac{|0\rangle + |1\rangle}{\sqrt{2}} \right) \right|^2 = \frac{1}{2} |ae^{-i\varphi} + b|^2 = \frac{1}{2} (a^2 + b^2 + 2ab \cos(\varphi))$$

$$P(-1) = \frac{1}{2} (a^2 + b^2 - 2ab \cos(\varphi))$$

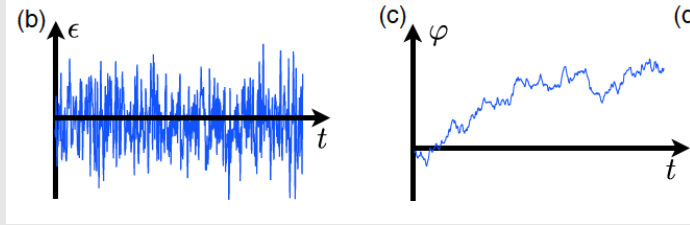


Figure 10: The energy of the two levels fluctuates around 0. Integration will give a unique phase value, $\phi = -\int_0^t \frac{\epsilon(t')}{\hbar} dt'$, that determines collapse probability. **This is for a single run.**

Averaging Averaging over the ± 1 will allow us to recover the $\langle \sigma_x \rangle \propto \cos(\varphi)$ dependence.

- Each run has an independent $\epsilon(t)$ and hence an independent $e^{i\varphi}$;
- Averaging will thus result in the classical average $\langle e^{i\varphi} \rangle_\varphi$.

And thus Eq. (17) will in practise be reading:

$$\langle \sigma_x \rangle = ab^* \langle e^{i\varphi} \rangle_\varphi + a^* b \langle e^{-i\varphi} \rangle_\varphi \xrightarrow{\text{a,b real}} 2ab \cos(\langle \varphi \rangle_\varphi).$$

Let us label this interference term factor

$$v(t) = \langle e^{i\varphi} \rangle_\varphi,$$

which is reflective of the noise suppression of interference: $v(t) \rightarrow 0$.

Why does it decrease with time? Making the assumption that $\epsilon(t)$ fluctuates around 0 we will find that

- Initially any $\varphi(0) = -\int_0^0 \frac{\epsilon(t')}{\hbar} dt' = 0$ (no phase has been allowed to accumulate) and therefore

$$\langle e^{i\varphi(0)} \rangle_\varphi = 1.$$

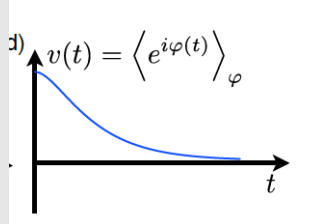


Figure 11: The longer we allow the phase, φ , to evolve the greater amount of cancellation between the independent runs we shall get. In this way and interference that we can infer will wash out.

- Subsequently, the random evolution of the phase will lead to

$$\begin{aligned}
 \langle e^{i\varphi(t)} \rangle_\varphi &= e^{i\phi_1(t)} + e^{i\phi_2(t)} + e^{i\phi_3(t)} + \dots \\
 &= x_1 + iy_1 + x_2 + iy_2 + x_3 + iy_3 + \dots \\
 &= \langle x \rangle + i \langle y \rangle \\
 &= 0 + i0 = 0
 \end{aligned}$$

and thus perfect cancellation - any agreement between the states will persist only for short times.

10.2 Pure dephasing from partial trace

We can arrive at Eq. (17) in a similar fashion by considering a system-bath state

$$|\Psi_{SB}\rangle = |\Psi\rangle \otimes |\chi_B\rangle \quad \text{where} \quad |\chi\rangle = \sum_i \sqrt{w_i} |\chi_i\rangle$$

where the bath is a weighted superposition of $|\chi_i\rangle$ states (normalised of course).

We postulate, that the state of the system will evolve according to the state of the bath:

$$U_{SB}(t) |1\rangle |\chi_i\rangle = e^{i\varphi_i(t)} |1\rangle |\chi_i\rangle$$

$$U_{SB}(t) |0\rangle |\chi_i\rangle = |0\rangle |\chi_i\rangle$$

acquiring a phase only for the $|1\rangle$ state and depending on the states of the bath.

Thus we shall get the following evolution:

$$\begin{aligned}
|\Psi_{SB}(t)\rangle &= aU_{SB}(t) \left[\sum_i \sqrt{w_i} |1\rangle |\chi_i\rangle \right] + bU_{SB}(t) \left[\sum_i \sqrt{w_i} |0\rangle |\chi_i\rangle \right] \\
&= a|1\rangle \sum_i \sqrt{w_i} e^{i\varphi_i(t)} |\chi_i\rangle + b|0\rangle \sum_i \sqrt{w_i} |\chi_i\rangle \\
&= a|1\rangle |\chi_1\rangle + b|0\rangle |\chi_0\rangle
\end{aligned}$$

Taking the expectation value of the operator $\mathbb{I} \otimes \sigma_x$, where we only operate on the system, we get

$$\begin{aligned}
\langle \sigma_x \rangle_S &= \langle \Psi_{SB}(t) | \mathbb{I} \otimes \sigma_x | \Psi_{SB}(t) \rangle \\
&= ab^* \langle \chi_0 | |\chi_1\rangle + a^* b \langle \chi_1 | |\chi_0\rangle \\
&= \sum_i w_i ab^* e^{i\varphi_i(t)} + cc. \\
&= ab^* \left\langle e^{i\varphi(t)} \right\rangle_\varphi + cc.
\end{aligned}$$

where $\left\langle e^{i\varphi(t)} \right\rangle_\varphi = \sum_i w_i e^{i\varphi_i} = \langle \chi_0 | |\chi_1\rangle$ and we recover the result Eq. (17). See how the environment picks up the state of the system

10.3 General roundup

In Sec. 10.1 and 10.2 we have come to two equivalent ways of recovering the state of the system:

$$|\Psi(t)\rangle_\varphi = a|1\rangle v(t) + b|0\rangle.$$

where the phase suppression term $v(t) = \langle e^{i\varphi} \rangle_\varphi$ is a consequence of:

- Classical noise process as we average over different runs that acquire different phases

$$|\Psi(t)\rangle_\varphi = \sum_i a|1\rangle e^{i\varphi_i(t)} + b|0\rangle.$$

- Quantum mechanical Interaction with the weighted superposition of the bath states $|\chi_i\rangle$,

$$\begin{aligned}
|\Psi\rangle_\varphi &= a|1\rangle \sum_i \sqrt{w_i} e^{i\varphi_i(t)} |\chi_i\rangle + b|0\rangle \sum_i \sqrt{w_i} |\chi_i\rangle \\
&= \left[a|1\rangle \sum_i e^{i\varphi_i(t)} + b|0\rangle \right] |\chi\rangle
\end{aligned}$$

Let us represent the state as a density matrix

$$\rho(t) = \begin{pmatrix} |a|^2 & ab^* \color{red}{v(t)} \\ a^* b \color{red}{v^*(t)} & |b|^2 \end{pmatrix},$$

Where we see that dephasing affects only the off-diagonal elements. Taking the purity

$$\begin{aligned} \text{Tr}\{\rho^2\} &= |a|^4 + 2|a|^2|b|^2|v(t)|^2 + |b|^4 \\ &= (|a|^2 + |b|^2)^2 - 2|a|^2|b|^2 + 2|a|^2|b|^2|v(t)|^2 \\ &= 1 - 2|a|^2|b|^2(1 - |v(t)|^2), \end{aligned}$$

and as $v(t) \rightarrow 0$ the purity goes $1 \rightarrow 1/2$ if we start from an even superposition.

Let us assume that the phase suppression term falls as an exponential (which we kind of show in Fig. 11)

$$v(t) = \left\langle e^{i\varphi(t)} \right\rangle_\varphi = e^{-\Gamma_\varphi t}$$

in which case we can write

$$\dot{\rho}_{10}(t) = -\Gamma_\varphi \rho_{10}(t). \quad (18)$$

We want to incorporate this into the evolution of the form

$$\mathcal{L}[\rho(\mathbf{0})] = \rho(\mathbf{t}).$$

10.4 Relaxation in the Linbland Equation

However, the Linbalnd equation, incorporating Eq. (18), cannot be written arbitraraly, because the density matrix is a weighted **probability** superposition

$$\rho = \sum_i |\psi_i\rangle \langle \psi_i|,$$

and therefore cannot have negative eigenvalues. If we, for example, take the decay of a state with initial off diagonal elements:

$$\begin{pmatrix} \rho_{00}(0) & \rho_{01}(0) \\ \rho_{10}(0) & \rho_{11}(0) \end{pmatrix} \rightarrow \begin{pmatrix} 0 & \rho_{01}(t) \\ \rho_{10}(t) & 1 \end{pmatrix} \rightarrow \text{negative eigenvalues!}$$

An arbitrary operator Φ has to be a completely positive:

$$\Phi(\rho) \geq 0$$

$$\Phi : B(\tilde{\mathcal{H}}) \rightarrow B(\mathcal{H})$$

where $\tilde{\mathcal{H}} = \mathcal{H} \otimes \mathcal{H}'$

and Φ acts on one product space and leaves the other untouched

This is fulfilled by the Kraus operator:

$$\Phi(\rho) = \sum_i K_i \rho K_i^\dagger \quad \sum_i K_i^\dagger K_i = \mathbb{I}.$$

A great example is unitary evolution $K = U(t)$, random unitary evolution $K_i = \sqrt{w_i}U_i(t)$ or the evolution of a system batch state:

$$\begin{aligned} \rho(t) &= \text{Tr} \left\{ U_{SB} \rho_S \otimes |\chi_B(0)\rangle \langle \chi_B(0)| U_{SB}^\dagger \right\} \\ &= \sum_j [\langle \chi_j | U_{SB} | \chi_B(0) \rangle] \rho_S \langle \chi_B(0) U_{SB}^\dagger | \chi_j \rangle \\ &= \sum_j K_j \rho_S K_j^\dagger, \end{aligned}$$

where the Kraus operators describe the traced out effect of the Bath state evolution. The full Hamiltonian reads:

$$\dot{\rho}(t) = -\frac{i}{\hbar} [\mathcal{H}, \rho] + \sum_j \left(R_j \rho R_j^\dagger - \frac{1}{2} \rho R_j^\dagger R_j - \frac{1}{2} \rho R_j^\dagger R_j \right)$$

Usually, relaxation operators are of a simple form, describing the operator that induces the dissipative transition, multiplied by the square root of the corresponding rate. **The decay rates must be much smaller than the transition frequencies of the system.**

- **Pure dephasing** due to energy level fluctuations as we set out to show in Eq. (18) is associated

with the σ_z term

$$R = \sqrt{\frac{\Gamma_\varphi}{2}} \sigma_z.$$

which leads to relaxation terms

$$\begin{aligned} R\rho R^\dagger - \frac{1}{2}R^\dagger R - \frac{1}{2}\rho R^\dagger R \\ = \Gamma_\varphi \begin{pmatrix} 0 & -\rho_{01} \\ -\rho_{10} & 0 \end{pmatrix}. \end{aligned} \quad (19)$$

It recovers the decaying off diagonal dynamics, and that is good enough for me.

- **Exponential relaxation** from excited to ground state, is associated with $\sigma_- = |0\rangle\langle 1|$

$$R = \sqrt{\Gamma} \sigma_-$$

giving

$$\Gamma \begin{pmatrix} +\rho_{11} & -\frac{1}{2}\rho_{01} \\ -\frac{1}{2}\rho_{10} & -\rho_{11} \end{pmatrix}, \quad (20)$$

which results in non-trivial **off diagonal elements**, which is exactly 1/2 of the decay rate.

Combining the effect of diagonal terms in Eq. (19), (20) we define

$$\Gamma_2 = \Gamma_\varphi + \frac{\Gamma_1}{2}$$

TWO LEVEL SYSTEM EVOLUTION

To represent a qubit state, we use a Bloch sphere, and say that

$$|\psi\rangle = \begin{cases} \cos\left(\frac{\theta}{2}\right)|0\rangle + e^{i\phi}\sin\left(\frac{\theta}{2}\right)|1\rangle \\ \alpha|0\rangle + \beta|1\rangle \end{cases},$$

from which we can express

$$\begin{cases} \alpha = \cos\left(\frac{\theta}{2}\right) \\ \beta = e^{i\phi}\sin\left(\frac{\theta}{2}\right) \end{cases} \Rightarrow \begin{cases} \left|\frac{\beta}{\alpha}\right| = \tan\left(\frac{\theta}{2}\right) \\ e^{i\phi} = \frac{\beta}{\sqrt{1-\alpha^2}} \Rightarrow \phi = i \ln\left(\frac{\sqrt{1-\alpha^2}}{\beta}\right) \end{cases}$$

Now consider a system with two wells. The state is determined by the well being occupied - $|0\rangle$ for one well and $|1\rangle$ for the other. Energy in each well is E_0 .

Now if we allow tunnelling through the barrier, the Hamiltonian of the system changes, to accommodate for the possibility of state exchange

$$\mathcal{H} = \begin{pmatrix} E_0 & 0 \\ 0 & E_0 \end{pmatrix} \Rightarrow \mathcal{H} = \begin{pmatrix} E_0 & -\Delta/2 \\ -\Delta/2 & E_0 \end{pmatrix} \xrightarrow{\text{set energies to zero}} \mathcal{H} = \begin{pmatrix} 0 & -\Delta/2 \\ -\Delta/2 & 0 \end{pmatrix}$$

Solving the eigenvalue equation ($\det(\mathcal{H} - \lambda\mathbb{I}) \equiv 0$), we find

$$E = \pm\Delta/2 \quad |\Psi\rangle = \frac{|0\rangle \pm |1\rangle}{\sqrt{2}},$$

and these two superposition states are represented diagrammatically as shown in Fig.12.

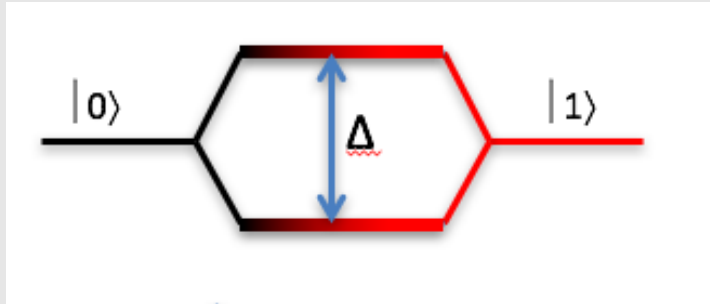


Figure 12: The original states have the same energy, but the superposition ones are split.

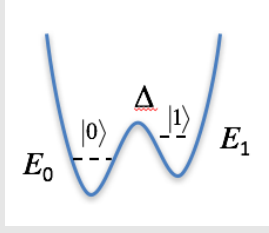


Figure 13: Adding an electric field, will mean that one well state is at a higher energy (higher potential energy).

Now we add an electric field to the quantum wells, see Fig.13. The energy shift from the field is $e\vec{E}\vec{d}$, where \vec{d} is the distance between the two wells. We have a two level system, and we define the zero energy to be halfway between them, making the Hamiltonian

$$\mathcal{H}_{\text{no tunneling}} = -\frac{\epsilon}{2}\sigma_z = \begin{pmatrix} -\epsilon/2 & 0 \\ 0 & \epsilon/2 \end{pmatrix}.$$

Now tunnelling + electric field gives us

$$\begin{aligned} \mathcal{H} &= \begin{pmatrix} -\epsilon/2 & 0 \\ 0 & \epsilon/2 \end{pmatrix} + \begin{pmatrix} 0 & -\Delta/2 \\ -\Delta/2 & 0 \end{pmatrix} = -\frac{\epsilon}{2}\sigma_z - \frac{\Delta}{2}\sigma_x \\ &= -\frac{\sqrt{\epsilon^2 + \Delta^2}}{2} \left(\frac{\epsilon}{\sqrt{\epsilon^2 + \Delta^2}}\sigma_z + \frac{\Delta}{\sqrt{\epsilon^2 + \Delta^2}}\sigma_x \right) \\ &= -\frac{\Delta E}{2} (\cos(\theta)\sigma_z + \sin(\theta)\sigma_x) \quad , \\ \Rightarrow \left\{ \begin{array}{l} \mathcal{H} = -\frac{\Delta E}{2} \begin{pmatrix} \cos(\theta) & \sin(\theta) \\ \sin(\theta) & -\cos(\theta) \end{pmatrix} \\ \Delta E = \sqrt{\epsilon^2 + \Delta^2} \\ \tan(\theta) = \frac{\Delta}{\epsilon} \end{array} \right. \end{aligned}$$

small θ = small mixing.. Finding eigenvalues and eigenvectors

$$E = \pm \frac{\Delta E}{2}, \quad |\psi\rangle_0 = \begin{pmatrix} \cos(\theta/2) \\ \sin(\theta/2) \end{pmatrix}, \quad |\psi\rangle_1 = \begin{pmatrix} \sin(\theta/2) \\ -\cos(\theta/2) \end{pmatrix}, \quad (21)$$

and we note that inside the Bloch Sphere, the eigenstates are now at an angle θ relative to the initial “north-south” eigenstates as seen in Fig.14

So we have gone from a purely potential system with $\mathcal{H} = -\epsilon/2\sigma_z$, and a purely kinetic system with $\mathcal{H} = -\Delta/2\sigma_x$, to a mixed one as shown in Fig.15.

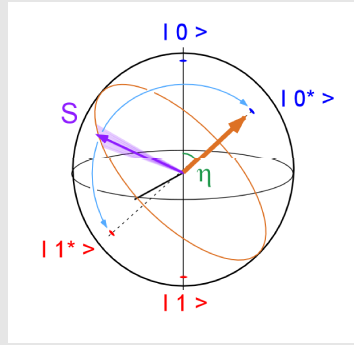


Figure 14: The drive Δ , tilts the eigenstates of the system. $\tan(\theta) = \frac{\Delta}{\epsilon}$

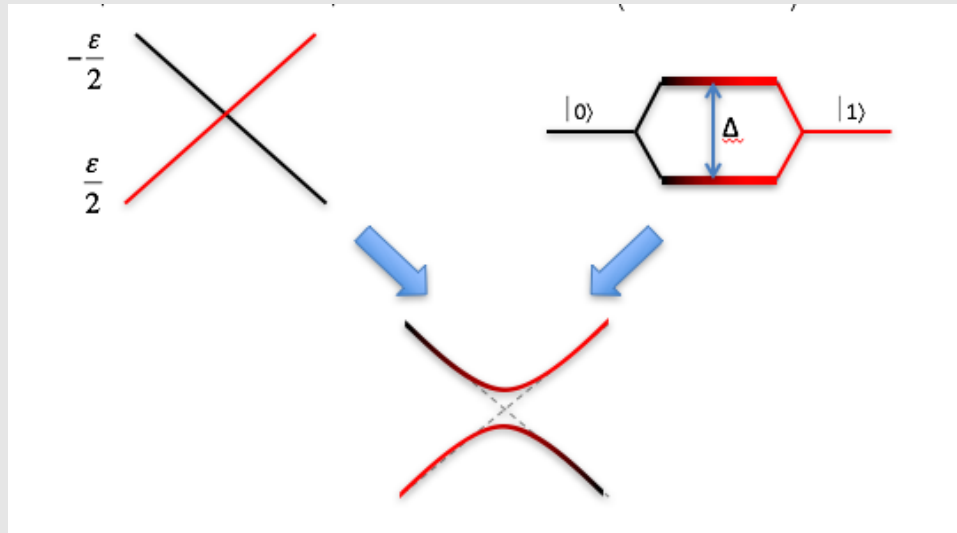


Figure 15: In the potential system, the energies of the eigenstates changed linearly with field. At the crossing point (no field), there is a degeneracy, where both wells are at the same potential. The kinetic tunnelling case we have also seen. Together they form a system whose eigenstates are split.

Considering the case with no bias $\epsilon = 0 \Rightarrow \Delta E = \Delta, \theta = \pi/2$:

$$\mathcal{H} = -\frac{\Delta}{2} \begin{pmatrix} 0 & 1 \\ 1 & 0 \end{pmatrix} = -\frac{\Delta}{2} \sigma_x.$$

Computing the unitary evolution of the state

$$\begin{aligned}
U &= \exp \left[\frac{-i\mathcal{H}t}{\hbar} \right] \\
&= \sum_k \frac{-i\Delta/2\sigma_x t}{k!} \\
&= \cos \left(\frac{\Delta}{2\hbar} t \right) \mathbb{I} + i \sin \left(\frac{\Delta}{2\hbar} t \right) \sigma_x = \begin{pmatrix} \cos \left(\frac{\Delta}{2\hbar} t \right) & i \sin \left(\frac{\Delta}{2\hbar} t \right) \\ i \sin \left(\frac{\Delta}{2\hbar} t \right) & \cos \left(\frac{\Delta}{2\hbar} t \right) \end{pmatrix},
\end{aligned}$$

so

$$U |0\rangle = \begin{pmatrix} \cos \left(\frac{\Delta}{2\hbar} t \right) \\ i \sin \left(\frac{\Delta}{2\hbar} t \right) \end{pmatrix},$$

so we can prepare any state perpendicular to the x-axis.

Thus no bias + tunneling \equiv bias + resonant field in RWA. In both cases, the interaction causes the same state evolution

CHAPTER 12 —

QUANTUM ELECTRODYNAMICS

FORMALISM

12.1 Superconductors

In superconductors CP carry charge. What happens is that the Fermi level splits into 2 bands that are $\pm\Delta$ above and below E_F , and each electron in the CP belongs to one of these bands.

Phase is quantised in a sc loop

$$\begin{aligned}\phi &= \phi_{\text{ext}} + 2\pi N \Leftrightarrow \Phi = \Phi_{\text{ext}} + \Phi_0 \\ (\Phi_0 &= \frac{\hbar}{2e}, \Phi/\Phi_0 = \phi/2\pi)\end{aligned}$$

12.2 Josephson junction

Now work with JJ. The states on the two sides of the JJ are $|\psi_0| e^{i\phi_1}$ and $|\psi_0| e^{i\phi_2}$. Solving the Schrodinger equation for the condensate state, when E=0

$$-\frac{\hbar^2}{2m} \frac{\partial^2}{\partial x^2} \psi + U\psi = 0 \Rightarrow \begin{cases} \psi = A_0 e^{-kx} + B_0 e^{+kx} \\ k = \frac{\sqrt{2mU}}{\hbar} \end{cases} \Rightarrow \begin{cases} \psi = A \cosh(kx) + B \sinh(kx) \\ k = \frac{\sqrt{2mU}}{\hbar} \end{cases}$$

Apply BC for JJ $\psi(a/2) = |\psi_0| e^{i\phi_2}$ and $\psi(-a/2) = |\psi_0| e^{i\phi_1}$ to find that

$$\begin{aligned}A &= \frac{|\psi_0|}{\cosh(ka/2)} \\ B &= \frac{|\psi_0|}{\sinh(ka/2)}.\end{aligned}$$

The super current is then

$$I = -\frac{i\hbar}{2m}(2e) \left[\psi^* \frac{\partial \psi}{\partial t} - \psi \frac{\partial \psi^*}{\partial t} \right] \equiv -\frac{2e\hbar}{m} \text{Im} \left[\psi^* \frac{\partial \psi}{\partial t} \right],$$

at $x = 0$ can be evaluated, as can the voltage and energy, which results in a phase dependence

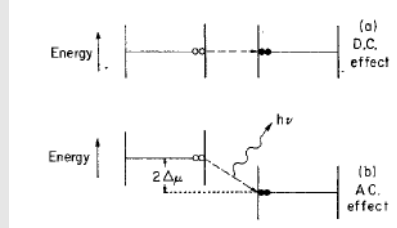
$$I = I_c \sin(\phi_2 - \phi_1); \quad \frac{d\phi}{dt} = \frac{2e}{\hbar} V \quad (22)$$

The phase across the JJ in a circuit is the phase induced by the external flux i.e.

$$\phi_1 + \phi_2 + \dots = \phi_{\text{ext}} = \frac{\Phi_{\text{ext}}}{\Phi_0} 2\pi, \quad (23)$$

$$\begin{cases} I = I_c \sin(\phi_2 - \phi_1) \equiv I_c \sin(\phi) \\ V = \dot{\Phi} \equiv \frac{\dot{\phi}}{2\pi} \Phi_0 \end{cases} \Rightarrow U = \begin{cases} \int_0^t IV dt = \int_0^t I_c \sin(\phi) \frac{\Phi_0}{2\pi} \frac{d\phi}{dt} dt \\ = \int_0^\phi E_J \sin(\phi) d\phi \\ = E_J(1 - \cos(\phi)), \quad E_J = \frac{\Phi_0 I_c}{2\pi}. \end{cases} \quad (24)$$

Increase $I \rightarrow$ Increase $\phi = \phi_2 - \phi_1$ to $\pi/2 \rightarrow$ Increase energy $U \rightarrow$ at some point, we reach critical current and highest energy - beyond this limit, we will generate voltage



Inductance is found by performing:

- Suppose a change in current, δ_I causes a change in phase $\delta_1\phi$:

$$I_0 + \delta_I = I_c \sin(\phi_0 + \delta_\phi) \Rightarrow \delta_I = I_c \cos(\phi_0) \delta_\phi.$$

- The voltage across the junction:

$$V = \frac{\dot{\phi}}{2\pi} \Phi_0 = \frac{\Phi_0}{2\pi} (\dot{\phi}_0 + \dot{\delta}_\phi) = \frac{\Phi_0}{2\pi} \frac{\dot{\delta}_I}{I_c \cos(\phi_0)}.$$

- Finally expressing the inductance

$$L = V / \frac{dI}{dt} = V / \dot{\delta}_I = \frac{\Phi_0}{2\pi} \frac{1}{I_c \cos(\phi_0)}.$$

$$L_J = \Phi/I = \frac{\Phi_0}{2\pi} \frac{1}{I_c} \frac{1}{\cos(\phi_0)}$$

The current is given by:

$$I_c R_n = \frac{\pi \Delta(T)}{2e} \tanh\left(\frac{\Delta(T)}{2k_b T}\right), \quad (25)$$

derived from BCS theory for a superconducting energy gap of $\Delta(T)$ and normal resistance R_n of the JJ.

Critical current I_c Taking the limit of $T \rightarrow 0$ we get

$$I_c R_n = \frac{\pi \Delta(0)}{2e} \quad (26)$$

Josephson Energy from JJ parameters Subbing in Eq. (26) into Eq. (24):

$$E_J = \frac{R_q}{R_n} \frac{\Delta(0)}{2}$$

$$R_n = 1.84 \text{ k}\Omega \text{ for } 100 \times 100 \text{ nm}^2$$

with $R_q = \frac{h}{(2e)^2}$. The larger the JJ, the lower the resistance of the junction and hence the bigger the Josephson energy.

JJ resistance increases by $\sim 10\%$ as one goes from room to cryogenic temperatures.

12.2.1 Inductance energy

Inductance energy derives from $\frac{\Phi_L^2}{2L} = \frac{\Phi_0^2}{(2\pi)^2 2L} (\phi_{\text{ext}} - \phi_J)^2 = E_L (\phi_{\text{ext}} - \phi_J)^2$

$$E_L = \frac{\Phi_0^2}{(2\pi)^2 2L}$$

$$L \propto R_n = 1.5 \text{ nH per } 100 \times 100 \text{ nm}^2$$

12.2.2 Summary of energies

Energy	Variable parameter	Energy ($N_{sq} = 10, N_{NbN} = 5$)
E_J	$\frac{R_q}{R_n} \frac{\Delta(0)}{2}$ $R_q = \frac{h}{(2e)^2} = 6.484 \text{ k}\Omega,$ $\Delta = 1.73 * (k_b \times 1.3 \text{ K}) = 3.1 \times 10^{-23},$ $R_n = 18.4 \text{ k}\Omega \text{ for } 100 \times 100 \text{ nm}^2$	77.5 GHz
E_C	$\frac{(2e)^2}{2C N_{sq}}$ $\varepsilon = 10, d = 2 \text{ nm},$ $A = 100 \times 100 \text{ nm}^2,$ $C = \frac{\varepsilon \varepsilon_0 A}{d} = 0.5 \text{ fF}$	17.4 GHz
E_L	$\frac{\Phi_0^2}{(2\pi)^2 2L N_{NbN}}$ $\Phi_0 = 2 \times -15 \text{ Wb},$ $L = 1.5 \text{ nH per NbN square}$	16.2 GHz

12.3 JJ Brief summary

Up to this point we have found from (Eq. 22)

$$I = I_c \sin(\phi_2 - \phi_1); \quad \frac{d\phi}{dt} = \frac{2e}{\hbar} V$$

So a constant voltage will result in an AC current across the JJ. The JJ itself will be modelled by

$$\begin{aligned} I(t) &= \text{JJ current} + \frac{d}{dt} [CV] + \frac{V}{R} \\ &= I_c \sin \varphi + \frac{\Phi_0}{2\pi} \left[C \frac{d^2 \varphi}{dt^2} + \frac{1}{R} \frac{d\varphi}{dt} \right] \end{aligned}$$

as shown in Fig. 61.

12.4 Shapiro steps

Now, let us irradiate the JJ with a frequency f_1 : This will drive a voltage

$$V = V_0 + V_1 \cos(2\pi f_1 t)$$

driving a phase change

$$\begin{aligned} \left| \frac{d\delta}{dt} \right| &= \frac{2eV_0}{\hbar} + \frac{2eV_1}{\hbar} \cos(2\pi f_1 t) \\ \Rightarrow \phi &= \phi_0 + \frac{2eV_0}{\hbar} t + \frac{2eV_1}{\hbar} \frac{1}{2\pi f_1} \sin(2\pi f_1 t) \\ &= \phi_0 + \frac{2eV_0}{\hbar} t + \alpha \sin(2\pi f_1 t) \end{aligned}$$

where due to the high frequency and finite V , $\alpha = \frac{2eV_1}{2\pi f_1} \ll 1$. This drives a current

$$\begin{aligned} I &= I_0 \sin \left(\phi_0 + \frac{2eV_0}{\hbar} t + \alpha \sin(2\pi f_1 t) \right) \\ &\approx I_0 \left[\sin \left(\phi_0 + \frac{2eV_0}{\hbar} t \right) + \alpha \sin(2\pi f_1 t) \cos \left(\phi_0 + \frac{2eV_0}{\hbar} t \right) \right]. \end{aligned}$$

Term by term:

- $\sin \left(\phi_0 + \frac{2eV_0}{\hbar} t \right)$ averages to 0.
- $\sin(2\pi f_1 t) \cos \left(\phi_0 + \frac{2eV_0}{\hbar} t \right)$ will only be non zero if the arguments of sin and cos are equal: $\int_0^T \sin(\beta t) \cos(\beta t) dt = \frac{1}{2} \int_0^T \sin(2\beta t) dt = \frac{1}{4\beta} [\cos(2\beta t)]_0^T \neq 0$ which apparently gives a non-zero average.

Therefore there is a set of frequencies

$$2\pi f_1 = \frac{2eV_0}{\hbar} n, n \in \mathbb{Z}$$

at which the current

$$I = \text{Some constant} \times \alpha \times I_0, \quad \alpha = \frac{2eV_1}{2\pi f_1}$$

takes on a finite value. These are the Shapiro steps.

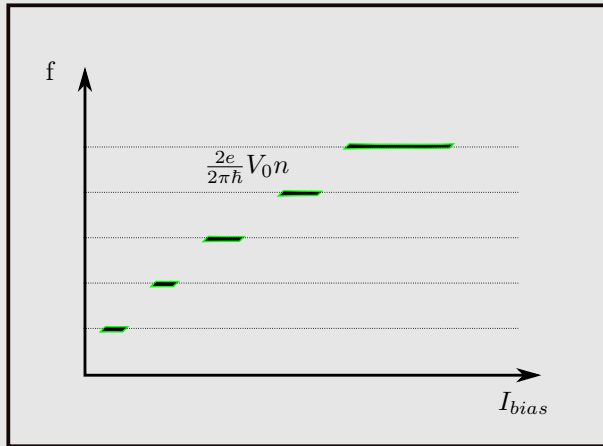


Figure 16: Shapiro steps 0 there is a non zero current at some frequencies for a given bias voltage V_0 .

12.5 Effective "ball" system

Now if we rewrite Subsec. 12.3

$$I = \textcolor{red}{I}_c \sin \varphi + \frac{\Phi_0}{2\pi} \left[\textcolor{green}{C} \frac{d^2 \varphi}{dt^2} + \frac{1}{R} \frac{d\varphi}{dt} \right]$$

in another form where we defined a characteristic time for the system

$$\tau = \frac{2\pi}{\Phi_0} I_c R t \quad \Rightarrow \quad \frac{d\tau}{dt} = \frac{2\pi}{\Phi_0} I_c R.$$

resulting in

$$\frac{I}{I_c} = \sin \delta + \beta_c \frac{d^2 \delta}{d\tau^2} + \frac{d\delta}{d\tau}$$

$$\left\{ \begin{array}{l} \beta_c = \frac{2\pi}{\Phi_0} I_c R^2 C \\ \frac{I_c}{\Phi_0} = \text{has units of inductance} \end{array} \right. \Rightarrow \beta_c = \frac{R^2 C}{L_J} = (\omega_p R C)^2 = Q^2 \quad \text{where } \omega_p = \frac{1}{\sqrt{L_J C}} = \text{plasma frequency}$$

where β_c is associated with the quality factor.

- $\beta_c \gg 1$ (underdamped), phase is very mobile and thus suffers from hysteresis
- $\beta_c \ll 1$ (overdamped), large energy dissipation.

This can be envisaged as a ball on a tilted washboard potential by integrating the effective force equation over δ

$$\underbrace{I - I_c \sin(\delta)}_{\text{non-linear restoring force}} = \underbrace{\frac{\Phi_0}{2\pi} C}_{\text{mass}} \underbrace{\frac{d^2 \delta}{dt^2}}_{\text{acceleration}} + \underbrace{\frac{\Phi_0}{2\pi} \frac{1}{R} \frac{d\delta}{dt}}_{\text{drag force}}$$

to get the potential landscape:

$$U(\delta) = I\delta - I_c \cos(\delta).$$

The potential is a washboard with 2 cases

- $I = 0$ and no current flows
- $I > I_c$ and there the “ δ ” particle is free to move, meaning that $\frac{d\delta}{dt} \neq 0$ and there is a finite voltage across the junction. **This is the JJ current exceeding the critical value and the JJ turning into normal state.**

12.6 SQUID to control E_J [22]

Inductance of a SQUID:

$$L_J(\Phi_{\text{ext}}) = V / \frac{dI}{dt} = \frac{\hbar}{4eI_c |\cos(\pi\Phi_{\text{ext}}/\Phi_0)|}. \quad (27)$$

Two JJ in a loop give a total current

$$I = I_{c1} \sin(\phi_1) + I_{c2} \sin(\phi_2),$$

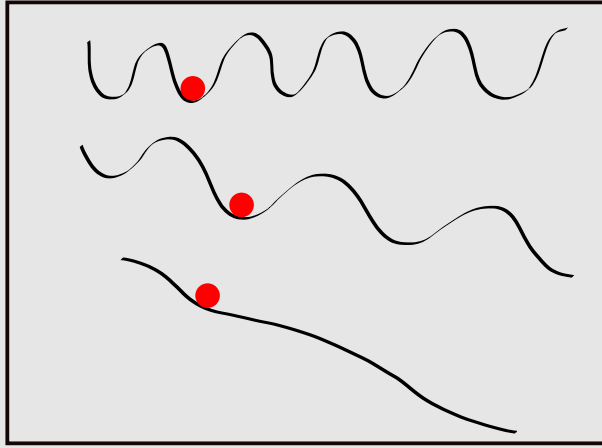


Figure 17: Phase exists on a washboard potential

which along with the phase quantisation condition Eq.(23) and symmetric JJs $I_{c1} = I_{c2} = I_c$ results in

$$\begin{aligned} I &= I_{cs}(\Phi_{\text{ext}}) \sin(\phi) \\ I_{cs} &= 2I_c |\cos(\pi\Phi_{\text{ext}}/\Phi_0)|, \\ \phi &= (\phi_1 + \phi_2)/2 \end{aligned}$$

which has a similar form to Eq.(22), but now the critical current I_{cs} is controlled by an external field. Taking the derivative

$$\frac{dI}{dt} = 2I_{cs}(\Phi_{\text{ext}}) \cos(\phi) \frac{d\phi}{dt},$$

and expressing the voltage using Eq.(22) and assuming $\cos(\phi) \approx 1$ for small excitations

$$V = \frac{\hbar}{2e} / \frac{d\phi}{dt} = \frac{\hbar}{4eI_{cs}} \frac{dI}{dt},$$

from which one finds the inductance ($\Phi = LI \rightarrow L = \frac{d\Phi}{dI} = \frac{d\Phi}{dt} / \frac{dI}{dt} = V / \frac{dI}{dt}$ for small excitations)

$$L_J(\Phi_{\text{ext}}) = V / \frac{dI}{dt} = \frac{\hbar}{4eI_c |\cos(\pi\Phi_{\text{ext}}/\Phi_0)|}.$$

Energy of two JJ forming a SQUID:

$$E_J = \sqrt{E_{J1}^2 + E_{J2}^2 + 2E_{J1}E_{J2} \cos\left(\frac{2e\Phi}{\hbar}\right)}$$

and a chain of SQUIDs has inductance

$$L = \frac{N\hbar^2}{4e^2 E_J}$$

Only valid for small currents not close to the critical current!

12.7 Building blocks for quantum circuits.

Quantum circuits are built from

- JJs, who posses an inductance L_J defined Eq.(27). The energy comes from the flux stored by the inductor

$$E_J(\Phi_{\text{ext}}) = \frac{\Phi_0}{2L_J(\Phi_{\text{ext}})}$$

- An inductor L with energy from the flux inside the inductor (coil)

$$E_L = \frac{\Phi^2}{2L}$$

- A capacitor with energy

$$E_c = \frac{Q^2}{2C}$$

12.7.1 Kinetic Inductance

This is the only inductance relevant for superconductors!

Drude model is the relationship between current and electric field due to the finite relaxation time (collision time, which is large in superconductors) of charge carriers τ , it takes some time for a change in voltage to accelerate the particle.

$$\begin{cases} m \langle v \rangle = qE\tau \\ j = nq \langle v \rangle \end{cases} \Rightarrow j = \left(\frac{nq^2\tau}{m} \right) E$$

Complex conductivity

$$\sigma(\omega) = \frac{ne^2\tau}{m(1-i\omega\tau)} = \frac{ne^2\tau}{m(1+\omega^2\tau^2)} - i \frac{ne^2\tau^2}{m(1+\omega^2\tau^2)}$$

We equate the kinetic energy of cooper pairs to the equivalent inductive energy ($(mv^2)(n_s l A) = \frac{1}{2} L_K I^2$), where l, A are the dimensions of the wire and n_s the cooper pair concentration, so that

$$L_K = \frac{ml}{2n_s e^2 A}.$$

Transforming conductivity to impedance $Z = \frac{L}{A} \frac{1}{\sigma}$:

$$Z = R + j\omega L_k.$$

For the most general discussion, we compare

Table 1

	Q and Φ	Mechanical	V and I
	$I = \dot{Q}$	$V = \dot{\Phi}$	
	$Q = CV$	$\Phi = LI$	
Kinetic	$\frac{Q^2}{2C}$ <i>Capacitor</i>	$\frac{p^2}{2m}$ $\frac{m\dot{x}^2}{2}$	<i>Inductor</i> $\frac{LI^2}{2} = \frac{LC^2\dot{V}^2}{2}$
Potential	$\frac{\Phi^2}{2L}$ <i>Inductor</i>	$\frac{kx^2}{2}$	$\frac{CV^2}{2}$ <i>Capacitor</i>
ω_0	$\frac{1}{\sqrt{LC}}$	$\sqrt{\frac{k}{m}}$	$\frac{1}{\sqrt{LC}}$
Energy	$\frac{Q^2}{2C} + \frac{1}{2}C\omega_0^2\Phi^2$	$\frac{p_m^2}{2m} + \frac{1}{2}m\omega_m^2x^2$ $\frac{m}{2}(\dot{x}^2 + \omega_0^2x^2)$	$\frac{LC^2}{2}(\dot{V}^2 + \omega_0V^2)$
Momentum	Q	p	$I = C\dot{V}$
Coordinate	Φ	x	V
Mass	C	m	LC^2
Stiffness	$\frac{1}{L}$	k	C
Solution	$\Phi = Ae^{i\omega_0 t} + Be^{-i\omega_0 t}$	$x = Ae^{i\omega_0 t} + Be^{-i\omega_0 t}$	$V = Ae^{i\omega_0 t} + Be^{-i\omega_0 t}$

We see that in either case, we are working with a harmonic oscillator system, with corresponding raising and lowering operators.

As a reminder, an equation with the form

$$\mathcal{H} = \frac{\hbar\omega_0}{2} \left(y^2 - \frac{2}{y^2} \right)$$

can be rewritten as

Table 2

	Q and Φ	Mechanical	V and I
Momentum	Q	p	$I = CV$
Coordinate	Φ	x	V
Mass	C	m	LC^2
Stiffness	$\frac{1}{L}$	k	C
Energy	$\frac{Q^2}{2C} + \frac{1}{2}C\omega_0^2\Phi^2$	$\frac{p_m^2}{2m} + \frac{1}{2}m\omega_m^2x^2$ $\frac{m}{2}(\dot{x}^2 + \omega_0^2x^2)$	$\frac{LC^2}{2}(\dot{V}^2 + \omega_0V^2)$
\mathcal{H}	$\frac{\hbar\omega_0}{2}\left(\frac{Q^2}{Q_0^2} + \frac{\Phi^2}{\Phi_0^2}\right)$ $\Phi_0 = \sqrt{\frac{\hbar\omega_0}{C}}, Q_0 = \sqrt{\frac{\hbar}{C\omega_0}}$	$\frac{\hbar\omega_0}{2}\left(\frac{\hat{p}^2}{p_0^2} + \frac{\hat{x}^2}{x_0^2}\right)$ $x_0 = \sqrt{\frac{\hbar}{m\omega_0}}, p_0 = \frac{\hbar}{x_0}$	$\frac{\hbar\omega_0}{2}\left(\frac{\hat{I}^2}{I_0^2} + \frac{\hat{V}^2}{V_0^2}\right)$ $V_0 = \sqrt{\frac{\hbar\omega_0}{C}}, I_0 = \sqrt{\frac{\hbar\omega_0}{L}}$
	$[\hat{\Phi}, \hat{Q}] = i\hbar$ since Φ and Q are exactly x and p	$[\hat{x}, \hat{p}] = i\hbar$	$[\hat{\Phi}, \hat{Q}] = [CV, LI] = i\hbar$ so $[\hat{V}, \hat{I}] = \frac{i\hbar}{LC}$
	$\hat{\Phi}$	\hat{x}	\hat{V}
	$\hat{Q} = -i\hbar\frac{d}{d\Phi}$	$\hat{p} = -i\hbar\frac{d}{dx}$	$\hat{I} = -i\frac{\hbar}{LC}\frac{d}{dV}$
	$a^\dagger = \sqrt{\frac{C\omega_0}{2\hbar}}\left(\hat{\Phi} - i\frac{\hat{Q}}{C\omega_0}\right)$	$a^\dagger = \frac{1}{\sqrt{2}}\left(\frac{\hat{x}}{x_0} - i\frac{\hat{p}}{p_0}\right)$	$a^\dagger = \frac{1}{\sqrt{2}}\left(\frac{\hat{V}}{V_0} - i\frac{\hat{I}}{I_0}\right)$

$$\mathcal{H} = \hbar\omega_0 \left(a^\dagger a + \frac{1}{2} \right) = \hbar\omega_0 \left(\hat{N} + \frac{1}{2} \right)$$

with eigenstates and eigenenergies

$$|\Psi\rangle_n = |n\rangle \quad E_n = \hbar\omega_0 \left(n + \frac{1}{2} \right).$$

The raising and lowering operators act in the following way on the eigenstates

$$\begin{cases} a|n\rangle = \sqrt{n}|n-1\rangle \\ a^\dagger|n\rangle = \sqrt{n+1}|n+1\rangle \end{cases} \Rightarrow \hat{N}|n\rangle = a^\dagger\sqrt{n}|n-1\rangle = \sqrt{n^2}|n\rangle = n|n\rangle,$$

and the matrix form, evaluated by finding the matrix coefficients $c_{ij} = \langle i|\hat{C}|j\rangle$

$$\hat{a} = \begin{pmatrix} 0 & \sqrt{1} & 0 & 0 \\ 0 & 0 & \sqrt{2} & 0 \\ 0 & 0 & 0 & \sqrt{3} \\ 0 & 0 & 0 & \ddots \end{pmatrix} \quad a^\dagger = \begin{pmatrix} 0 & 0 & 0 & 0 \\ \sqrt{0+1} & 0 & 0 & 0 \\ 0 & \sqrt{1+1} & 0 & 0 \\ 0 & 0 & \sqrt{2+1} & \ddots \end{pmatrix} \quad \hat{N} = \begin{pmatrix} 0 & 0 & 0 & 0 \\ 0 & 1 & 0 & 0 \\ 0 & 0 & 2 & 0 \\ 0 & 0 & 0 & \ddots \end{pmatrix}$$

For the Harmonic oscillator which the system replicates, the energy levels are evenly spaced, making it impossible to address individual states. But by replacing the inductor with a JJ

$$E_L = \frac{\Phi^2}{2L} \longrightarrow U = -E_J \cos(\phi),$$

changing the quadratic to a cosine potential.

CHARGE BASIS

The charge basis is used, when the energy is mostly capacitive.

- It is not continuous wavefunctions, but raising and lowering operators and discrete charge states $|0\rangle, |1\rangle, |2\rangle, |3\rangle \dots$;
- The operators are defined as

$$\hat{N} |n\rangle = n |n\rangle \quad e^{\pm i\phi} = \sum_n |n \pm 1\rangle \langle n| \quad [\phi, \hat{N}] = \frac{2\pi}{\hbar} [\Phi, Q] \frac{1}{2e} = i$$

n , is the number of Cooper pairs that have tunneled to an island via the Josephson junction.

13.1 Prooving the phase raising effect

Let us understand, where the phase operator definition

$$e^{\pm i\phi} = \sum_n |n \pm 1\rangle \langle n|,$$

is coming from.

1. Looking at the commutation relation

$$\begin{aligned} [\hat{N}, e^{\pm i\hat{\phi}}] &= \left[\hat{N}, \sum_{\alpha=0}^{\infty} \frac{(\pm i\hat{\phi})^\alpha}{\alpha!} \right] \\ &= \sum_{\alpha=0}^{\infty} (\pm i)^\alpha \frac{[\hat{N}, \hat{\phi}^\alpha]}{\alpha!} \quad [\hat{N}, \hat{\phi}] = -i, [A, BC] = B[A, C] + [A, B]C \\ &= \sum_{\alpha=0}^{\infty} (\pm i)^\alpha \frac{-\alpha i \hat{\phi}^{\alpha-1}}{\alpha!} \\ &= \pm \sum_{\alpha=1}^{\infty} i^{\alpha-1} \frac{(\pm \hat{\phi})^{\alpha-1}}{(\alpha-1)!} \\ &= \pm e^{\pm i\hat{\phi}} \end{aligned}$$

2. Next, if we evaluate

$$\begin{aligned} \hat{N} \left[e^{\pm i\hat{\phi}} |n\rangle \right] &= \left[\pm e^{\pm i\hat{\phi}} + e^{\pm i\hat{\phi}} \hat{N} \right] |n\rangle \\ &= (n \pm 1) \left[e^{\pm i\hat{\phi}} |n\rangle \right] \end{aligned}$$

3. So in effect, what we can say is that the action of the phase operator increments the n number like a ladder operator:

$$\begin{aligned} e^{\pm i\hat{\phi}} |n\rangle &= C |n \pm 1\rangle \quad (\text{since } e^{\pm i\hat{\phi}} \text{ is unitary}) \\ &= |n \pm 1\rangle \end{aligned}$$

4.

So therefore, we can write the phase operator in the following form

$$\begin{aligned} e^{\pm i\hat{\phi}} &= \sum_n |n \pm 1\rangle \langle n| \\ \hat{N} &= \sum_n n |n\rangle \langle n|. \end{aligned}$$

PHASE BASIS

The phase basis is used, when the energy is mostly from the JJ, such as an RF-SQUID

- We work with wavefunction $\psi(\phi)$ in phase-space;
- For the operators we take

$$\hat{\phi} \quad \hat{N} = -i \frac{d}{d\phi} \quad [\phi, N] = \frac{2\pi}{\frac{\hbar}{2e}} [\Phi, Q] \frac{1}{2e} = i$$

The Cooper pair box Hamiltonian will read

$$\mathcal{H} = E_c \left(-i \frac{d}{d\phi} - n_g \right)^2 - E_J \cos(\phi).$$

TWO LEVEL SYSTEM

- Cause dissipation and decoherence in qubits with JJ.
- Can be an electron or ion with two potential wells and tunneling between them.
- Phase difference across the junction will couple via the electric field across the junction:

$$\varepsilon = \frac{\dot{\phi}}{d},$$

where d is the thickness of the JJ.

- Activated when the frequency across the JJ matches their energy separation:

$$\hbar\omega_J$$

and after which Rabi oscillations can occur. The rate of rabi oscillation (Ω_R) depends on the strength of the coupling.

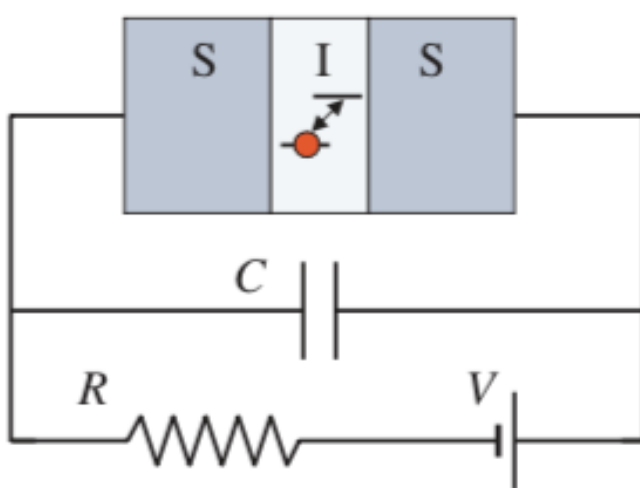


Figure 18: Setup

CHAPTER 16

SINGLE COOPER PAIR BOX SYSTEM

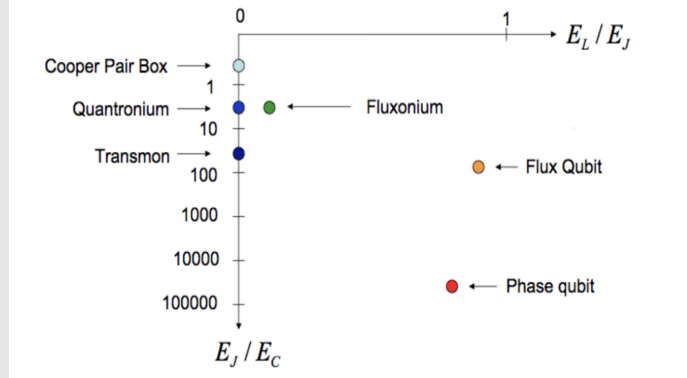


Figure 19: General overview of energy parameters

- Starting with Fig. 20 and remembering Faraday's law ($V = -\dot{\Phi}$), we read the **charging kinetic part**, that comes as a result of the time-varying flux on the cooper pair island.

$$T = \frac{C_g}{2} \dot{\Phi}_J^2 + \frac{C_J}{2} \dot{\Phi}_J^2 = \frac{C_\Sigma}{2} \dot{\Phi}_J^2.$$

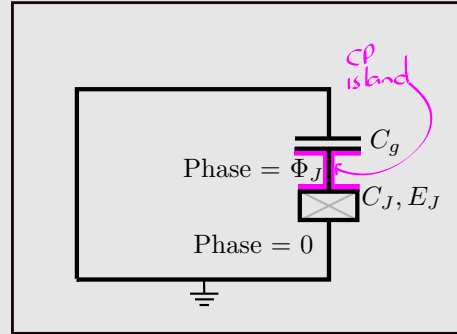


Figure 20: The Cooper pairs are trapped on an island between a gated capacitor and a Josephson junction.

- The potential energy part** comes from the JJs and the energy of the gate voltage acting on the induced charge on the capacitor.

$$\begin{cases} E_J = 1 - E_J \cos\left(\frac{2\pi}{\Phi_0} \Phi_J\right) \\ E_{\text{gate}} = V_g \times Q_g \\ bQ_g = C_g \times -\dot{\Phi}_J b \end{cases} \rightarrow U = -E_J \cos\left(\frac{2\pi}{\Phi_0} \Phi_J\right) - V_g C_g \dot{\Phi}_J.$$

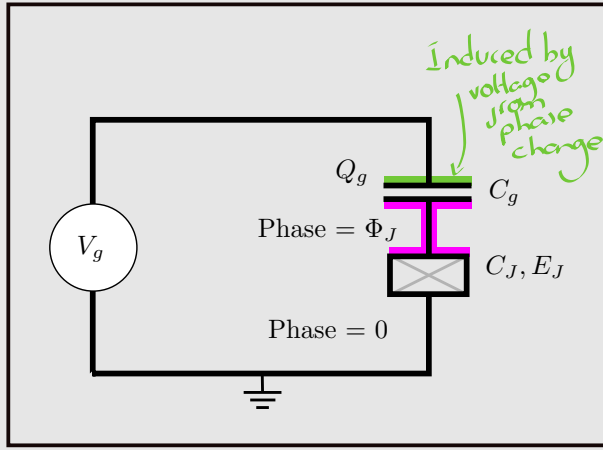


Figure 21: Addition of bias voltage

3. The full **Lagrangian** now reads

$$\mathcal{L} = T - U = \frac{C_{\Sigma}}{2} \dot{\Phi}_J^2 + E_J \cos\left(\frac{2\pi}{\Phi_0} \Phi_J\right) + V_g C_g \dot{\Phi}_J.$$

4. The **conjugate momentum**, which gives useful set of generalised coordinates to work with,

$$Q_J = \frac{d\mathcal{L}}{d\dot{\Phi}_J} = C_{\Sigma} \dot{\Phi}_J + V_g C_g,$$

turns out to be the **induced charge on the capacitor due to the JJ voltage offset by the charge induced by the gate voltage V_g** .

5. So we arrive at the following set of variables

$$\mathbf{x} \leftrightarrow \Phi \leftrightarrow \phi \text{ (position/flux)} \quad \mathbf{p} \leftrightarrow \mathbf{Q} \leftrightarrow \mathbf{N} \text{ (momentum/electrons)}$$

with the commutation relations:

$$\begin{aligned} [\mathbf{x}, \mathbf{p}] &= i\hbar & [\Phi, \mathbf{Q}] &= i\hbar & [\phi, \mathbf{N}] &= \frac{2\pi}{\hbar} [\Phi, \mathbf{Q}] \frac{1}{2e} = i \\ \hat{\mathbf{p}} &= -i\hbar \frac{\partial}{\partial \mathbf{x}} & \hat{\mathbf{Q}} &= -i\hbar \frac{\partial}{\partial \Phi} & \hat{\mathbf{N}} &= -i \frac{\partial}{\partial \phi} \end{aligned}$$

6.

The Hamiltonian is then:

$$\begin{aligned}
\mathcal{H} &= Q_J \dot{\Phi}_J - \mathcal{L} \\
&= \frac{(Q_J - C_g V_g)^2}{2C_\Sigma} - E_J \cos\left(\frac{2\pi}{\Phi_0} \Phi_J\right) \\
&= 4\mathbf{E}_C \left(\hat{\mathbf{N}} - \mathbf{N}_{\text{ext}} \right)^2 - \mathbf{E}_J \cos(\phi) \quad E_c = \frac{e^2}{2C_\Sigma}
\end{aligned}$$

We will call $N_{\text{ext}} = \frac{C_g V_g}{2e}$ the effective offset charge and $C_\Sigma = C_g + C_J$.

16.1 Adding a parallel JJ

A parallel JJ will allow one to tune the energy of the system by varying the biasing magnetic field.

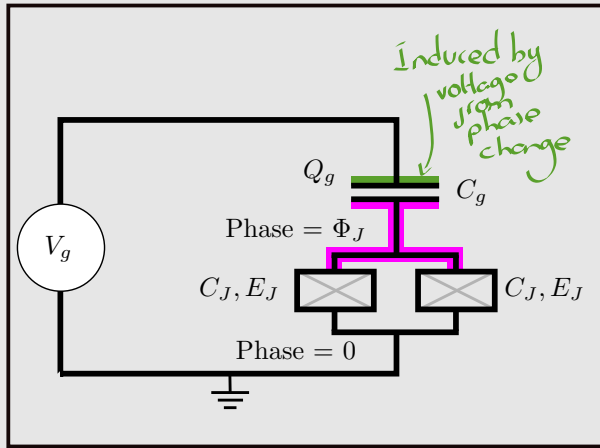


Figure 22: Adding a second JJ will allow one to control the effective energy E_J and thus the energy of the system.

- The two currents through the JJ will give a total current

$$I = I_{c1} \sin(\phi_1) + I_{c2} \sin(\phi_2),$$

- The phase quantisation ($\phi_1 - \phi_2 = \phi_{\text{ext}} + 2\pi m, m \in \mathbb{Z}$) and symmetric JJs ($I_{c1} = I_{c2} = I_{c0}$) results in

$$\begin{aligned}
I &= 2I_{c0} \sin\left(\frac{\phi_1 + \phi_2}{2}\right) \cos\left(\frac{\phi_1 - \phi_2}{2}\right) \\
&= 2I_{c0} \cos\left(2\pi \frac{\Phi_{\text{ext}}}{2\Phi_0}\right) \sin\left(\frac{\phi_1 + \phi_2}{2}\right)
\end{aligned}$$

In effect, the two JJ acts as a single JJ with current

$$I = \textcolor{teal}{I}_c \sin(\phi)$$

where the critical current, I_c is a magnetic-field-controlled parameter.

$$I_c(\Phi_{\text{ext}}) = 2I_{c0} |\cos(\pi\Phi_{\text{ext}}/\Phi_0)| \quad \phi = (\phi_1 + \phi_2)/2$$

- The potential energy $U(\Phi_{\text{ext}})$ is now a field-controlled parameter:

$$\begin{cases} I = \textcolor{teal}{I}_c(\Phi_{\text{ext}}) \sin(\phi) \\ V = \dot{\Phi} \equiv \frac{\dot{\phi}}{2\pi} \Phi_0 \end{cases} \Rightarrow U = \begin{cases} \int_0^t IV dt = \int_0^t \textcolor{teal}{I}_c(\Phi_{\text{ext}}) \sin(\phi) \frac{\Phi_0}{2\pi} \frac{d\phi}{dt} dt \\ = \int_0^\phi E_J \sin(\phi) d\phi \\ = \textcolor{red}{E}_J(1 - \cos(\phi)) \quad \textcolor{red}{E}_J = \frac{\Phi_0 I_{c0}}{2\pi} \times 2|\cos(\pi\Phi_{\text{ext}}/\Phi_0)|. \end{cases}$$

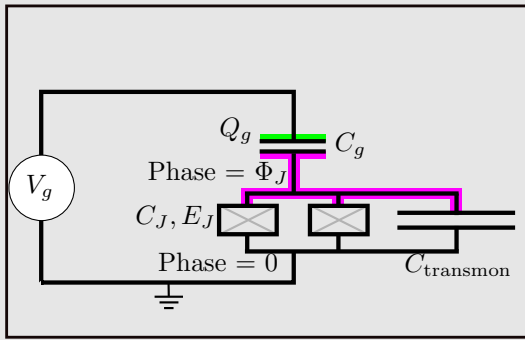
Thus the Josephson energy from the JJ elements acquires an additional factor which can now be controlled:

$$E_J = \textcolor{teal}{E}_{J0} \times 2|\cos(\pi\Phi_{\text{ext}}/\Phi_0)|$$

16.2 Transmon

A transmon extends the cooper pair box, by boosting the ratio $\frac{E_J}{E_C}$. This is done by decreasing the charging energy $E_c = \frac{e^2}{2C_\Sigma}$ by introducing a large shunt capacitance in parallel to the JJs.

$$C_\Sigma = \textcolor{orange}{C}_{\text{transmon}} + C_g + C_J.$$

Figure 23: Transmon suppresses E_C with a large shunt capacitance.

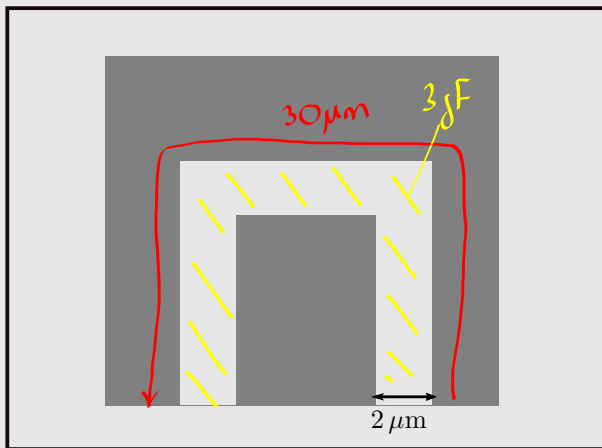
Summarising up to now:

$$\begin{aligned} \mathcal{H} &= 4E_C \left(\hat{N} - N_{\text{ext}} \right)^2 - E_J(\Phi_{\text{ext}}) \cos(\phi) \\ E_c &= \frac{e^2}{2C_\Sigma} \\ N_{\text{ext}} &= \frac{C_g V_g}{2e} \quad \text{Induced charge from the gate} \\ C_\Sigma &= C_{\text{transmon}} + C_g + C_J \\ E_J(\Phi_{\text{ext}}) &= E_{J0} \times 2|\cos(\pi\Phi_{\text{ext}}/\Phi_0)| \quad \text{controlled by the applied external flux.} \end{aligned} \tag{28}$$

16.2.1 Capacitance through parallel structures

As stated in Sec. 2.6, each $10 \mu\text{m}$ of parallel structures adds on 1 fF of capacitance (10^{-10} F/m).

$$C_g \text{ or } C_{\text{transmon}} = 1 \text{ fF} \times \text{per } 10\mu\text{m of interface.}$$



16.2.2 Capacitances from JJ

- The JJ (see below) act like capacitors due to the Al_0x oxide layer between them:

$$C_J = \frac{\varepsilon \varepsilon_0 A_{JJ}}{d}$$

where A_{JJ} is the contact area of the JJ, $d = 2 \text{ nm}$, $\varepsilon = 10$.

This contribution will be relatively small for the Transmon.

16.3 The critical current and E_{J0}

$$I_c R_n = \frac{\pi \Delta(T)}{2e} \tanh\left(\frac{\Delta(T)}{2k_b T}\right)$$

can derived from BCS theory (see Eq.(25)) for a superconducting energy gap of $\Delta(T)$ and normal resistance R_n of the JJ, which in the limit $T \rightarrow 0$ read $I_c R_n = \frac{\pi \Delta(0)}{2e}$ so that

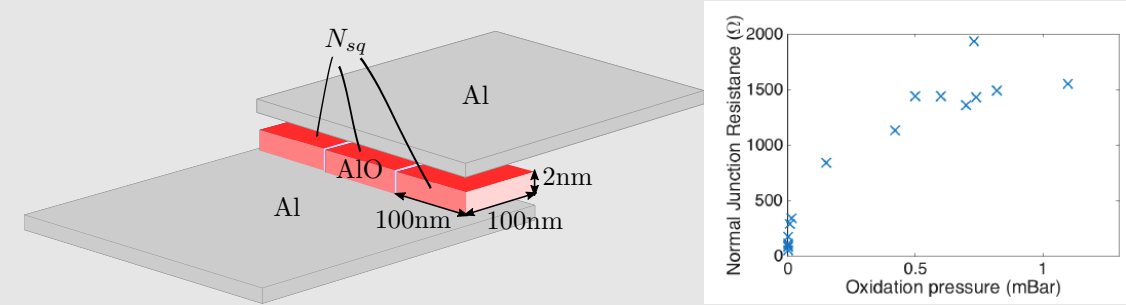
$$E_{J0} = \Phi_0 I_c \frac{1}{2\pi} = \frac{\hbar}{2e} \frac{\pi \Delta(0)}{2e R_n} \frac{1}{2\pi} \equiv \frac{R_q}{R_\square / N_{sq}} \frac{\Delta(0)}{2}$$

where

- $R_q = \frac{\hbar}{(2e)^2}$;
- $R_n = R_\square / N_{sq}$ is the resistance of the JJ oxide layer. The more $100 \times 100 \text{ nm}^2$ squares (N_{sq}), the lower the resistance.

$$R_\square = 3.57 \text{ k}\Omega (1.84 \text{ k}\Omega before) \text{ for } 100 \times 100 \text{ nm}^2.$$

At room temperature, the resistances are 10% lower than at cryogenic temperatures.



- BCS theory says that at zero temperature, there is a universal value

$$\Delta(0) = 1.73 \times k_b \times T_c,$$

that depends on the critical temperature of the metal. For aluminium it is 1.3 K.

16.4 Quantising the Hamiltonian

16.4.1 Charge energy dominates, $E_C/E_J \gg 1$

If charge is the important variable, then we shall work with the charge basis $\{N\}$. We use the number of phase operators derived in Sec. 13.

$$\begin{aligned} e^{\pm i\hat{\phi}} &= \sum_n |n \pm 1\rangle \langle n| \\ \hat{N} &= \sum_n n |n\rangle \langle n|. \end{aligned}$$

and exponentiating \cos , Eq.(28) becomes

$$\begin{aligned} \mathcal{H} &= 4E_C (\hat{N} - N_{\text{ext}})^2 - E_J \cos(\hat{\phi}) \\ &= 4E_C (\hat{N} - N_{\text{ext}})^2 - E_J \frac{1}{2} (e^{+i\hat{\phi}} + e^{-i\hat{\phi}}) \\ &= \sum_n \left[4E_C(n - N_{\text{ext}})^2 |n\rangle \langle n| - \frac{E_J}{2} \left(|n+1\rangle \langle n| + |n-1\rangle \langle n| \right) \right] \end{aligned}.$$

which takes on the matrix form:

$$\begin{pmatrix} 4E_C(-2 - N_{\text{ext}})^2 & -E_J/2 & 0 & 0 & 0 \\ -E_J/2 & 4E_C(-1 - N_{\text{ext}})^2 & -E_J/2 & 0 & 0 \\ 0 & -E_J/2 & 4E_C(N_{\text{ext}})^2 & -E_J/2 & 0 \\ 0 & 0 & -E_J/2 & 4E_C(1 - N_{\text{ext}})^2 & -E_J/2 \\ 0 & 0 & 0 & -E_J/2 & 4E_C(2 - N_{\text{ext}})^2 \end{pmatrix}$$

In Fig. 24 we demonstrate the energy spectrum and contributions of the various charge states ($|i\rangle$) to the ground state Ψ_g :

$$|\Psi_g\rangle = \sum_i^{\text{charge states}} \alpha_i |i\rangle.$$

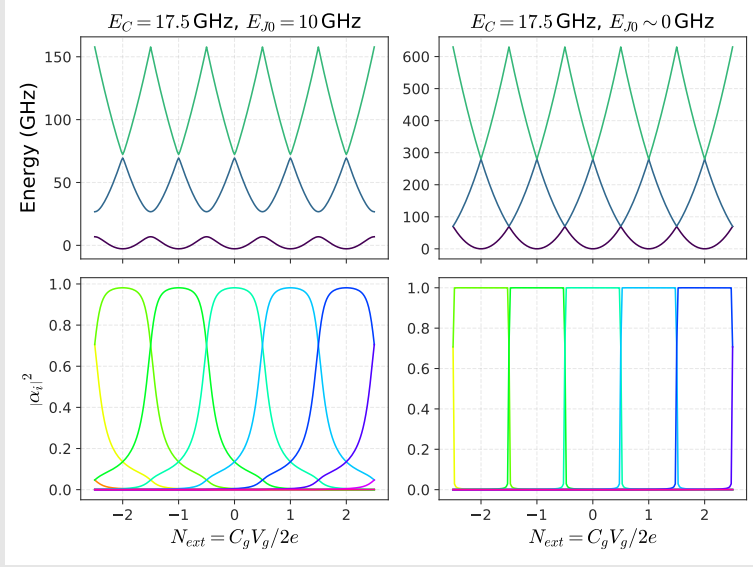


Figure 24: Plot of energies and ground-eigenstate contributions - taken at $\Phi_{\text{ext}} = 0$

The stronger the coupling (E_{J0}) the greater the splitting at the degeneracy points ($N_{\text{ext}} = \frac{2n+1}{2}, n \in \mathbb{Z}$).

Furthermore, we can run the simulation at a fixed gate charge ($N_{\text{ext}} = 0$) but varying external flux (Φ_{ext}) (as done in an experiment in which we sweep the field) - Fig. 25.

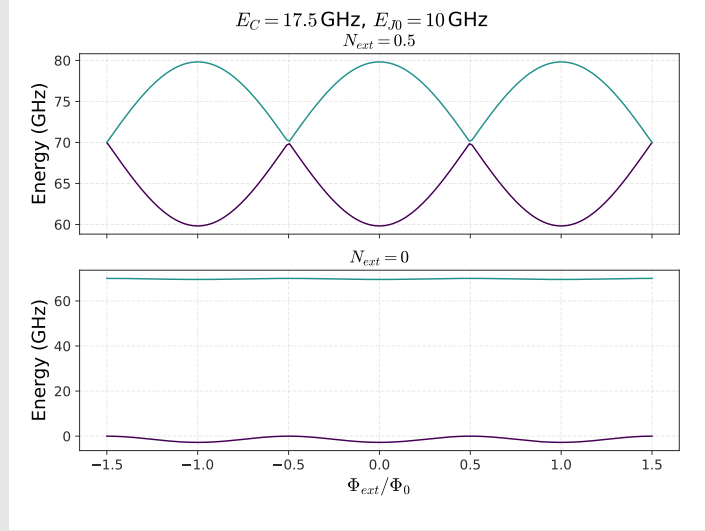


Figure 25: Fixed charge but varied flux (what we would typically see experimentally).

16.5 Deriving energy from geometry

In Fig. 24 and Fig. 25 we hard-coded in the charging energy ($E_C = 70$ GHz) and Josephson energy ($E_{J0} = 10$ GHz), but from Eq. 28 these parameters are determined by the geometry of the qubit depicted in Fig. 26.

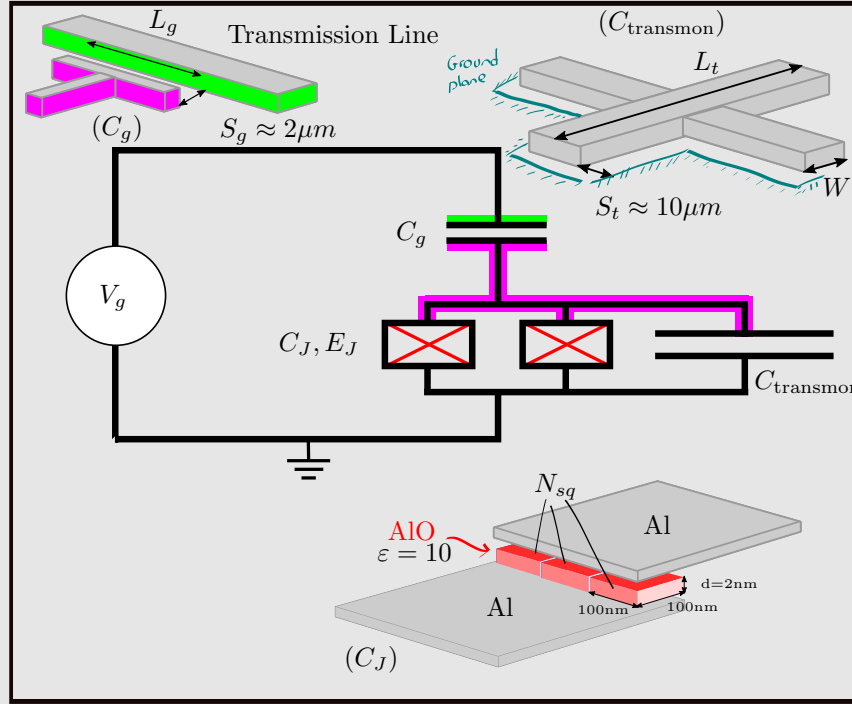


Figure 26: Energy defined by geometry of transmon

Reading off the diagram

$$\left\{ \begin{array}{l} E_c = \frac{e^2}{2C_\Sigma} \\ C_\Sigma = C_{\text{transmon}} + C_g + C_J \\ C_g = L_g \times 10^{-10} \\ C_{\text{transmon}} = 4 \times (L_t - 2S_{\text{transmon}}) \times 10^{-10} \\ C_J = \frac{\varepsilon \varepsilon_0 N_{sq} \times A_{100 \times 100 nm^2}}{d} \quad \text{where } d = 2 \text{ nm}, \varepsilon = 10 \\ E_{J0} = \frac{R_q}{R_\square/N_{sq}} \frac{\Delta(0)}{2} \\ R_\square = 3.57 \text{ k}\Omega (1.84 \text{ k}\Omega \text{ before}) \text{ for } 100 \times 100 \text{ nm}^2 \quad (1.5 \text{ k}\Omega \text{ at room temperature}) \\ \Delta(0) = 1.73 \times k_b \times T_c \quad \text{For aluminium } T_c \text{ is 1.3 K.} \end{array} \right.$$

Figure 27 shows the energy and transition spectrum for typical experimental geometry values.

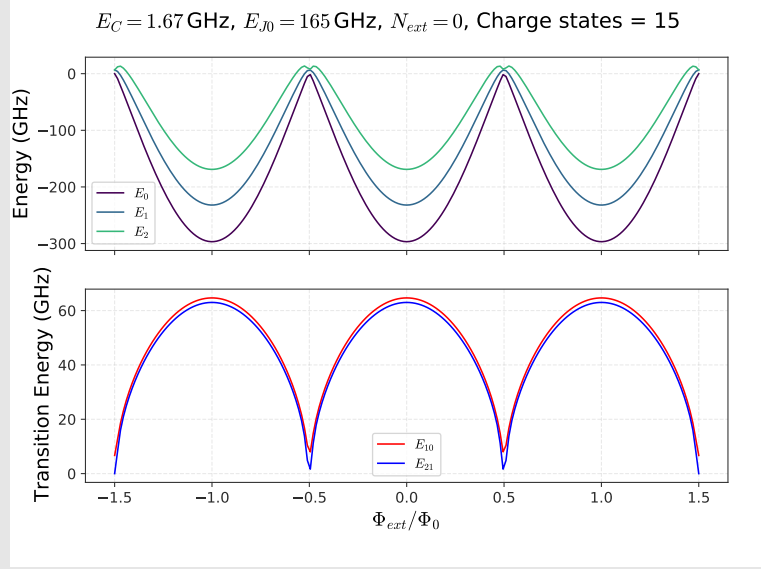


Figure 27: Parameters used: $L_g = 15 \mu m$, $L_t = 150 \mu m$, $2S_{transmon} = 10 \mu m$, $N_{sq} = 2$, $d = 2 \text{ nm}$, $\varepsilon = 10$.

16.5.1 Effect of N_{ext} is negligible in transmon

The ratio $E_C/E_{J0} \ll 0$ due to the shunting capacitance that suppresses the charging energy, meaning that charge will not strongly affect the energy spectrum. In Fig. 24 we can see much flatter (with respect to N_{ext}) energies when E_{J0} is much great than E_C .

This can be confirmed, by varying N_{ext} in Fig. 28.

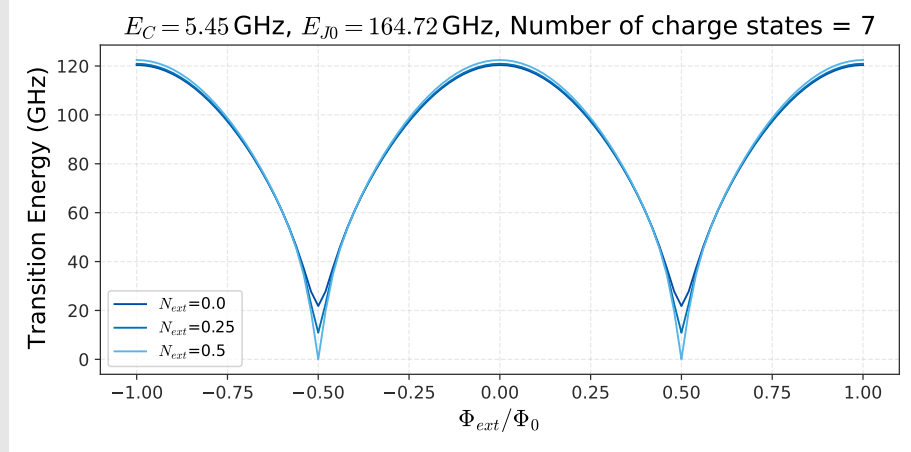


Figure 28: Sweeping the gate-induced charge, $N_{ext} = \frac{V_q C_g}{2e}$ has little effect on the energy of the system, since any variations are suppressed by the big shunting capacitance.

16.5.2 Using sufficient number of charge states for simulation

It is always best to utilise as many charge states for a simulation - convergence occurs as in Fig. 29.

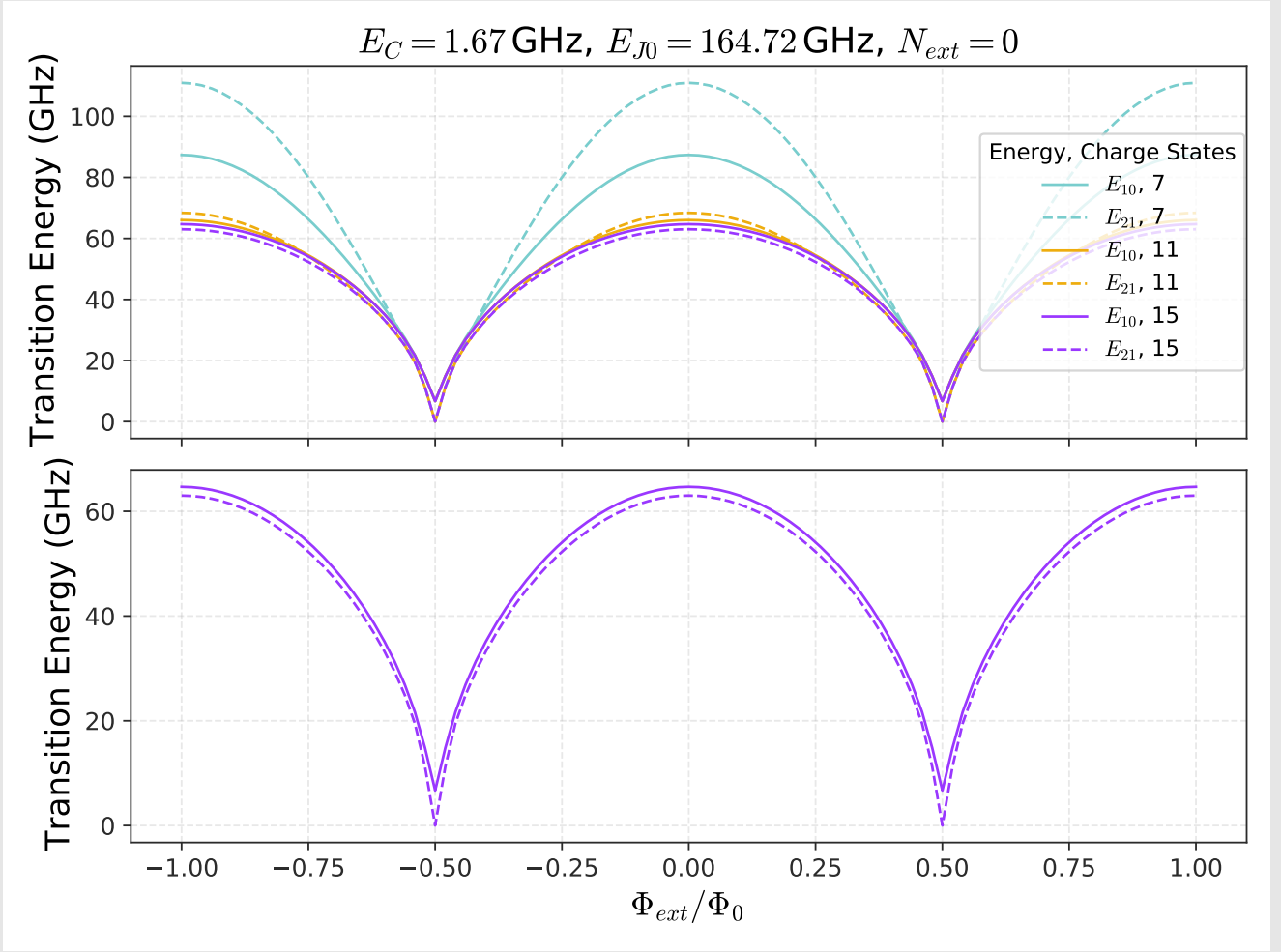


Figure 29: Including more charge states in the simulation results in a more accurate simulation - at some point the energies stop changing, at which point the simulation is good enough.

16.5.3 Maintaining anharmonicity

The robustness to charge noise, that is always present in electrical systems, demonstrated in Ch. 16.5.1 is countered by the vanishing assymetry between the transitions

$$\alpha = \frac{E_{21} - E_{10}}{E_{10}}.$$

Increasing E_J/E_C will lead to the domination of $\cos(\hat{\phi})$ in $E_C(\hat{N} - N_{ext})^2 - E_J \cos(\hat{\phi})$. The state of the system can be viewed as a particle in a periodic potential, becoming exceedingly localised in the potential

minima. [Insert derivation from Bader](#).

Just compare the anharmonicity for different values of E_C in Fig. 30.

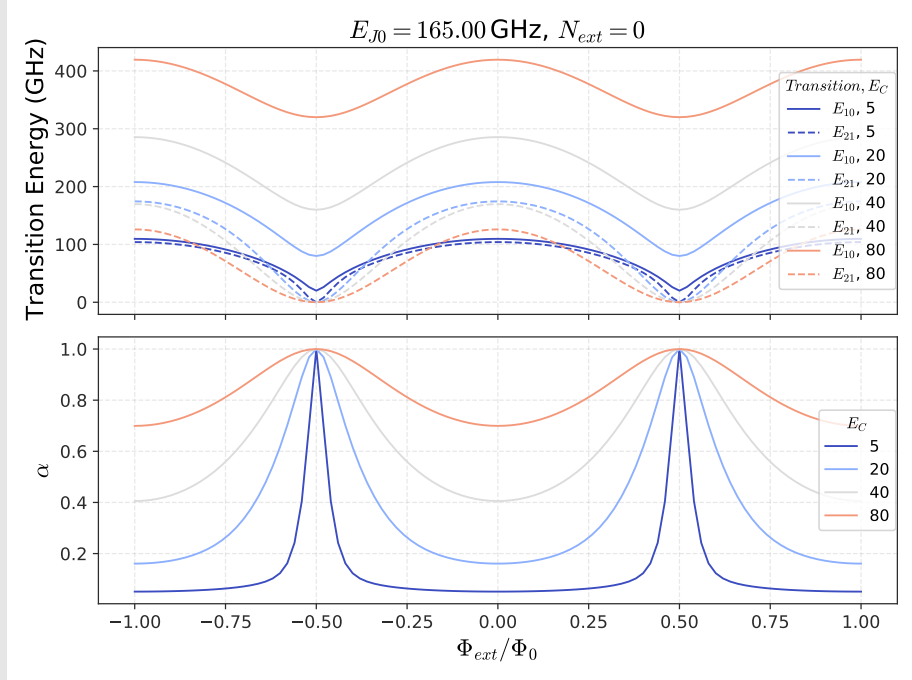


Figure 30: Anharmonicity vanishes when $E_C/E_{J0} \ll 1$

16.6 Charge dispersion

The transmon must be robust against charge variations (maximise E_J/E_C) so that charge variations in the circuit do not affect the energy levels. [Bader derivation](#) goes through how deep decoupled states in the well it is best to assume that the energy levels of individual wells are known, but coupling between these “wells” perturbs the initial energies.

The wavefunction is suppressed by the potential barrier. The higher the relative size of the barrier (high E_J/E_C) the higher the decoupling and the less

16.7 Summary for transmon

The addition of a shunt capacitance, $C_{transmon}$, reduces E_C - energy associated with the capacitance circuit elements, which has two counter-opposing effects that are demonstrated in Fig. 32

- Robustness of the system against charge noise, which occurs for $E_{J0}/E_C > 5$ Ch. 16.5.1;
- Vanishing of the anharmonicity required for addressing individual transitions - **the anharmonicity needs to be at least larger than the spectrum width of the 0-1 transition. This will**

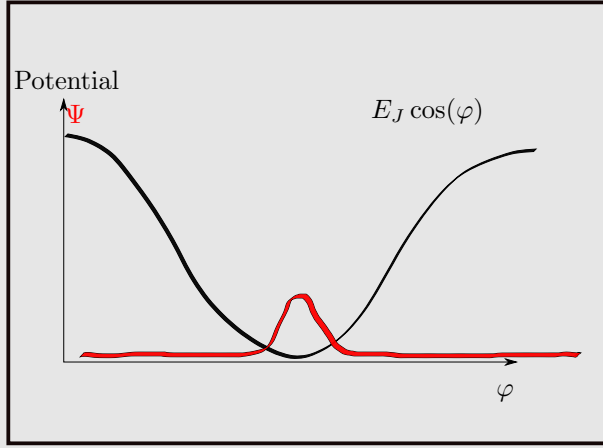


Figure 31: View system as a particle in a periodic potential. It has very little Kinetic energy, so it will be localised in the minima.

typically be 200MHz, meaning that for a spacing of 5 – 20 GHz one will need $\alpha > 0.04$ [9]

Ch. 16.5.3.

Now as per Tab. 2, increasing $C_{transmon}$ is equivalent to a particle in the potential acquiring more mass - it becomes localised in one of the potential minima, in which case we approximate cosine with a parabolic potential and according to [10] find that

$$\alpha = \frac{-E_C}{\omega_{10}} = -\frac{1}{\sqrt{8E_{J0}/E_C} - 1} \quad \Rightarrow \quad \frac{E_{J0}}{E_C} = \frac{1}{8} \left(1 - \frac{1}{\alpha}\right)^2,$$

so for $\alpha > 0.04$ one would need $E_{J0}/E_C < 70$:

We need to find a compromise that fulfills the following criteria:

- Maintain anharmonicity $|\alpha| \geq 0.04 \quad E_{J0}/E_C < 70;$
- Reduce the charge dispersion $\varepsilon_m < 0.0001 \quad E_{J0}/E_C > 5;$
- We need the transition energy to be within the window that our laboratory equipment can register
5 – 20 GHz;

16.7.1 Choosing ratio

Let us choose E_C and E_{J0} to fulfil the above criteria. Hard-coding some values, in Fig. 33, we get a selection of E_C and E_{J0} energies to use, which we will keep a log of in Tab. 3. In order to use consistent cross sizes

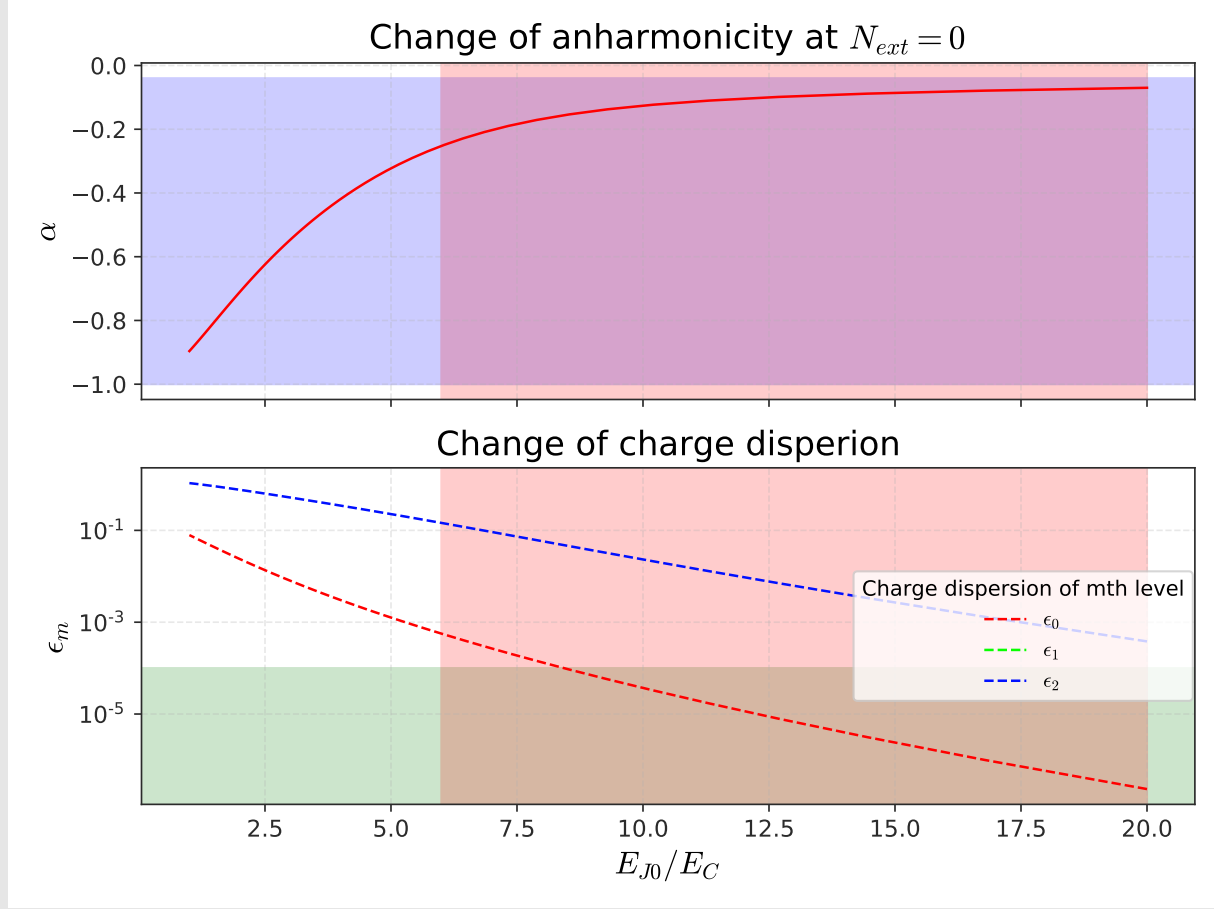


Figure 32: We want to maximise the anharmonicity α (have it in the blue region) and minimise sensitivity to charge ($\epsilon_m = \frac{E_m(N_{ext}=0.5) - E_m(N_{ext}=0)}{E_{10}}$) (green region). This is achieved by having $5 \leq E_{J0}/E_C \leq 70$ We need to use many charge states in order to get a good approximation (50 used here, and it is still only an approximation)

(simpler to draw) we will choose the $E_C = 1\text{GHz}$ for a transmon length of L_{transmon}

$E_C(L_{\text{transmon}})$ and $E_{J0}(N_{sq})$ where the calibration curves are given in Fig. 34 - this completes Tab. 3.

$$\left\{ \begin{array}{l} L_{\text{gate}} = 15 \mu\text{m} \\ C_{\text{gate}} = L_{\text{gate}} \times 10^{-10} = 1.5 \text{ fF} - \text{negligible} \\ 2S_{\text{transmon}} = 10 \mu\text{m} \\ C_{\text{transmon}} = 4 \times (L_{\text{transmon}} - 2S_{\text{transmon}}) \times 10^{-10} \\ A_{JJ} = N_{sq} \times 100 \times 100 \text{ nm}^2 \\ C_J = \frac{\epsilon \epsilon_0 A_{JJ}}{d} \quad d = 2 \text{ nm}, \epsilon = 10 \\ C_{\Sigma} = C_{\text{transmon}} + C_g + C_J \approx C_{\text{transmon}} \\ E_c = \frac{e^2}{2C_{\Sigma}} \\ E_{J0} = \frac{R_q}{R_{\square}/N_{sq}} \frac{\Delta(0)}{2} \quad R_q = 6.43 \text{ k}\Omega \quad R_{\square} = 3.57 \text{ k}\Omega (1.84 \text{ k}\Omega \text{ before}) \text{ for } 100 \times 100 \text{ nm}^2 \end{array} \right.$$

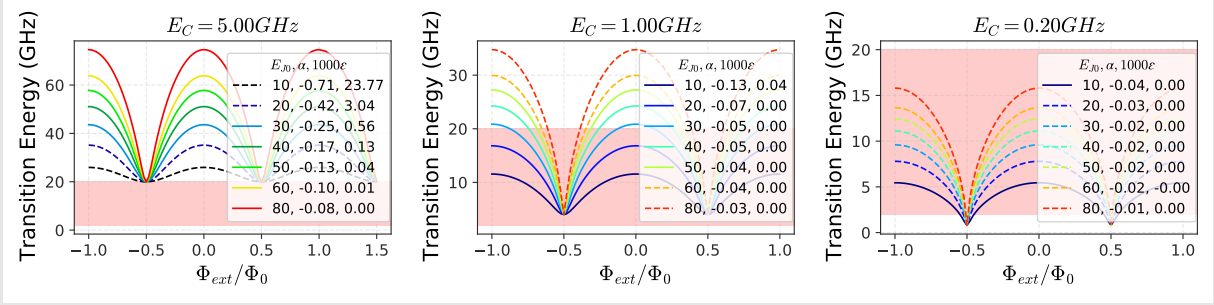


Figure 33: Optimal parameters for transmon. Left to right we increase E_C and within each plot display values for varying E_{J0} , Red region shows the window of devies. Solid lines show $\alpha \geq 0.04$. We will choose the bigger transmon (suppressing E_C) as it allows for a broader range of E_{J0} values.

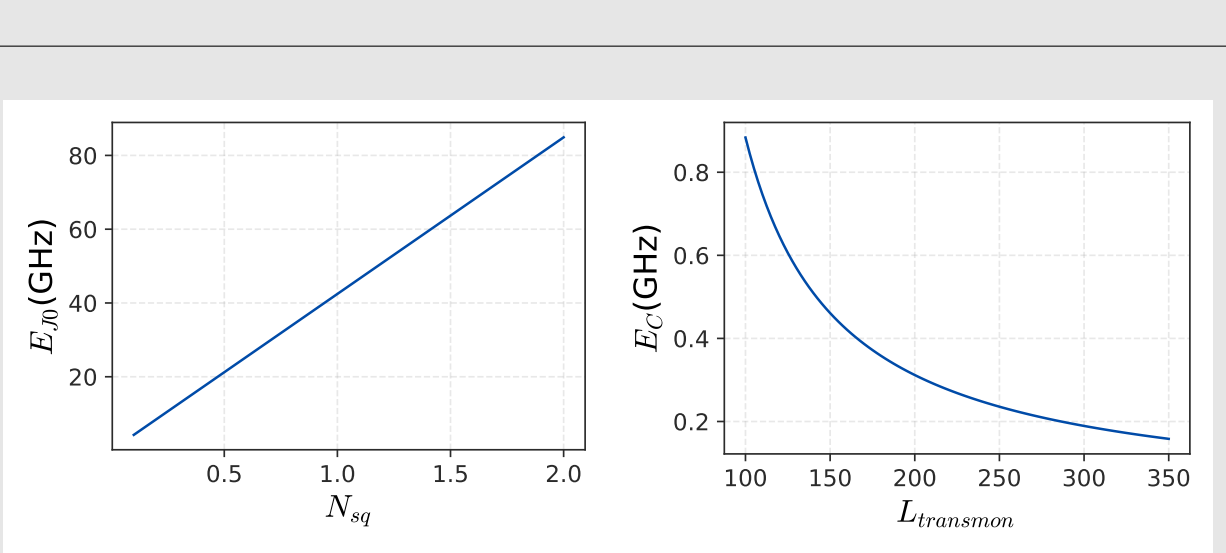
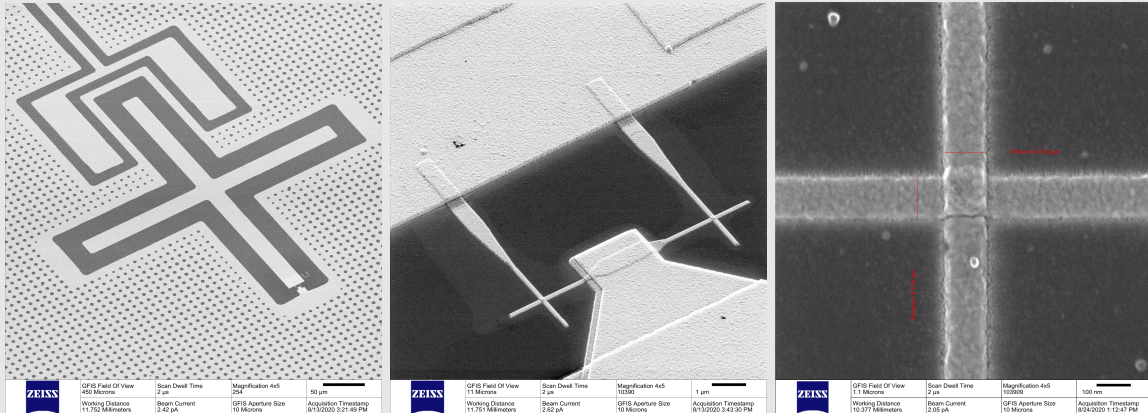


Figure 34: More JJ squares mean smaller resistance and higher critical current $\Rightarrow E_{J0}$ increases. Large transmon size means less charge concentration $\Rightarrow E_C$ decreases. @ $E_C(L_{transmon} = 350) = 0.59 \text{ GHz}$

An example of the resulting structure is given in table Tab. 3.

Table 3: Example E_C and E_{J0} values for fabrication. $2S_{\text{transmon}} = 24 \mu\text{m}$

E_C (GHz)	E_{J0} (GHz)	Ratio	L_{transmon} (μm)	N_{sq}	Square side (nm)	Resistance/RT (k Ω)
0.85	10	11.8	251	0.12	34.6	15.33/12.50
0.85	17	20.0	251	0.21	45.8	9.67/7.89
0.85	40	47.1	251	0.49	70.	3.75/3.06
0.85	80	94.1	251	0.97	98.5	1.90/1.55
1	20	20.0	217	0.24	49.0	7.67/6.25
0.6	100	166.7	345	1.22	110.	1.508/1.23
0.6	120	200.0	345	1.46	121.	1.26/1.03



16.8 Transmon 2-level approximation

Normally N_{ext} is biased at a sweet spot **close to $-1/2$** . Then the only number of electrons n on out island that will give a low energy (due to the energy dispersion in Fig. 24) is either 0 or -1. The other level will be far separated. Then we take out the Hamiltonian

$$\mathcal{H}_{0 \text{ or } -1} = \begin{pmatrix} E_C(-1 - N_{\text{ext}})^2 & -E_J/2 \\ -E_J/2 & E_C(N_{\text{ext}})^2 \end{pmatrix}$$

And we have a two level system just as in the previous lecture Eq.(21). Redefining the zero point energy to be in the middle of the diagonal terms

$$\mathcal{H} = \begin{pmatrix} -\epsilon/2 & -E_J/2 \\ -E_J/2 & \epsilon/2 \end{pmatrix}$$

$$\epsilon/2 = \frac{\text{energy diff}}{2} = \frac{E_C N_{\text{ext}}^2 - E_C(1 + N_{\text{ext}})^2}{2} = -\frac{E_C}{2}(1 + 2N_{\text{ext}})$$

This will have solutions

$$E = \pm \frac{\Delta E}{2}, \quad |\psi\rangle_0 = \begin{pmatrix} \cos(\theta/2) \\ \sin(\theta/2) \end{pmatrix}, \quad |\psi\rangle_1 = \begin{pmatrix} \sin(\theta/2) \\ \cos(\theta/2) \end{pmatrix}, \quad \Delta E = \sqrt{\epsilon^2 + \Delta^2}$$

16.9 Charge energy dominates: E_C/E_J :

- High charge noise - gate voltage changes, affects the energy levels severely
- High anharmonicity - quadratic n dependance dominates, allowing individual addressing of the levels;

16.10 Flux energy dominates: $E_C/E_J \ll 1$

If flux is the important variable, then we shall work with the flux basis using the wavefunctions $\psi(\phi)$

$$\hat{\mathcal{N}} = -i \frac{d}{d\phi}$$

and we rewrite

$$\begin{aligned}\mathcal{H} &= E_C \left(\hat{\mathcal{N}} - N_{\text{ext}} \right)^2 - E_J \cos(\hat{\phi}) \\ &= E_C \left(-i \frac{d}{d\phi} - n_g \right)^2 - E_J \cos(\varphi).\end{aligned}$$

16.10.1 Numerical solution

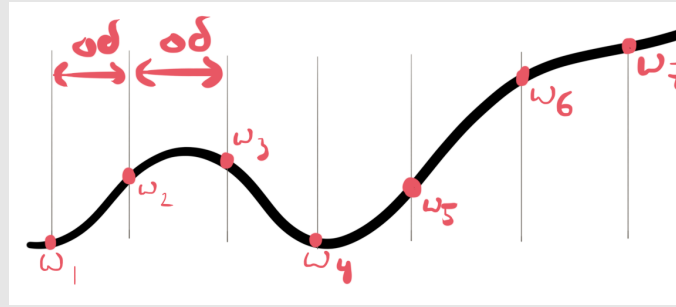
We dice up the state of the system into individual values at discretised positions, with a step of $\Delta\delta$ in order to solve

$$\mathcal{H}\Psi(\varphi) = E\Psi(\varphi)$$

$$\Psi(\varphi) \rightarrow \begin{pmatrix} \Psi(0) \\ \Psi(\Delta\delta) \\ \Psi(2\Delta\delta) \\ \vdots \\ \Psi(n\Delta\delta) \end{pmatrix} \equiv \begin{pmatrix} w_0 \\ w_1 \\ w_2 \\ \vdots \\ w_n \end{pmatrix}$$

and solve for this wavefunction made up of a lot of small contributions at different phases.

$$\frac{d}{d\varphi} (\omega_i) = \frac{w_{i+1} - w_{i-1}}{2\Delta\delta}$$



We rewrite Subsec. 16.10 for w_1 for example:

$$\begin{aligned} E_C \left[\left(\frac{w_{i+1} - w_{i-1}}{2\Delta\delta} \right)^2 + 2in_g \frac{w_{i+1} - w_{i-1}}{2\Delta\delta} + n_g^2 w_i \right] - E_J \cos(\delta) w_i &= E w_i \\ \frac{E_C}{4\Delta\delta^2} [w_{i+1}^2 - w_{i-1}^2 - 2w_{i+1}w_{i-1} + 4in_g \Delta\delta (w_{i+1} - w_{i-1})] + U(w_i) w_i &= E w_i \end{aligned}$$

where $U(w_n) = E_C n_g^2 - E_J \cos(n \times \delta)$

$$\begin{aligned} \left[-\frac{E_C}{\Delta\delta^2} [\omega_2 + \omega_0 - 2\omega_1] + U(w_1) \right] w_1 &= E w_1 \\ \left[-\frac{E_C}{\Delta\delta^2} [\omega_3 + \omega_1 - 2\omega_2] + U(w_2) \right] w_2 &= E w_2 \end{aligned}$$

...

where we defined

$$\begin{pmatrix} 2\frac{E_c}{\Delta\delta^2} + U(w_1) & -\frac{E_c}{\Delta\delta^2} & 0 & 0 \\ -\frac{E_c}{\Delta\delta^2} & 2\frac{E_c}{\Delta\delta^2} + U(w_2) & -\frac{E_c}{\Delta\delta^2} & 0 \\ 0 & -\frac{E_c}{\Delta\delta^2} & 2\frac{E_c}{\Delta\delta^2} + U(w_3) & -\frac{E_c}{\Delta\delta^2} \\ \vdots & \vdots & \vdots & \ddots \end{pmatrix} \begin{pmatrix} w_1 \\ w_2 \\ w_3 \\ \vdots \end{pmatrix} = E \begin{pmatrix} w_1 \\ w_2 \\ w_3 \\ \vdots \end{pmatrix}$$

where

$$\begin{cases} \mathbf{U}(\phi_{\mathbf{J}}) = \mathbf{E}_{\mathbf{L}}(\phi_{\text{ext}} - \phi_{\mathbf{J}})^2 - \mathbf{E}_{\mathbf{J}} \cos(\phi_{\mathbf{J}}) \\ E_c = \frac{(2e)^2}{2C} \\ E_L = \frac{\Phi_0^2}{2L(2\pi)^2} \\ E_J = \frac{\Phi_0 I_c}{2\pi} = \frac{\Phi_0}{2\pi} \frac{\pi \Delta(0)}{2eR} \end{cases}$$

The eigentates can be evaluated in MatLab:

To complete

16.10.2 Periodic analogy

- Let us compare this to Hamiltonian in a periodic potential

$$\mathcal{H}_{\text{crystal}} = \frac{-\hbar^2}{2m} \frac{d^2}{dx^2} + V(x) \quad V(x+a) = V(x),$$

which, according to Bloch's theorem, states that the eigenstates will be of the form

$$\psi_{kn}(x) = e^{ikx} u_{kn}(x),$$

which, when plugged in will result in an effective Hamiltonian

$$\mathcal{H}_{\text{eff},k} = \frac{\hbar^2}{2m} \left(-i \frac{d}{dx} + k \right)^2 + V(x)$$

- We can see this mapping between

$$\begin{aligned} \mathcal{H}_{\text{eff},k} &= \frac{\hbar^2}{2m} \left(-i \frac{d}{dx} + k \right)^2 + V(x) \\ \mathcal{H} &= E_C \left(-i \frac{d}{d\phi} - n_g \right)^2 - E_J \cos(\phi), \end{aligned}$$

so, will look for solutions of a similar form.

- As E_C/E_J gets smaller, the potential well from the $E_J \cos(\phi)$ gets deeper **and the states within each well localise, and stop interacting with one another.** Solving, as in the Transmon Paper, will lead to anharmonicity relation

$$\frac{E_{12} - E_{01}}{E_{01}} \approx -(8E_J/E_C)^{-1/2},$$

which decreases as we continue to increase E_J .

COUPLING TRANSMON WITH RESONATOR

Following is extract from Bader which explains coupling to a transmon via a resonator.

In the following we perform the following approximation:

- Consider transmon to have a single JJ (using $E_J(\Phi_{\text{ext}}) = E_{J0} \times 2|\cos(\pi\Phi_{\text{ext}}/\Phi_0)|$);

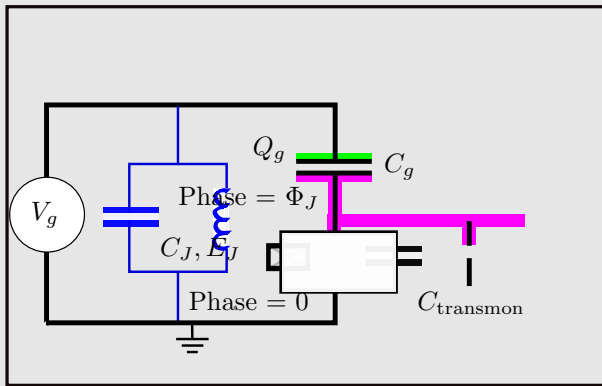


Figure 35: Adding resonator that is interacting with the transmon

17.0.1 Coupling strength

It will be found that the matrix element that gives the coupling strength

$$g = (2e\beta V_{\text{rms}}^0/\hbar) \left(\frac{E_J}{8E_C} \right)^{1/4}$$

which is paradoxical since:

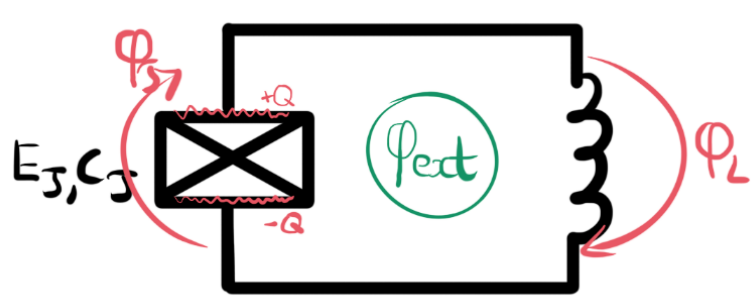
- Charge sensitivity is reduced by using the shunt capacitance of the transmon
- So therefore a bigger C (lower E_C) should **reduce coupling to environmental fields**.

But this is because the transmon was considered in the static case - where we monitor response of transmon to DC charge offsets.

But for dynamic coupling (when field is close to the frequency of the qubit) this is not the case. In fact, because flux terms are more dominant in the transmon, compared to the CPB, more charge terms are involved in the dynamics making the transmon more polarizable. (see Bader).

RF SQUID (FLUX QUBIT). $E_J/E_C \sim 50$

The RF SQUID composes of a JJ in a loop with a big inductor. This inductor was neglected for the CPB in the previous section, since $E_C, E_J \gg E_L$.



18.1 Regimes of RF SQUIDs [15]

Taking the loop inductance L_s and the inductance of the JJ $L_J = \frac{\Phi_0}{2\pi I_0}$ (see Fig. 12.2) we have regimes when

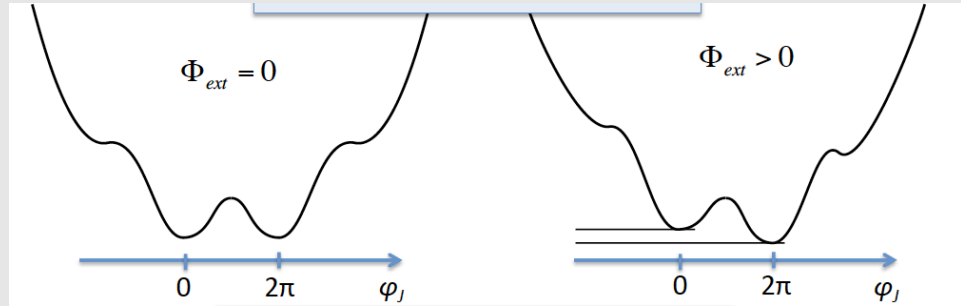
- $L_J \gg L_s$ - the current induced in the loop (by the biasing flux) is negligible compared to the current on the JJ:
 - Aluminium loops;
 - $E_C = \frac{e^2}{2C}$
 - $E_J = \frac{I_0 \Phi_0}{2\pi}$
 - Negligible inductance energy of the loop (loop except the JJ)
 - Use number is a good quantum number
- $L_J \ll L_s$ - the current induced in the loop (by the biasing flux) is important:
 - Niobium;
 - The quantum variables can be related to the flux in the loops and their time derivatives;
 - Circulating current states - persistent current states.

The paper then goes onto the standard derivation of Hamiltonian from the Lagrangian - applying the tight binding model for two parts of the wavefunction in the different minima at different biasing fields.

18.2 Hamiltonian

1. **Potential energy part** comes from the JJ and the inductor, where we use the phase quantisation in a loop to get

$$U = 1 - E_J \cos(\phi_J) + \frac{\Phi_0^2}{(2\pi)^2 2L} (\phi_{ext} - \phi_J)^2,$$



resulting in a ‘wiggled’ parabolic potential.

2. **The charging kinetic part** is from the voltage being induced by the changing flux on the JJ

$$T = \frac{C_J}{2} \dot{\Phi}_J^2.$$

3. The full **Lagrangian** now reads

$$\mathcal{L} = T - U = \frac{C_J}{2} \dot{\Phi}_J^2 + E_J \cos(\phi_J) - \frac{\Phi_0^2}{(2\pi)^2 2L} (\phi_{ext} - \phi_J)^2.$$

4. The **conjugate momentum**

$$Q_J = \frac{d\mathcal{L}}{d\dot{\Phi}_J} = C_J \dot{\Phi}_J,$$

is just an offset of the induced charge on the capacitor due to the JJ voltage.

5. So we arrive at the following set of operators

$$\mathbf{x} \leftrightarrow \Phi \leftrightarrow \phi \text{ (position/flux)} \quad \mathbf{p} \leftrightarrow \mathbf{Q} \leftrightarrow \mathbf{N} \text{ (momentum/electrons)}$$

with the commutation relations:

$$\begin{aligned} [\textcolor{blue}{x}, \textcolor{red}{p}] &= i\hbar & [\Phi, \textcolor{blue}{Q}] &= i\hbar & [\phi, N] &= \frac{2\pi}{\frac{\hbar}{2e}} [\Phi, Q] \frac{1}{2e} = i \\ \hat{p} &= -i\hbar \frac{\partial}{\partial \textcolor{blue}{x}} & \hat{Q} &= -i\hbar \frac{\partial}{\partial \Phi} & \hat{N} &= -i \frac{\partial}{\partial \phi} \end{aligned}$$

6.

Expressing the **Hamiltonian** in the standard fashion

$$\begin{aligned} \mathcal{H} &= \hat{Q}_J \dot{\hat{\Phi}}_J - \mathcal{L} \\ &= \frac{\hat{Q}_J^2}{2C_J} - E_J \cos(\hat{\phi}_J) + \frac{\Phi_0^2}{(2\pi)^2 2L} (\phi_{\text{ext}} - \hat{\phi}_J)^2 \\ &= \mathbf{E}_{\mathbf{C}} \hat{\mathbf{N}}^2 - \mathbf{E}_{\mathbf{J}} \cos(\hat{\phi}_{\mathbf{J}}) + \mathbf{E}_{\mathbf{L}} (\phi_{\text{ext}} - \hat{\phi}_{\mathbf{J}})^2 \quad E_c = \frac{(2e)^2}{2C_J} \quad E_L = \frac{\Phi_0^2}{(2\pi)^2 2L}. \end{aligned}$$

7. So now one has a parabolic potential term in the Hamiltonian, unlike in the Cooper Pair box case where there was only the cosine potential

- ϕ_{ext} controls the shape of the potential and hence the energies of each eigenstate
- ϕ_{JJ} is the dynamic parameter of the qubit.

18.3 Numerical solution of Hamiltonian

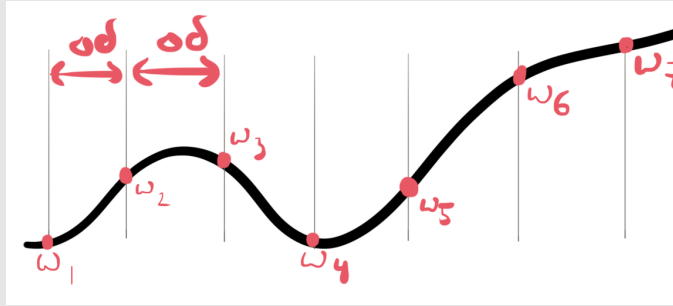
There is a numerical method to solve for the RF-SQUID, whereby we dice up the state of the system into individual values at discretised positions, with a step of $\Delta\delta$

$$\psi \rightarrow \begin{pmatrix} \psi(0) \\ \psi(\Delta\delta) \\ \psi(2\Delta\delta) \\ \vdots \\ \psi(n\Delta\delta) \end{pmatrix} \equiv \begin{pmatrix} w_0 \\ w_1 \\ w_2 \\ \vdots \\ w_n \end{pmatrix}$$

and solve

$$\begin{aligned} \mathcal{H}\psi &= \left[E_c \hat{N}^2 - E_J \cos(\hat{\phi}_J) + E_L (\phi_{\text{ext}} - \hat{\phi}_J)^2 \right] \psi \\ &= \left[-E_C \frac{\partial}{\partial \phi_J^2} + U(\phi_J) \right] \psi \end{aligned} \quad \equiv E\psi \quad (29)$$

for this wavefunction made up of a lot of small contributions.



The derivative, can be evaluated using neighbouring points:

$$\frac{d}{d\phi_J^2} (\omega_i) = \frac{\frac{\omega_{i+1}-\omega_i}{\Delta\delta} - \frac{\omega_i-\omega_{i-1}}{\Delta\delta}}{\Delta\delta} = \frac{1}{\Delta\delta^2} [\omega_{i+1} + \omega_{i-1} - 2\omega_i]. \quad (30)$$

We rewrite Eq. (29) with the derivative Eq. (30) to get

$$\begin{aligned} \left[-\frac{E_C}{\Delta\delta^2} [\omega_2 + \omega_0 - 2\omega_1] + U(w_1) \right] \omega_1 &= Ew_1 \\ \left[-\frac{E_C}{\Delta\delta^2} [\omega_3 + \omega_1 - 2\omega_2] + U(w_2) \right] \omega_2 &= Ew_2 \end{aligned}$$

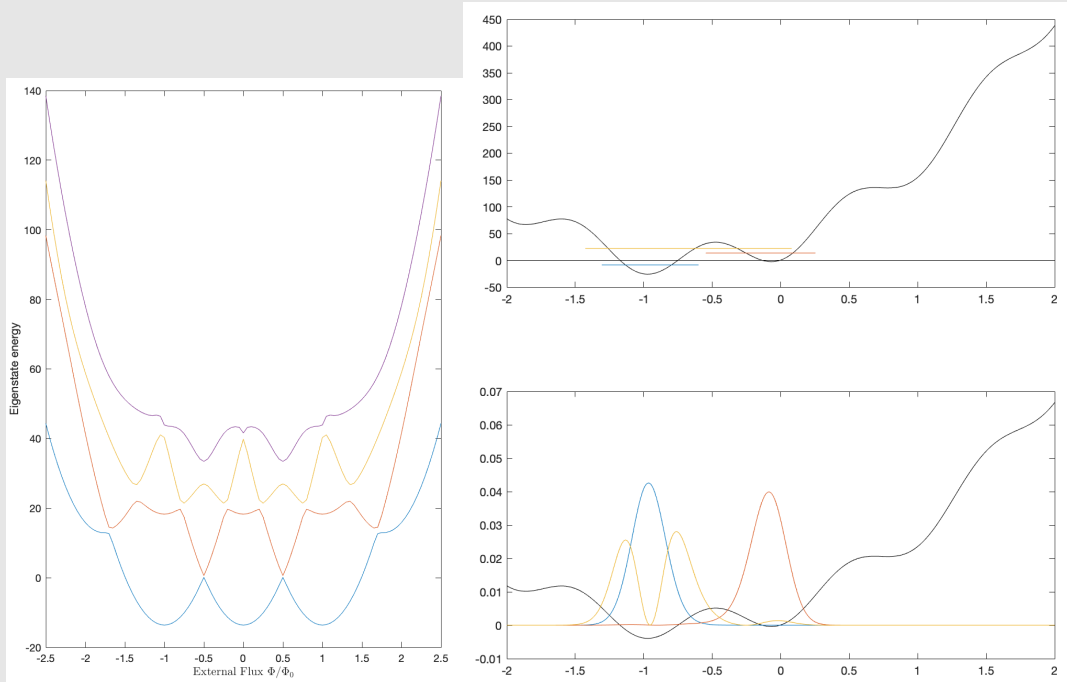
...

$$\begin{pmatrix} 2\frac{E_c}{\Delta\delta^2} + U(w_1) & -\frac{E_c}{\Delta\delta^2} & 0 & 0 \\ -\frac{E_c}{\Delta\delta^2} & 2\frac{E_c}{\Delta\delta^2} + U(w_2) & -\frac{E_c}{\Delta\delta^2} & 0 \\ 0 & -\frac{E_c}{\Delta\delta^2} & 2\frac{E_c}{\Delta\delta^2} + U(w_3) & -\frac{E_c}{\Delta\delta^2} \\ \vdots & \vdots & \vdots & \ddots \end{pmatrix} \begin{pmatrix} w_1 \\ w_2 \\ w_3 \\ \vdots \end{pmatrix} = E \begin{pmatrix} w_1 \\ w_2 \\ w_3 \\ \vdots \end{pmatrix}$$

where

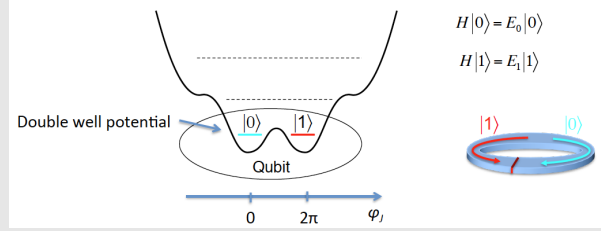
$$\begin{aligned} U(\phi_J) &= \mathbf{E}_L(\phi_{\text{ext}} - \phi_J)^2 - \mathbf{E}_J \cos(\phi_J) \\ E_c &= \frac{(2e)^2}{2C} \\ E_L &= \frac{\Phi_0^2}{2L(2\pi)^2} \\ E_J &= \frac{\Phi_0 I_c}{2\pi} = \frac{\Phi_0}{2\pi} \frac{\pi \Delta(0)}{2eR} \end{aligned}$$

The eigenstates can be evaluated in MatLab:



18.4 Solution in the degenerate case

There is a nice solution when eigenstates are degenerate, that occurs with a symmetrical double well potential. Eigenstates $|\psi(0)\rangle$ and $|\psi(2\pi)\rangle$ constitute to the two circulating current directions.



1. We look for contribution to the wavefunction at $\phi_J = 0$ and $\phi_J = 2\pi$, ‘sampling’ much more strictly than in Section 18.3:

$$\psi \rightarrow \begin{pmatrix} \psi(0) \\ \vdots \\ \psi(n\Delta\delta) \end{pmatrix} \xrightarrow{\Delta = 2\pi, n=1} \begin{pmatrix} \psi(0) \\ \psi(2\pi) \end{pmatrix} = \psi(0)|0\rangle + \psi(2\pi)|1\rangle$$

looking for solutions to solve

2. The potential consists of

$$-E_J \cos(\phi_J) \rightarrow \text{symmetric about } \phi_J = \pi(2n+1) \quad n \in \mathbb{Z}$$

$$E_L(\phi_{\text{ext}} - \phi_J)^2 \rightarrow \text{symmetric about } \phi_J = \phi_{\text{ext}}.$$

3. Thus the potential is symmetrical and states $|0\rangle$ or $|1\rangle$ are degenerate if

$$\phi_{\text{ext}} \approx \pi + \delta\phi.$$

4. The energy difference between the two wells located at $\phi_{J1} = 0$ and $\phi_{J2} = 2\pi$ (or equivalently at a separation of 2π).

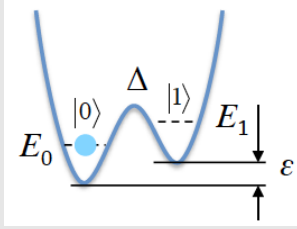


Figure 36: The two lowest energies for the system near the double potential well. The loop is biased by a flux corresponding to $\phi_{\text{ext}} \approx \pi - \text{half a flux quantum}$.

$$\varepsilon = E_0 - E_{2\pi}$$

$$\begin{aligned} &= [-E_J \cos(0) + E_L(\phi_{\text{ext}} - 0)^2] - [-E_J \cos(2\pi) + E_L(\phi_{\text{ext}} - 2\pi)^2] \\ &= E_L \left[\phi_{\text{ext}}^2 - \phi_{\text{ext}}^2 + 4\pi\phi_{\text{ext}} - 4\pi^2 \right] = 4\pi E_L \left[\phi_{\text{ext}} - \pi \right] \\ &\approx 4\pi E_L \left[\pi + \delta\phi - \pi \right] = 4\pi E_L \delta\phi = 4\pi \frac{\Phi_0^2}{(2\pi)^2 2L} \delta\phi = \frac{1}{2\pi} \frac{\Phi_0^2}{2L} \delta\phi \\ &\varepsilon = \frac{\Phi_0}{2L} \delta\Phi = I_p \delta\Phi \end{aligned}$$

Recalling that $E_J = \frac{\Phi_0 I_c}{2\pi}$, where I_c is the maximal persistent current (critical current)

5. So for the potential part accounts for two states, $|\psi(0)\rangle$ and $|\psi(2\pi)\rangle$ at two different energies, which we can write as a diagonal matrix

$$U = \begin{bmatrix} |\psi(0)\rangle & |\psi(2\pi)\rangle \\ \langle\psi(0)| & \langle\psi(2\pi)| \end{bmatrix} \quad \varepsilon = \frac{\Phi_0}{2L} \delta\Phi = I_p \delta\Phi.$$

6. The kinetic term $-E_C \frac{\partial}{\partial \phi_J^2}$ is evaluated as in Chapter 18.3

$$\begin{aligned} \frac{d}{d\phi_J^2} \omega_i &= \frac{\frac{\omega_{i+1}-\omega_i}{\Delta\delta} - \frac{\omega_i-\omega_{i-1}}{\Delta\delta}}{\Delta\delta} = \frac{1}{\Delta\delta^2} [\omega_{i+1} + \omega_{i-1} - 2\omega_i] \\ \bullet \frac{d}{d\phi_J^2} \psi(0) &= \frac{1}{(2\pi)^2} [\psi(2\pi) + \psi(-2\pi) - 2\psi(0)] \approx \frac{1}{4\pi^2} [\psi(2\pi) - 2\psi(0)] \\ \bullet \frac{d}{d\phi_J^2} \psi(2\pi) &= \frac{1}{(2\pi)^2} [\psi(4\pi) + \psi(0) - 2\psi(2\pi)] \approx \frac{1}{4\pi^2} [\psi(0) - 2\psi(2\pi)], \end{aligned}$$

where we assume that for the lowest energy states the wavefunction is negligible outside the well: $\psi(4\pi) = \psi(-2\pi) = 0$.

7. In matrix form this looks like

$$-E_C \frac{d}{d\phi_J^2} = \begin{matrix} |\psi(0)\rangle & |\psi(2\pi)\rangle \\ \langle\psi(0)| & \langle\psi(2\pi)| \end{matrix} \begin{bmatrix} \frac{1}{4\pi^2} 2E_C & -\frac{1}{4\pi^2} E_C \\ -\frac{1}{4\pi^2} E_C & \frac{1}{4\pi^2} 2E \end{bmatrix} \equiv \begin{matrix} |\psi(0)\rangle & |\psi(2\pi)\rangle \\ \langle\psi(0)| & \langle\psi(2\pi)| \end{matrix} \begin{bmatrix} 0 & -\frac{\Delta}{2} \\ -\frac{\Delta}{2} & 0 \end{bmatrix} \quad \Delta = \frac{2E_C}{4\pi^2}$$

8.

The Hamiltonian can be written as that for a two level system

$$\mathcal{H} \approx -\frac{\epsilon}{2}\sigma_z - \frac{\Delta}{2}\sigma_x = \begin{matrix} |\psi(0)\rangle & |\psi(2\pi)\rangle \\ \langle\psi(0)| & \langle\psi(2\pi)| \end{matrix} \begin{bmatrix} -\epsilon/2 & -\Delta/2 \\ -\Delta/2 & \epsilon/2 \end{bmatrix} \quad \text{when } \phi_{\text{ext}} \approx \pi$$

$$\epsilon = \frac{\Phi_0}{2L} \delta\Phi \quad \text{controlled by bias flux}$$

$$\Delta = \frac{2E_C}{4\pi^2} \quad \text{anticrossing energy between states } |0\rangle \text{ and } |1\rangle$$

9. Solving as in Chapter 11 using a unitary rotation

$$\begin{aligned} \mathcal{H} &= -\frac{\epsilon}{2}\sigma_z - \frac{\Delta}{2}\sigma_x \\ &= -\frac{\sqrt{\epsilon^2 + \Delta^2}}{2} \left(\frac{\epsilon}{\sqrt{\epsilon^2 + \Delta^2}} \sigma_z + \frac{\Delta}{\sqrt{\epsilon^2 + \Delta^2}} \sigma_x \right) \\ &= -\frac{\Delta E}{2} (\cos(\theta) \sigma_z + \sin(\theta) \sigma_x) \\ \Delta E &= \sqrt{\epsilon^2 + \Delta^2} \\ \tan(\theta) &= \frac{\Delta}{\epsilon} \end{aligned},$$

with eigenvectors and eigenvalues being a mixture of persistence current states $|\circlearrowleft\rangle$, $|\circlearrowright\rangle$.

$$E = \pm \frac{\Delta E}{2}, \quad |0\rangle = \begin{pmatrix} \cos(\theta/2) \\ \sin(\theta/2) \end{pmatrix}, \quad |1\rangle = \begin{pmatrix} \sin(\theta/2) \\ -\cos(\theta/2) \end{pmatrix}$$

10. With states $|\circlearrowleft\rangle \equiv +I_p$ and $|\circlearrowright\rangle \equiv -I_p$ the expectation values of the current:

$$\begin{aligned} \langle I \rangle_{|0\rangle} &= I_p \cos(\theta/2)^2 - I_p \sin(\theta/2)^2 = I_p \cos(\theta) \\ \langle I \rangle_{|1\rangle} &= I_p \sin(\theta/2)^2 - I_p \cos(\theta/2)^2 = -I_p \cos(\theta) \end{aligned}$$

11. Now we perform a transformation to rotate the state by $2\alpha = \theta$

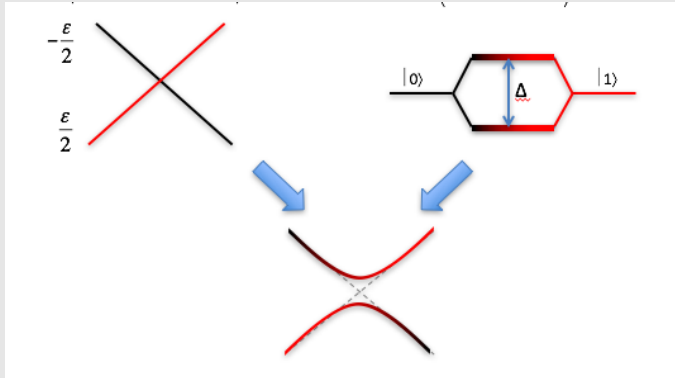
$$U = e^{i\frac{\theta}{2}\sigma_y} = \cos(\alpha)\mathbb{I} + i \sin(\alpha)\sigma_y$$

to rotate the basis in this plane. **Note that the transformation uses an angle HALF of the required turn.** The time independent Hamiltonian will be transformed and evaluating using the commutation relations Eq.(10)

$$\begin{aligned} \mathcal{H}' &= U\mathcal{H}U^\dagger = U \left[-\frac{\Delta E}{2} (\sigma_z \cos(\theta) + \sigma_x \sin(\theta)) \right] \left[\cos(\theta/2)\mathbb{I} - i \sin(\theta/2)\sigma_y \right] \\ &= U \left[\cos(\theta/2)\mathbb{I} + i \sin(\theta/2)\sigma_y \right] \left[-\frac{\Delta E}{2} (\sigma_z \cos(\theta) + \sigma_x \sin(\theta)) \right] \\ &= UU\mathcal{H} = -\frac{\Delta E}{2} \left[\cos(\theta)\mathbb{I} + i \sin(\theta)\sigma_y \right] \left[(\sigma_z \cos(\theta) + \sigma_x \sin(\theta)) \right] \\ &= -\frac{\Delta E}{2} \left[\cos^2(\theta)\sigma_z + \sin(\theta) \cos(\theta)\sigma_x + i \sin(\theta) \cos(\theta)\sigma_y\sigma_z + i \sin^2(\theta)\sigma_y\sigma_x \right] \\ &= -\frac{\Delta E}{2} \left[\cos^2(\theta)\sigma_z + \sin(\theta) \cos(\theta)\sigma_x + i \sin(\theta) \cos(\theta)i\sigma_x + i \sin^2(\theta)-i\sigma_z \right] \\ &= -\frac{\Delta E}{2}\sigma_z, \end{aligned}$$

12.

In the rotated frame we have a two level system, where the biasing flux, and the anticrossing energies come together to create new system eigenstates:



$$\mathcal{H}' = -\frac{\Delta E}{2}\sigma_z$$

With eigenstates $|\psi(0)\rangle, |\psi(2\pi)\rangle$ (mix of persistent current states) at energies

$$\pm \frac{\Delta E}{2} \quad \Delta E = \sqrt{\varepsilon^2 + \Delta^2} \quad \varepsilon = \frac{\Phi_0}{2L} \delta\Phi \quad \Delta = \frac{2E_C}{4\pi^2}.$$



Fig.37 depicts the approximated wavefunctions and Fig.38 the energies for different external fields.

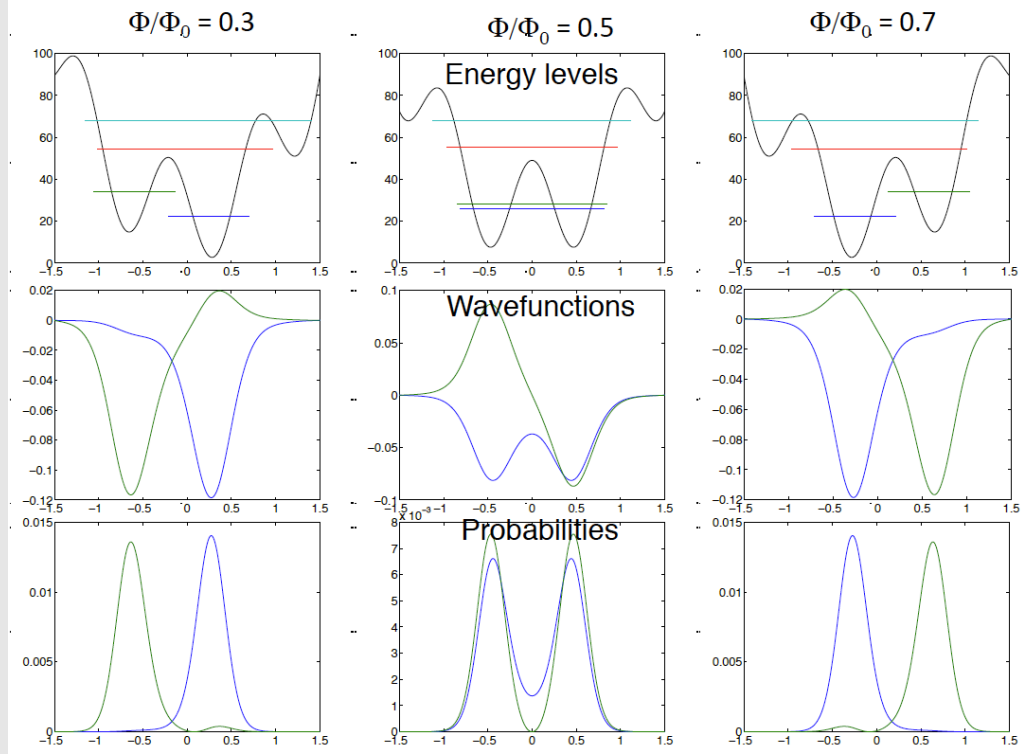


Figure 37: The wavefunctions of the RF SQUID as a function of ϕ_J for different external flux ϕ_{ext} biases. Notice how the different flux biases change the symmetry of the potential and the shape of the wavefunctions

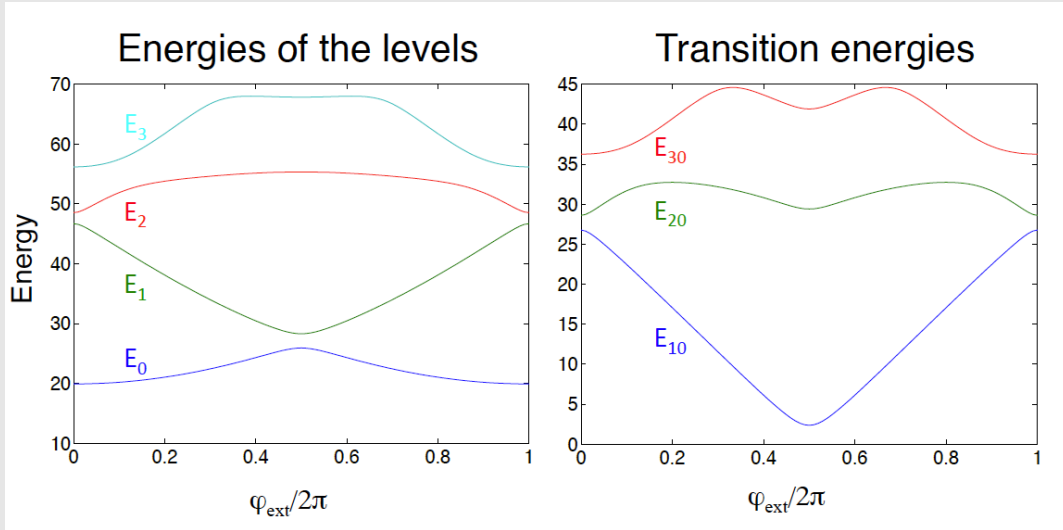


Figure 38: The energy levels and their differences as a function of the **applied flux** ϕ_{ext} . At the degeneracy point, the levels come close together.

18.5 Question about fabrication

There is a technological limitation to this kind of device. Once needs a large inductance L , but be able to keep a relatively small size. Otherwise the capacitance C of the system grows too large, which prevents the tunnelling of the localised states.

A proposal is to replace the classical inductor with a JJ, which provides plenty of inductance, while keeping a considerable size. Will it work? Lets evaluate the potential energy

$$\begin{aligned}
 & -E_J \cos(\phi_{J1}) - \alpha E_J \cos(\phi_{J1} - \phi_{\text{ext}}) \\
 &= -E_J \left[\cos(\phi_{J1} - \frac{\phi_{\text{ext}}}{2} + \frac{\phi_{\text{ext}}}{2}) + \alpha \cos(\phi_{J1} - \frac{\phi_{\text{ext}}}{2} - \frac{\phi_{\text{ext}}}{2}) \right] \\
 &= -E_J \left[\cos(\phi' + \frac{\phi_{\text{ext}}}{2}) + \alpha \cos(\phi' - \frac{\phi_{\text{ext}}}{2}) \right] \\
 \left\{ \begin{array}{l} U^{\text{potential}} = -E_J \cos(\phi_{J1}) - \alpha E_J \cos(\phi_{J2}) \\ \phi_{J1} - \phi_{J2} = \phi_{\text{ext}} \end{array} \right. &\Rightarrow -E_J \left[\cos(\phi') \cos(\frac{\phi_{\text{ext}}}{2}) + \alpha \cos(\phi') \cos(\frac{\phi_{\text{ext}}}{2}) \right. \\
 &\quad \left. - \sin(\phi') \sin(\frac{\phi_{\text{ext}}}{2}) + \alpha \sin(\phi') \sin(\frac{\phi_{\text{ext}}}{2}) \right] \\
 &\approx -E_J(1 + \alpha) \left[\cos(\phi') \cos(\frac{\phi_{\text{ext}}}{2}) \right]
 \end{aligned}$$

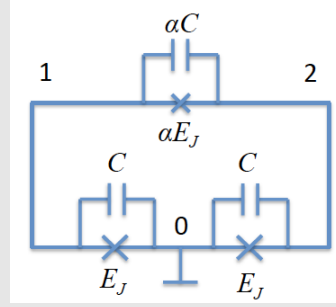
There is no parabolic dependence, making the localised states unsuitable - the eigenstates will tunnel across all of the possible wells formed by the cosine potential. **So this is not possible with just replacing an inductor with a JJ.**

CHAPTER 19

3 JJ QUBIT

From [7]:

- To create a double potential well we need $\alpha > 0.5$ and to reduce flux noise we need $\alpha < 0.7$;



1. **Potential energy** comes from all three JJs, where we denote the phases

$$e^{i\phi_{01}} = e^{i(\phi_0 - \phi_1)}$$

$$\begin{aligned} U_{\text{potential}} &= E_J(1 - \cos(\phi_{01})) + \alpha E_J(1 - \cos(\phi_{12})) + E_J(1 - \cos(\phi_{20})) \\ &= E_J \left[2 + \alpha - \cos(\phi_{01}) - \cos(\phi_{20}) - \alpha \cos(\phi_{\text{ext}} - \phi_{01} - \phi_{20}) \right]. \end{aligned}$$

2. **The kinetic energy** comes from the charging energy. Its better to work with the capacitance matrix for the system which links a given charge vector \vec{n} with a potential vector \vec{V}

$$\begin{cases} \vec{n} = \begin{pmatrix} n_1 \\ n_2 \end{pmatrix} \\ \vec{V} = \begin{pmatrix} V_1 \\ V_2 \end{pmatrix} \\ C = \begin{pmatrix} C_{01} + C_{12} & -C_{12} \\ -C_{12} & C_{02} + C_{12} \end{pmatrix} \end{cases} \Rightarrow \vec{n} = \frac{C\vec{V}}{2e} \equiv \begin{bmatrix} C_{01}(V_1 - 0) + C_{12}(V_1 - V_2) \\ C_{01}(V_2 - 0) + C_{12}(V_2 - V_1) \end{bmatrix},$$

which is just the typical evaluating of charge on a capacitor from $Q = CV$. For evaluating the kinetic energy from the charges

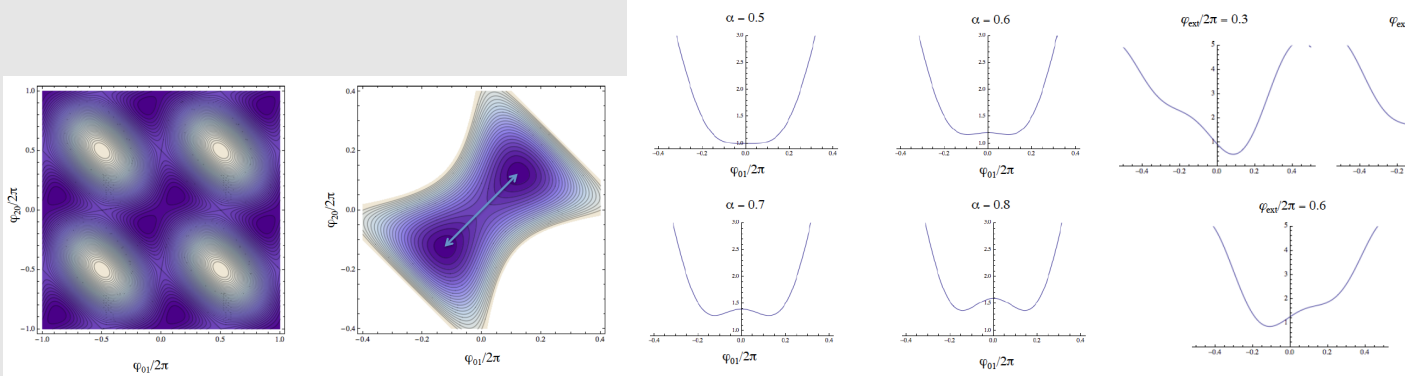


Figure 39: α determines the height of the barrier in the middle of the two wells. Larger alpha raises the barrier up. ϕ_{ext} determines the symmetry of the wells (as in the previous section).

$$\left\{ \begin{array}{l} \vec{V} = 2eC^{-1}\vec{n} \\ \vec{Q} = 2e\vec{n} \quad \Rightarrow U_{\text{kinetic}} = \frac{1}{2} (2e\vec{n}^T) (2eC^{-1}\vec{n}) = \frac{(2e)^2}{2} \vec{n}^T C^{-1} \vec{n}, \\ U_{\text{kinetic}} = \frac{1}{2} Q \cdot V \end{array} \right.$$

3. The total Hamiltonian for the 3JJ/3 capacitor system being

$$\begin{aligned} \mathcal{H} &= U_{\text{kinetic}} + U_{\text{potential}} \\ &= \frac{(2e)^2}{2} \vec{n}^T C^{-1} \vec{n} + E_J \left[2 + \alpha - \cos(\phi_{01}) - \cos(\phi_{20}) - \alpha \cos(\phi_{\text{ext}} - \phi_{01} - \phi_{20}) \right]. \end{aligned}$$

For simple representation in matrix form, we write it out in the **charge basis**. In such a basis we have the results summarised in Table.

4. We draw parallels to rewrite our new Hamiltonian in matrix form (using exponential form of trigonometric functions and zeroing constant offsets and replacing the last exponential with explicit dependence on the phase across the junction)

Table 4: Note how the phase operators increase and decrease the islands associated to a given phase.

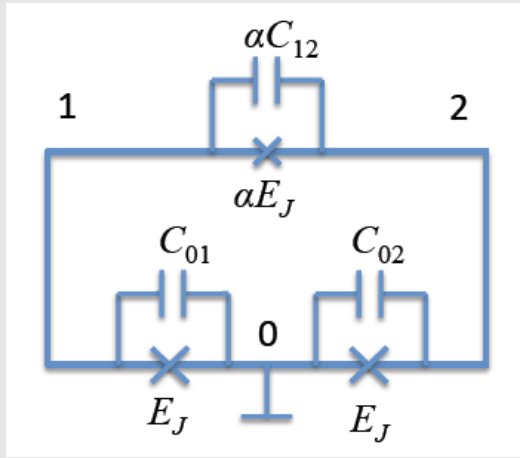
One island (Sec.12)	Two islands
$\hat{N} = \sum_N N\rangle\langle N $	$\frac{(2e)^2}{2} \begin{pmatrix} n_1 & \\ & n_2 \end{pmatrix} C^{-1} \begin{pmatrix} n_1 \\ n_2 \end{pmatrix} = \sum_{N_1, N_2} \mathbf{U}(n_1, n_2) n_1, n_2\rangle\langle n_1, n_2 $
$e^{i\phi} = \sum_N N+1\rangle\langle N $	$e^{i\phi_{01}} = e^{i(\phi_0 - \phi_1)} = \left[\sum_{n_1} n_1 - 1\rangle\langle n_1 \right] \otimes \left[\sum_{n_2} n_2 + 1\rangle\langle n_2 \right] - \text{ignore}$ $e^{-i\phi_{01}} = e^{i(\phi_1 - \phi_0)} = \sum_{n_1} n_1 + 1\rangle\langle n_1 $ $e^{i\phi_{20}} = e^{i(\phi_2 - \phi_0)} = \sum_{n_2} n_2 + 1\rangle\langle n_2 $ $e^{-i\phi_{20}} = e^{i(\phi_0 - \phi_2)} = \sum_{n_2} n_2 - 1\rangle\langle n_2 $ $e^{i\phi_{12}} (\equiv e^{\phi_{\text{ext}} - \phi_{01} - \phi_{20}}) = e^{i(\phi_1 - \phi_2)} = \left[\sum_{n_1} n_1 + 1\rangle\langle n_1 \right] \otimes \left[\sum_{n_2} n_2 - 1\rangle\langle n_2 \right]$ $e^{-i\phi_{12}} = e^{i(\phi_2 - \phi_1)} = \left[\sum_{n_1} n_1 - 1\rangle\langle n_1 \right] \otimes \left[\sum_{n_2} n_2 + 1\rangle\langle n_2 \right]$

$$\mathcal{H} = \frac{(2e)^2}{2} \vec{n}^T C^{-1} \vec{n} - \frac{E_J}{2} (e^{i\phi_{01}} + e^{-i\phi_{01}}) - \frac{E_J}{2} (e^{i\phi_{20}} + e^{-i\phi_{20}}) - \frac{\alpha E_J}{2} (e^{i\phi_{12}} + e^{-i\phi_{12}})$$

$$\begin{aligned}
&\Rightarrow \sum_{n_1, n_2} U(n_1, n_2) |n_1, n_2\rangle\langle n_1, n_2| \\
&\quad - \frac{E_J}{2} \left[|n_1 - 1\rangle\langle n_1| + |n_1 + 1\rangle\langle n_1| \right] \otimes \mathbb{I}_2 \\
&\quad - \frac{E_J}{2} \mathbb{I}_1 \otimes \left[|n_2 + 1\rangle\langle n_2| + |n_2 - 1\rangle\langle n_2| \right] \\
&\quad - \frac{\alpha E_J}{2} \left[|n_1 + 1\rangle\langle n_1| |n_2 - 1\rangle\langle n_2| + |n_1 - 1\rangle\langle n_1| |n_2 + 1\rangle\langle n_2| \right] \\
&\Rightarrow \sum_{n_1, n_2} U(n_1, n_2) |n_1, n_2\rangle\langle n_1, n_2| \\
&\quad - \frac{E_J}{2} \left[|n_1 - 1, \mathbf{n}_2\rangle\langle n_1, \mathbf{n}_2| + |n_1 + 1, \mathbf{n}_2\rangle\langle n_1, \mathbf{n}_2| \right] \rightarrow n_2 \text{ constant} \\
&\quad - \frac{E_J}{2} \left[|\mathbf{n}_1, n_2 + 1\rangle\langle \mathbf{n}_1, n_2| + |\mathbf{n}_1, n_2 - 1\rangle\langle \mathbf{n}_1, n_2| \right] \rightarrow n_1 \text{ constant} \\
&\quad - \frac{\alpha E_J}{2} \left[|n_1 + 1, n_2 - 1\rangle\langle n_1, n_2| + |n_1 - 1, n_2 + 1\rangle\langle n_1, n_2| \right]
\end{aligned}$$

and writing out in matrix form

$$\mathcal{H} = \begin{bmatrix} | -1,0 \rangle & | 0,-1 \rangle & | 0,0 \rangle & | 0,1 \rangle & | 1,0 \rangle \\ \langle -1,0 | & U(-1,0) & -\frac{E_J}{2} & -\frac{E_J}{2} & 0 & 0 \\ \langle 0,-1 | & -\frac{E_J}{2} & U(0,-1) & -\frac{E_J}{2} & 0 & 0 \\ \langle 0,0 | & -\frac{E_J}{2} & -\frac{E_J}{2} & U(0,0) & -\frac{E_J}{2} & -\frac{E_J}{2} \\ \langle 0,1 | & 0 & 0 & -\frac{E_J}{2} & U(0,1) & -\frac{E_J}{2} \\ \langle 1,0 | & 0 & 0 & -\frac{E_J}{2} & -\frac{E_J}{2} & U(1,0) \end{bmatrix}$$



System of tunnelling electrons between the three junctions

4JJ-SERIES FLUX QUBIT [20]

This qubit behaves like a 3JJ qubit, albeit with some **differences**:

- Can be operated in the single or double potential well regime;
- Has a lower **flux** sensitivity and thus better to tune;
- Under certain conditions **only** $|1\rangle \leftrightarrow |2\rangle$ allowed. In other systems other transitions are also possible
- no state leakage to $|3\rangle$.

20.1 Derivation of the Hamiltonian

It's a load of bloat including:

1. Using phase loop quantisation

$$\varphi_1 + \varphi_2 + \varphi_\alpha + \varphi_\beta + 2\pi f_{\text{tot}} = 0;$$

2. Kinetic energy evaluation, using emf induction $V = \dot{\Phi}$:

$$\begin{aligned} \mathcal{T} &= \frac{1}{2} \sum C_i V_i^2 \\ &= \frac{C}{2} \left(\frac{\Phi_0}{2\pi} \right)^2 \left\{ \dot{\varphi}_1^2 + \dot{\varphi}_2^2 + \alpha \dot{\varphi}_\alpha^2 + \beta \left[\dot{\varphi}_1 + \dot{\varphi}_2 + \dot{\varphi}_\alpha + 2\pi \dot{f}_{\text{tot}} \right]^2 \right\}; \end{aligned}$$

3. Potential energy

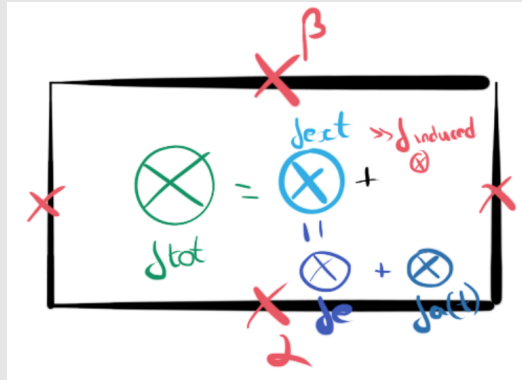
$$U = \sum E_{Ji} [1 - \cos(\varphi_i)].$$

4. Inductive energy

$$U_L = \frac{\Phi_0^2}{2L} (f_{\text{tot}} - f_{\text{ext}})^2.$$

5. Some complicated transformation that maps $\varphi_1, \varphi_2, \varphi_\alpha \rightarrow \varphi_+, \varphi_-, \varphi, \xi$, where

$$\xi = f_{\text{tot}} - f_e \approx f_a(t) \text{ (negligible flux linked by current),}$$



is the time dependent component of the magnetic field to arrive at the lagrangian

$$\begin{aligned}\mathcal{L} &= \mathcal{T} - U \\ &= \frac{C}{2} \left(\frac{\Phi_0}{2\pi} \right)^2 (\dot{\varphi}^2 + \Gamma_+ \dot{\varphi}_+^2 + \Gamma_- \dot{\varphi}_-^2 + \Gamma_\xi \dot{\xi}^2) \\ &\quad - U(\varphi, \varphi_+, \varphi_-, \xi) - \frac{\Phi_0^2}{2L} (\xi - f_a)^2\end{aligned}$$

6. Finding the canonical momenta

$$P_i = \frac{d\mathcal{L}}{d\dot{\varphi}_i}$$

and evaluating the Hamiltonian, $\mathcal{H} = \sum P_i \dot{\varphi}_i - \mathcal{L}$.

7. Splitting the Hamiltonian up into a Harmonic oscillator part

$$\mathcal{H} = 4E_C \left(P_+^2 + \frac{P_+^2}{\Gamma_+} + P_-^2 + \frac{P_-^2}{\Gamma_-} \right) + U(\varphi, \varphi_+, \varphi_-, \xi) + \mathcal{H}_{\text{osc}},$$

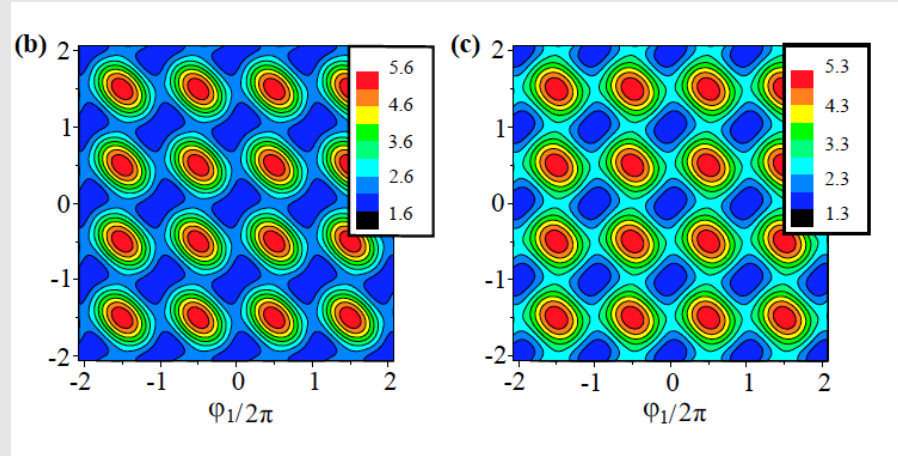
which is always in the ground state, due to its energy being much higher than the qubit levels. Thus it can be dropped from consideration.

20.2 Bloat over

So now lets have a look at some implications of this Hamiltonian.

1.

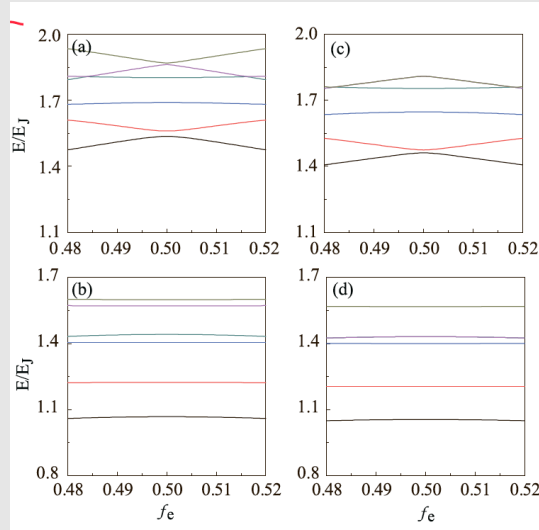
The potential landscape that forms has adjustable single and double wells through the 0.5 threshold in 3 JJ qubit.



2. The solution of $\mathcal{H}_0\psi(\varphi) = E\psi(\varphi)$ is looked for in a block wave form

$$\Psi(\varphi) = u(\varphi) = \sum_{\mathbf{K}} a_{\mathbf{K}} e^{i\mathbf{K}\cdot\varphi}.$$

3. In the single well configuration (**bottom**, $\beta < 0.3$) the bands are flatter and less susceptible to flux noise than in the double well (**top**, $\beta > 0.3$) case.



Note the superior separation of the levels in both the 3JJ

The addition of a time dependent field changes the hamiltonian to give a perturbation:

$$\mathcal{H} = \mathcal{H}_0 - I\Phi_a(t)$$

I = effective current, which is a monster of an equation

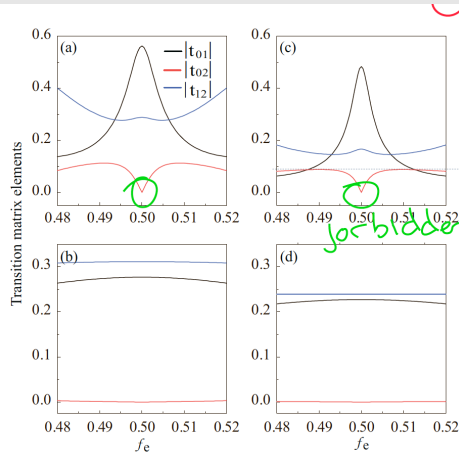
$$\Phi_a(t) = |\Phi_a| \cos(\omega_a t).$$

and we have a transition that is calculated using the eigenstates of the original Hamiltonian

$$t_{ij} = \langle i | I\Phi_a | j \rangle.$$

4. The results are:

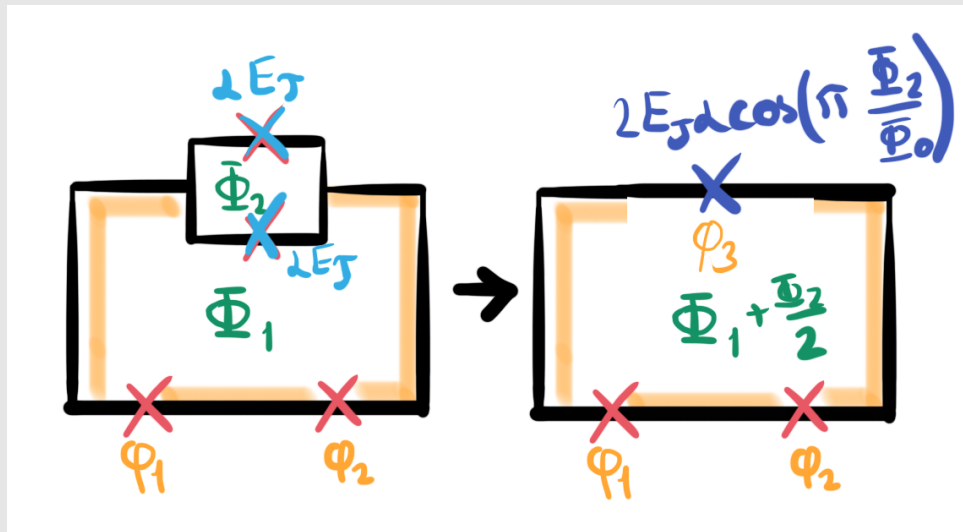
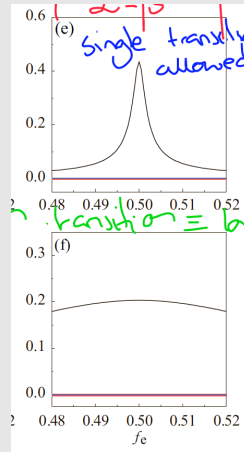
- At the degeneracy point, $|1\rangle \leftrightarrow |3\rangle$ is forbidden, and we have a Ξ energy ladder. Everywhere else it's a Δ



- For low β all transitions are suppressed except $|1\rangle \leftrightarrow |2\rangle$. This makes it a perfect qubit system, with no leakage to other energy levels.

FLUX QUBIT 4 JJ [13]

1. The two JJ's of SQUID come together like in Chapter 16.1 to create a single Josephson junction with a tuneable energy:



$$E_{SQUID} = \frac{\Phi_0 I_c}{2\pi} \times 2|\cos(\pi\Phi_2/\Phi_0)|$$

$$\equiv E_J \times 2|\cos(\pi\Phi_2/\Phi_0)|.$$

2. The effective flux penetrating the full loop is

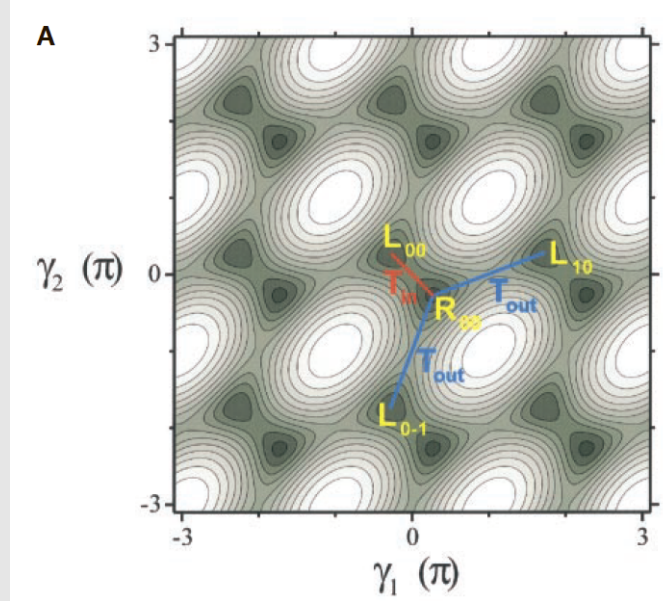
$$\Phi_{\text{total}} = \Phi_1 + \frac{1}{2}\Phi_2.$$

One can think of the flux in the SQUID loop, Φ_2 , affecting the lower one only through one of the JJs.

3. **The potential energy** of the terms $1 - \cos(\phi_{ij})$ of the JJs around the circuit (using the quantisation condition $\phi_3 - \phi_1 + \phi_2 - 2\pi f_{\text{total}} = 2\pi n$):

$$U_{\text{potential}} = E_J \left[2 + 2\alpha - \cos(\phi_1) - \cos(\phi_2) - 2 \cos(\pi f_2) \cos \left(\phi_1 - \phi_2 + 2\pi(f_1 + \frac{1}{2}f_2) \right) \right].$$

And this is what it looks like:



circulate in the same direction, state R in the opposite. The link between the states depends on parameters α and f_2 .

4.

If $f_1 + \frac{1}{2}f_2 = 1$, we recover the 3JJ potential from Chapter 19.

5. **The kinetic energy** is harder to evaluate.

$$\left\{ \begin{array}{l} \vec{V} = 2eC^{-1}\vec{n} \\ \vec{Q} = 2e\vec{n} \quad \Rightarrow U_{\text{kinetic}} = \frac{1}{2} (2e\vec{n}^T) (2eC^{-1}\vec{n}) = \frac{(2e)^2}{2} \vec{n}^T C^{-1} \vec{n}, \\ U_{\text{kinetic}} = \frac{1}{2} \vec{Q} \cdot \vec{V} \end{array} \right.$$

where \vec{n} is the charge state on the 3 islands in the system and C is the capacitance matrix for the system (confusingly, the capacitance for JJ's 1 and 2 is also given the symbol C).

It is common to work classical analogues, where we would write:

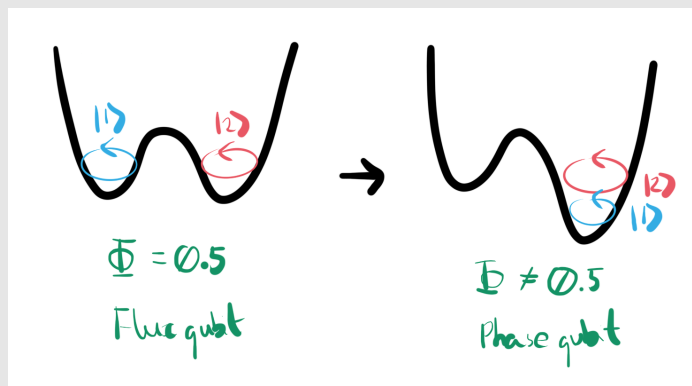
$$\frac{(2e)^2}{2} \vec{n}^T C^{-1} \vec{n} = \frac{1}{2} \vec{p}^T M^{-1} \vec{p}.$$

M is the mass tensor, with normalisation value $\hbar^2 / \frac{(2e)^2}{2C}$, where we have applied $[x, p] = i\hbar$ and $[\phi, n] = i$ to generate the \hbar .

Depending on the direction that we are looking at tunneling across, we get two tensors:

- $M_a = \frac{1}{4}M$ for the $\phi_1 - \phi_2 = 0$ direction (across the tall barrier);
- $M_b = M$ for the $\phi_1 + \phi_2 = 0$ direction (across the small barrier);

6. The result is two different transitions, with two different oscillation frequencies.
7. **Make sure barrier is high enough, to localise state, and small enough to allow sufficient tunneling to occur.**

PHASE QUBIT. $E_J/E_C \sim 10^6$ 

- Confined to a single potential well;
- Has a bias current that controls it's state.

TRANSMON SOURCE

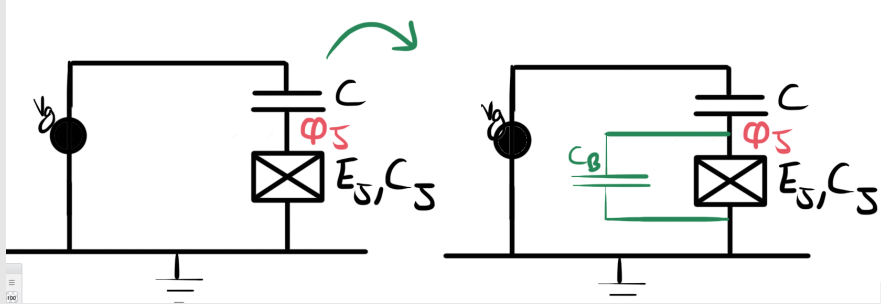
It has experimental coherence times of $\sim 100 \mu\text{s}$. The Transmon paper by Sam Bader December 2013. There are two main factors to consider when making a Cooper pair box

$$\mathcal{H} = E_C \left(\hat{N} - N_{\text{ext}} \right)^2 - E_J \cos \left(\hat{\phi} \right),$$

which was discussed in Ch. 16.

- $E_C/E_J \gg 1$ High anharmonicity, $\frac{E_{12}-E_{01}}{E_{01}} \approx -(8E_J/E_C)^{-1/2}$, allowing addressation of individual transitions;
- $E_C/E_J \ll 1$ Low charge noise sensitivity, so that N_{ext} does not jump and affect the quadratic energy dependance;

It is usually better to have $E_C/E_J \ll 1$, because anharmonicity decreases slowly, while the charge sensitivity will greatly improve. To do this, we need to increase the apparent capacitance of the junction with a large shunt capacitance:



The same equations are used as for the Cooper pair box, except the capacitance $C_J \rightarrow C_B$, which is magnitudes larger.

$$\mathcal{H}_{\text{transmon}} = E_C \left(\hat{N} - N_{\text{ext}} \right)^2 - E_J \cos \left(\hat{\phi} \right),$$

RESONATORS

24.1 Deriving resonator equations

We treat the transmission line as a chain of inductors and capacitors and that is lossless (i.e $R = 0$ and $G = 0$ = no conductance between the lines) with

$l \approx \mu_0$ - the inductance per unit length $c \approx \epsilon_0$ - the capacitance per unit length,

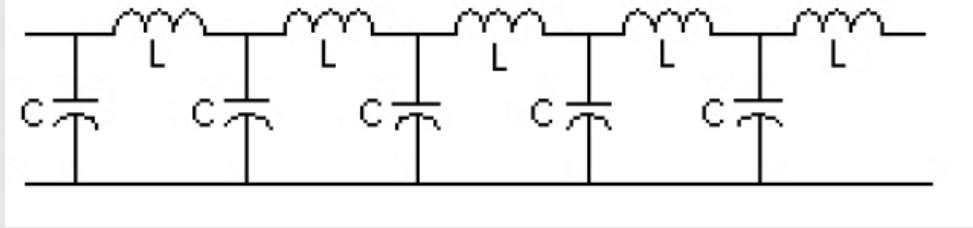
as shown in Fig.40. Recall that for a device of size α , the capacitance will be $C \approx \epsilon_0\alpha$. The current and the voltage in the line will have components going in opposite directions

$$\mathbf{V}_\pm = \mathbf{V}_0 e^{\pm ikx - i\omega t}; \quad \mathbf{I}_\pm = \mathbf{I}_0 e^{\pm ikx - i\omega t}, \quad (31)$$

and be related to each other via the complex impedance. (**Impedance** is equivalent to **Resistance** but for an AC circuit, where charge buildup and current through coils will create time-varying emf in the circuit)

$$V_\pm = \pm Z I_\pm$$

Figure 40: Treat the transmission line as a chain of inductors and capacitors and that is lossless



We write the following equations from their classical analogues

$$\begin{cases} V = -\frac{d\Phi}{dt} = -L \frac{dI}{dt} \\ I = -\frac{dQ}{dt} = -C \frac{dV}{dt} \end{cases} \Rightarrow \text{per unit length} \Rightarrow \begin{cases} \frac{dV}{dx} = -l \frac{dI}{dt} \\ \frac{dI}{dx} = c \frac{dV}{dt} \end{cases}, \quad (32)$$

- We substitute Eq.(31) into Eq.(32) to get

$$\begin{cases} ikV_0 = i\omega l I_0 \\ -i\omega I_0 = -ickV_0 \end{cases} \Rightarrow \begin{cases} Z_0 = \frac{V_0}{I_0} = \frac{\omega l}{k} \\ Z_0 = \frac{V_0}{I_0} = \frac{k}{\omega c} \end{cases} \Rightarrow \mathbf{Z}_0 = \sqrt{\frac{l}{c}} \approx 100\Omega$$

- We differentiate Eq.(32)

$$\frac{d^2V}{dx^2} = -l \frac{d^2I}{dt\partial x} = -l \left(-c \frac{d^2V}{dt^2} \right) \Rightarrow V_{xx} = \frac{1}{1/lc} V_{tt},$$

which has the exact same form as the wave equation $y_{xx} = \frac{1}{v^2} y_{tt}$, from which one can get the speed of wave propagation

$$v = \frac{1}{\sqrt{lc}}$$

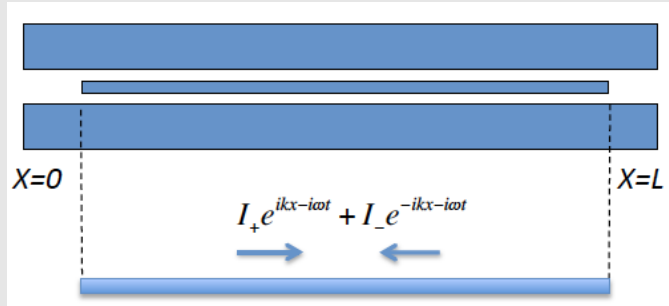


Figure 41

So far we have had a transmission line with no boundary conditions. But now lets us look at a resonator, depicted in figure which has two ends which are cut off and at which

- **The current $I = 0$:** no charge may flow at these points of cut.

Mathematically speaking

$$\begin{cases} I(x = 0) = I_+(x = 0) + I_-(x = 0) = 0 \\ I(x = L) = I_+(x = L) + I_-(x = L) = 0 \end{cases} \Rightarrow \begin{aligned} I_+ &= -I_- \\ I_+ &= -I_- e^{-i2kL} \end{aligned} \Rightarrow k = \frac{\pi n}{L},$$

and the total current at any point in the resonator will be a point on a standing wave

$$I(x, t) = I_+(x, t) + I_-(x, t) = I_+ e^{i\frac{\pi n}{L}x - i\omega t} - I_+ e^{-i\frac{\pi n}{L}x - i\omega t} = I_0 \sin \left[\frac{\pi n}{L}x \right] e^{-i\omega t}. \quad (33)$$

Evaluating the voltage using Eq.(32) and Eq.(33)

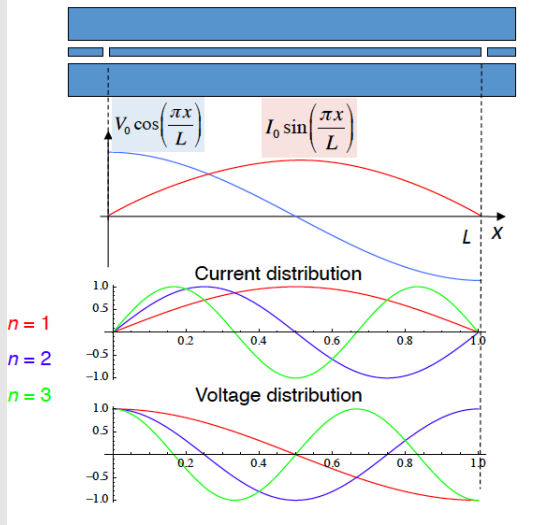


Figure 42: Voltage has an anti-node at the two sides, while current has a node. Multiple modes can be accommodated by the resonator

$$\begin{aligned}
 \frac{dI}{dx} &= -c \frac{dV}{dt} \\
 kI_0 \cos(kx)e^{-i\omega t} &= -c \frac{dV}{dt} \\
 \frac{-1}{i\omega} kI_0 \cos(kx)e^{-i\omega t} &= -cV \\
 \Rightarrow V &= -i \frac{k}{\omega c} I_0 \cos(kx)e^{-i\omega t} \\
 &= |Z| I_0 \cos(kx)e^{-i\omega t} e^{-i\pi/2} \\
 &= V_0 \cos\left(\frac{\pi n}{L} x\right) \exp\left[-i\omega t - i\pi/2\right]
 \end{aligned}$$

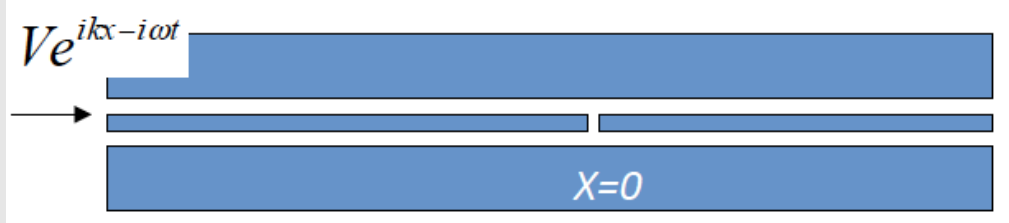
or fully the result is (and depicted in Fig.42)

$$\begin{aligned}
 V &= V_0 \cos\left(\frac{\pi n}{L} x\right) \exp\left[-i\omega t - i\frac{\pi}{2}\right] \\
 I &= I_0 \sin\left(\frac{\pi n}{L} x\right) \exp\left[-i\omega t\right] \\
 V_0 &= |Z| I_0
 \end{aligned}$$

24.2 The voltages at the gaps of the resonator

Now when we consider a boundary, we shall label **+** as moving towards a boundary, and **-** as moving away.

By defining the transmission and reflection as



$$t = \frac{|V_L^-|}{|V_L^+|}; \quad r = \frac{|V_L^-|}{|V_L^+|}; \quad t = 1 + r,$$

we shall write the propagating waves as follows

$$V_L^+ = V_0 e^{ikx-i\omega t}$$

$$V_L^- = rV_0 e^{-ikx-i\omega t}$$

$$V_R^+ = tV_0 e^{ikx-i\omega t},$$

where we assume that no wave is incident from the right hand side ($V_R^+ = 0$). Recalling Eq.(32) that relates the current to the voltage in a line, let us evaluate the current corresponding to each voltage component in the table below

Table 5: In the last step $\mathbf{I}_0 = V_0 \frac{k}{\omega l} = V_0 \frac{1}{vl} = V_0 \frac{\sqrt{c}}{l} = V_0 / Z_0$.

Component	Voltage, V	$\frac{dV}{dx} \equiv -l \frac{dI}{dt}$	$\frac{dI}{dt}$	Current I
Left +	$\mathbf{V}_0 e^{ikx-i\omega t}$	$\Rightarrow ikV_0 e^{ikx-i\omega t}$	$\Rightarrow -\frac{ik}{l} V_0 e^{ikx-i\omega t}$	$\Rightarrow \frac{k}{\omega l} V_0 e^{ikx-i\omega t} = \mathbf{I}_0 e^{ikx-i\omega t}$
Left -	$r\mathbf{V}_0 e^{-ikx-i\omega t}$	$-ikrV_0 e^{-ikx-i\omega t}$	$\frac{ikr}{l} V_0 e^{-ikx-i\omega t}$	$-\frac{k}{\omega l} rV_0 e^{-ikx-i\omega t} = -r\mathbf{I}_0 e^{-ikx-i\omega t}$
Right +	$t\mathbf{V}_0 e^{ikx-i\omega t}$	$iktV_0 e^{ikx-i\omega t}$	$\frac{ik}{l} tV_0 e^{ikx-i\omega t}$	$\frac{k}{\omega l} tV_0 e^{ikx-i\omega t} = t\mathbf{I}_0 e^{ikx-i\omega t}$

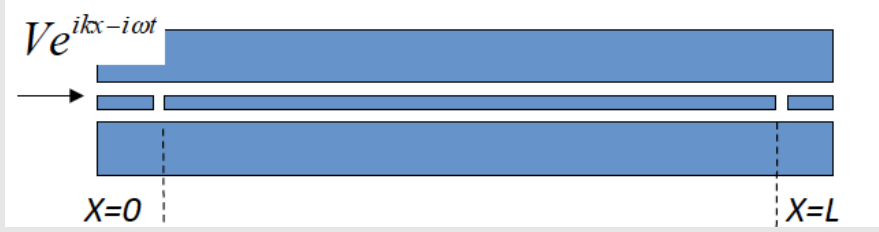
Now, the equality of the currents and voltages on the two sides of the gap at $x = 0$ **and including the potential difference drop across the gap**, $V_{\text{drop}} = I_R^+ Z_{\text{gap}} = \frac{tI_0 e^{-i\omega t}}{i\omega C_{\text{gap}}}$, that causes the current on the other side of the gap

$$\begin{cases} I_0 e^{-i\omega t} - rI_0 e^{-i\omega t} = tI_0 e^{-i\omega t} \\ V_0 e^{-i\omega t} + rV_0 e^{-i\omega t} = tV_0 e^{-i\omega t} + \frac{tI_0}{i\omega C_{\text{gap}}} \end{cases} \Rightarrow \begin{cases} 1 - r = t \\ 1 + r = \left(1 + \frac{1}{i\omega C_{\text{gap}} Z}\right)t \end{cases}$$

and one can simply solve for r and t coefficients

$$\mathbf{t} = \frac{1}{1 + \frac{1}{i2\omega C_{\text{gap}} Z}} = \frac{i\alpha}{1 + i\alpha}; \quad \mathbf{r} = \frac{1}{1 + i\alpha}; \quad \alpha = 2\omega C_{\text{gap}} Z.$$

Now suppose that we defined another gap further down the line. Let us see what the resulting voltage at $x = L$ would be. The voltage that is transmitted across the gap initially is tV_0 .



$$tV_0 \rightarrow \{\text{travels } L \text{ to } x = L\} \rightarrow tV_0 e^{ikL - i\omega t}$$

$$\rightarrow \{\text{reflects, travels } L \text{ to } x = 0, \text{ reflects, travels } L \text{ to } x = L\} \rightarrow r^2 tV_0 e^{ik3L - i\omega t}$$

$$\rightarrow \{\text{reflects, travels } L \text{ to } x = 0, \text{ reflects, travels } L \text{ to } x = L\} \rightarrow r^4 tV_0 e^{ik5L - i\omega t}$$

$$\rightarrow \{\text{reflects, travels } L \text{ to } x = 0, \text{ reflects, travels } L \text{ to } x = L\} \rightarrow r^6 tV_0 e^{ik7L - i\omega t}$$

$\rightarrow \dots$

so that the total voltage

$$\begin{aligned} V(x = L) &= tV_0 e^{ikL - i\omega t} \left(1 + r^2 e^{i2kL} + r^4 e^{i4kL} + r^6 e^{i6kL} + \dots \right) \\ &= tV_0 e^{ikL - i\omega t} \sum_{n=0}^{\infty} \left(r^2 e^{i2kL} \right)^n, \quad \text{and since } r < 1 \text{ this is a convergent power series} \\ &= \frac{tV_0 e^{ikL - i\omega t}}{1 - r^2 e^{i2kL}}. \end{aligned}$$

To make good use of this, we need to use

$$\begin{cases} e^{i\alpha + i\alpha^2/2} = 1 + i\alpha + O(\alpha^3) \text{ (proof by simple expansion)} \\ r = (1 + i\alpha)^{-1} \text{ (from before)} \end{cases} \Rightarrow r^2 \approx e^{-i2\alpha + \alpha^2}$$

This and further mathematical stuff will lead to the voltage inside the resonator to be

$$V_r = \frac{V_0}{\alpha} \frac{i(-1)^n e^{-i\omega t}}{1 + i \frac{2\delta\omega}{\Delta\omega}}; \quad \Delta\omega = 2\alpha^2 f_0; \quad \delta\omega = \text{offset from } n^{\text{th}} \text{ resonance.}$$

As can be seen, the maximum voltage inside the resonator is $1/\alpha$ times larger than the external field - we

have boosted the total field from the combination of reflections. In a similar way the voltage/power leaving the resonator are

$$V_{out} = tV_r = \frac{V_0}{\alpha} \frac{i(-1)^{n+1} e^{-i\omega t}}{1 + i \frac{2\delta\omega}{\Delta\omega}}; \quad P_{out} = \frac{P_0}{1 + \left(\frac{2\delta\omega}{\Delta\omega}\right)^2}.$$

Important is the quality factor of the resonator. This is the ratio of the resonance frequency to the width of the resonance peak

$$Q = \frac{\omega_{\text{resonance}}}{\Delta\omega} = \frac{\pi}{(2\omega Z C_{gap})^2}.$$



Using results of Table.2, with $V = V_0(a + a^\dagger)$; $I = iI_0(a - a^\dagger)$, and the results from the classical resonator $V = V_0 \cos(\frac{\pi n}{L}x)$; $I = I_0 \sin(\frac{\pi n}{L}x)$, the quantum field is

$$\begin{aligned}\hat{V} &= \sqrt{\frac{\hbar\omega}{2c}}(a + a^\dagger) \cos\left(\frac{\pi n}{L}x\right) \\ \hat{I} &= i\sqrt{\frac{\hbar\omega}{2l}}(a - a^\dagger) \sin\left(\frac{\pi n}{L}x\right)\end{aligned}$$

and the total energy, given by the Hamiltonian is

$$\begin{aligned}\mathcal{H} &= \frac{1}{L} \int_0^L \left(\frac{l\hat{I}^2}{2} + \frac{c\hat{V}^2}{2} \right) dx \\ &= \frac{l}{2} \frac{-\hbar\omega}{2l} (a - a^\dagger)^2 \frac{1}{L} \int_0^L \cos^2\left(\frac{\pi n}{L}x\right) dx + \frac{c}{2} \frac{\hbar\omega}{2c} (a + a^\dagger)^2 \frac{1}{L} \int_0^L \sin^2\left(\frac{\pi n}{L}x\right) dx \\ &= -\frac{\hbar\omega}{4} \frac{1}{2} (aa - aa^\dagger - a^\dagger a + a^\dagger a^\dagger) + \frac{\hbar\omega}{4} \frac{1}{2} (aa + aa^\dagger + a^\dagger a + a^\dagger a^\dagger) \\ &= \frac{\hbar\omega}{8} (aa^\dagger + a^\dagger a) = \frac{\hbar\omega}{8} ((a^\dagger a + 1) + a^\dagger a) = \hbar\omega \left(\hat{N} + \frac{1}{2} \right),\end{aligned}$$

so the resonator is a quantum harmonic oscillator.

24.3 Resonator types

- $\lambda/2$ resonator - transmission lines at either end. Transmission is maximum;
- $\lambda/4$ resonator - one end is grounded, other is coupled to transmission line. Transmission has a dip.

24.4 Resonator Emission

This is based off a slightly related paper [6] which talks about shining a light on a cavity. In general, the intensity of a signal from a resonator can be fitted by:

$$\text{Intensity} = I_0 + I_1 \frac{[q + 2(\omega - \omega_0)/\Gamma]^2}{1 + [2(\omega - \omega_0)/\Gamma]^2}$$

where apart from scaling and offset I_0, I_1 there is:

- $q = \frac{\text{Resonant scattering amplitude}}{\text{Non-resonant amplitude}}$;
- Γ is the FWHM of the scattering (linewidth)

Light shone on the cavity in Fig. 43 will be reflected in one of two regimes

- Emission at the cavity frequency and inevitable emission to continuum (non-resonant) frequency $q \approx 1$
Fig. 43a - asymmetric fit;
- Non-resonant emission at a continuum of available frequencies $q \ll 0$ Fig. 43b - flipped lorentzian;
- (Not observed - very strong resonant emission - standard lorentzian) $q \gg 1$.

24.5 Resonator example [2]

In this experiment a $\lambda/2$ resonator was used (coupled to transmission line at both ends) which had

$$\begin{cases} l_1 = \frac{L_{sq}}{W} = \frac{0.7 \text{ nH}}{3 \mu\text{m}} = 2.3 \times 10^{-4} \text{ H/m} \\ c_1 = 0.85 \times 10^{-10} \text{ F/m} \end{cases} \Rightarrow Z_1 = \sqrt{\frac{l_1}{c_1}} = 1.6 \text{ k}\Omega, v = \frac{1}{\sqrt{l_1 c_1}} = 7.2 \times 10^6 \text{ m/s}$$

- Due to the big different inductance, there would be a current maximum at the edges
- Only odd modes will be coupled, so that the current in the center of the resonator (where the cqs is) is not zero.

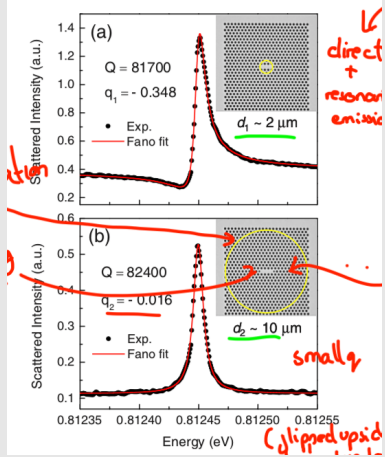


Figure 43: Bigger area of reflect light means that there is more contribution from non-resonant processes. Note that in figure B, the lorentzian is flipped by the experiment (from formula is should be upside down).

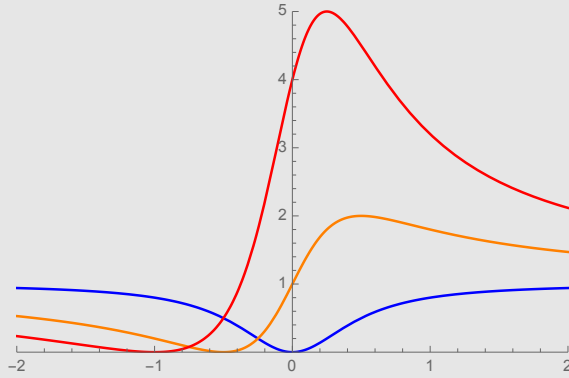


Figure 44: Red: $q = 2$, Orange: $q = 1$, Blue: $q = 0$. Note that when there is very weak resonant emission, we are centred on the dip, otherwise the dip will actually be off-center.

- The decay in such a resonator is:

$$\kappa = \frac{4Z_0}{Z_1} \frac{v}{L}.$$

24.6 Resonator Fabrication

Example sizes: [19]:

- Separation of $20 \mu\text{m}$ from ground plane;
- Width of line is $5 \mu\text{m}$

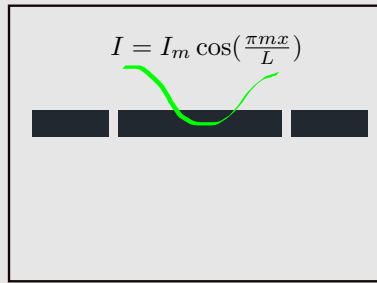


Figure 45: Maximum current at the interface - **very different to the usual case where there is no current at the boundaries!**

To realise, we put the atom at the maximum voltage of a ‘cut out’ resonator. Full details are given in [4].

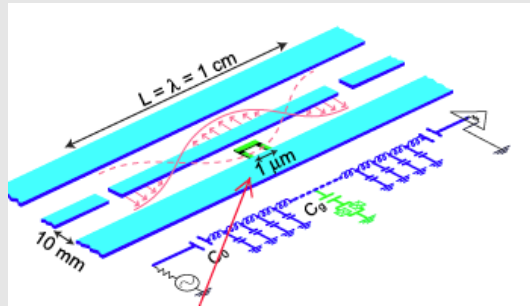


Figure 46: Qubit is placed at the antinode of resonator. The transmission line itself is modelled as a sequence of capacitors and inductors.

- The coupling strength is very large because of the small sizes of the elements. The voltage between the ground plane and resonator is 0.2 V/m , which is 100 times stronger than for a regular cavity;
- The geometry of the resonator fixes its frequency \rightarrow no $1/f$ noise;
- Atom will emit directly into the line, and with a high enough quality factor, losses are minimised.

CHAPTER 25

QUBIT-RESONATOR INTERACTION [4]

Please see Sec. 24 for a derivation formulas for the resonator itself.

1. The two-level qubit with a separation between the energy levels ΔE has the Hamiltonian

$$\mathcal{H}_a = -\frac{\Delta E}{2} \sigma_z.$$

2. This qubit is placed in close proximity with a resonator, which, as we have seen in the previous chapter, has a harmonic oscillator-like Hamiltonian

$$\mathcal{H}_r = \hbar\omega \left(\hat{N} + \frac{1}{2} \right) \quad a^\dagger |N\rangle = \sqrt{N+1} |N+1\rangle; \quad a |N\rangle = \sqrt{N} |N=1\rangle.$$

where for simplicity we neglect the constant energy term.

3. The general state of a system, where the qubit is in state n and the resonator in state N (i.e. N photons) will be

$$|n, N\rangle.$$

Qualitatively speaking, the way the qubit interacts with the resonator in one of the two ways

- Qubit absorbs a photon and transitions to the excited state: $|0, N+1\rangle \rightarrow |1, N\rangle$;
- Qubit relaxes to ground state and releases a photon into the resonator: $|1, N\rangle \rightarrow |0, N+1\rangle$.

This can be expressed via the interaction Hamiltonian

$$\mathcal{H}_{\text{int}} = a\sigma^+ + a^\dagger\sigma^-.$$

$$\mathcal{H} = -\frac{\Delta E}{2}\sigma_z + \hbar\omega_r a^\dagger a + \hbar g_0 \left(a\sigma^+ + a^\dagger\sigma^- \right),$$

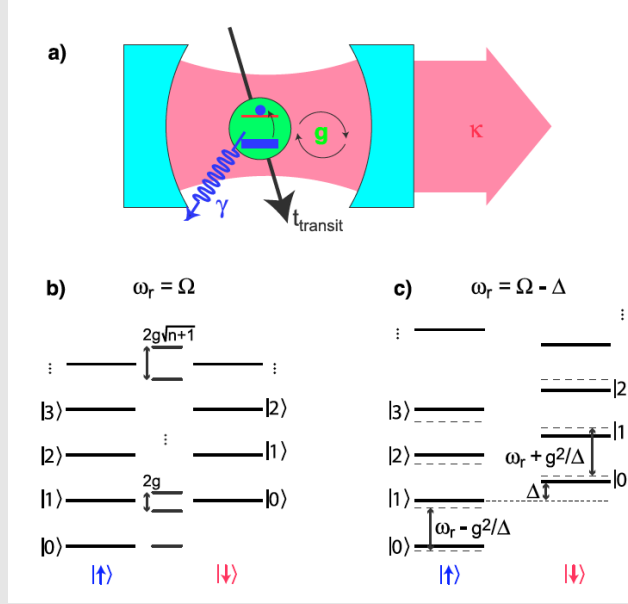


Figure 47: Interaction between states with same energy creates the superposed states in the middle.

This gives rise to energy levels depicted in Fig.47 which we write out in terms of the basis states, recalling that $\sigma_z = |e\rangle\langle e| - |g\rangle\langle g|$, $\sigma^+ = |e\rangle\langle g|$, $\sigma^- = |g\rangle\langle e|$, $a = \sqrt{N+1}|N\rangle\langle N+1|$, $a^\dagger = \sqrt{N+1}|N+1\rangle\langle N|$:

$$\begin{aligned} \mathcal{H} &= \left[\frac{\Delta E}{2} (|e\rangle\langle e| - |g\rangle\langle g|) \right] \otimes \mathbb{I}_N + \mathbb{I}_n \otimes \left[\hbar\omega_r \sum_N N |N\rangle\langle N| \right] + \\ &\quad + \hbar g_0 \left[|e\rangle\langle g| \sqrt{N+1} \sum_N |N\rangle\langle N+1| + |g\rangle\langle e| \sum_N \sqrt{N+1} |N+1\rangle\langle N| \right] \\ &= \sum_N \left(\hbar N \omega_r - \frac{\Delta E}{2} \right) |g, N\rangle\langle g, N| + \left(\hbar N \omega_r + \frac{\Delta E}{2} \right) |e, N\rangle\langle e, N| \leftarrow \text{diagonal} \\ &\quad + \hbar g_0 \sqrt{N+1} \left[|e, N\rangle\langle g, N+1| + |g, N+1\rangle\langle e, N| \right] \leftarrow \text{cross terms} \end{aligned}$$

and in matrix form

$$\mathcal{H} = \begin{bmatrix} |g,N\rangle & |e,N\rangle & |g,N+1\rangle & |e,N+1\rangle \\ \langle g,N| & \hbar N \omega_r - \frac{\Delta E}{2} & 0 & 0 \\ \langle e,N| & 0 & \hbar N \omega_r + \frac{\Delta E}{2} & \hbar g_0 \sqrt{N+1} \\ \langle g,N+1| & 0 & \hbar g_0 \sqrt{N+1} & \hbar(N+1)\omega_r - \frac{\Delta E}{2} \\ \langle e,N+1| & 0 & 0 & \hbar(N+1)\omega_r + \frac{\Delta E}{2} \end{bmatrix}$$

25.1 General solutions

1. For the ground state, we take the top row, which will have the lowest energy

$$|g, 0\rangle = \begin{pmatrix} 1 \\ 0 \\ \vdots \end{pmatrix} \text{ with energy } -\frac{\Delta E}{2}.$$

2. Then diagonalising an arbitrary middle matrix (N value incremented for convenience)

$$\begin{aligned} \mathcal{H}_{\text{middle}} &= \begin{bmatrix} |e,N\rangle & |g,N+1\rangle \\ \langle e,N| & \hbar \omega_r(N + \frac{1}{2}) + \hbar \Delta & \hbar g_0 \sqrt{N+1} \\ \langle g,N+1| & \hbar g_0 \sqrt{N+1} & \hbar \omega_r(N + \frac{1}{2}) - \hbar \Delta \end{bmatrix} \\ &= \hbar \omega_r(N + \frac{1}{2}) \mathbb{I} + \frac{\hbar \Delta}{2} \sigma_z + \hbar g_0 \sqrt{N+1} \sigma_x \\ &= \hbar \omega_r(N + \frac{1}{2}) \mathbb{I} + \frac{1}{2} \sqrt{(\hbar \Delta)^2 + 4 \hbar^2 g_0^2 (N+1)} \left(\cos(\theta) \sigma_z + \sin(\theta) \sigma_x \right) \\ &= \hbar \omega_r(N + \frac{1}{2}) \mathbb{I} + E_{\text{coupled}} (\cos(\theta) \sigma_z + \sin(\theta) \sigma_x) \\ \text{where } E_{\text{coupled}} &= \frac{\hbar}{2} \sqrt{\Delta^2 + 4 g_0^2 (N+1)}; \quad \tan(\theta) = \frac{g_0 \sqrt{N+1}}{\Delta/2}. \end{aligned}$$

Rotated frame

$$\mathcal{H}' = \hbar \omega_r(N + \frac{1}{2}) \mathbb{I} + \frac{E_{\text{coupled}}}{2} \sigma_z = \begin{pmatrix} \hbar \omega_r(N + \frac{1}{2}) + \frac{E_{\text{coupled}}}{2} & 0 \\ 0 & \hbar \omega_r(N + \frac{1}{2}) - \frac{E_{\text{coupled}}}{2} \end{pmatrix}$$

- Eigenstates: $|\tilde{0}\rangle, |\tilde{1}\rangle;$
- Eigenenergies: $\hbar \omega_r(N + \frac{1}{2}) \pm \frac{E_{\text{coupled}}}{2}.$

3. By applying a rotation of $\frac{\theta}{2}$ about the y-axis

$$U = \exp\left[i\frac{\theta}{2}\sigma_y\right] = \cos(\frac{\theta}{2})\mathbb{I} + i\sin(\frac{\theta}{2})\sigma_y,$$

we will end up with

Raw frame

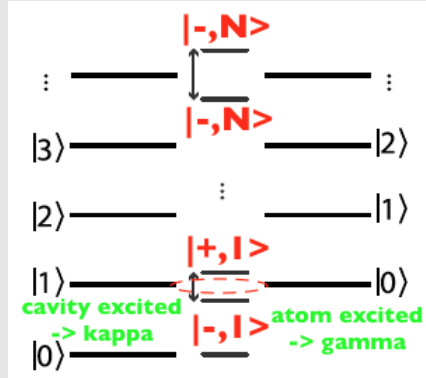
- Eigenstates:

$$|+, N\rangle = U^\dagger |\tilde{1}\rangle = \left(\cos(\frac{\theta}{2})\mathbb{I} - i\sin(\frac{\theta}{2})\sigma_y \right) \begin{pmatrix} 1 \\ 0 \end{pmatrix} = \begin{pmatrix} \cos(\frac{\theta}{2}) \\ \sin(\frac{\theta}{2}) \end{pmatrix}$$

$$|-, N\rangle = U^\dagger |\tilde{0}\rangle = \begin{pmatrix} -\sin(\frac{\theta}{2}) \\ \cos(\frac{\theta}{2}) \end{pmatrix} \equiv -\sin(\frac{\theta}{2}) |e, N\rangle + \cos(\frac{\theta}{2}) |g, N+1\rangle$$

- Eigenenergies:

$$\text{Energies}_\pm = \hbar\omega_r(N + \frac{1}{2}) \pm \frac{E_{\text{coupled}}}{2}$$



25.2 Resonant case

The eigenstate spectrum of the $|\pm, N\rangle$ states is ladder-like (down the middle). For a single photon, and on resonance ($\Delta = 0$) the entangled states are

$$|\pm, 1\rangle = \frac{|e, 0\rangle \pm |g, 1\rangle}{\sqrt{2}} \quad \text{with energies } \hbar\omega_r(N + \frac{1}{2}) \pm \hbar g_0 \sqrt{N + 1},$$

will flip flop between the original levels with a Rabi frequency $2g_0/2\pi$. As the atom is excited for exactly half of the state, with a decay rate γ , and the cavity is excited for the other half of the state, with a decay rate κ the net decay rate is $\frac{\gamma+\kappa}{2}$ and to observe Rabi oscillations between the original states

$$2g > \frac{\kappa + \gamma}{2} \quad \text{to see Rabi oscillation before decay == strong coupling}$$

- If a cavity is resonant with the atom, then the atom can emit and reabsorb photons coherently. Alternatively, if the atom is far detuned from any cavity mode, its eigenstates are very nearly the eigenstates of the system;
- The rate at which an atomic level decays is proportional (by Fermi's golden rule) to the density of states of the local electromagnetic field at that atomic frequency;
- But the mode quantization enforced by a cavity redefines the density of states available to the atom, increasing it in the case of resonance or diminishing it in the case of far detuning. By this channel, the cavity can enhance or reduce the spontaneous emission rate of an atom [20, 21] in what is known as the Purcell effect.

25.3 Non-resonant case

In the case that large detuning $\Delta \gg g$ is applied (detuning is much greater than the coupling) we expand

$$|\pm, 1\rangle = -\sin\left(\frac{\theta}{2}\right)|e, 0\rangle + \cos\left(\frac{\theta}{2}\right)|g, 1\rangle \quad \tan(\theta) = \frac{g_0\sqrt{N+1}}{\Delta/2}.$$

$$|-, 1\rangle \approx \frac{-g}{\Delta}|e, 0\rangle + |g, 1\rangle$$

- Atom decays at a rate $\frac{-g}{\Delta}$;
- Cavity decays at a rate 1;
- $\Gamma = (g/\Delta)^2\gamma + \kappa$

and

$$|+, 1\rangle \approx |g, 0\rangle + \frac{g}{\Delta}|e, 1\rangle$$

- Atom decays at rate 1;

- Cavity decays at rate $\frac{-g}{\Delta}$;

- $\Gamma = \gamma + (g/\Delta)^2 \kappa$.

If we apply a unitary transformation ($U = \exp(\frac{g}{\Delta}(a\sigma^+ + a^\dagger\delta^-))$):

$$\begin{aligned} U\mathcal{H}U^\dagger &\approx \hbar\omega_r a^\dagger a + \left[\frac{\hbar\Omega}{2} + \frac{g^2}{\Delta} \left(a^\dagger a + \frac{1}{2} \right) \right] \sigma_z \\ &= \hbar \left[\omega_r + \frac{g^2}{\Delta} \sigma_z \right] a^\dagger a + \frac{\hbar}{2} [\Omega + \frac{g^2}{\Delta}] \sigma_z \end{aligned}$$

which we can interpret as

- **Stark/Lambda shift:** photon-number-dependent shift of the atom's energy by $\frac{g^2}{\Delta} (a^\dagger a + \frac{1}{2})$;
- **Dispersive shift (cavity energy shifts by χ):** The atom “pulls” the cavity frequency by $\chi = \pm g^2/\Delta$ depending on the atomic state (we can neglect the constant offset as it will not affect transition energies).

Because of the Purcell effect (cavity limits density of state that an excited qubit can decay into) suppresses the local electromagnetic density of states at the detuned qubit frequency, thus inhibiting excited state decay.

An example of this effect can be found in the following paper about SAW [11]

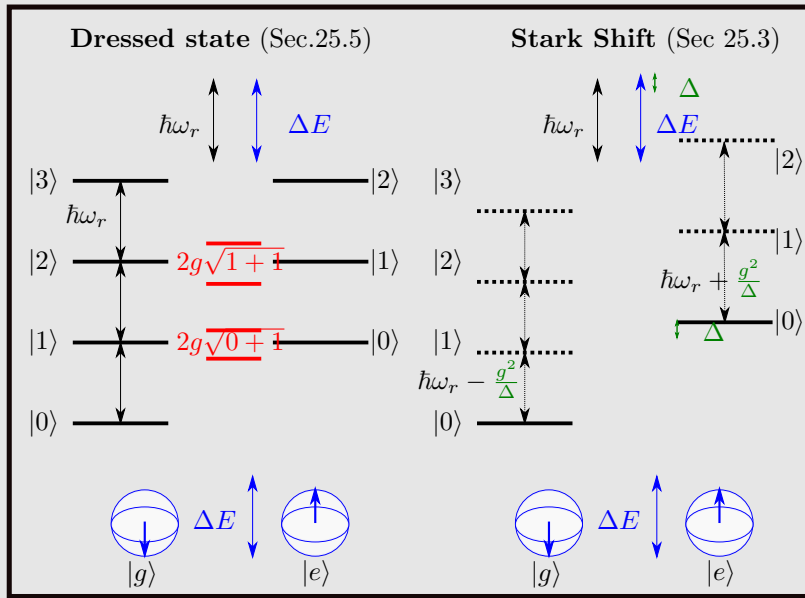


Figure 48: When there is 0 detuning (right, $\hbar\omega_r = \Delta E$) the dressed states create a degeneracy which is lifted by the coupling. When there is a sizeable detuning Δ (left), there will be no degeneracy. Instead - per Subsec. 25.3 the energy of the atom shifts by a constant factor (not interesting) whereas the resonator ladder energy separation changes by $\pm \frac{g^2}{\Delta}$ depending on state of atom.

25.4 Stark shift measurements

Let us use the dispersive shift of the resonator frequency, dependent on the state of the qubit as in Fig. 49. Measurements can be done at either:

- $\omega'_r \pm \chi$: amplitude for the two state will be different;
- ω'_r : phase for the two states will be different (shifted by π).

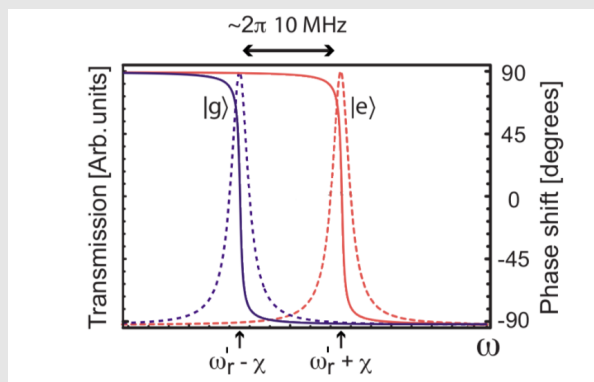


Figure 49: There will be 2 transmission profiles, depending on the state of the qubit. Transmission (dotted) vs phase (solid)

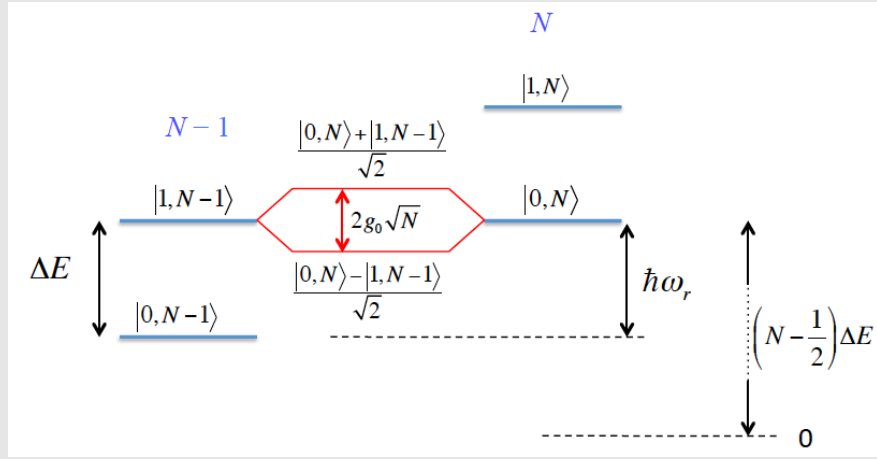


Figure 50: Degeneracy between different photon states . Note that relative to zero energy (for $|0,0\rangle$) one is shifted by $N\hbar\omega_r - \frac{\Delta E}{2} = \left(N - \frac{1}{2}\right)\Delta E$

25.5 Resonant case = Dressed States

$$\hbar\omega_r \equiv \Delta E$$

$$\mathcal{H} = \begin{bmatrix} |0,N-1\rangle & |1,N-1\rangle & |0,N\rangle & |1,N\rangle \\ \langle 0,N-1| & \Delta E(N - \frac{3}{2}) & 0 & 0 \\ \langle 1,N-1| & 0 & \Delta E(N - \frac{1}{2}) & \hbar g_0 \sqrt{N} \\ \langle 0,N| & 0 & \hbar g_0 \sqrt{N} & \Delta E(N - \frac{1}{2}) \\ \langle 1,N| & 0 & 0 & \Delta E(N + \frac{1}{2}) \end{bmatrix},$$

and a degeneracy appears between the two middle states as in Fig.50. The middle part of the Hamiltonian is treated as a two levels system

$$\mathcal{H}_{\text{middle}} = \begin{pmatrix} \Delta E(N - \frac{1}{2}) & \hbar g_0 \sqrt{N} \\ \hbar g_0 \sqrt{N} & \Delta E(N - \frac{1}{2}) \end{pmatrix} \Rightarrow \begin{bmatrix} |1,N-1\rangle & |0,N\rangle \\ \langle 1,N-1| & 0 \\ \langle 0,N| & \hbar g_0 \sqrt{N} \end{bmatrix},$$

which can be diagonalised with two states separated by an energy $g_0\sqrt{N}$, also depicted in Fig.50. The degeneracy is lifted for every single state, and these states are known as dressed.

$$|\Psi\rangle = \frac{|0,N\rangle \pm |1,N-1\rangle}{\sqrt{2}} \quad E = \pm g_0\sqrt{N}.$$

Fig.51 is interpreted as follows:

1. We have a qubit, that is either in state $|0\rangle$ or $|1\rangle$, whose energy spectrum is shown by the green lines. By controlling some bias e.g. gate voltage, we choose the energy difference ΔE between the two levels.
2. A resonator will create an energy ladder of the mixed system, shifted by $\hbar\omega_r$.
3. At the degeneracy point for the new qubit-resonator system, degeneracy will be lifted by the qubit-resonator interaction \rightarrow we have just seen that two states $|0, N\rangle, |1, N-1\rangle$ will interact and develop a splitting of $2g_0\sqrt{N}$ at the degeneracy point.

This happens where $\Delta E = \hbar\omega_r$ i.e. the level separation matches the drive from the resonator. For all other cases there is no splitting/mixing.

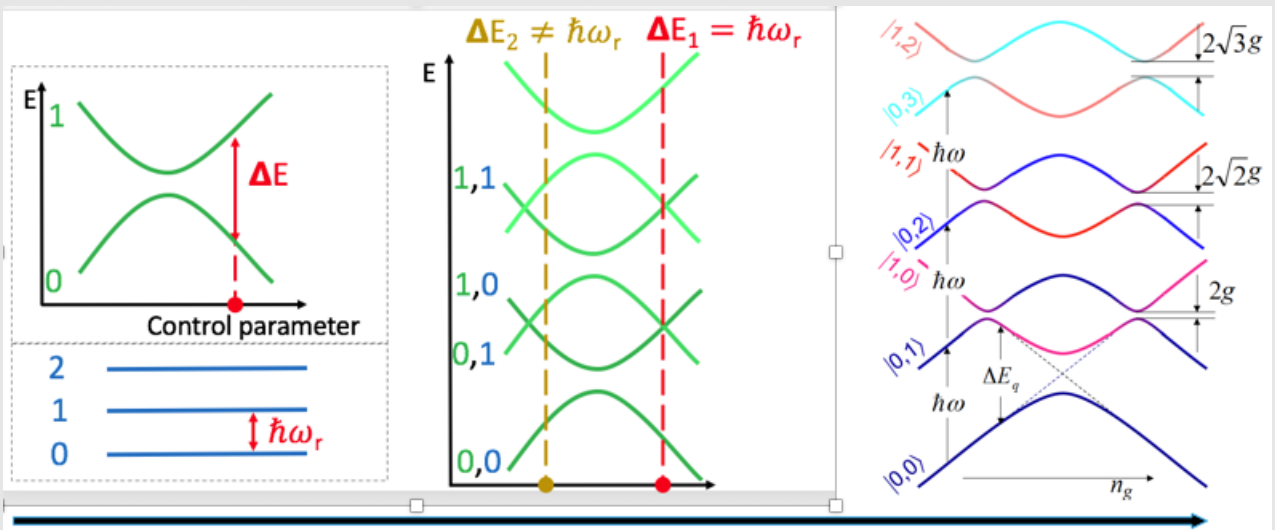


Figure 51: Degeneracy for the qubit-resonator system occurs when $\hbar\omega_r \equiv \Delta E$. As seen with the above matrix, interaction between $|0, N\rangle$ and $|1, N-1\rangle$ will lift the degeneracy at this anticrossing.

Now let us perform measurements on this system.

1. We bias the qubit to an arbitrary ΔE and couple it with a resonator, with frequency ω_r .
2. Then we send a weak field probe signal, measuring its transmission as we sweep it. It will have a peak at the frequency of resonator ω_0 , which corresponds to the excitation of the qubit.
3. We plot the maximum of this peak as shown in Fig.52.
4. Then we step the control parameter, to move along the qubit curve and repeat.
5. Everywhere apart from the degeneracy point, there will be a single transition - the $\hbar\omega_0$ one that will dominate.

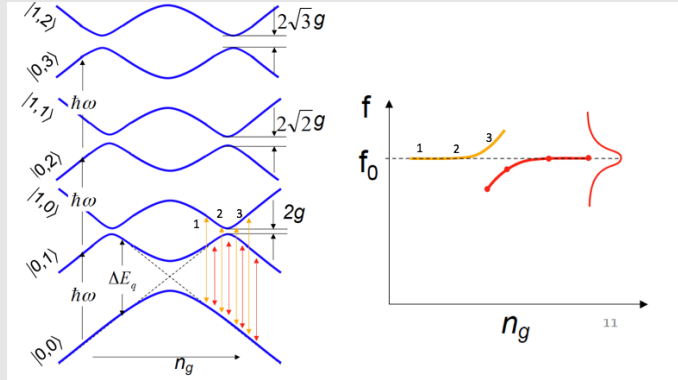


Figure 52: We use a weak probe field and measure its transmission curve. The peak corresponds to a favourable transition frequency. **We cannot see the qubit - only where the energy separation happens to match the resonator frequency.**

6. However near the degeneracy point, two transitions, symmetrical about ω_0 will be present. This is a result of the $\pm g_0\sqrt{N}$ splitting that occurs at the crossing point.
7. Thus at the degeneracy point one observes two peaks for the transmission as in Fig.?? - the two strong transitions at the splitting point. Generally the lower peak will be stronger - smaller energy difference in the process.
8. The width of the peak γ corresponds to the width of the level - the area to which one can excite to. One needs $\gamma \ll g_0$ to observe such a transitions. This is fulfilled for a strong drive.

$$\hbar\Omega_{\text{splitting}} = 2g\sqrt{N},$$

defines the Rabi frequency $\Omega_{\text{splitting}}$ and becomes constant for $N \gg 1$.

The configuration in Fig.?? is the Mollow triplet - it is probed either by a weak field (as explained above) or directly observed in the spectrum emitted by the atom.

25.6 Actual simulations

When performing the actual simulations, I found that we need to consider the atom Hamiltonian not as:

$$\frac{\Delta E}{2} \begin{pmatrix} 1 & 0 \\ 0 & -1 \end{pmatrix}$$

but as

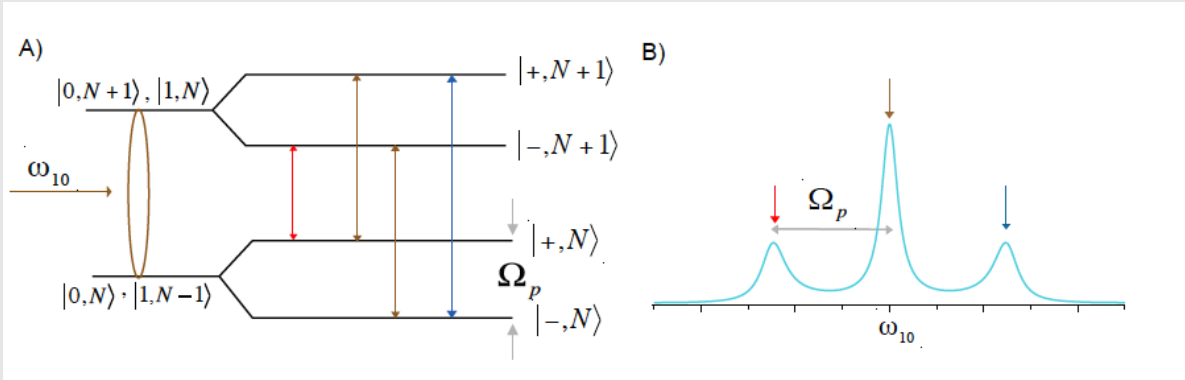


Figure 53: Mollow triplet is formed when driving the system at resonance

$$\Delta E \begin{pmatrix} 1 & 0 \\ 0 & 0 \end{pmatrix}$$

Reason is, that we cannot have negative energy in the resonator ($E_{\text{res}} = \hbar\omega_r N$) and $N \geq 0$. Therefore the matrices from above are now:

$$\mathcal{H} = \begin{bmatrix} |g,N\rangle & |e,N\rangle & |g,N+1\rangle & |e,N+1\rangle \\ \langle g,N| & \hbar N \omega_r & 0 & 0 \\ \langle e,N| & 0 & \hbar N \omega_r + \Delta E & \hbar g_0 \sqrt{N+1} \\ \langle g,N+1| & 0 & \hbar g_0 \sqrt{N+1} & \hbar(N+1)\omega_r \\ \langle e,N+1| & 0 & 0 & \hbar(N+1)\omega_r + \Delta E. \end{bmatrix}$$

and where we will wind up with the following:

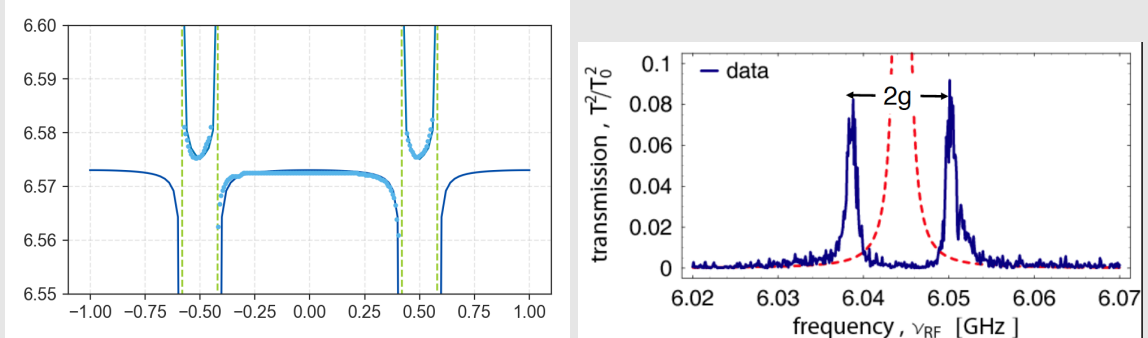


Figure 54: Anticrossing fit to experimental data. At the degeneracy point, when the resonator field coincides with the qubit transition, two types of transitions appear from the splitting at the degeneracy point. The splitting $\pm g_0 \sqrt{N}$ will put two peaks either side of the central one (which disappears - there is no longer a level to accommodate this transition). γ characterises the width of the split levels and hence the width of the peak. If the width is too big, no splitting shall be seen.

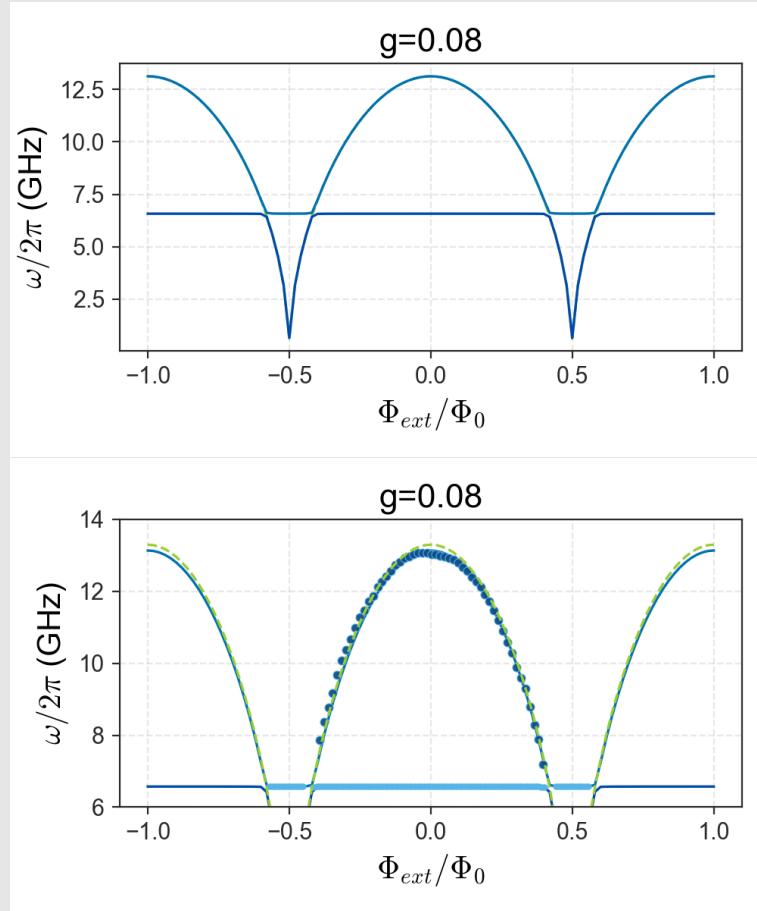


Figure 55: When g is small, there the qubit and resonator energies are hardly affected. Then the coupling is large, there will be a large amount of mixed states.

25.7 Decay rates and quality factors

There are two ways in which the system can decay:

- Resonator (cavity) decay to the continuum:

$$\kappa = \frac{\omega_r}{Q}$$

- Atom decays to modes other than the resonator modes

$$\gamma$$

25.8 Second order effects

Just to refresh our memory, our Hamiltonian has the following form

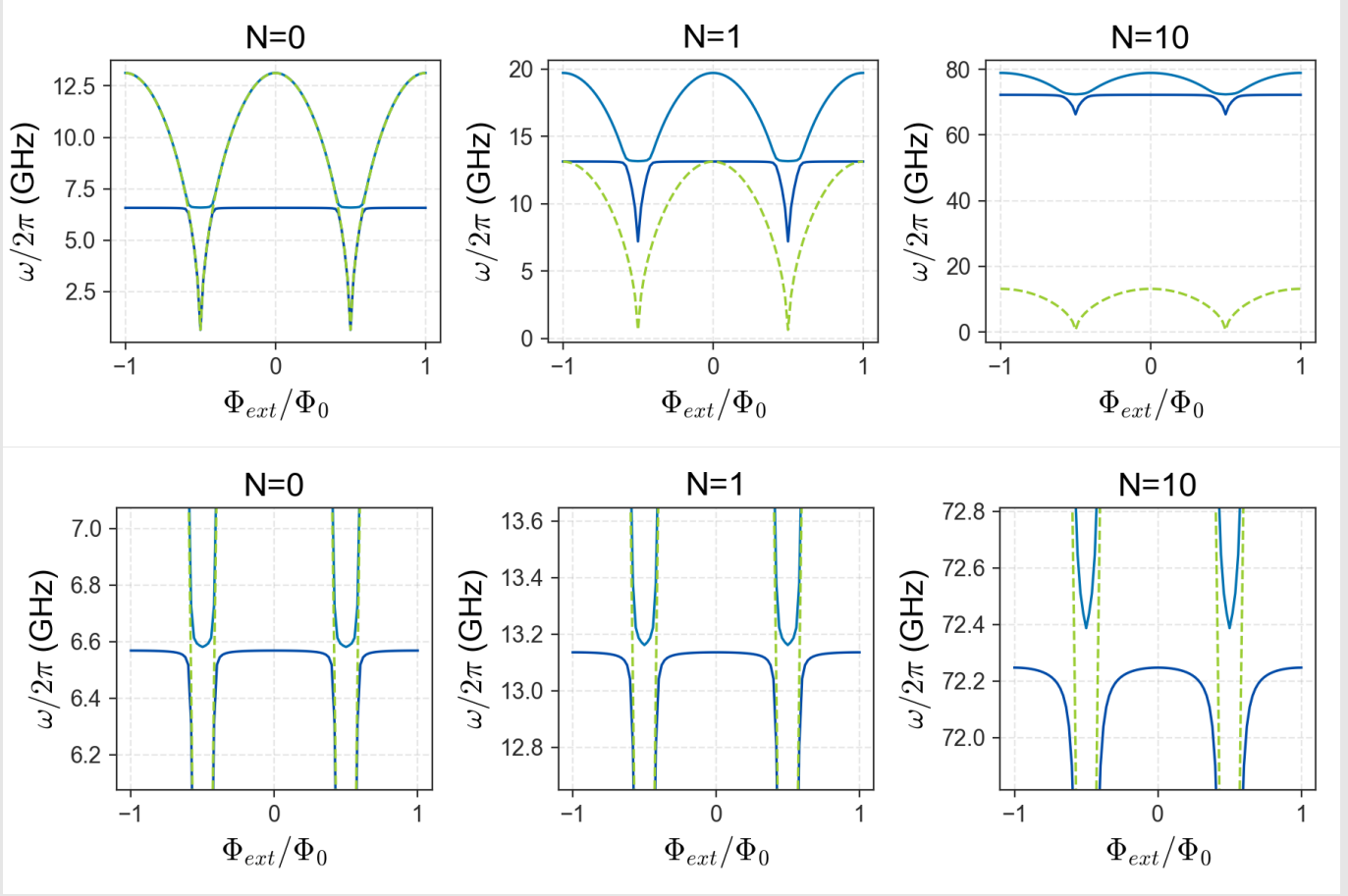


Figure 56: When $N \neq 0$, the anticrossing will be visible at shifted spectra by $\hbar\omega_r$. The splitting itself will be $\propto g\sqrt{N+1}$

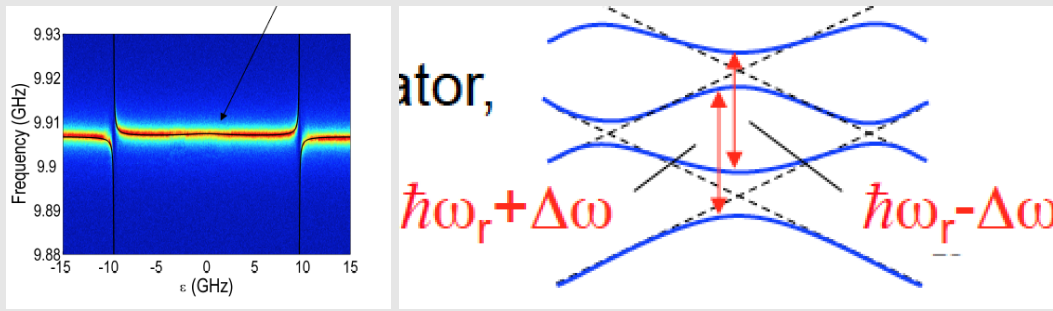
$$-\frac{\Delta E}{2}\sigma_x + \hbar\omega_r a^\dagger a + \hbar g_0(a\sigma^+ + a^+\sigma^-),$$

and without the [interaction term](#) one had the following eigenstates and eigenenergies

$$\begin{aligned} &|n, N\rangle \\ &(n - \frac{1}{2})\Delta E + \hbar\omega N. \end{aligned}$$

Now we consider second order effects, where there is a frequency shift when the qubit is in the excited state. These second order effects will change the energies and eigenstates

$$E'_{n,N} = E_{n,N}^{(0)} + E_{n,N}^{(1)}; \quad |\Psi'_{n,N}\rangle = |\Psi_{n,N}^{(0)}\rangle + |\Psi_{n,N}^{(1)}\rangle + |\Psi_{n,N}^{(2)}\rangle.$$



From time independent perturbation theory, one finds that the first order energy shift term is

$$E_{n,N}^{(1)} = \langle \Psi_{n,N}^{(0)} | V | \Psi_{n,N}^{(0)} \rangle = \langle n, N | g_0 (a\sigma^+ + a^\dagger\sigma^-) | n, N \rangle \equiv 0,$$

while the second order energy shift

$$E_{n,N}^{(2)} = \sum_{m,M} \frac{|\langle m, M | g_0 (a\sigma^+ + a^\dagger\sigma^-) | n, N \rangle|^2}{E_{n,N} - E_{m,M}}.$$

For the two states of the qubit this evaluates to

$$E_{0,N}^{(2)} = |g_0|^2 \sum_{m,M} \frac{|\langle m, M | (a\sigma_+ + a^\dagger\sigma_-) | 0, N \rangle|^2}{E_{0,N} - E_{m,M}} = |g_0|^2 \frac{\left| \langle 1, N-1 | \sqrt{N} | 1, N-1 \rangle \right|^2}{E_{0,N} - E_{1,N-1}} = -\frac{|g_0|^2 N}{\Delta E - \hbar\omega}$$

and

$$E_{1,N}^{(2)} = |g_0|^2 \sum_{m,M} \frac{|\langle m, M | (a\sigma_+ + a^\dagger\sigma_-) | 1, N \rangle|^2}{E_{1,N} - E_{m,M}} = |g_0|^2 \frac{\left| \langle 0, N+1 | \sqrt{N+1} | 0, N+1 \rangle \right|^2}{E_{1,N} - E_{1,N+1}} = \frac{|g_0|^2 (N+1)}{\Delta E - \hbar\omega}$$

From this we evaluate the energy difference between atomic and resonator transitions:

- **Atomic transition** can be seen to depend on the number of photons in the resonator

$$\begin{aligned} E'_{1,N} - E'_{0,N} &= E_{1,N}^{(0)} + E_{1,N}^{(1)} + E_{1,N}^{(2)} - E_{0,N}^{(0)} - E_{1,N}^{(1)} - E_{0,N}^{(2)} \\ &= \Delta E + \frac{|g_0|^2 (N+1)}{\Delta E - \hbar\omega} - \left(-\frac{|g_0|^2 N}{\Delta E - \hbar\omega} \right) \\ &= \Delta E + \frac{|g_0|^2 (2N+1)}{\Delta E - \hbar\omega} \end{aligned}$$

- **Resonator transition** depends on the state of the qubit

$$E'_{n,N+1} - E'_{n,N} = \begin{cases} \hbar\omega - \frac{|g_0|^2}{\Delta E - \hbar\omega} & \text{for } n=0 \\ \hbar\omega + \frac{|g_0|^2}{\Delta E - \hbar\omega} & \text{for } n=1 \end{cases}$$

25.9 Driving qubit-resonator system

The drive Hamiltonian for a qubit-resonator system we add a coherent field that will couple with the qubit via the resonator with the same coupling strength g .

$$\mathcal{H} = -\frac{\Delta E}{2}\sigma_z + \hbar\omega_r a^\dagger a + \hbar g_0 (a\sigma^+ + a^\dagger\sigma^-) + \hbar g (\alpha^*\sigma^- + \alpha\sigma^+).$$

25.10 Dynamics using Linbalnd equation

Solving for the Harmonic oscillator alone, with a relaxation rate κ between the levels, it is convenient to write the Linblad term and the density matrix as

$$\mathcal{H} = \hbar\omega_r a^\dagger a + \hbar\Omega(a + a^\dagger) \cos(\omega t); \quad \rho^{(r)} = \sum_{M,N=0}^{\infty} \rho_{NM}^{(r)} |N\rangle \langle M|; \quad \mathcal{L}^{(r)} = \frac{\kappa}{2} \left(2a\rho a^\dagger - a^\dagger a\rho - \rho a^\dagger a \right),$$

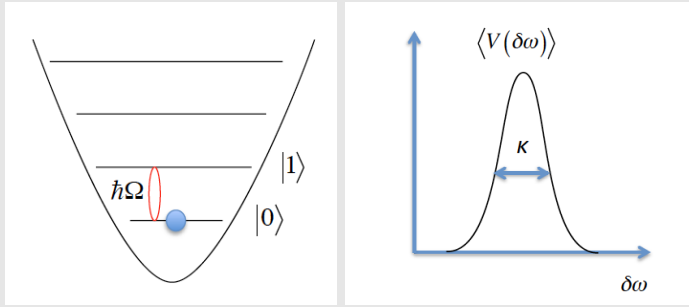
which ultimately results in the following contribution to from the Linblad term

$$\dot{\rho}_{NN}^{(r)} \rightarrow \kappa(N+1)\rho_{N+1}^{(r)} - \kappa N\rho_{NN}^{(r)}.$$

1. The Hamiltonian for the resonator is transformed by moving into the corresponding rotating frame

$$\mathcal{H}' = -\hbar\delta\omega a^\dagger a + \frac{\hbar\Omega}{2}(a + a^\dagger).$$

2. Solving the Master equation for the continuous drive for the stationary condition and assuming that the driving is weak (and thus only the bottom photon levels will be occupied), the solution can be truncated to have only the $|0\rangle$ and $|1\rangle$ photon states.
3. The expectation value for the field in the resonator is found using the density matrix for the stationary condition



$$\langle V \rangle = V_0 \langle a + a^\dagger \rangle = V_0 \text{Tr} \{ (a + a^\dagger) \rho \} \approx \frac{2\Omega}{\kappa + 2\delta\omega},$$

which is a Lorentzian, whose peak occurs for the case when $\delta\omega = 0$ and the field being driven through the resonator is exactly in resonance with it.

Now include the atom with the resonator system

$$\begin{aligned} \mathcal{H} &= -\frac{\Delta E}{2}\sigma_z + \hbar\omega_r a^\dagger a + g_0 \left(a\sigma^+ + a^\dagger\sigma^- \right) \\ \mathcal{L}^{(a)} &= \frac{\Gamma_1}{2} \left(2\sigma^-\rho\sigma^+ - \sigma^+\sigma^-\rho - \rho\sigma^+\sigma^- \right); \quad \mathcal{L}^{(r)} = \frac{\kappa}{2} \left(2a\rho a^\dagger - a^\dagger a \rho - \rho a^\dagger a \right) \\ \dot{\rho} &= -\frac{i}{\hbar} [\mathcal{H}, \rho] + \mathcal{L}^{(a)} + \mathcal{L}^{(r)}; \quad \rho = \sum_{m,n=0}^1 \sum_{M,N=0}^{\infty} \rho_{nm,NM} |nN\rangle \langle mM| \end{aligned}$$

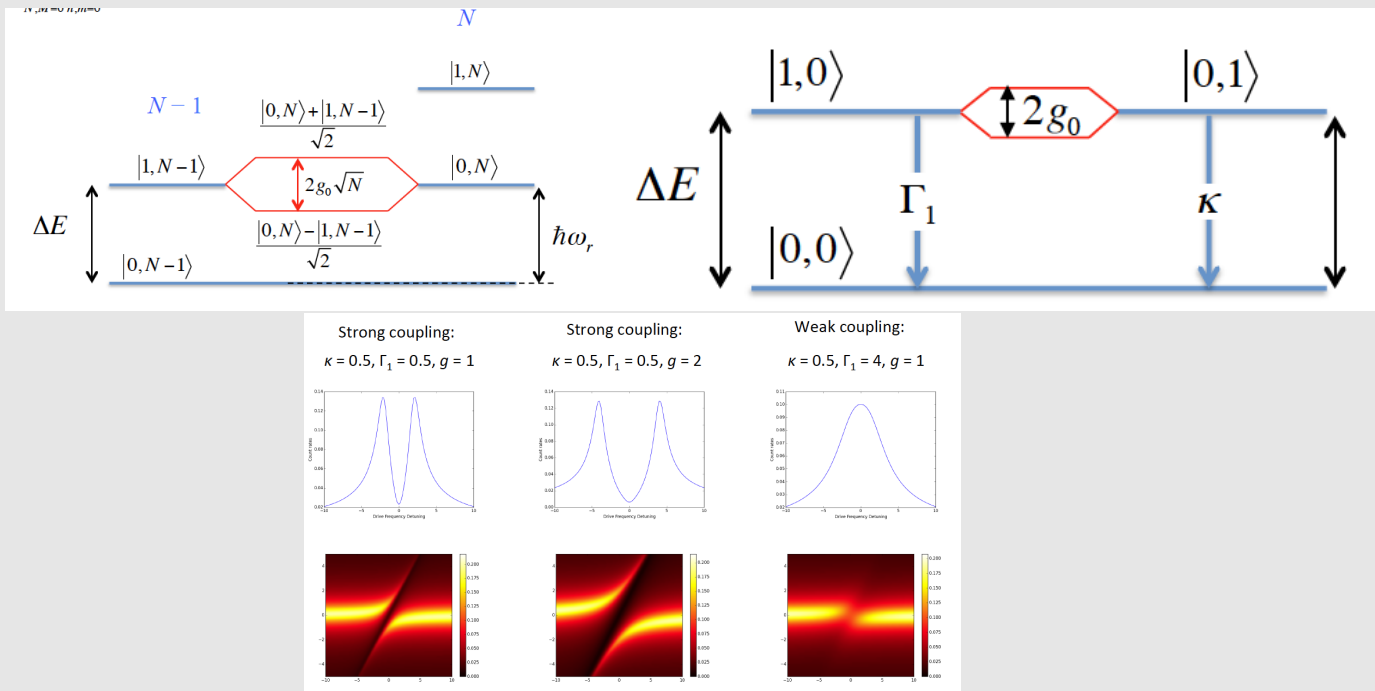
and this kind of system has been solved before, but now there are decay mechanisms also. The states decay with a rate

$$\gamma = \frac{\kappa + \Gamma_1}{2},$$

meaning that in order to couple the qubit and resonator, the energy exchange must occur faster than this decay time. The energy exchange occurs at a rate $\hbar/g_0 \ll 1/\Gamma_1, 1/\kappa$, imposing the condition that

$$g_0 \gg \hbar\Gamma_1, \hbar\kappa,$$

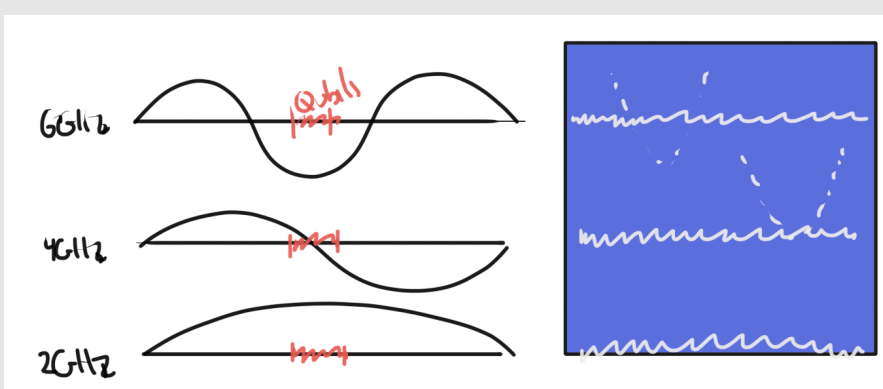
in which the characteristic energy is higher than incoherent processes.



MEASUREMENT WITH RESONATOR

There are some simple rules, when it comes to measuring with a resonator:

1. Current has nodes on the end of the resonator - voltage has antinodes;
2. Flux qubit needs current maxima;
3. Charge qubits need voltage maxima;
4. Say the resonator has a resonance $n = 1$ of 2 GHz. When measuring the qubit, each of the resonance lines corresponds to a particular standing wave profile:



Tune the VNA (probe) to the best resonance for your position of the qubit in **two-tone measurements**.

When making a resonator:

1. The length of the resonator effects the wavelength λ of the standing waves;
2. Speed is determined by

$$v = \frac{1}{\sqrt{LC}}.$$

and in turn

$$L \propto R \propto \text{length/width};$$

3. Thus, in order to raise the resonator frequency **while keeping the same standing wave for interaction with the qubit**, make the resonator **wider**.

A useful way of figuring out which resonance you are firing with the first tone, is to look for **vertical lines** in the spectrum. Whenever the qubit cross **your resonance** (e.g. resonator at 3GHz, and we move to field where the qubit is at 6GHz) **then irrelevant of what the generator sweeps, the qubit will always be giving a response so you get a vertical white line**.

26.1 Choosing power

1. For two-tone measurements, make the probe signal **1st tone** fairly weak so that there is a single photon in the resonator.

Keep raising the power, until resonator lines become distorted.

2. The generator signal **2nd tone** should be weak enough to get a thin response from resonator, but powerful enough to get a response at all.

3. For anti crossings you must have much less than a photon in the resonator on average.

CHAPTER 27

CREATING A DARK STATE IN A 3-LEVEL SYSTEM[21][1]

We drive a 3-level system in such a way that one of its states is never populated.

We can use a flux qubit, solved in Chapter 18, for the 3-level system.

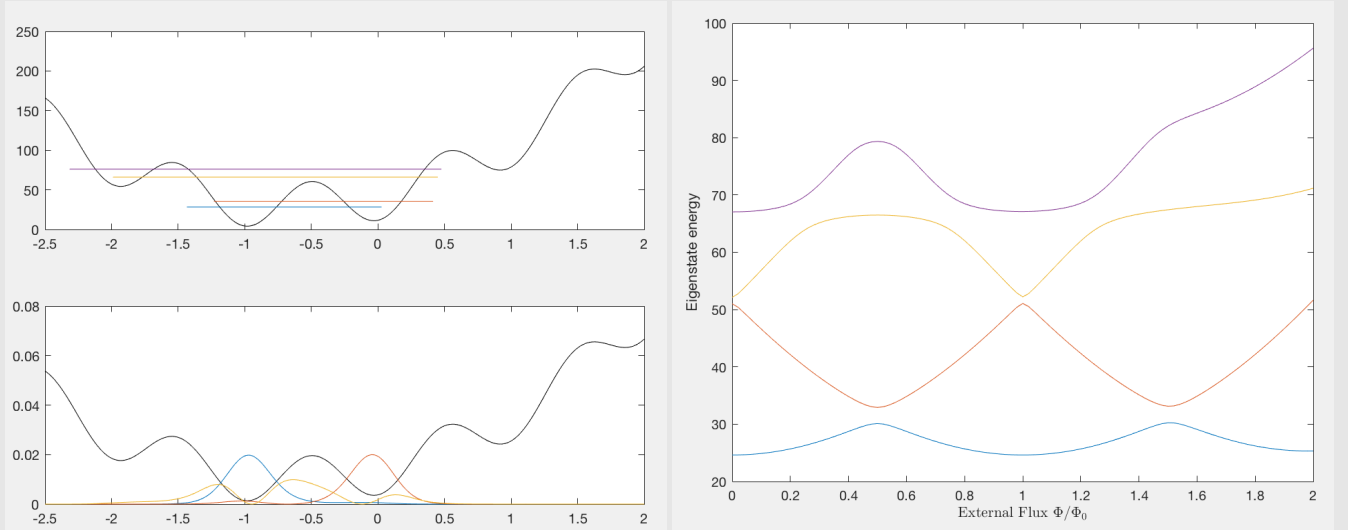


Figure 57: $|0\rangle$ migrates to the lower potential well as one increases the external flux. Black lines show the potential in the system.

27.1 Driving the three level atom

The Hamiltonian for a Three-Level atom, in a corresponding basis of eigenstates $|1\rangle$, $|2\rangle$, $|3\rangle$, by which the three levels are labelled, can be written as

$$\mathcal{H}_{\text{atom}} = \begin{pmatrix} E_1 & 0 & 0 \\ 0 & E_2 & 0 \\ 0 & 0 & E_3 \end{pmatrix} = \begin{pmatrix} E_3 - \hbar\omega_{31} & 0 & 0 \\ 0 & E_3 - \hbar\omega_{32} & 0 \\ 0 & 0 & E_3 \end{pmatrix}, \quad (34)$$

where $\hbar\omega_{31} = E_3 - E_1$ and $\hbar\omega_{32} = E_3 - E_2$. Considering driving fields Ω_{32} , Ω_{31} driving transitions $|2\rangle \leftrightarrow |3\rangle$ and $|1\rangle \leftrightarrow |3\rangle$ that arise due to capacitive or inductive coupling ($\hbar\Omega_{ij} \propto \vartheta_{ij}$ is derived in Chapter 4)

$$\mathcal{H}_{\text{int}} = -\hbar\Omega_{31} \cos(\omega_{31}^d t) \begin{pmatrix} 0 & 0 & 1 \\ 0 & 0 & 0 \\ 1 & 0 & 0 \end{pmatrix} - \hbar\Omega_{32} \cos(\omega_{32}^d t) \begin{pmatrix} 0 & 0 & 0 \\ 0 & 0 & 1 \\ 0 & 1 & 0 \end{pmatrix}, \quad (35)$$

where the non-zero matrix elements indicate the states coupled by the fields. The total Hamiltonian, $\mathcal{H}_a = \mathcal{H}_{\text{atom}} + \mathcal{H}_{\text{int}}$, is a sum of Eq. (34), (35), written for convenience with complex exponentials,

$$\begin{aligned} \mathcal{H}_a &= \begin{pmatrix} E_3 - \hbar(\omega_{31}^d - \delta\omega_{31}) & 0 & -\frac{\hbar\Omega_{31}}{2} \left(e^{i\omega_{31}^d t} + e^{-i\omega_{31}^d t} \right) \\ 0 & E_3 - \hbar(\omega_{32}^d - \delta\omega_{32}) & -\frac{\hbar\Omega_{32}}{2} \left(e^{i\omega_{32}^d t} + e^{-i\omega_{32}^d t} \right) \\ -\frac{\hbar\Omega_{31}}{2} \left(e^{i\omega_{31}^d t} + e^{-i\omega_{31}^d t} \right) & -\frac{\hbar\Omega_{32}}{2} \left(e^{i\omega_{32}^d t} + e^{-i\omega_{32}^d t} \right) & E_3 \end{pmatrix} \\ &= \begin{pmatrix} H_{11} & H_{12} & H_{13} \\ H_{21} & H_{22} & H_{23} \\ H_{31} & H_{32} & H_{33} \end{pmatrix}, \end{aligned} \quad (36)$$

where $\delta\omega_{31} = \omega_{31} - \omega_{31}^d$, $\delta\omega_{32} = \omega_{32} - \omega_{32}^d$ represent the detunings of the driving fields from the resonant frequencies of the atom. The Hamiltonian Eq. (36) governs the time evolution of the system state

$$|\Psi\rangle = c_1 |1\rangle + c_2 |2\rangle + c_3 |3\rangle,$$

through the standard Schrödinger equation, which takes on the matrix form

$$\begin{pmatrix} H_{11} & H_{12} & H_{13} \\ H_{21} & H_{22} & H_{23} \\ H_{31} & H_{32} & H_{33} \end{pmatrix} \begin{pmatrix} c_1 \\ c_2 \\ c_3 \end{pmatrix} = i\hbar \begin{pmatrix} \dot{c}_1 \\ \dot{c}_2 \\ \dot{c}_3 \end{pmatrix}. \quad (37)$$

By applying a time dependent **unitary transformation**

$$\tilde{c}_i = e^{i\phi_i(t)} c_i,$$

where $i = 1, 2, 3$, one can rewrite Eq. (37) as

$$\begin{pmatrix} H_{11} - \hbar\dot{\phi}_1 & H_{12}e^{i\phi_{12}} & H_{13}e^{i\phi_{13}} \\ H_{21}e^{i\phi_{21}} & H_{22} - \hbar\dot{\phi}_2 & H_{23}e^{i\phi_{23}} \\ H_{31}e^{i\phi_{31}} & H_{32}e^{i\phi_{32}} & H_{33} - \hbar\dot{\phi}_3 \end{pmatrix} \begin{pmatrix} \tilde{c}_1 \\ \tilde{c}_2 \\ \tilde{c}_3 \end{pmatrix} = i\hbar \begin{pmatrix} \dot{\tilde{c}}_1 \\ \dot{\tilde{c}}_2 \\ \dot{\tilde{c}}_3 \end{pmatrix},$$

where $e^{i\phi_{kj}} = e^{i(\phi_k - \phi_j)}$. Setting

$$\phi_1 = \left(\frac{E_3}{\hbar} - \omega_{31}^d \right) t; \quad \phi_2 = \left(\frac{E_3}{\hbar} - \omega_{32}^d \right) t; \quad \phi_3 = \frac{E_3}{\hbar} t,$$

which effectively rotates the state vector components at the natural atomic evolution and detuning frequencies,⁴ will give a simple expression for the Hamiltonian

$$\tilde{\mathcal{H}}_a = \begin{pmatrix} \hbar\delta\omega_{31} & 0 & -\frac{\hbar\Omega_{31}}{2} \\ 0 & \hbar\delta\omega_{32} & -\frac{\hbar\Omega_{32}}{2} \\ -\frac{\hbar\Omega_{31}}{2} & -\frac{\hbar\Omega_{32}}{2} & 0 \end{pmatrix} + \begin{pmatrix} 0 & 0 & -\frac{\hbar\Omega_{31}}{2}e^{-i2\omega_{31}^d t} \\ 0 & 0 & -\frac{\hbar\Omega_{32}}{2}e^{-i2\omega_{32}^d t} \\ -\frac{\hbar\Omega_{31}}{2}e^{-i2\omega_{31}^d t} & -\frac{\hbar\Omega_{32}}{2}e^{-i2\omega_{32}^d t} & 0 \end{pmatrix}. \quad (38)$$

In the rotating-wave-approximation, one ignores the contribution from the fast rotating $2\omega_{31}^d$, $2\omega_{32}^d$ in the second term, since their oscillations will be averaged out at the time-scales of significant processes - physically they correspond to energy non-conserving processes. One is left with the following driving cases

⁴The full unitary transformation applied:

$$U(t) = \exp \left[\frac{i t}{\hbar} [(E_1 - \hbar\delta\omega_{31}) |1\rangle \langle 1| + (E_2 - \hbar\delta\omega_{32}) |2\rangle \langle 2| + E_3 |3\rangle \langle 3|] \right]$$

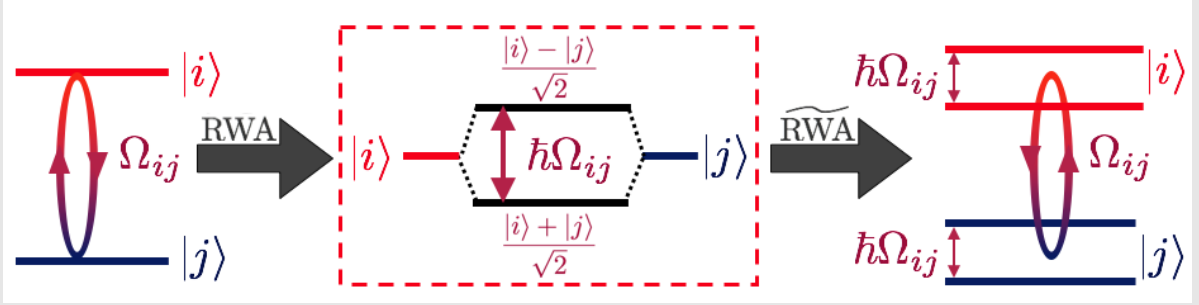


Figure 58: **The Rabi splitting of the energies in a Two-Level system.** A driving field with angular frequency ω_{ij}^d and Rabi amplitude Ω_{ij} in resonance with the atomic transition ω_{ij} , couples the states $|i\rangle$ and $|j\rangle$. In the rotated frame, the eigenstates $(|i\rangle \pm |j\rangle)/\sqrt{2}$ are separated by an energy $\hbar\Omega_{ij}$. Retuning to the original frame will map the Rabi splitting onto the original levels.

$$\begin{aligned}
 |1\rangle \leftrightarrow |3\rangle \text{ and } |2\rangle \leftrightarrow |3\rangle \quad & \tilde{\mathcal{H}}_a = -\frac{\hbar}{2} \begin{pmatrix} -2\delta\omega_{31} & 0 & \Omega_{31} \\ 0 & -2\delta\omega_{32} & \Omega_{32} \\ \Omega_{31} & \Omega_{32} & 0 \end{pmatrix}; \\
 |1\rangle \leftrightarrow |3\rangle \text{ and } |1\rangle \leftrightarrow |2\rangle \quad & \tilde{\mathcal{H}}_b = -\frac{\hbar}{2} \begin{pmatrix} 0 & \Omega_{21} & \Omega_{31} \\ \Omega_{21} & 2\delta\omega_{21} & 0 \\ \Omega_{31} & 0 & 2\delta\omega_{31} \end{pmatrix}; \\
 |1\rangle \leftrightarrow |2\rangle \text{ and } |2\rangle \leftrightarrow |3\rangle \quad & \tilde{\mathcal{H}}_c = -\frac{\hbar}{2} \begin{pmatrix} 0 & \Omega_{21} & 0 \\ \Omega_{21} & 2\delta\omega_{21} & \Omega_{32} \\ 0 & \Omega_{32} & 2\delta\omega_{21} + 2\delta\omega_{32} \end{pmatrix}.
 \end{aligned} \tag{39}$$

For various $\delta\omega_{ij} \approx 0$, certain energy levels in the rotated frame become degenerate, shown in Fig. 58b for a two level system. The off-diagonal terms induce a splitting $\hbar\Omega$ between the eigenstates of the system,⁵ lifting this degeneracy. In the original unrotated frame, these Rabi splittings persist, resulting in a richer energy level structure as in Fig. 58.

⁵For a Two-Level $|0\rangle, |1\rangle$, system,

$\mathcal{H} = \hbar \begin{pmatrix} 0 & -\Omega/2 \\ -\Omega/2 & 0 \end{pmatrix}$ has eigenenergies $\pm\hbar\Omega$ and eigenstates $(|0\rangle \mp |1\rangle)/\sqrt{2}$.

27.2 Driving to the dark state

If $\delta\omega_{32} = \delta\omega_{21} = 0$ then Eq. (39) will read

$$\tilde{\mathcal{H}}_c = -\frac{\hbar}{2} \begin{pmatrix} 0 & \Omega_{21} & 0 \\ \Omega_{21} & 0 & \Omega_{32} \\ 0 & \Omega_{32} & 0 \end{pmatrix},$$

with eigenvalues found from $\det(\tilde{\mathcal{H}} - \lambda\mathbb{I}) \equiv 0$ and eigenvectors from $(\tilde{\mathcal{H}} - \lambda\mathbb{I})\vec{v} = 0$:

$$\begin{aligned} E_0 = 0 & \quad E_1 = -\frac{\hbar}{2}\sqrt{\Omega_{21}^2 + \Omega_{32}^2} & E_2 = \frac{\hbar}{2}\sqrt{\Omega_{21}^2 + \Omega_{32}^2} \\ \vec{v}_0 = \frac{1}{\sqrt{\Omega_{21}^2 + \Omega_{32}^2}} \begin{pmatrix} \Omega_{32} \\ 0 \\ -\Omega_{21} \end{pmatrix} & \vec{v}_1 = \begin{pmatrix} \Omega_{21} \\ -\sqrt{\Omega_{21}^2 + \Omega_{32}^2} \\ \Omega_{32} \end{pmatrix} & \vec{v}_2 = \begin{pmatrix} \Omega_{21} \\ \sqrt{\Omega_{21}^2 + \Omega_{32}^2} \\ \Omega_{32} \end{pmatrix}, \end{aligned}$$

The state indicated in red is known as the dark state i.e. completely unpopulated $|1\rangle$. It happens when both the probe ($|0\rangle \leftrightarrow |1\rangle$) and control ($|1\rangle \leftrightarrow |2\rangle$) are on resonance:

$$|\Psi_0\rangle = \cos(\Theta)|0\rangle - \sin(\Theta)|2\rangle; \quad \tan(\Theta) = \frac{\Omega_{21}}{\Omega_{32}}.$$

To get the ground state we do $\sin(\Theta) = 0 \rightarrow \Omega_p \ll \Omega_c$:

$$|\Psi_0\rangle \approx |0\rangle$$

COHERENT QUANTUM PHASE SLIP (CQPS) [14]

28.1 Literature

- Trivia

1. Dual to the JJ effect, where instead of coherent transfer of charge, we have coherent transfer of flux
2. Each phase slip event releases an energy $I\Phi_0$.
3. In [14] there is a simplifying assumption that CQPS “just happens” with $E_s/h = 100$ GHz;
4. Wires must have **large kinetic inductance** and **small capacitance**. This will give impedance

$$Z_c = \sqrt{\frac{L}{C}}$$

and for frequent phase slips $Z_c > R_q = \frac{h}{4e^2}$.

5. Just like in JJ, the CQPS has trapped voltage in potential minima for voltages that do not exceed

$$V_C = \frac{2\pi E_S}{2e}$$

6. Need to have large normal state resistivity in order to have large impedance when in superconducting state - **large inductance**
7. We will observe when the flux is localised i.e. weak phase slip, $E_L \gg E_s$
8. Quantum phase slip process is a tunneling one:

$$E_S = E_0 \exp(-\kappa\bar{\omega})$$

where $\bar{\omega}$ is the line width and κ is the characteristic width at which the wire becomes a one-dimensional channel **with large quantum fluctuations possible**

- Experiment

1. Fabricate with strongly disordered superconductors near the superconductor-insulator transition (Niobium Nitride for example) - this will prevent gapless excitations [2].

2. Fabricate several thin superconducting bridges with meanders;
3. Measure the DC voltage, V , across then as a function of the applied gate voltage, V_c , from underneath the chip;
4. Some samples have big oscillations in V with gate voltage - Single Electron Transistor regime, where nanowire is composed of grains, which feel a Coulomb Blockade;
5. Quantum Phase Slip possible in other samples, where there are no grains in the wire.

Initially quantum phase slips were a result of thermal activation in thin wires.

28.2 Cooper box duality

The system is dual to the cooper pair box system, where the charging energy creates a parabolic dependence, and the Josephson coupling energy E_J mixes states lifting degeneracy as in Sec 16:

$$\mathcal{H} = \textcolor{red}{E_c}(\hat{n} - n_g)^2 - \frac{E_J}{2} [|n+1\rangle\langle n| + |n\rangle\langle n+1|].$$

In the quantum phase slip, we do the same thing, but now with inductor-component energy, $E_L = \frac{\Phi_0^2}{2L}$, is parabolic and degeneracy is lifted by the coupling, E_s , due to the tunneling of fluxes (we do not specify yet the exact derivation of this energy):

$$\mathcal{H} = \textcolor{red}{E_L}(\hat{n} - f)^2 - \frac{E_s}{2} [|n+1\rangle\langle n| + |n\rangle\langle n+1|],$$

with $f = \Phi/\Phi_0$.

The discussion then stems off into how the Cooper pair tunneling is dual to the phase slip, how one gets similar steps in voltage current characteristics. There is a lot of math, which I don't want to get into.

In both cases, a truncation of the Hamiltonian results in states (solving like in Sec. 11) and setting $\delta\Phi = \Phi_{\text{ext}} - (N + \frac{1}{2})\Phi_0$ as the deviation from a degeneracy point between states $|N\rangle$ and $|N+1\rangle$:

$$\mathcal{H} = \begin{pmatrix} \frac{\Phi_0^2}{2L} \left(N - \frac{\Phi_{\text{ext}}}{\Phi_0} \right) & -\frac{E_s}{2} \\ -\frac{E_s}{2} & \frac{\Phi_0^2}{2L} \left(N + 1 - \frac{\Phi_{\text{ext}}}{\Phi_0} \right) \end{pmatrix} = \begin{pmatrix} \frac{\Phi_0}{2L} (\Phi_0 N - \Phi_{\text{ext}}) & -\frac{E_s}{2} \\ -\frac{E_s}{2} & \frac{\Phi_0}{2L} (\Phi_0 N + \Phi_0 - \Phi_{\text{ext}}) \end{pmatrix} = \begin{pmatrix} -\delta\Phi I_p + \frac{\Phi_0 I_p}{2} & -\frac{E_s}{2} \\ -\frac{E_s}{2} & +\delta\Phi I_p + \frac{\Phi_0 I_p}{2} \end{pmatrix}$$

we get

$$\left\{ \begin{array}{l} \mathcal{H} = -\frac{\Delta E}{2} \begin{pmatrix} \cos(\theta) & \sin(\theta) \\ \sin(\theta) & -\cos(\theta) \end{pmatrix} \\ \Delta E = \sqrt{\epsilon^2 + \Delta^2} \\ \tan(\theta) = \frac{\Delta}{\epsilon} \end{array} \right.$$

in which case $\Delta \equiv E_s$ and $\epsilon = 2I_p\delta\Phi = \frac{\Phi_0}{L_k}\delta\Phi$ is the energy difference between neighbouring states (neighbours on the diagonal).

28.3 Mooij 2006 paper [14]

$$E_L \equiv E_C$$

$$E_J \equiv E_s$$

$$n_g \equiv f$$

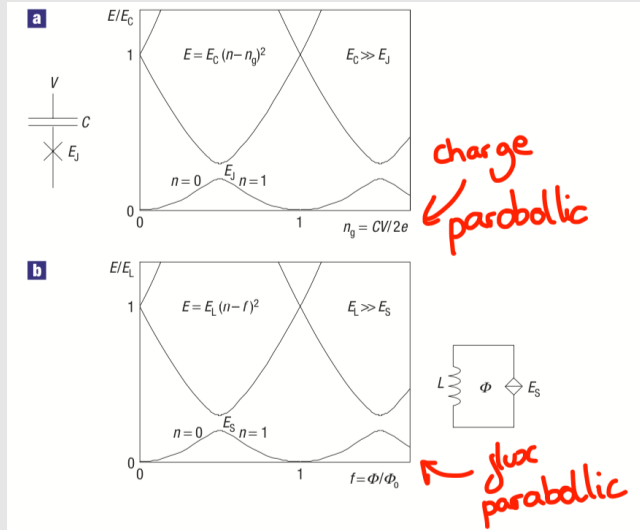


Figure 59: The energy spectra are dual for the two systems - from. In a) $E_C >> E_J$ so that charge is the relevant quantum number and in b) $E_L >> E_s$ so that phase is the quantum number. [14].

28.4 Derivation

There is a theory written in the book **Devoret: Quantum Fluctuation in electrical circuits** about how **any linear circuit can be presented by an equivalent circuit with a frequency-dependent resistor**.

- Current biased: Resistor is in parallel Phase across junction
- Voltage biased: Resistor is in series No of CP transferred.

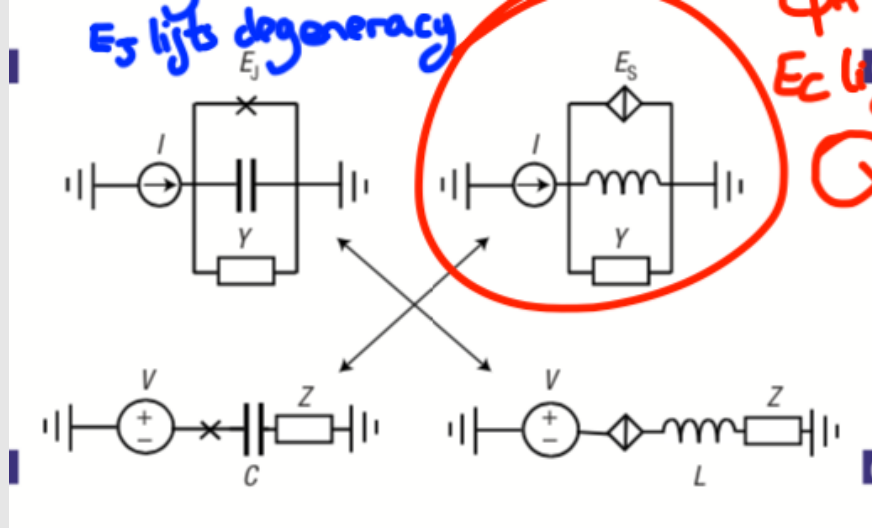


Figure 60: **JJ on left vs CQPS on right.** The capacitor is replaced with an inductor to make phase the new defined quantum variable.

The main transformation applied that links the following hamiltonians (we simply match the inductive and QPS terms from Subsec. 28.2) and we add the necessary 2π factors

$$\begin{aligned}\mathcal{H}_{JJ} &= E_C \hat{q}^2 - E_J \cos \hat{\varphi} \\ \mathcal{H}_{CQPS} &= E_L \frac{\hat{\varphi}^2}{(2\pi)^2} - E_S \cos(2\pi \hat{q})\end{aligned}$$

This requires the following set of transformations:

- $\hat{q} \rightarrow -\frac{\varphi}{2\pi}$
- $\hat{\varphi} \rightarrow 2\pi q$
- $E_s \rightarrow E_J$
- $E_L \rightarrow E_C$
- $I \Leftrightarrow \frac{V}{R_q}$
- $Y(\omega) \Leftrightarrow \frac{Z(\omega)}{R_q^2}$

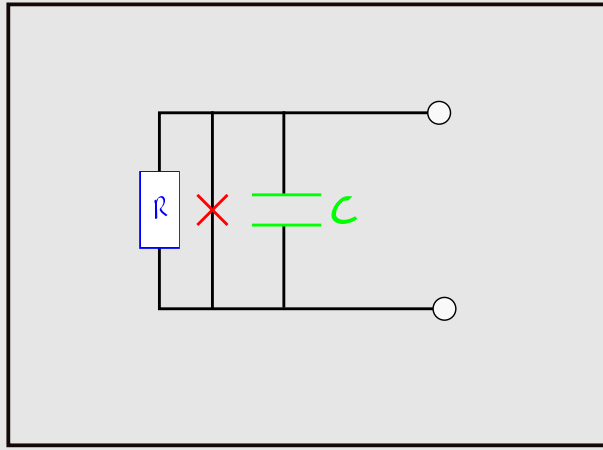


Figure 61: Modelling a JJ

28.5 Inverse shapiro steps

Now if we take the aforementioned mappings and apply them to the equation used to model a typical JJ

$$I(t) = I_c \sin \varphi + \frac{\Phi_0}{2\pi} \left[C \frac{d^2 \varphi}{dt^2} + \frac{1}{R} \frac{d\varphi}{dt} \right]$$

which leads to Shapiro steps. Add explanation from metrology notes.

Upon subbing in

$$V(t) = V_c \sin(2\pi q) + 2e \left[L \frac{d^2 q}{dt^2} + R \frac{dq}{dt} \right]$$

where we now deal with the voltage drops across the CQPS (in becomes a linear circuit). **Valid when the charge is the relevant quantum number (just like for JJ phase is the quantum number as we are localised in a potential minimum)**

28.6 Plasma Frequency

The JJ can be viewed as an inductance with a shunt capacitor due to it's finite size (inductance actually depends on the phase across the JJ, $L_{\text{kin}} = \frac{\Phi_0}{2\pi I_c \cos(\varphi_0)}$):

$$\begin{cases} Z = Z_c + Z_L \\ Z_C = \frac{1}{j\omega C} \Rightarrow Z = \frac{L/C}{j(\omega L - \frac{1}{\omega C})} \Rightarrow \omega_{\text{res}} = \frac{1}{\sqrt{LC}}. \\ Z_L = j\omega L \end{cases}$$

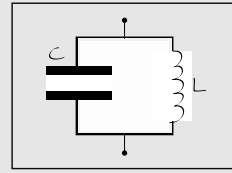


Figure 62: LC circuit that is set up inside the JJ

28.7 What sets the energies

JJ

1. $E_J = \frac{R_q}{R_{\square}/N_{sq}} \frac{\Delta(0)}{2}$ $E_J \propto N_{sq}$
2. $E_C = \frac{e^2}{2C_{\Sigma}}$ $E_C \propto \frac{1}{Area}$

CQPS

1. $E_L = \frac{\Phi_0^2}{2L}$ $E_L \propto \frac{1}{Wire\ Length}$
2. $E_S \propto Wire\ length$

28.8 Standard of voltage

Just like JJ has a damping factor (Subsec. 12.5) so does the CQPS

$$Q_{QPS}^2 = \beta_L = 2\pi \frac{V_c}{2e} \frac{L}{R^2} = 2\pi^2 \frac{E_s}{E_L} \left(\frac{R_q}{R} \right)^2.$$

Too much damping is bad, as on the washboard potential is gives rise to hysteresis, and while E_s and E_L are fixed in order to operate in the voltage localisation regime, it is possible to increase R to 60 kΩ.

28.9 Coherent quantum phase slip 2012 [2]

Oleg drove the CQPS system in the two level approximation by a resonant drive.

The Hamiltonian near a degeneracy point can be written

$$\mathcal{H} \approx -\frac{\varepsilon}{2}\sigma_z - \frac{\Delta}{2}\sigma_x = \begin{pmatrix} -\varepsilon/2 & -\Delta/2 \\ -\Delta/2 & \varepsilon/2 \end{pmatrix} \quad \text{when } \Phi \approx (N + \frac{1}{2})\Phi_0$$

$$\varepsilon = \frac{\Phi_0}{L}\delta\Phi = 2I_p\delta\Phi \quad \text{controlled by bias flux, and yes, there is a factor of 2 - not an error!}$$

$$\Delta = E_s \quad \text{Degeneracy lifted by the coupling of the flux states}$$

which can be rotated to give

$$\mathcal{H}' = -\frac{\Delta E}{2}\sigma_z \quad \Delta E = \sqrt{\varepsilon^2 + \Delta^2}$$

Now we applying a driving field (labelling $\omega_0 = \Delta E/\hbar$). From Sec. 4 the coupling $\hbar\Omega = |I_{mw}|MI_p\zeta = MI_p|I_{mw}|\frac{E_s}{\Delta E}$

$$\mathcal{H}'' = -\frac{\hbar\omega_0}{2}\sigma_z - \hbar\Omega \cos(\omega_0 t)\sigma_x,$$

and applying a rotating wave $U(t) = \exp[-i\frac{\omega_0 t}{2}\sigma_z]$ and removing fast-oscillating terms

$$\mathcal{H}''' = -\frac{\hbar\Omega}{2}\sigma_x$$

which evolves the state $U(t) = e^{-i\mathcal{H}'''/\hbar t} = e^{i\Omega t/2\sigma_x}$ which evolves

$$|\Psi\rangle = U|0\rangle = \cos\left(\frac{\Omega t}{2}\right)|0\rangle + e^{i\pi/2}\sin\left(\frac{\Omega t}{2}\right)|1\rangle.$$

Since $\hbar\Omega \neq 0$ only is $E_s \neq 0$ this will directly show CQPS if one finds that the field interacts with the system.

28.9.1 Choosing material

CQPS occurs due to fluctuations in the order parameters Ψ ($|\Psi|^2$ is proportional to number of CP.)
Surprisingly to see CQPS, we need to have a low CP concentration to have a big Ginsburg parameter

$$G_i = \frac{1}{\nu \Delta \xi^3}$$

where ν = DOS, Δ is the sc gap and ξ is the coherence length. To get small ξ we need to be close to the superconductor-insulator transition at which point

$$\text{Cohrence length } \xi \approx \xi_{localisation}$$

An alternative explanation is to limit the number of conductive channels

$$N_{ch} = \frac{R_K}{R}, \quad R_K = \frac{h}{e^2}$$

since $E_s \propto e^{-aN_{ch}}$, so we need a highly resistive material.

Materials that fit are NbN and TiN where $\xi = 30$ nm.

At around 2.7 K the sheet inductance is

$$R_{sq} = 1.7 \text{ k}\Omega$$

$$L_{sq} = \frac{\hbar R_{sq}}{\pi \Delta} \approx 0.7 \text{ nH}$$

Another great way to get material parameters is done by **Peltonen** [19]:

- Measure resonator whose frequency:

$$\begin{cases} f_n = \frac{nv}{2L}, & n \in \mathbb{Z} \\ v = \frac{1}{\sqrt{lc}} \end{cases}$$

- Estimate $c_l \approx 7 \times 10^{-10} \text{ F/m}$ and thus deduce l .

28.9.2 Fitting of results

Results are measured using two-tone spectroscopy and fitting performed using $\Delta E = \sqrt{(2I_p \delta \Phi)^2 + E_s^2}$ to get

- $E_s = 10 \text{ GHz}$ $\zeta = 10 \text{ nm}$
- $L_k = 42 \text{ nH}$ (compared to prediction from BCS of 23 nH)

- Proof that there is a linear inductance in the system (not the non linear one as for JJ) by two-tone data with different excitation paths

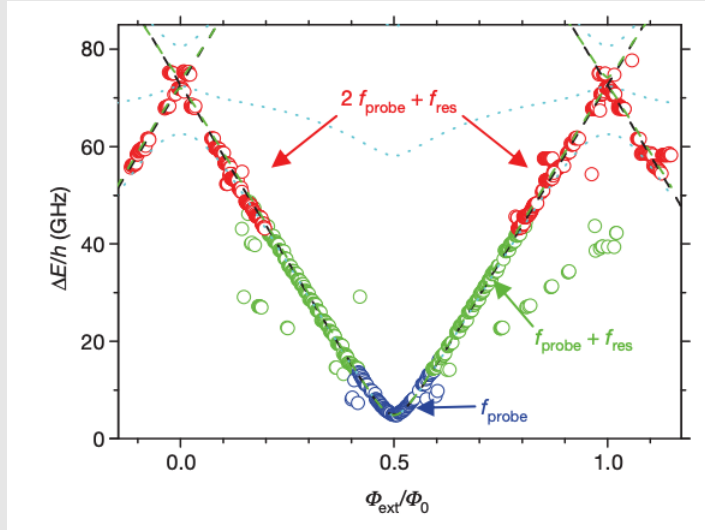


Figure 63: Energy to excite the system comes from either **second tone**, **second tone + first tone**, **two second tone + one first tone**. In contrast, the prediction using a JJ RF-SQUID is very different.

It is not identical to BCS prediction due to exponential dependence of the sample on material parameters.

28.10 Evidence for coherent quantum phase-slips across a Josephson junction array [12]

- A phase slip destroys superconducting order in a narrow wire
- There will be shifting of energies, turning energy-level shifts into linewidths.
- Gradient of order parameter Ψ , gives the non-dissipative current (supercurrent) **that is constant along the wire**.
- Thinner wire == more phase slips
- Phase slip can occur by $\pm 2\pi$ and preserve the single-valuedness of the macroscopic wave function Ψ . Summing up the total phase slips that can occur anywhere $m = \sum_i m_i$.
- Phase slips do not have to be **dissipative** - multiple CPS in different location can interfere with each other.
- A phase slip dissipates and energy $I\Phi_0$, where I is the bias current.

- Phase slip energy can vary **by a lot** so it may be hard to catch it within the laboratory ranges.

So in this experiment, they take a long chain of JJ (to minimize effect of lumped circuits).

Phase slips will change the inductance of this chain, which will be registered by a fluxonium qubit.

- **Fluxonium qubit** is single JJ shunted by an array of JJ. Readout by coupling it to a resonator
- Large E_J/E_C mean that phase fluctuations are small - not a lot of phase slips.

28.11 Coherent flux tunneling through NbN nanowires [18]

- Tunneling rate depends exponentially on the number of conducting channels N_{ch}
- For the following

$$E_S = E_0 \exp(-\kappa \bar{\omega})$$

one can get

$$E_0 = \frac{\Delta}{\xi^2} \frac{(h/4e^2)}{R_{\square}} l \bar{\omega}$$

$$\kappa = a \frac{(h/4e^2)}{R_{\square}} \frac{1}{\xi}$$

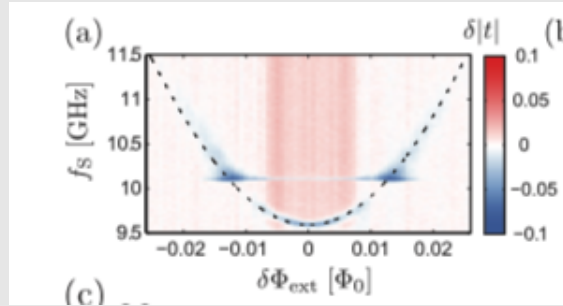
where $l \approx 500$ nm, $\Delta \approx 1.6$ meV, $\xi = 4$ nm.

- BCS theory fails in disordered material

28.12 Coherent dynamics and decoherence in a superconducting weak link [17]

- NbN thickness of 2 – 3 nm
- First deposition creates the large grounds planes → second deposition using negative resist **calixarene** and **reactive ion etching** etches away the pieces of NbN that are uncovered.
- **Do not remove negative resist afterwards** - it protects against ageing.

- Two tone spectroscopy to measure energies - **Nont-resonant coupling between qubit and resonator** allows one to map out the qubit energies through changes in the resonator
- Fitting of $\sqrt{(2I_p\delta\Phi)^2 + E_s^2}$ to the spectrum allows one to find:
 - $I_p \approx 40 \text{ nA}$
 - $L_K = \frac{\Phi_0}{2I_p} \approx 25 \text{ nH}$



- **Stark shift** (Subsec. 25.3) tells us that

$$U\mathcal{H}U^\dagger \approx \hbar\omega_r a^\dagger a + \left[\frac{\hbar\Omega}{2} + \frac{g^2}{\Delta} \left(a^\dagger a + \frac{1}{2} \right) \right] \sigma_z$$

depending on number of photon in resonator, the atom's energy will shift

- When big powers are applied, the **Lorentzian dip** will deform into a Gaussian blur. At low power the FWHM=26 MHz gives a dephasing rate (total dephasing) $\Gamma_2 = \pi \times \text{FWHM} = 8 \times 10^7$ per second
- Authors show that as magnetic field is moved from $\delta\Phi = 0$ relaxation rate Γ_1 stays constant, but decoherence rate Γ_2 increases due to low frequency flux fluctuations into the flux degree of freedom

CHAPTER 29

SINGLE PHOTON

- High efficiency;
- On-demand, deterministic operation;
- Low timing jitter;
- Control shape of wave packet [5]

29.1 What is spectral density

An excellent paper [8] says that **for an atom to transition $|1\rangle \rightarrow |0\rangle$ the rate of transition, according to Fermi's golden rule, is proportional to the spectral density of electromagnetic modes.**

Thus, measuring lifetime of an atom probes the local strength of vacuum fluctuations at that transition frequency. **The frequency-dependent spatial structure of the vacuum**

Once a relaxation occurs, a photon of frequency ω_{qubit} and wavelength

$$\lambda(\Phi) = \frac{2\pi v}{\omega_{\text{qubit}}}, \quad v = \frac{1}{\sqrt{lc}}$$

is emitted into the line.

29.2 Making measurement

For normalisation, subtract the reference when the photon source it turned off for the different measurements [16]:

- Power ($|V|$)
- $|\langle a \rangle|$
- $\langle a^\dagger a \rangle$
- $\langle a^\dagger a^\dagger aa \rangle$

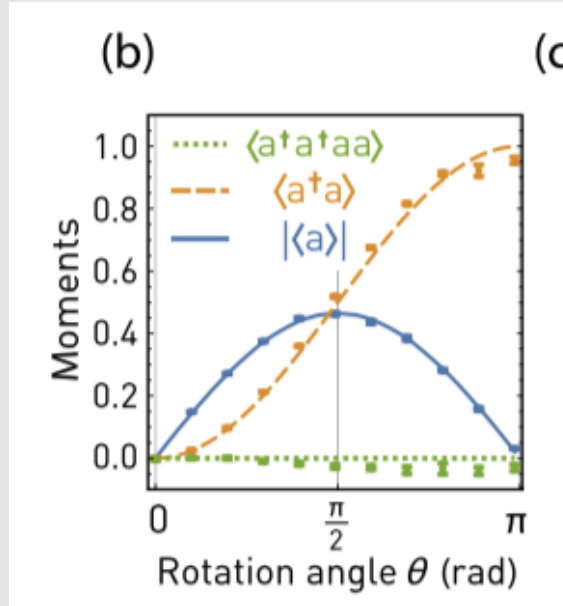
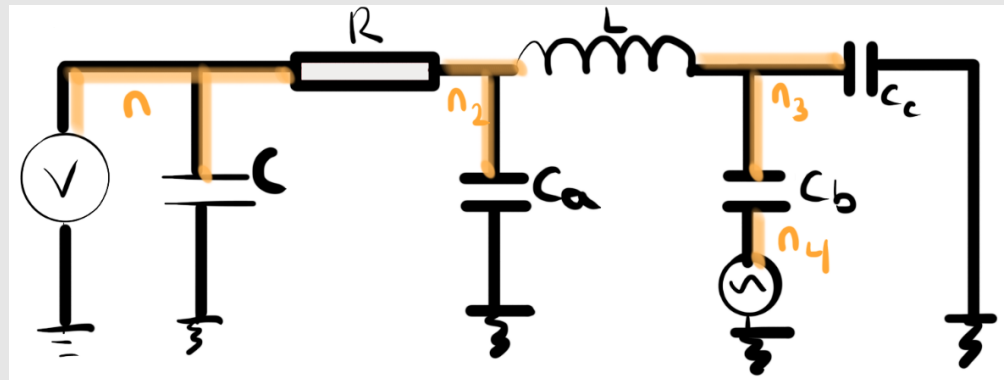


Figure 64: Ignore the green line. $a \propto$ equator component (coherent), and $a^\dagger a \propto$ relaxation from excited state (incoherent)

SIMULATING CIRCUITS

Oleg went through how one would simulate a circuit, such as the one below (in fact this is the setup for the inverse Shapiro step):



Constraints in this system are that we solve the current for

- Work with n number of CP of charge **2e**;
- V the DC voltage that we fix;

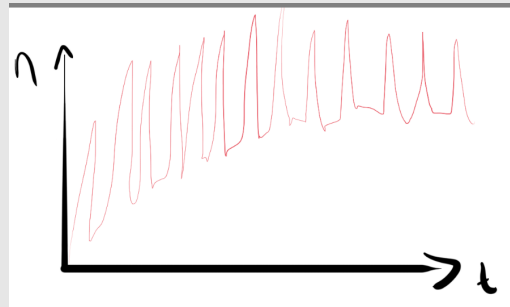
- f is the frequency of the rf-bias.
- Ignore that large capacitance C - it's so large that it has no effect on the whole system.

Next we write out a system of simultaneous equations that Oleg solves numerically in **Mathematica** for $n(t)$.

$$\begin{cases} V = 2eR\dot{n} + \frac{2e}{C_a}n_2 \\ V = L\frac{d}{dt}(\dot{n} - \dot{n}_2) + \frac{2e}{C_b}(n_3 - n_4) - V_{rf} \cos(2\pi ft) \\ V = L\frac{d}{dt}(\dot{n} - \dot{n}_2) + \frac{2e}{C_c}n_3 \end{cases}$$

- Charge passing through resistor R and inductor, $V = LI$;
- Potential difference across capacitors due to onset charge;
- RF-voltage source in action.

What we find if oscillations in this charge number $n_1(t)$. Evaluating $\langle I(V) \rangle = \int_{t_1}^{t_2} 2en(t)dt$ for different bias voltages V , we can plot a V vs $\langle I(V) \rangle$ graph, which will show Shapiro steps.



PROPERTIES OF PHOTONS

If we have a decay of radiation

$$E^{(+)}(t) = E_0 e^{-2\pi i \nu_0 t} e^{-\frac{\kappa}{2} t}$$

and take its Fourier transform, we get a Lorentzian, with an intensity

$$|f(\nu)|^2 = \frac{4 |E_0|^2}{\kappa^2 + [4\pi(\nu_0 - \nu)]^2}.$$

It has a half-width of

$$\Delta\nu = \frac{\kappa}{2\pi},$$

and since $\Delta t = \kappa^{-1}$, we get the relationship

$$\Delta\nu\Delta t \approx \frac{1}{2\pi}$$

31.1 Emission and line broadening

Classically, we have an ensemble of atoms, the relaxing $|2\rangle \rightarrow |1\rangle$. If we hit particles to take away the ‘unradiated’ energy, the relaxation terminates, and atoms emit only part of the full energy $\hbar\omega_{21}$. Because this is an ensemble, on average the energy $\hbar\omega_{21}$ will still be emitted, just with a smaller Δt , so the line broadens.

Quantum mechanically, we cannot emit ‘parts’ of $\hbar\omega_{21}$. Either the photon is emitted, or the photon is not. Absurdly, if the atom has been emitting for a certain time, and then the energy is taken away (say during a collision), then it is free to track back and not release the photon, or release it fully.

31.2 Classical vs Quantum pulses

Suppose that an atom emits a photon of frequency hf and we start catching it by a localised detector (or just leave it to interact with the environment, which implicitly performs measurements for us)

- Classically the energy is spread out over space → **we never measure the total energy of the pulse**;
- Quantum the photon will be absorbed or not absorbed at different points in space. Performing an average over all the positions, we find an exponential decay with a vertical front.

Now, when emission takes place, the wavefunction evolves from $\Psi_2 \Phi_{\text{vacuum}}$ to

$$e^{-\frac{\Gamma}{2}t} \Psi_2 \Phi_{\text{vacuum}} + \sqrt{1 - e^{-\Gamma t}} \Psi_1 \Phi_{\text{photon}(t)}.$$

What is important here?

- Upon measurement, the wavefunction collapses to one of the two states: 1) either the atom is still excited; 2) the photon has been emitted;
- As the relaxation occurs, $\Phi_{\text{photon}}(t)$ evolves, to have a smaller and smaller ‘tail’ in the atom. The change occurs over a time Γ^{-1} .

When the atom gives all its excitation energy away during a collision and nothing is left to the radiation field, the atom need not “reel back” any field because, until that moment, no real emission took place. The latter emission happened only virtually – whatever that might mean!

- If we leave the system for long enough, it will, by itself, transfer irreversibly to state $\Psi_1 \Phi_{\text{photon}}$ (normally quantum mechanics is reversible, as long as measurement is not made);
- The photon has a size

$$cT = \frac{c}{\Gamma}.$$

This extension explains interference effects

The photon is spread over space **before** measurement, with a distribution:

$$\langle \hat{E}^{(-)}(\mathbf{r}, t) \hat{E}^{(+)}(\mathbf{r}, t) \rangle,$$

and the probability of detectors response is proportional to it.

Upon each measurement the photon will be localised in a single space, as the wavefunction collapses. Two important errors are:

- The photon is not localised before measurement - it's not a particle, it's a wavefunction with collapses only upon detection;
- The photons energy is not spread out - it's not a wave, it's a wavefunction.

- Photons are never split → in this case we would have photons of energy $\frac{1}{2}hf$, which would disappear from the observable world, as they have no atoms to be absorbed with.

- For interference we need two beams from the same source, so that phase fluctuations are the same - same as in the master beam.

But what if now, we measure over a timescale **of the order of the coherence time**, preventing washing out of the pattern? This was done with lasers (enough power to have many photons for clear interference) and an interference pattern was setup.

- A really cool way to measure interference patterns with very weak sources, is to take two beams, and beam split each one.
 - The stronger beams should interfere on a controlled detector. The interference pattern will constantly change (as the phase changes randomly in each beam). We pick on such pattern, and produce a square pulse **only** when it is formed;
 - This pulse is used to open a shutter on another screen, where the weaker beams are sent through. Thus, we will be building up a pattern of the two beams at a fixed phase, even though they come from two sources!

Note that for such weak intensities, the photon picture of light completely fails - if they were particles then its extremely improbable that both will be passing through the shutter at the same time to interfere with one another. Here light behaves more like a wave.

31.3 More about photons

We can also apply laser pulses to form superpositions of 2 atomic states. It is possible for the system to transition into one energy level simultaneously. **The emitted photon will have elements of both excited atomic states - this will show up as the photon having two frequencies!**

- **Parametric fluorescence:** during parametric down conversion in a non-linear medium, a single photon spontaneously decays into two more (idler and signal), abiding energy and momentum conservation:

$$\hbar(\omega_p) = \hbar(\omega_i + \omega_s);$$

$$\hbar\mathbf{k_p} = \hbar(\mathbf{k_i} + \mathbf{k_s}).$$

The emitted photons become entangled and will have a very strong correlation in terms of total energy and simultaneous measurement.

Such fluorescence photons are good to use as single photon sources - registering the idler photon, we can be 100% sure that a corresponding signal photon is flying in a specific direction

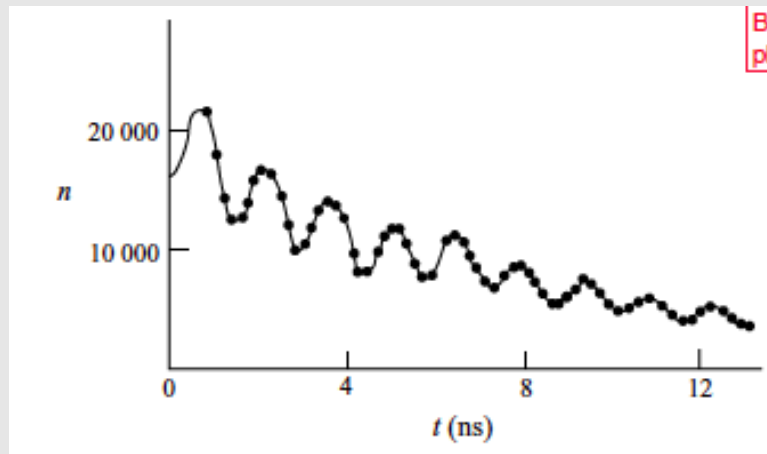


Figure 65: Suppose that we create a superposition in the atom $\frac{|1\rangle+|2\rangle}{\sqrt{2}}$. Then there are two possible ways for the atom to decay to the ground energy state and create an outgoing photon. When we measure the intensity of the photon, with the outgoing detector, the photons $1 \rightarrow 0$ and $2 \rightarrow 0$ components will interfere to produce beatings. The photon is thus imprinting the full information of the atomic excitation. Oh, did I mention this is a single photon? Classically this would be impossible to do with a single photon.

- Now consider forming an interference pattern with photons. The clarity of the interference pattern depends on the uncertainty of the phase, $\Delta\phi$. The phase and photon number abide the relationship

$$\Delta n \Delta \phi \geq \frac{1}{2},$$

so surely with decreasing photon number (decreasing Δn), the phase should diverge and wash out interference! \Rightarrow In reality the phase uncertainty accumulates in the vacuum state $|0\rangle$, which does not contribute to the interference pattern.

- To ensure good matching of frequencies from two sources, one can measure beats in interference patterns, and only open the shutter when the beats oscillate slowly (good frequency matching).

31.4 Photon bunching

We began with discussing that when observing stars. We use something similar to an interferometer, and pick up an interference pattern on the telescope screen.

Now consider a second light source (different part of the planet). It will fly in at an ever smaller different angle, and its' pattern will be shifted, relative to the initial one. An overlap will occur if we increase the separation of the telescope mirrors (increasing the phase difference between the patterns). This is called the coherence length - separation at which interference vanishes

Probability that two photons arrive at the same place shortly one after another i.e. $\tau < t_{coh}$ is higher than if they arrive with a larger time delay $\tau > t_{coh}$.

This is exactly analogous to the coherence length above, except in time!

If one thinks in the photon picture, this implies that photon sources communicate with each other to release photons in pairs. **But this is seriously wrong!** It is actually due to interference between the waves emitted by completely different atoms!

31.5 Types of light

Coherence volume or time is over which the **instantaneous** phase does not change significantly within it.

The photon number is related to the mode volume $V_{coherence}$. In experiments we must be working within this volume, or within the related time T , over which coherence persists. **If a fraction of the volume (time) is observed, then only a fraction of photons present are observed**

1. **Thermal light, is formed of partial waves with random phases.** The intensity fluctuates in time. **The bandwidth of scattered light is very narrow**, giving a large Δt for intensity correlation measurements.

It follows a Bose Einstein distribution which is very broad and **the photons are subject to bunching!**

2. **Laser light** has a constant amplitude (intensity) and follows a Poisson distribution, which is much narrower than the Bose one for thermal light.

Laser light does not tend to bunch (unlike thermal light) with the coincidence photon rate being the same as the random one - same probability of detecting photons for all kinds of different time delays.

31.6 Photon antibunching

Occurs with photons with a sharp photon number $\langle n \rangle$.

So now consider the case of a detector, which accumulates over a time (or volume) V_{obs} . It has probability

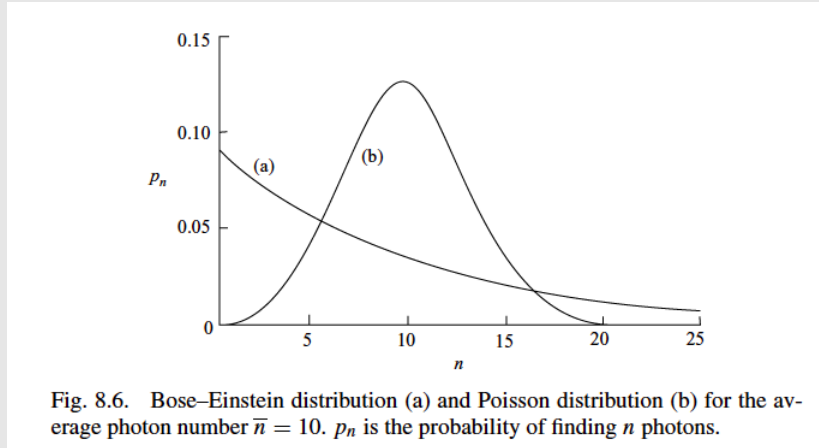


Fig. 8.6. Bose-Einstein distribution (a) and Poisson distribution (b) for the average photon number $\bar{n} = 10$. p_n is the probability of finding n photons.

$$t = \frac{V_{\text{obs}}}{V_{\text{coh}}} \eta, \quad (40)$$

of detecting a photon, which depends on the ratio of the observed to the coherence volume (**recall that photon numbers are associated with the mode volume V_{coh} , so if we observe a smaller volume, than we register a fraction of the photons.**)

The detector either detects or photon (with probabiltiy t) or it doesn't. So the probability of transmitting k out of n photons follows a binomial distribution

$$\text{Prob}(k \text{ photons}) = \binom{n}{k} t^k r^{n-k},$$

which has a variance

$$\Delta k^2 = (1 - t) \langle k \rangle \quad (\equiv \langle k^2 \rangle - \langle k \rangle^2).$$

Now, look out!

- The lower the detection probability in Eq. (40), due to shorter integration time or lower efficiency, the large the variance Δk^2 .
- If however we are able to detect all photon in the mode volume V_{coh} , then there should be no variance.

Unlike with bunched light, where photon number is undefined, the ratio of random clicks to simultaneous clicks

$$R = \frac{\Delta n^2 - \langle n \rangle}{\langle n \rangle^2},$$

can be negative! Negative relative to the counts we would measure outside the coherence time/volume, where statistics were random.

This is showing photon antibunching, whereby photon do not tend to be simultaneously detected in the same coherence volume.

Let us discuss this more fully

- Classically the coincidence counting rate (simultaneous clicks) $\propto I(t)I(t + \tau)$, which has a maximum at $\tau = 0$ (opposite of antibunching);
- **Antibunching:** (Sub-)Poisson statistics for $\langle n \rangle \rightarrow 0$. $\Delta n < \langle n \rangle$. Only when we fire single photons.;
- **Bunching:** Poisson statistics for $\langle n \rangle \rightarrow \infty$. $\Delta n > \langle n \rangle$.
-

31.7 Creating antibunching

To create a stream of bullets (which is not how we imagined light classically - we used to think of it as a wave)

- Use atoms flying through cavity \rightarrow excite and allow some of them to relax \rightarrow then measure with an ionisation detector to recover photon statistics from the de-excited atom statistics;
- Create electron hole pairs and create light emission in a controlled way;

31.8 Squeezed light

Squeezed light has a Δx or Δp smaller than vacuum. The other component is correspondingly blown up. These two quantities arise when we rewrite the field

$$\mathbf{E}(\vec{r}, t) = A e^{i(\vec{k}\vec{r} - \omega t)} + A^* e^{-i(\vec{k}\vec{r} - \omega t)},$$

The quantum mechanical description of the field is

$$\hat{E} = \hat{E}^{(+)} + \hat{E}^{(-)} = e^{-i\omega t} \hat{a} + e^{i\omega t} \hat{a}^\dagger,$$

where the amplitude is replaced with the quantum mechanical field operators, telling how many photons are in the field. The energy of the field is

$$\hat{H} = \hbar\omega \hat{a}^\dagger \hat{a}$$

- Electric field strength $\langle \hat{E} \rangle = 0$ for states with well defined photon number $|n\rangle$. (The \hat{a} operators raise and lower this number, so that the product of two different ‘kets’ is 0.)

in terms of two new variables $x = \mathcal{R}A, p = \mathcal{I}\hat{A}$

$$E(\vec{r}, t) = C \left[x \cos(\omega t - \vec{k}\vec{r}) + p \sin(\omega t - \vec{k}\vec{r}) \right]$$

31.9 Phase distribution

Say we want to measure the phase distribution of the field

$$E(z, t) \propto \cos(\omega t - \phi - kz),$$

which we rewrite

$$\frac{\cos(\phi) \cos(\omega t - kz)}{\sqrt{x^2 + p^2}} + \frac{\sin(\phi) \sin(\omega t - kz)}{\sqrt{x^2 + p^2}}.$$

So by measuring the quadrates of the field, we can map out the x and the p components. There are multiple ways of describing x, p distribution in phase space (where distance from axis, ρ , is amplitude, and angle, ϕ):

- Through the Q function

$$w(x, p) = \frac{1}{\pi} |\langle \psi | \alpha \rangle|^2,$$

which loses some information about the x and p distribution, due to them being non-commutable observables;

- Wigner function, which gives full information about the state

$$W(x, p) = \frac{1}{\pi} \int_{-\infty}^{\infty} e^{i2py} \psi(x-y) \psi^*(x+y) dy.$$

This turns into the Q function, if we convolute it with a Gaussian, which smooths the function out.

)

INTERACTION PICTURE

Given an eigenstates of \hat{H}_0 , we can easily compute the system evolution

$$|\psi(t)\rangle = \sum_j \alpha_j e^{-iE_j t/\hbar} |\phi_j\rangle.$$

Now to find the state for a system with a Hamiltonian

$$\hat{H} = H_0 + V,$$

we define the interaction picture state

$$|\psi(t)\rangle_I = U_0(t)^\dagger |\psi(t)\rangle_S,$$

Substituting $|\psi(t)\rangle_S = U_0(t) |\psi(t)\rangle_I$ into the Schrödinger equation $i\hbar \frac{\partial}{\partial t} |\psi(t)\rangle_S = \hat{H} |\psi(t)\rangle_S$

$$i\hbar \frac{\partial}{\partial t} (U_0(t) |\psi(t)\rangle_I) = i\hbar \left(U_0(t) \frac{\partial |\psi(t)\rangle_I}{\partial t} + \frac{-iH_0}{\hbar} U_0(t) |\psi(t)\rangle_I \right) \equiv H U_0(t) |\psi(t)\rangle_I,$$

multiplying by $U_0^\dagger(t)$

$$\begin{aligned} i\hbar \frac{\partial |\psi(t)\rangle_I}{\partial t} &= H_I |\psi(t)\rangle_I \\ H_i &= U_0^\dagger(t) [H - H_0] U_0(t) = U_0^\dagger(t) [V] U_0(t). \end{aligned} \tag{41}$$

Ultimately, what we have found is that to solve for $H = H_0 + V$, one needs to

1. Find $H_I = U_0^\dagger(t) V U_0(t)$
2. Solve the interaction Scrodinger equation $i\hbar \frac{\partial |\psi(t)\rangle_I}{\partial t} = H_I |\psi(t)\rangle_I$
3. Find the Schroinger picture states by unwinding i.e. $|\psi(t)\rangle_S = U_0(t) |\psi(t)\rangle_I$

It can be easily shown that expectation values are preserved

$${}_I \langle \psi | \hat{O}_I | \psi \rangle_I = {}_S \langle \psi | U_0 U_0^\dagger \hat{O}_S U_0 U_0^\dagger | \psi \rangle_s \equiv_S \langle \psi | \hat{O}_S | \psi \rangle_S$$

CHAPTER 33

INTERACTION BETWEEN LIGHT AND ATOM

We construct the Hamiltonian for the full system

$$\hat{H} = \hat{H}_{\text{atom}} + \hat{H}_{\text{light}} + \hat{H}_{\text{atom - light}}.$$

- \hat{H}_{atom} comes from the energy levels of the atom

$$\hat{H}_{\text{atom}} = \hbar\omega_a |e\rangle\langle e| \otimes \mathbb{I}_{\text{light}},$$

- \hat{H}_{light} from before ([find reference](#)) is the Hamiltonian for the photon modes

$$\hat{H}_{\text{light}} = \mathbb{I}_{\text{atom}} \otimes \hbar\omega_j \left(\hat{a}^\dagger \hat{a} + \frac{1}{2} \right),$$

- and $\hat{H}_{\text{atom - light}} = -\hat{E} \cdot \hat{D}$ from Sec.34

$$\begin{aligned} \hat{H}_{\text{atom - light}} &= -(\mathbf{E}_{0x}(\hat{a} + \hat{a}^\dagger) \sin(\mathbf{k}\mathbf{z})) (\tilde{\mathbf{d}}(|g\rangle\langle e| + |e\rangle\langle g|)) \\ &= \hbar\mathbf{g}(\vec{r}) (\hat{a} + \hat{a}^\dagger) (|g\rangle\langle e| + |e\rangle\langle g|), \end{aligned}$$

where $\hbar\mathbf{g}(\vec{r}) = E_{0x} \sin(kz) \tilde{\mathbf{d}}$ is the coupling strength. Although ideally we should be writing state via the tensor product notation, we shall do this instead save space and write

$$|g, n\rangle = |g\rangle \otimes |n\rangle$$

The full Hamiltonian is then

$$\hat{H} = \hbar\omega_a |e\rangle\langle e| + \hbar\omega_j \left(\hat{a}^\dagger \hat{a} + \frac{1}{2} \right) + \hbar\mathbf{g}(\vec{r}) (\hat{a} + \hat{a}^\dagger) (|g\rangle\langle e| + |e\rangle\langle g|),$$

which we split up into two parts, to use the interaction picture, covered in Sec.32

$$\begin{cases} H = H_0 + \mathbf{V} \\ H_0 = \hbar\omega_a |e\rangle\langle e| + \hbar\omega_j \left(\hat{a}^\dagger \hat{a} + \frac{1}{2} \right) \\ \mathbf{V} = \hbar\mathbf{g}(\vec{r}) (\hat{a} + \hat{a}^\dagger) (|g\rangle\langle e| + |e\rangle\langle g|) \end{cases} \quad (42)$$

We compute the interaction Hamiltonian

$$\begin{cases} H_I = U_0^\dagger V U_0 \\ U_0 = \exp [-i\omega_j (\hat{a}^\dagger \hat{a} + 1/2) t] \exp [-i\omega_a |e\rangle \langle e| t] \end{cases} \Rightarrow$$

$$\Rightarrow \hbar g(\vec{r}) \times$$

$$\exp [+i\omega_j (\hat{a}^\dagger \hat{a} + 1/2) t] (\hat{a} + \hat{a}^\dagger) \exp [-i\omega_j (\hat{a}^\dagger \hat{a} + 1/2) t] \times \\ \exp [+i\omega_a |e\rangle \langle e| t] (|g\rangle \langle e| + |e\rangle \langle g|) \exp [-i\omega_a |e\rangle \langle e| t]$$

Then we proceed term by term

- $\exp [+i\omega_j (\hat{a}^\dagger \hat{a} + 1/2) t] \hat{a} \exp [-i\omega_j (\hat{a}^\dagger \hat{a} + 1/2) t] = \exp [+i\omega_j \hat{a}^\dagger \hat{a} t] \hat{a} \exp [-i\omega_j \hat{a}^\dagger \hat{a} t]$

The lowering operator

$$\hat{a} = \begin{bmatrix} \langle 0 | \hat{a} | 0 \rangle & \langle 0 | \hat{a} | 1 \rangle & \dots \\ \langle 1 | \hat{a} | 0 \rangle & \langle 1 | \hat{a} | 1 \rangle & \dots \\ \langle 2 | \hat{a} | 0 \rangle & \langle 2 | \hat{a} | 1 \rangle & \dots \\ \vdots & \vdots & \ddots \end{bmatrix} = \begin{bmatrix} \langle 0 | 0 & \langle 0 | \sqrt{1} | 0 \rangle & \dots \\ \langle 1 | 0 & \langle 1 | \sqrt{1} | 0 \rangle & \dots \\ \langle 2 | 0 & \langle 2 | \sqrt{1} | 0 \rangle & \dots \\ \vdots & \vdots & \ddots \end{bmatrix} = \begin{bmatrix} 0 & \sqrt{1} & \dots \\ 0 & 0 & \dots \\ 0 & 0 & \dots \\ \vdots & \vdots & \ddots \end{bmatrix}$$

$$= \sum_n \sqrt{n} |n-1\rangle \langle n|$$

and thus evaluating

$$\begin{aligned} & e^{+i\omega_j t \hat{a}^\dagger \hat{a}} \left[\sum_n \sqrt{n} |n-1\rangle \langle n| \right] e^{+i\omega_j t \hat{a}^\dagger \hat{a}} \\ &= \sum_n \sqrt{n} e^{+i\omega_j t \hat{a}^\dagger \hat{a}} |n-1\rangle \langle n| e^{-i\omega_j t \hat{a}^\dagger \hat{a}} \quad \leftarrow \text{expand exponential operator} \\ &= \sum_n \sqrt{n} e^{+i\omega_j (n-1)t} |n-1\rangle \langle n| e^{-i\omega_j nt} \\ &= e^{+i\omega_j (n-1)t} \left[\sum_n \sqrt{n} |n-1\rangle \langle n| \right] e^{-i\omega_j nt} \\ &= e^{+i\omega_j (n-1)t} \hat{a} e^{-i\omega_j nt} \\ &\equiv \mathbf{exp}[-i\omega_j t] \hat{a} \end{aligned}$$

- $\exp [+i\omega_j (\hat{a}^\dagger \hat{a} + 1/2) t] \hat{a}^\dagger \exp [-i\omega_j (\hat{a}^\dagger \hat{a} + 1/2) t] = \mathbf{exp}[+i\omega_j t] \hat{a}^\dagger$

•

$$\begin{aligned}
& \exp[+i\omega_a |e\rangle\langle e| t] |g\rangle\langle e| \exp[-i\omega_a |e\rangle\langle e| t] \\
&= \left[\exp[+i\omega_a t (\mathbb{I} - |g\rangle\langle g|)] |g\rangle \right] \left[\langle e| \exp[-i\omega_a |e\rangle\langle e| t] \right] \\
&= \left[\exp[+i\omega_a t (1 - 1)] |g\rangle \right] \left[\langle e| \exp[-i\omega_a 1t] \right] \\
&= \left[\exp[+i\omega_a t 0] \right] |g\rangle\langle e| \left[\exp[-i\omega_a t] \right] \\
&\equiv \exp[-i\omega_a t] |g\rangle\langle e|
\end{aligned}$$

• $\exp[+i\omega_a |e\rangle\langle e| t] |g\rangle\langle e| \exp[-i\omega_a |e\rangle\langle e| t] \equiv \exp[+i\omega_a t] |e\rangle\langle g|$

Combining the results

$$\begin{aligned}
H_I &= \hbar g(\vec{r}) \left[\exp^{-i\omega_j t} \hat{a} + \exp^{+i\omega_j t} \hat{a}^\dagger \right] \left[\exp^{-i\omega_a t} |g\rangle\langle e| + \exp^{+i\omega_a t} |e\rangle\langle g| \right] \\
&= \hbar g(\vec{r}) \left(\exp[-i(\omega_j - \omega_a)t] \hat{a} |e\rangle\langle g| + \exp[i(\omega_j - \omega_a)t] \hat{a}^\dagger |g\rangle\langle e| \right. \\
&\quad \left. + \exp[-i(\omega_j + \omega_a)t] \hat{a} |g\rangle\langle e| + \exp[i(\omega_j + \omega_a)t] \hat{a}^\dagger |e\rangle\langle g| \right) \tag{43}
\end{aligned}$$

33.1 Resonance

Looking at Eq.(43) at resonance, i.e. $\omega_a = \omega_j = \omega$

$$H_I = \hbar g(\vec{r}) \left(\hat{a} |e\rangle\langle g| + \hat{a}^\dagger |g\rangle\langle e| + \exp[-i2\omega t] \hat{a} |g\rangle\langle e| + \exp[i2\omega t] \hat{a}^\dagger |e\rangle\langle g| \right),$$

The two terms in red are neglected in the **ROTATING WAVE APPROXIMATION** - this is suitable for when the oscillations are much faster than the time-scales of the most significant physical processes.

Physically speaking, we keep energy conserving processes, where excitation/de-excitation processes pair up with photon destruction/creation.

$$H_I = \hbar g(\vec{r}) \left(\hat{a} |e\rangle\langle g| + \hat{a}^\dagger |g\rangle\langle e| \right). \tag{44}$$

Now we solve for the initial condition $|\psi(0)\rangle_I = |g, 1\rangle$. Notice that since

$$H_I |g, 1\rangle = \hbar g |e, 0\rangle \quad H_I |e, 0\rangle = \hbar g |g, 1\rangle, \tag{45}$$

which means that there is only coupling between $|g, 1\rangle$ and $|e, 0\rangle$ states. As proof of this, recall the evolution of the density matrix from Eq.(47), $\rho(t) = \sum_{i=1}^n p_i U(t) |\Psi_i\rangle\langle\Psi_i| U(t)^\dagger$, and “zooming-in” on

$$\begin{aligned} U(t) |\Psi_i\rangle &= e^{-i\frac{\hat{H}}{\hbar}t} |\Psi_i\rangle = \sum_k \frac{\left(-i\frac{\hat{H}}{\hbar}t\right)^k}{k!} |\Psi_i\rangle \\ &= \sum_k \frac{\left(\frac{-it}{\hbar}\right)^k}{k!} \hat{H}^k |\Psi_i\rangle, \end{aligned}$$

and thus if the only $|\Psi_i\rangle$ was $|g, 1\rangle$, which we showed can only transform to something proportional to $|e, 0\rangle$ in the red, these will be the only states in the system.

Thus the general state of the system will be

$$|\psi(t)\rangle_I = \alpha(t) |g, 1\rangle + \beta(t) |e, 0\rangle.$$

Substituting into the Schroedinger equation, using Eq.(44) and Eq.(45),

$$\begin{aligned} \frac{\partial |\psi\rangle_I}{\partial t} &= -\frac{i}{\hbar} H_I |\psi\rangle_I \\ \frac{\partial \alpha}{\partial t} |g, 1\rangle + \frac{\partial \beta}{\partial t} |e, 0\rangle &= -\frac{i}{\hbar} \left(\alpha H_I |g, 1\rangle + \beta H_I |e, 0\rangle \right) \\ \frac{\partial \alpha}{\partial t} |g, 1\rangle + \frac{\partial \beta}{\partial t} |e, 0\rangle &= -ig \left(\alpha |e, 0\rangle + \beta |g, 1\rangle \right) \end{aligned}$$

Multiplying by $|g, 1\rangle$ and $|e, 0\rangle$

$$\begin{cases} \frac{\partial \alpha}{\partial t} = -ig\beta \\ \frac{\partial \beta}{\partial t} = -ig\alpha \end{cases} \Rightarrow \begin{cases} \frac{\partial \alpha^2}{\partial t} = -ig\frac{\partial \beta}{\partial t} = -ig(-ig\alpha) = -g^2\alpha \\ \frac{\partial \beta^2}{\partial t^2} = -ig\frac{\partial \alpha}{\partial t} = -ig(-ig\beta) = -g^2\beta \end{cases}$$

And solving for the initial conditions $\alpha(0) = 1, \beta(0) = 0$

$$\begin{cases} \alpha(t) = \exp[igt] \\ \beta(t) = \exp[igt] \end{cases} \Rightarrow \begin{cases} \alpha(t) = \cos(gt) \\ \beta(t) = i \sin(gt) \end{cases},$$

resulting in

$$\begin{aligned} |\psi(t)\rangle_I &= \cos(gt) |g, 1\rangle + i \sin(gt) |e, 0\rangle \\ |\psi(t)\rangle_S &= \cos(gt) U_0(t) |g, 1\rangle + i \sin(gt) U_0(t) |e, 0\rangle \\ &= \cos(gt) \exp[-it\hat{H}_0/\hbar] |g, 1\rangle + i \sin(gt) \exp[-it\hat{H}_0/\hbar] |e, 0\rangle. \end{aligned}$$

Using Eq.(42)

$$\begin{aligned}
\hat{H}_0 |g\rangle |1\rangle &= \left[\hbar\omega |e\rangle \langle e| \otimes \mathbb{I}_{\text{light}} + \mathbb{I}_{\text{atom}} \otimes \hbar\omega \left(\hat{a}^\dagger \hat{a} + \frac{1}{2} \right) \right] |g\rangle \otimes |1\rangle \\
&= \hbar\omega |e\rangle \langle e| |g\rangle \otimes |1\rangle + |g\rangle \otimes \hbar\omega \left(\hat{n} + \frac{1}{2} \right) |1\rangle \\
&= 0 |g\rangle \otimes |1\rangle + |g\rangle \otimes \hbar\omega(1 + 1/2) |1\rangle \\
&= (0 + 3\hbar\omega/2)) |g, 1\rangle = \frac{3\hbar\omega}{2} |g, 1\rangle \\
\hat{H}_0 |e\rangle |0\rangle &= (\hbar\omega + \hbar\omega/2) = \frac{3\hbar\omega}{2} |e, 0\rangle
\end{aligned}$$

one gets a constant phase factor

$$|\psi(t)\rangle_s = \exp[-i3\omega t/2] \left[\cos(gt) |g, 1\rangle + i \sin(gt) |e, 0\rangle \right]$$

For any arbitrary n , it can be shown that

$$|\psi(t)\rangle_I = \cos(\sqrt{n}gt) |g, n\rangle + i \sin(\sqrt{n}gt) |e, n-1\rangle$$

CHAPTER 34

THE DIPOLE APPROXIMATION

Classically, for a dipole $\vec{D} = q\vec{r}$, for example an atom and an electron orbiting at a radius \vec{r} . In an electric field \vec{E} , it gives rise to an interaction energy

$$U = -\vec{D} \cdot \vec{E}.$$

The expression for \vec{E} has already been found before (insert reference) to be $E_{0x}(\hat{a} + \hat{a}^\dagger) \sin(kz)$.

As for the quantum operator for \vec{D} , we begin by assuming a two level atom, with a Hamiltonian

$$\hat{H} = 0|g\rangle\langle g| + \hbar\omega_a|e\rangle\langle e|,$$

for a separation $\hbar\omega_a$ between the two levels. This approximation for a many level atom is good, as long as the photon mode energy $\hbar\omega_j = \hbar\omega_a$, with all other transitions off resonance.

With such a two level system, the matrix for \vec{D} will be

$$\begin{bmatrix} \langle g | \hat{D} | g \rangle & \langle g | \hat{D} | e \rangle \\ \langle e | \hat{D} | g \rangle & \langle e | \hat{D} | e \rangle. \end{bmatrix}$$

However, from parity (\vec{r} is odd), $\langle g | \hat{D} | g \rangle = \langle e | \hat{D} | e \rangle \equiv 0$, and so only the off diagonal elements are non zero. We label $\langle g | \hat{D} | e \rangle = \langle e | \hat{D} | g \rangle \equiv \vec{d}$ resulting in

$$\hat{D} = \begin{bmatrix} 0 & \vec{d} \\ \vec{d} & 0 \end{bmatrix} = \vec{d}(|g\rangle\langle e| + |e\rangle\langle g|).$$

CHAPTER 35

BACKGROUND ON QUANTUM MECHANICS

PRINCIPLES

35.1 The density matrix

First we introduce the concept of the density matrix, derived fully in [quantum course]. To begin with we consider a system with probabilities p_1 and p_2 of being in state Ψ_1 and a Ψ_2 . The expectation value for the observable \hat{O} is then

$$\langle \hat{O} \rangle = p_1 \langle \Psi_1 | \hat{O} | \Psi_1 \rangle + p_2 \langle \Psi_2 | \hat{O} | \Psi_2 \rangle,$$

which is some form of numerical value. Taking the trace of this value, which can be viewed as a 1-dimensional matrix, and remembering trace is a linear operator and that its cyclic invariance, one gets

$$\begin{aligned} \text{Tr}(\langle \hat{O} \rangle) &= \text{Tr}(p_1 \langle \Psi_1 | \hat{O} | \Psi_1 \rangle) + \text{Tr}(p_2 \langle \Psi_2 | \hat{O} | \Psi_2 \rangle) \\ &= p_1 \text{Tr}(\hat{O} |\Psi_1\rangle \langle \Psi_1|) + p_2 \text{Tr}(\hat{O} |\Psi_2\rangle \langle \Psi_2|) \\ &= \text{Tr}\left(p_1 \hat{O} |\Psi_1\rangle \langle \Psi_1| + p_2 \hat{O} |\Psi_2\rangle \langle \Psi_2|\right) \\ &= \text{Tr}(\hat{O} \rho), \end{aligned}$$

where $\rho = p_1 |\Psi_1\rangle \langle \Psi_1| + p_2 |\Psi_2\rangle \langle \Psi_2|$ is the density operator. Generalising for n states,

$$\begin{aligned} \rho &= \sum_{i=1}^n p_i |\Psi_i\rangle \langle \Psi_i| \\ \langle \hat{O} \rangle &= \text{Tr}(\hat{O} \rho). \end{aligned} \tag{46}$$

Note that the states do **not** need to be orthogonal. This notation is convenient when there is uncertainty in the preparation of states in our system. When the density matrix is

$$\rho = |\Psi\rangle \langle \Psi|,$$

then it is a pure state, otherwise is is mixed. Generally one shall work in the matrix representation of the density matrix, in which case one inserts the closure relation $\sum |\phi\rangle \langle \phi|$ to get

$$\begin{aligned}\rho &= \sum_j |\phi_j\rangle \langle \phi_j| \rho \sum_k |\phi_k\rangle \langle \phi_k| \\ &= \sum_{jk} \rho_{jk} |\phi_j\rangle \langle \phi_k|,\end{aligned}$$

where $\rho_{jk} = \langle \phi_j | \rho | \phi_k \rangle$. In such a way, the density matrix can be written

$$\rho = \begin{pmatrix} \rho_{11} & \rho_{12} & \rho_{13} \\ \rho_{31} & \rho_{22} & \rho_{23} \\ \rho_{31} & \rho_{32} & \rho_{33} \end{pmatrix}.$$

The density matrix has several important properties.

- $\rho = \rho^\dagger$
- ρ has unit trace. This is seen by looking at Eqn.(46) and noting that in the basis of the given vectors, the trace must be 1, since the sum of the probabilities is 1. Trace is invariant under the basis that one chooses, so $\text{Tr}(\rho) = 1$
- Finally one can test for the purity of the system, by evaluating $\text{Tr}(\rho^2)$. From Eqn.(46) its is obvious that the diagonal elements will be squared. Since they are all ≤ 1 , summing them up will lead to
 - $\text{Tr}(\rho^2) = 1$, in which case the state is pure (only one element, with $p = 1$).
 - $\text{Tr}(\rho^2) < 1$, in which case the state is mixed **and cannot be expressed via a single projector**

Purity does not change under unitary evolution (prove using cyclic invariance of trace)

An important operation involving the density matrix is the partial trace. Consider first a system in an entangled state - that is we consider two quantum systems A and B and observe their joint state. If this state **cannot** be factorised into distinct states for system A and B , then the system is entangled.

Next consider the density matrix for a compound system, which is represented in the orthonormal basis $\{|a_j, b_k\rangle\}$ of the joint system

$$\rho = \sum_{j,k} \sum_{l,m} \rho_{j,k,l,m} |a_j, b_k\rangle \langle a_l, b_m|,$$

with $\rho_{j,k,l,m} = \langle a_j, b_k | \rho | a_l, b_m \rangle$. If one is dealing with an entangled states, then it is not possible to separate the state into an individual description of the two systems. What one can do, is trace out one of the system, while retaining all the information about the observable of the other. To see this, consider how one would find the expectation value of an observable in A

$$\begin{aligned}
\langle \hat{O}_A \rangle &= \text{Tr} \left\{ (\hat{O}_A \otimes \mathbb{I}_{\rho_{AB}}) \right\} \\
&= \sum_{jk} \langle a_j, b_k | \hat{O}_A \otimes \mathbb{I}_{\rho_{AB}} | a_j, b_k \rangle \\
&= \sum_j \langle a_j | \hat{O}_A \left(\sum_k \langle b_k | \rho_{AB} | b_k \rangle \right) | a_j \rangle \\
&= \sum_j \langle a_j | \hat{O}_A \rho_A | a_j \rangle \\
&= \text{Tr} \left\{ (\hat{O}_A \rho_A) \right\},
\end{aligned}$$

where we defined $\rho_A = \text{Tr} \{(\rho_{AB})\}_B = \sum_k \langle b_k | \rho_{AB} | b_k \rangle$. This has effectively traced out/took partial trace to give a reduced state of the system. The action of the tracing out

$$\begin{aligned}
\rho_A &= \text{Tr} \{(\rho_{AB})\}_B = \sum_{k'} \langle b_{k'} | \rho_{AB} | b_{k'} \rangle \\
&= \sum_{jk} \sum_{lm} \sum_{k'} \langle b_{k'} | \rho_{j,k,l,m} | a_j, b_k \rangle \langle a_l, b_m | | b_{k'} \rangle \\
&= \sum_{jk} \sum_{lm} \sum_{k'} \rho_{j,k,l,m} | a_j \rangle \langle b_{k'} | | b_k \rangle \langle b_m | | b_{k'} \rangle \langle a_l | \\
&= \sum_{jk} \sum_{lm} \sum_{k'} \rho_{j,k,l,m} | a_j \rangle \langle a_l | \delta_{k'k} \delta_{mk'} \\
&= \sum_j \sum_l \sum_{k'} \rho_{j,k',l,k'} | a_j \rangle \langle a_l | \\
&= \sum_j \sum_l \left(\sum_k \rho_{j,k',l,k'} \right) | a_j \rangle \langle a_l|,
\end{aligned}$$

and in the last line we see that the result is a set of operators with weights $\sum_k \rho_{j,k',l,k'}$. The reduced state ρ_A will only be pure if there was no entanglement.

The evolution of the density matrix will be

$$\begin{aligned}
\rho(0) &= \sum_{i=1}^n p_i |\Psi_i\rangle \langle \Psi_i| \longrightarrow \rho(t) = \sum_{i=1}^n p_i U(t) |\Psi_i\rangle \langle \Psi_i| U(t)^\dagger \\
&\quad = U(t) \rho(0) U^\dagger(t),
\end{aligned} \tag{47}$$

where $U(t) = e^{-i \frac{\hat{H}}{\hbar} t}$, which, as a reminder, can be written out in matrix form as

$$U(t) = e^{-i \frac{\hat{H}}{\hbar} t} = \sum_k \frac{\left(-i \frac{\hat{H}}{\hbar} t\right)^k}{k!}.$$

The most important question of why use it? It widens the state vector formalism to represent states prepared probabilistically, which do **Cannot be described by a**

wavefunction.

One can get a version of the Schrödinger equation, by differentiating Eq.(47)

$$\begin{aligned}
 \frac{\partial \rho(t)}{\partial t} &= \dot{U}(t)\rho(0)U^\dagger(t) + U(t)\rho(0)\dot{U}^\dagger(t) \\
 &= -\frac{i}{\hbar}\hat{H}U(t)\rho(0)U^\dagger(t) + \frac{i}{\hbar}\hat{H}U(t)\rho(0)U^\dagger(t) \\
 &= \frac{i}{\hbar} [\rho(t), \hat{H}]
 \end{aligned} \tag{48}$$

CHAPTER 36

OPEN QUANTUM SYSTEMS

When system interacts with the environment, in other words the system is not isolated, then it becomes exceedingly hard to solve the Schrödinger for the whole system. There are too many interacting modes for this to be feasible.

Such quantum systems are referred to as *open quantum systems*. We wish to solve the evolution of this specific subsystem. A key point is that in this case, states become entangled, and the global state can no longer be factored as a specific environment and system states. The density matrix formalism allows one to overcome this (the reduced state of an entangled state is a mixed state, which density matrices can represent).

36.1 How a mixed state arises

Since unitary operators preserve purity, it's impossible to create a mixed state from a pure one, using unitary evolution. **Now we examine quantum evolutions which allow this**

1. Classical Randomness

Start off with a pure state

$$\rho = |\Psi\rangle\langle\Psi|.$$

and perform a unitary transformation U_j with probability p_j . The result is

$$\rho \rightarrow \rho' = \sum_j p_j U_j \rho U_j^\dagger,$$

recall Eq.(47). Thus classical randomness has prepared a mixed state.

2. From entanglement

Begin with an entangled state - tensor product of two density matrices

$$\hat{\rho}_{SB} = \hat{\rho}_S \otimes \hat{\rho}_B.$$

Unitary evolution under the **Full Hamiltonian**

$$\rho'_{SB} = U \left[\rho_S(0) \otimes \rho_B(0) \right] U^\dagger,$$

Then we trace out the unwanted B component (by taking the sandwich with the basis vectors $\{|e_i\rangle\}$)

$$\begin{aligned}\rho'_S &= \text{Tr}_B \{ \rho'_{SB} \} \\ &= \sum_k \langle e_k | U \left[\rho_S(0) \otimes \rho_B(0) \right] U^\dagger | e_k \rangle.\end{aligned}$$

Assuming that $\rho_B(\mathbf{0}) = |\mathbf{e}_0\rangle\langle\mathbf{e}_0|$,

$$\begin{aligned}\rho'_S &= \sum_k \left[\langle e_k | U | e_0 \rangle \right] \rho_S(0) \left[\langle e_0 | U^\dagger | e_k \rangle \right] \\ &= \sum_k S_k \rho_S(0) S_k^\dagger,\end{aligned}$$

S_k being introduced for the super-operator concept below.

36.2 Superoperators

In parallel with the way that an operator maps one vector to another

$$|\psi'\rangle = \hat{O} |\psi\rangle,$$

a super-operator maps one operator (density matrix) into another

$$\rho' = S[\rho],$$

for the two examples above it would have been

$$\rho' = S[\rho] = \begin{cases} \sum_j p_j U_j \rho U_j^\dagger \\ \sum_k [\langle e_k | U | e_0 \rangle] \rho [\langle e_0 | U^\dagger | e_k \rangle]. \end{cases}$$

All superoperators in quantum mechanics can be written in the form

$$S[\rho] = \sum_j K_j \rho K_j^\dagger,$$

$$\sum_j K_j^\dagger K_j = \mathbb{I}.$$

For the above Example 1, $K_j = \sqrt{p_j} U_j$.

Important properties

1. Does NOT need to be unitary
2. If ρ is Hermitian, trace 1 and non negative eigenvalues, then ρ' has the same properties.

36.3 Deriving equation for open quantum system

We would like to derive an evolution equation of the form

$$\dot{\rho}(t) = S[\rho(t)],$$

i.e. find such a superoperator $S[]$, that returns the rate of change of the density matrix (analogy to Schrödinger's $|\dot{\psi}(t)\rangle = \frac{-i\hat{H}}{\hbar} |\psi(t)\rangle$). It only depends on the state of the system **immediately before**.

A system, whose evolution only depends on the state **RIGHT NOW**, is known as Markovian. No dependence on $\rho(t')$ much earlier than t . An example is Snakes and Ladders.

Furthermore, it should only depend on the reduced state of our system of interest (**not on the state of the other system**) \equiv flow of information out of the system like the interaction of atoms with electromagnetic field - emitted photons will never return to the system practically.

We make three assumptions to find an expression for

$$\dot{\rho}(t) = S[\rho(t)].$$

1. We work with $\rho(0)$ and $\rho(\delta t)$, instead of $\rho(t)$ and $\rho(t + \delta t)$.
2. There is a superoperator which takes $\rho(0) \rightarrow \rho(\delta t)$ (i.e. Markovian evolution)

$$\rho(\delta t) = S[\rho(0)] = \sum_j K_j(\delta t) \rho(0) K_j^\dagger(\delta t). \quad (49)$$

3.

$$\begin{aligned} \dot{\rho}(t) &= \lim_{\delta t \rightarrow 0} \frac{\rho(t + \delta t) - \rho(t)}{\delta t} \quad \Rightarrow \quad \rho(t + \delta t) = \rho(t) + \dot{\rho}(t) \delta t \\ &\Rightarrow \rho(\delta t) = \rho(0) + \underbrace{\dot{\rho}(0)}_{\dot{\rho}(0)} \delta t \end{aligned} \quad (50)$$

This is accurate in the limit $\delta t \rightarrow 0$. The highlighted $\dot{\rho}(0)$ is what we want to find.

In order for Eq.(50) and Eq.(49) to be the same, the Kraus operators must be

$$K_j = \begin{cases} K_0 &= \mathbb{I} + \delta t A \\ K_j &= \sqrt{\delta t} L_j \end{cases},$$

where A and L_j are linear operators, and this is proven by direct substitution into Eq.(49)

$$\left\{ \begin{array}{l} \text{Eq.(49)} \quad \rho(\delta t) = K_0 \rho(0) K_0^\dagger + \sum_{j=1}^{\infty} K_j(\delta t) \rho(0) K_j^\dagger(\delta t) \\ = (\mathbb{I} + \delta t A) \rho(0) (\mathbb{I} + \delta t A^\dagger) + \delta t \sum_{j=1}^{\infty} L_j \rho(0) L_j^\dagger \\ = \rho(0) + \delta t A \rho(0) + \delta t \rho(0) A^\dagger + \underbrace{O(\delta t^2)}_{=} + \delta t \sum_{j=1}^{\infty} L_j \rho(0) L_j^\dagger \Rightarrow \\ = \rho(0) + \delta t \left(A \rho(0) + \rho(0) A^\dagger + \sum_{j=1}^{\infty} L_j \rho(0) L_j^\dagger \right) \\ \text{Eq.(50)} \quad \rho(\delta t) = \rho(0) + \dot{\rho}(0) \delta t \\ \Rightarrow \dot{\rho}(0) = A \rho(0) + \rho(0) A^\dagger + \sum_{j=1}^{\infty} L_j \rho(0) L_j^\dagger \\ \Rightarrow \dot{\rho}(t) = A \rho(t) + \rho(t) A^\dagger + \sum_{j=1}^{\infty} L_j \rho(t) L_j^\dagger \end{array} \right. \quad (51)$$

Next, express the linear operator A as a sum of **Hermitian** operators $H = H^\dagger, M = M^\dagger$

$$A = -\frac{i}{\hbar} H + M \quad \Rightarrow \quad K_0 = \mathbb{I} + \delta t \left(-\frac{i}{\hbar} H + M \right). \quad (52)$$

Recall, that Kraus operators must fulfil $\sum_j K_j^\dagger K_j = \mathbb{I}$, meaning that there is a constraint on the values of H and M :

$$\begin{aligned} \mathbb{I} &= \sum_j K_j^\dagger K_j = \left(\mathbb{I} + \delta t \left(+\frac{i}{\hbar} H + M \right) \right) \left(\mathbb{I} + \delta t \left(-\frac{i}{\hbar} H + M \right) \right) + \sum_j \sqrt{\delta t} L_j^\dagger \sqrt{\delta t} L_j \\ &= \mathbb{I} + \delta t \left(+\frac{i}{\hbar} H + M \right) + \delta t \left(-\frac{i}{\hbar} H + M \right) + \underbrace{O(\delta t^2)}_{=} + \delta t \sum_{j=1}^{\infty} L_j^\dagger L_j \\ &= \mathbb{I} + 2\delta t M + \delta t \sum_{j=1}^{\infty} L_j^\dagger L_j \quad \Rightarrow \quad M = -\frac{1}{2} \sum_{j=1}^{\infty} L_j^\dagger L_j. \end{aligned} \quad (53)$$

Whoa, that's a lot. Lets tie in the results of Eq.(51), Eq.(52) and Eq.(53)

$$\begin{aligned}
\dot{\rho}(t) &= A\rho(t) + \rho(t)A^\dagger + \sum_{j=1}^{\infty} L_j \rho(t) L_j^\dagger \\
&= \left(-\frac{i}{\hbar} H + M \right) \rho(t) + \rho(t) \left(+\frac{i}{\hbar} H + M \right) + \sum_{j=1}^{\infty} L_j \rho(t) L_j^\dagger \\
&= -\frac{i}{\hbar} \left(H - i\frac{\hbar}{2} \sum_{j=1}^{\infty} L_j^\dagger L_j \right) \rho(t) + \frac{i}{\hbar} \rho(t) \left(H + i\frac{\hbar}{2} \sum_{j=1}^{\infty} L_j^\dagger L_j \right) + \sum_{j=1}^{\infty} L_j \rho(t) L_j^\dagger, \\
&\Rightarrow \begin{cases} H_{\text{eff}} = H - i\frac{\hbar}{2} \sum_{j=1}^{\infty} L_j^\dagger L_j \\ \dot{\rho}(t) = -\frac{i}{\hbar} H_{\text{eff}} \rho(t) + \frac{i}{\hbar} \rho(t) H_{\text{eff}} + \sum_{j=1}^{\infty} L_j \rho(t) L_j^\dagger \end{cases}
\end{aligned}$$

or fully, the Lindblad form of the Master equation:

$$\begin{cases} \dot{\rho}(t) = -\frac{i}{\hbar} [H_{\text{eff}}, \rho(t)] + \sum_{j=1}^{\infty} L_j \rho(t) L_j^\dagger \\ H_{\text{eff}} = H - i\frac{\hbar}{2} \sum_{j=1}^{\infty} L_j^\dagger L_j \end{cases}. \quad (54)$$

Note that H_{eff} is NOT Hermitian. But note how this is similar to the Von Neumann equation (Eq.(48)) $\dot{\rho}(t) = -i\hbar[H, \rho(t)]$ form. This allows us to digest what the different parts of the master equation contribute:

- **System Hamiltonian**

$-\frac{i}{\hbar} [H_{\text{eff}}, \rho(t)]$ - the deterministic part of the equation, describing the evolution of closed system with Hamiltonian H_{eff} . It is

1. Deterministic (can predict evolution)
2. Non-unitary, so purity is **is not preserved**.

- **Quantum jumps**

$\sum_{j=1}^{\infty} L_j \rho(t) L_j^\dagger$ - irreversible dynamics due to coupling with the environment.

36.4 Example application

As an example, consider spontaneous emission by an atom. We need to identify the two parts of Eq.(54).

1. The closed system, is that of an atom in state $|e\rangle$ or $|g\rangle$, with a Hamiltonian

$$H = \hbar\omega |e\rangle \langle e|. \quad (55)$$

2. Irreversible dynamics occur due to the atom interacting with the modes in the surrounding electromagnetic field. We use the Jaynes-Cummings Hamiltonian for the single mode in Sec.33. In that case, the photon could be reabsorbed by the atom, **but not in this case**, so the evolution is Markovian. A single jump operator

$$L = \gamma |g\rangle\langle e|, \quad (56)$$

is used, to embody the spontaneous decay of an atom.

Next we evaluate the effective Hamiltonian

$$\begin{aligned} H_{\text{eff}} &= H - i\frac{\hbar}{2} \sum_{j=1}^{\infty} L_j^\dagger L_j \\ &= \hbar\omega |e\rangle\langle e| - i\frac{\hbar}{2} (\gamma |g\rangle\langle e|)^\dagger (\gamma |g\rangle\langle e|) \\ &= \hbar\omega |e\rangle\langle e| - i\frac{\hbar}{2} |\gamma|^2 |e\rangle\langle g| |g\rangle\langle e| \\ &= \left(\hbar\omega - \frac{i\hbar}{2} |\gamma|^2 \right) |e\rangle\langle e|, \end{aligned}$$

and as an aside, we can see that $U = \exp \left[-i\frac{\hbar\omega_{\text{eff}}|e\rangle\langle e|}{\hbar} t \right] = \exp \left[-|\gamma|^2 t |e\rangle\langle e| \right] \exp \left[i\omega t |e\rangle\langle e| \right]$ is not norm preserving (with and exponential decay).

We want to find the time evolving state of the form

$$\begin{aligned} \rho(t) &= \rho_{ee}(t) |e\rangle\langle e| + \rho_{gg}(t) |g\rangle\langle g| \\ \dot{\rho}(t) &= \dot{\rho}_{ee}(t) |e\rangle\langle e| + \dot{\rho}_{gg}(t) |g\rangle\langle g| \end{aligned} \quad (57)$$

Subbing Eq.(55), Eq.(56) and Eq.(57) into the master equation

$$\left\{ \begin{array}{l} \dot{\rho}(t) = -\frac{i}{\hbar} [H_{\text{eff}}\rho(t) - \rho(t)H_{\text{eff}}^\dagger] + L\rho(t)L^\dagger \\ H_{\text{eff}}\rho(t) = \hbar \left(\omega - \frac{i}{2} |\gamma|^2 \right) \rho_{ee}(t) |e\rangle\langle e| \\ \rho(t)H_{\text{eff}}^\dagger = \hbar \left(\omega + \frac{i}{2} |\gamma|^2 \right) \rho_{ee}(t) |e\rangle\langle e| \\ L\rho(t)L^\dagger = \gamma |g\rangle\langle e| \left(\rho_{ee}(t) |e\rangle\langle e| + \rho_{gg}(t) |g\rangle\langle g| \right) \gamma^* |e\rangle\langle g| = |\gamma|^2 \rho_{ee}(t) |g\rangle\langle g| \end{array} \right. \Rightarrow \begin{aligned} \dot{\rho}(t) &= -\frac{i}{\hbar} \left(-i\hbar|\gamma|^2 \right) \rho_{ee}(t) |e\rangle\langle e| + |\gamma|^2 \rho_{ee}(t) |g\rangle\langle g| \\ &= -|\gamma|^2 \rho_{ee}(t) |e\rangle\langle e| + |\gamma|^2 \rho_{ee}(t) |g\rangle\langle g| \end{aligned},$$

resulting in

$$\dot{\rho}(t) = \begin{cases} \dot{\rho}_{ee}(t) |e\rangle\langle e| + \dot{\rho}_{gg}(t) |g\rangle\langle g| & \leftarrow \text{desired solution} \\ -|\gamma|^2 \rho_{ee}(t) |e\rangle\langle e| + |\gamma|^2 \rho_{ee}(t) |g\rangle\langle g| & \leftarrow \text{Master equation} \end{cases},$$

or in matrix form

$$\dot{\rho}(t) = \begin{bmatrix} \dot{\rho}_{ee} & \dot{\rho}_{eg} \\ \dot{\rho}_{eg} & \dot{\rho}_{gg} \end{bmatrix} = \begin{bmatrix} -|\gamma|^2 \rho_{ee} & 0 \\ 0 & |\gamma|^2 \rho_{ee} \end{bmatrix}.$$

These simple first order differential equations are solved for the initial state $\rho(0) = |e\rangle\langle e|$ to get (using the fact that trace sum must be 1, so $\rho_{gg} = 1 - \rho_{ee}$)

$$\begin{aligned} \rho_{ee}(t) &= e^{-|\gamma|^2 t} \\ \rho_{ee}(t) &= 1 - e^{-|\gamma|^2 t}, \end{aligned}$$

so the probability of an atom being in the excited state decays, as expected.

36.5 Summary of method

1. Find the Hamiltonian for the system H .
2. Find the relevant jump operators L_j .
3. Compute the effective Hamiltonian $H_{\text{eff}} = H - i\frac{\hbar}{2} \sum_{j=1}^{\infty} L_j^\dagger L_j$.
4. Express the desired form of the state we want to find $\rho(t)$ e.g $\rho_{ee}(t) |e\rangle\langle e| + \rho_{gg}(t) |g\rangle\langle g| + \rho_{ge}(t) |g\rangle\langle e| + \rho_{eg}(t) |e\rangle\langle g|$.
5. Substitute $\rho(t)$ and H_{eff} into the master equation and evaluate the rate of change $\dot{\rho}(t) = -\frac{i}{\hbar} [H_{\text{eff}}\rho(t) - \rho(t)H_{\text{eff}}^\dagger] + L\rho(t)L^\dagger$.
6. Integrate the density matrix, to get the state at any given time. Or for the stationary state $\dot{\rho} = 0$, solve set of linear differential equations.

CHAPTER 37

REPRESENTING 2-LEVEL SYSTEM AS A SPIN

We call the magnetic dipole the quantity

$$\vec{\mu} = IA,$$

the product of the current around a loop, by the area it encompasses. It points perpendicular to the plane of the loop.

When placed inside a uniform magnetic field, the torque on the setup will be (can be proven by geometry and $\vec{F} = l \cdot \vec{I} \times \vec{B}$

$$\tau = \vec{\mu} \times \vec{B},$$

which attempts to rotate the moment to the lowest energy configuration, when the magnetic moment falls in line with the magnetic field. The energy of a magnetic moment we measure relative to the case when the magnetic moment is \perp to the magnetic field, and taking the integral $\int \tau d\theta$, one gets the energy

$$U = -\vec{\mu} \cdot \vec{B}.$$

Evaluating the moment for a simple electron in orbit like in Sec. 37

$$\mu = \left[-|e| \frac{v}{2\pi r} \right] \pi r^2 = -\frac{|e|}{2} rv,$$

and remembering that $mrv = L$ - the angular momentum

$$\vec{\mu} = -\frac{|e|}{2m} \vec{L} \quad U = -\frac{|e|}{2m} \vec{L} \cdot \vec{B}.$$

Following commutation relations for angular momentum, follows the quantisation of angular momentum into ladder like states (we guess the way that L_z and L^2 act on their eigenstates. The general direction that this is done for is the z-direction, whereby L_z and \hat{L}^2 both become quantised. In momentum space this means that for a fixed angular momentum in one direction, we know nothing of the other two components.

The Stern-Gerlach experiment on measuring the deflection of electrons, resulted in the speculation that there was an additional type of ‘hidden’ momentum - the spin. By analogy the magnetic moment from spin is

$$\vec{\mu}_s = -g_e \frac{|e|}{2m_e} \vec{S}. \quad (58)$$

Using similar arguments, one finds two eigenvectors

$$|s = 1/2, m = +1/2\rangle = \begin{bmatrix} 1 \\ 0 \end{bmatrix} \quad |s = 1/2, m = -1/2\rangle = \begin{bmatrix} 0 \\ 1 \end{bmatrix},$$

which are expressed in their eigenbasis, that form a complete set (as long as we don't introduce other degrees of freedom).

Writing out the way spin operators affect these eigenstates (i.e. when we measure spin)

$$\begin{aligned} \hat{S}_z |\uparrow\rangle &= +\frac{\hbar}{2} |\uparrow\rangle \hat{S}_z |\downarrow\rangle = -\frac{\hbar}{2} |\downarrow\rangle \\ \hat{S}^2 |\uparrow\rangle &= \frac{3}{4}\hbar^2 |\uparrow\rangle \hat{S}^2 |\downarrow\rangle = \frac{3}{4}\hbar^2 |\downarrow\rangle, \\ \hat{S}_+ |\uparrow\rangle &= 0 \hat{S}_+ |\downarrow\rangle = \hbar |\uparrow\rangle \\ \hat{S}_- |\uparrow\rangle &= \hbar |\downarrow\rangle \hat{S}_- |\downarrow\rangle = 0 \end{aligned}$$

and taking the sandwiches $\langle \uparrow | S | \downarrow \rangle$ to evaluate the matrix elements (and using $S_x = \frac{S_+ + S_-}{2}$ etc)

$$\hat{S}_z = \frac{\hbar}{2}\sigma_x \quad \hat{S}_y = \frac{\hbar}{2}\sigma_y \quad \hat{S}_x = \frac{\hbar}{2}\sigma_z$$

Thus the general spin operator is found by combining (58) and Eq. 37

$$\hat{\mu} = -g_e \frac{|e|}{2m_e} \hat{S} = -g_e \frac{|e|}{2m_e} \frac{\hbar}{2} \begin{bmatrix} \sigma_x \\ \sigma_y \\ \sigma_z \end{bmatrix} = -\mu \begin{bmatrix} \sigma_x \\ \sigma_y \\ \sigma_z \end{bmatrix}$$

The Hamiltonian $\mathcal{H} = \hat{\mu} \cdot \vec{B}$ is then

$$\begin{aligned} \mathcal{H} &= -\mu (B_x \sigma_x + B_y \sigma_y + B_z \sigma_z) \\ &= -\frac{\hbar}{2} \left(\omega_x \sigma_x + \omega_y \sigma_y + \omega_z \sigma_z \right), \end{aligned}$$

where we introduced a convenient frequency. **Any two level system has this energy spectrum, with an offset energy.** The dynamics are then:

$$i\hbar \frac{d\vec{\sigma}}{dt} = \mathcal{H} \vec{\sigma} \propto \vec{B} \cdot \vec{\sigma} \quad (59)$$

Further, the density matrix for an arbitrary two level system can always be written in the form (remember normalisation $|\alpha|^2 + |\beta|^2 = 1$)

$$\begin{aligned}
 \rho &= \begin{pmatrix} \alpha \\ \beta \end{pmatrix} \begin{pmatrix} \alpha^* & \beta^* \end{pmatrix} = \begin{pmatrix} |\alpha|^2 & \alpha\beta^* \\ \beta\alpha^* & |\beta|^2 \end{pmatrix} \\
 &= \begin{pmatrix} |\alpha|^2 & (\Re[\alpha] + i\Im[\alpha])(\Re[\beta] - i\Im[\beta]) \\ (\Re[\beta] + i\Im[\beta])(\Re[\alpha] - i\Im[\alpha]) & |\beta|^2 \end{pmatrix} \\
 \begin{bmatrix} \alpha \\ \beta \end{bmatrix} \Rightarrow &= \begin{pmatrix} |\alpha|^2 & \Re[\alpha]\Re[\beta] + \Im[\alpha]\Im[\beta] + i(\Im[\alpha] - \Im[\beta]) \\ \Re[\alpha]\Re[\beta] + \Im[\alpha]\Im[\beta] - i(\Im[\alpha] - \Im[\beta]) & |\beta|^2 \end{pmatrix} \\
 &= \begin{pmatrix} |\alpha|^2 & X + iY \\ X - iY & 1 - |\alpha|^2 \end{pmatrix} \\
 &= \begin{pmatrix} \frac{1}{2} & 0 \\ 0 & \frac{1}{2} \end{pmatrix} + \begin{pmatrix} |\alpha|^2 - \frac{1}{2} & 0 \\ 0 & -[|\alpha|^2 - \frac{1}{2}] \end{pmatrix} + \begin{pmatrix} 0 & X \\ X & 0 \end{pmatrix} + \begin{pmatrix} 0 & +iY \\ -iY & 0 \end{pmatrix} \\
 \rho &= \frac{1}{2} \left(\mathbb{I} + \mathbf{u}_x \sigma_x + \mathbf{u}_y \sigma_y + \mathbf{u}_z \sigma_z \right)
 \end{aligned}$$

CHAPTER 38

RABI OSCILLATIONS

Rabi oscillations - occur between two levels when subjected to their resonant transition frequency ω_r , and occur with a frequency of Ω between the two levels i.e. **The Rabi frequency = Amplitude of the driving field**. In the original frame the state evolves between $|0\rangle$ and $|1\rangle$ in a cyclic manner. In the rotated frame, two eigenstates of the Hamiltonian are $(|0\rangle \pm |1\rangle)/\sqrt{2}$ and the state also evolves coherently between them.

This drive will also lead to the splitting of the energy levels, with a characteristic width Ω as well. So the amplitude dictates the oscillation frequency and the splitting of the two level system.

So one applies a pulse for a time t at a given power Ω , so that Rabi oscillations are driven for a time t . Next one removes the drive, and measures the resulting state of the qubit (by measuring emission from the atom). The position of the final state on the Bloch sphere, determines the output signal.

Now, the data capturing device has a minimum bandwidth of 1Hz i.e. averages the signal over 1 second. We repeat the above experiment (same power and pulse length) 1 million times, and output the cumulative signal acquired. It will be proportional to the analytic probability of the qubit being in its final state.

Then we elongate the length of the pulse, so that the state now finishes on a different part of the Bloch sphere. And repeat. We thus get oscillations, with Rabi period (from analytical calculations).

Because of dephasing, longer pulses will mean that one acquires more and more random phases. When the pulses were short, the phases didn't have time to evolve freely and deviate from the exact value. For longer pulses, the separate measurements differ more and more in phase i.e. the integral of the different phases will get closer and closer to zero. This is the decay of the collective signal.

CHAPTER 39

PERTURBATION THEORY

A **perturbation** applied to a system

$$\hat{H}(t) = \hat{H}_0 + \lambda \hat{V}(t).$$

We need to find the evolution of the initial state to the final state

$$|\psi(0)\rangle \rightarrow |\psi(t)\rangle.$$

We use eigenstates $|\phi\rangle_i$ of the Hermitian operator \hat{H}_0 that form a basis.

1. The state at an arbitrary time is a weighted superposition

$$|\psi(t)\rangle_I = \sum_j c_j(t) |\phi_j\rangle \quad \text{interaction picture - operator evolves}$$

$$|\psi(t)\rangle_S = \sum_j c_j(t) \exp\left[\frac{-iE_j\hbar}{t}\right] |\phi_j\rangle \quad \text{Schrodinger picture - state evolves}$$

2. Solving the Schrödinger equation in the interaction picture (see Chapter 32)

$$i\hbar \frac{\partial |\psi(t)\rangle_I}{\partial t} = \left(U_0^\dagger \lambda \hat{V}(t) U_0\right) |\psi(t)\rangle_I \Rightarrow$$

$$i\hbar \frac{\partial}{\partial t} \left[\sum_j c_j(t) |\phi_j\rangle \right] = \left(U_0^\dagger \lambda \hat{V}(t) U_0\right) \left[\sum_k c_k(t) |\phi_k\rangle \right].$$

3. Taking out the time dependent terms, and ‘sandwiching’

$$\sum_j \frac{\partial c_j(t)}{\partial t} \langle \phi_m | |\phi_j\rangle = \frac{\lambda}{i\hbar} \sum_k \left[\langle \phi_m | U_0^\dagger \right] \hat{V}(t) c_k(t) \left[U_0 | \phi_k \rangle \right] \Rightarrow$$

$$\sum_j \frac{\partial c_j(t)}{\partial t} \delta_{mj} = \frac{\lambda}{i\hbar} \sum_k \left[\langle \phi_m | e^{+iE_m t/\hbar} \right] \hat{V}(t) c_k(t) \left[e^{-iE_k t/\hbar} | \phi_k \rangle \right] \Rightarrow$$

where we used

$$U(t) |\psi(t)\rangle = \exp[-i\hat{H}t/\hbar] |\psi\rangle = \sum_n \frac{1}{n!} \left[\frac{-i\hat{H}t}{\hbar} \right]^n |\psi\rangle = \sum_n \frac{1}{n!} \left[\frac{-iEt}{\hbar} \right]^n |\psi\rangle = \exp[-iEt/\hbar] |\psi\rangle.$$

4. This evaluates to

$$\frac{\partial c_m(t)}{\partial t} = \frac{\lambda}{i\hbar} \sum_k c_k(t) e^{i(\mathbf{E}_m - E_k)t/\hbar} \langle \phi_m | \hat{V}(t) | \phi_k \rangle \Rightarrow$$

$$\frac{\partial c_m(t)}{\partial t} = \frac{\lambda}{i\hbar} \sum_k c_k(t) e^{i(\mathbf{E}_m - E_k)t/\hbar} \langle \hat{V}(t) \rangle_{mk}.$$

5. A useful thing to do now, is to expand the ‘weighting factors’ $c_m(t)$ as a power series of the small parameter λ :

$$c_m(t) = c_m^{(0)}(t) + \lambda c_m^{(1)}(t) + \lambda^2 c_m^{(2)}(t) + \dots$$

Now lets sub in this expansion into Eq. 4 and compare terms with λ powers on the LHS and RHS:

(a)

$$\lambda^0 \rightarrow \frac{dc_m^{(0)}(t)}{dt} = 0.$$

The initial state of the system before any perturbation ($\lambda = 0$) is an eigenstate $|\Psi(0)\rangle = |\phi_i\rangle$.

Since this initial weight $c_j^{(0)}$ doesn’t change:

$$c_m^{(0)}(t) = \text{constant} = \langle \phi_m | \Psi(0) \rangle = \delta_{m,i}.$$

(b) λ^1

$$\begin{aligned} \frac{dc_m^{(1)}(t)}{dt} &= \frac{1}{i\hbar} \sum_k c_k^{(0)}(t) e^{i\omega_{mk}t} \langle \hat{V}(t) \rangle_{mk} \\ &= \frac{1}{i\hbar} \sum_k \delta_{k,i} e^{i\omega_{mk}t} \langle \hat{V}(t) \rangle_{mk} \\ &= \frac{1}{i\hbar} e^{i\omega_{mi}t} \langle \hat{V}(t) \rangle_{mi} \end{aligned}$$

giving weights of the for the initial state component, $c_i^{(1)}(t)$ and the others that arise, $c_m^{(1)}(t)$:

$$\begin{aligned} c_i^{(1)}(\tau) &= \frac{1}{i\hbar} \int_0^\tau dt \hat{V}_{ii}(t) \\ c_m^{(1)}(\tau) &= \frac{1}{i\hbar} \int_0^\tau dt \hat{V}_{mi}(t) \exp[i\omega_{mi}t] \end{aligned}$$

1. λ^2

$$\begin{aligned}\frac{dc_m^{(2)}(t)}{dt} &= \frac{1}{i\hbar} \sum_k c_k^{(1)}(t) e^{i\omega_{mk} t} \langle \hat{V}(t) \rangle_{mk} \\ &= \frac{1}{i\hbar} \sum_k \left[\frac{1}{i\hbar} \int_0^t dt \hat{V}_{mi}(t) \exp[i\omega_{mi}t] \right] e^{i\omega_{mk} t} \langle \hat{V}(t) \rangle_{mk}\end{aligned}$$

39.1 Fermi's golden rule

So up to this point, we have determined that we have the evolution following a perturbation in the interactin picture

$$\begin{aligned}|\psi\rangle &\rightarrow |\Psi(t)\rangle = \sum_m c_m(t) |m\rangle \equiv |\psi\rangle + \sum_m c_m^{(1)}(t) |m\rangle \\ c_m(t) &= c_m^{(0)}(t) + \lambda c_m^{(1)}(t) + \lambda^2 c_m^{(2)}(t) + \dots \\ c_m^{(0)}(t) &= \text{const} = \delta_{m,i} \\ c_i^{(1)}(\tau) &= \frac{1}{i\hbar} \int_0^\tau dt \hat{V}_{ii}(t) \\ c_m^{(1)}(\tau) &= \frac{1}{i\hbar} \int_0^\tau dt \hat{V}_{mi}(t) \exp[i\omega_{mi}t]\end{aligned}$$

The probability that upon measurement, we collapse into state $|j\rangle$:

$$\text{Prob(collapsing into } |j\rangle) = |\langle j| |\Psi(t)\rangle|^2 = \left| \langle j| \left(|\psi\rangle + \lambda \sum_m c_m^{(1)}(t) |m\rangle \right) \right|^2.$$

The **first term** goes to zero, as states $|\psi\rangle$, $|j\rangle$ are othogonal, and in the **second term** only $|m\rangle = |j\rangle$ will be selected:

$$\begin{aligned}\text{Prob collapsing into } |j\rangle &= \left| \lambda c_j^{(1)}(t) \right|^2 \\ c_j^{(1)}(t) &= \frac{1}{i\hbar} \int_0^\tau dt \hat{V}_{mi}(t) \exp[i\omega_{ji}t] \\ \hat{V}_{ji}(t) &= \langle j| \hat{V}(t) |i\rangle\end{aligned}$$

In the special case, that the perturbation has a frequency corresponding to the energy separation of states $|i\rangle$, $|j\rangle$:

$$\lambda \hat{V}(t) = \hat{A} e^{-i\omega_{ji}t},$$

the rotation in the integral cancels out, leaving:

$$\text{Prob collapsing into } |j\rangle = \left| \frac{1}{i\hbar} \langle j | \hat{A} | i \rangle \tau \right|^2 \propto \left| \langle j | \hat{A} | i \rangle \right|^2.$$

Driving something in resonance between two states, will mean that the probability of transition (transition rate) is proportional to

$$t_{ij} \propto \left| \langle j | \hat{A} | i \rangle \right|^2.$$

CHANGING THE BASIS

An operator is **unitary** if its Hermitian conjugate is its inverse i.e. $UU^\dagger = U^\dagger U = \mathbb{I}$

Unitary operators are

- Norm preserving;
- Inner product preserving,

Making them ideal for transformation of basis to

One can always transform from $\{|\beta_i\rangle\}$ to $\{|\alpha\rangle\}$ by $U|\beta_i\rangle = |\alpha_i\rangle$.

Let us find the matrix form of the operator U that results in $|\alpha_i\rangle \xrightarrow{U} |\beta_i\rangle$.

We begin with

$$|\Psi\rangle = \sum_j c_j |\alpha_j\rangle,$$

and apply the closure relation, using the $\{|\beta_i\rangle\}$ basis.

$$\begin{aligned} |\Psi\rangle &= \sum_j c_j \left(\sum_k |\beta_k\rangle \langle \beta_k| \right) |\alpha_j\rangle \\ &= \sum_k \left(\sum_j c_j \langle \beta_k | \alpha_j \rangle \right) |\beta_k\rangle \\ &= \sum_{j,k} c_j \color{red} U_{kj} |\beta_k\rangle, \end{aligned}$$

the result of which is the transformation of $|\Psi_{\{|\alpha_j\rangle\}}\rangle$ to $|\Psi_{\{|\beta_j\rangle\}}\rangle$, by applying suitable weightings U_{kj} in the new basis.

The elements $U_{k,j} = \langle \beta_k | \alpha_j \rangle$ are the matrix elements on the unitary of operator

$$U = \begin{bmatrix} U_{00} & U_{01} & U_{02} & \cdots & U_{0n} \\ U_{10} & U_{11} & U_{12} & \cdots & U_{1n} \\ \vdots & \vdots & \vdots & \ddots & \vdots \\ U_{m0} & U_{m1} & U_{m2} & \cdots & U_{mn} \end{bmatrix} = \begin{bmatrix} \langle \beta_0 | \alpha_0 \rangle & \langle \beta_0 | \alpha_1 \rangle & \langle \beta_0 | \alpha_2 \rangle & \cdots & \langle \beta_0 | \alpha_n \rangle \\ \langle \beta_1 | \alpha_0 \rangle & \langle \beta_1 | \alpha_1 \rangle & \langle \beta_1 | \alpha_2 \rangle & \cdots & \langle \beta_1 | \alpha_n \rangle \\ \vdots & \vdots & \vdots & \ddots & \vdots \\ \langle \beta_m | \alpha_0 \rangle & \langle \beta_m | \alpha_1 \rangle & \langle \beta_m | \alpha_2 \rangle & \cdots & \langle \beta_m | \alpha_n \rangle \end{bmatrix}$$

Thus when one perform the unitary operation

$$\begin{aligned} |\alpha_k\rangle = U|\beta_k\rangle \equiv U_{kj}|\beta_k\rangle &= \begin{bmatrix} \langle \beta_0 | \alpha_0 \rangle & \langle \beta_0 | \alpha_1 \rangle & \langle \beta_0 | \alpha_2 \rangle & \cdots & \langle \beta_0 | \alpha_n \rangle \\ \langle \beta_1 | \alpha_0 \rangle & \langle \beta_1 | \alpha_1 \rangle & \langle \beta_1 | \alpha_2 \rangle & \cdots & \langle \beta_1 | \alpha_n \rangle \\ \vdots & \vdots & \vdots & \ddots & \vdots \\ \langle \beta_m | \alpha_0 \rangle & \langle \beta_m | \alpha_1 \rangle & \langle \beta_m | \alpha_2 \rangle & \cdots & \langle \beta_m | \alpha_n \rangle \end{bmatrix} \begin{bmatrix} 0 \\ 0 \\ \vdots \\ 1 \\ \vdots \end{bmatrix} \xleftarrow{\text{in } \{|\beta_j\rangle\} \text{ basis}} \\ &= \begin{bmatrix} \langle \beta_0 | \alpha_k \rangle \\ \langle \beta_1 | \alpha_k \rangle \\ \vdots \\ \langle \beta_m | \alpha_k \rangle \end{bmatrix} \xleftarrow{\text{now expressed in the } \{|\alpha_j\rangle\} \text{ basis}} \\ &= \sum_j \langle \beta_j | \alpha_k \rangle |\beta_j\rangle, \end{aligned}$$

so one has effectively projected $|\alpha_k\rangle$ onto **every single component** of the $\{|\beta_i\rangle\}$ basis.

CHAPTER 41

FLUCTUATION DISSAPATION THEORY

FROM BRIAN COWANS NOTES

41.1 Summary

- How correlation functions of voltage and current can be integrated to give the resistances in a given circuit:

$$R = \frac{1}{2kT} \int \langle V(0)V(t) \rangle dt \quad \frac{1}{R} = \frac{1}{2kT} \int \langle I(0)I(t) \rangle dt.$$

- When a system feels an effect $B(\tau)$, it responds with $M(t)$ according to the dynamical susceptibility X .

$$M(t) = \int_{-\infty}^t X(t-\tau)B(\tau)d\tau.$$

- For a sinusidal excitation $B(t) = be^{-i\omega t}$ the response is

$$\begin{aligned} M(t) &= be^{-i\omega t}\chi(\omega) \\ \chi(\omega) &= \int_{-\infty}^{\infty} X(\tau)e^{i\omega t}d\tau \end{aligned}$$

The real and imaginary parts of dynamical susceptibility are even and add respectively.

- Working in frequency domain

Given a superposition of forces (expressed by $b(\omega)$ in the frequency range)

$$B(t) = \frac{1}{2\pi} \int_{-\infty}^{\infty} b(\omega)e^{-i\omega t}d\omega,$$

the response can be found by evaluating the response at frequency:

$$m(\omega) = \chi(\omega)b(\omega),$$

and ‘summing’ them up, which is equivalent to taking the fourier transform

$$M(t) = \frac{1}{2\pi} \int_{-\infty}^{\infty} m(\omega)e^{-i\omega t}d\omega.$$

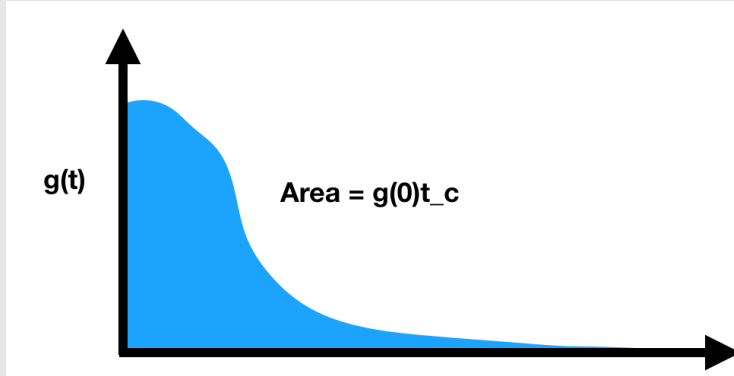


41.2 Correlation function

The correlation function

$$g(\tau) = \langle X(0)X(\tau) \rangle - \langle X^2 \rangle,$$

measures how fast variations in a system will go away. Effectively what is happening is we are averaging the fluctuation $X(t)$ over time from its equilibrium value $\langle X \rangle$. Of course, a decay should slowly decay (on average, and hence that is why we take the expectation value $\langle X(t) \rangle$).



Because fluctuations are symmetrical about the equilibrium value, we need to multiply the fluctuation by its initial value $X(0)$ to avoid averaging out to 0. *This is a very clever trick indeed.*

41.3 Fluctuation dissipation theory

This is a very general theory, applied here for current and voltage respectively. The idea is to write out the dynamics of one variable, and equate the energy found to the energy available. This constrains the value of some of the parameters.

1. Write out the equation of motion:

$$L \frac{dI}{dt} + RI(t) = V(t) \quad (\text{Kirchoffs 2nd}) \qquad C \frac{dV}{dt} + \frac{1}{R}V(t) = I(t) \quad (\text{Kirchoffs 1st}).$$

2. Propose a trial solution (this is called the integrating factor method, and I covered on Wikipedia):

$$I(t) = I(0)e^{-tR/L} + \frac{1}{L} \int_0^t e^{(u-t)\frac{R}{L}} V(u) du \qquad V(t) = V(0)e^{-t/CR} + \frac{1}{C} \int_0^t e^{(u-t)/CR} I(u) du \quad (60)$$

3. Assume that the correlation of the random fluctuation is very short:

$$\langle I(t_1)I(t_2) \rangle = I^2 \delta(t_1 - t_2) \quad \langle V(t_1)V(t_2) \rangle = V^2 \delta(t_1 - t_2) \quad (61)$$

4. Compute the mean power deposited from Eq. (60) after a long time (so the first exponentially decaying terms go away):

$$\begin{aligned} \langle I^2 \rangle &= \frac{1}{L} 2e^{-2Rt/L} \int_0^t e^{uR/L} \langle I(0)V(u) \rangle du + \frac{e^{-2Rt/L}}{L^2} \int_0^t du \int_0^t dw e^{(u+v)R/L} \langle V(u)V(w) \rangle \\ \langle V^2 \rangle &= \frac{1}{C} 2e^{-2t/RC} \int_0^t e^{u/RC} \langle V(0)I(u) \rangle du + \frac{e^{-2t/RC}}{C^2} \int_0^t du \int_0^t dw e^{(u+v)/RC} \langle I(u)I(w) \rangle. \end{aligned}$$

The red terms dissapear, because there is no correlation between current and voltage

$$\langle V(t_1)I(t_2) \rangle = 0,$$

while for the blue terms, we need to use Eq. (61) to get cancelation of one of the integrals:

$$\begin{aligned} \langle I^2 \rangle &= V^2 \frac{e^{-2Rt/L}}{L^2} \int_0^t du e^{2uR/L} = V^2 \frac{1}{2RL} (1 - e^{-2Rt/L}) \xrightarrow{t \rightarrow \infty} \frac{V^2}{2RL} \\ \langle V^2 \rangle &= I^2 \frac{e^{-2t/RC}}{C^2} \int_0^t du e^{2u/RC} = I^2 \frac{R}{2C} (1 - e^{-2t/RC}) \xrightarrow{t \rightarrow \infty} = \frac{I^2 R}{2C} \end{aligned} \quad (62)$$

5. In thermal equilibrium, a system in an environment at temperature T , will have $\frac{1}{2}k_bT$ of energy associated with each degree of freedom in the system. For circuits there is one degree of freedom (current or voltage determines the value of the other), and so

$$\frac{1}{2}k_bT = \frac{1}{2}L \langle I \rangle^2 \quad (\text{inductor}) \quad \frac{1}{2}k_bT = \frac{1}{2}C \langle V \rangle^2,$$

Combined with Eq. (62) this gives

$$\frac{V^2}{2R} = kT \quad \frac{I^2 R}{2} = kT. \quad (63)$$

6. Combining Eq. (63) with Eq. (61) we wind up at the result fluctuation dissipation result:

$$R = \frac{1}{2kT} \int \langle V(0)V(t) \rangle dt \quad \frac{1}{R} = \frac{1}{2kT} \int \langle I(0)I(t) \rangle dt.$$

Expression of dissipation through the area under the correlations.

41.4 Responses

In the following sections we consider the dynamic susceptibility X , that transforms an input B to an output M .

The response of a system, M , to an external force B we treat by assuming that the system responds to the history $B(\tau)$ via the **dynamical susceptibility** function

$$X(t - \tau). \quad (64)$$

We write out the history of the forces, and use the mapping Eq. (64), to find how each of these forces manifests itself at time t .

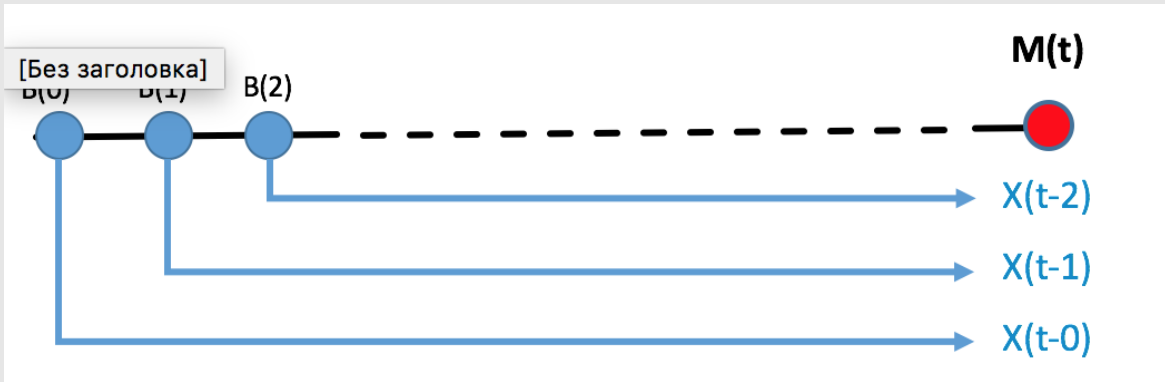


Figure 66: We break up the force in time, and mapping their effect using the susceptibility function, we can evaluate the response of the system at a later time.

Two assumptions are made:

- Linearity - the effect of the different forces $X(t - t_i)B(t_i)$ is linearly summed up to find the resultant;
- Causality implies that $t_i < t$, since the force cannot precede its own effect.

to write the formula:

$$M(t) = \int_{-\infty}^t X(t - \tau)B(\tau)d\tau. \quad (65)$$

41.4.1 Sinusoidal Excitation

An excitation of the form:

$$B(t) = b \cos(\omega t) - ib \sin(\omega t) = be^{-i\omega t},$$

results in the response (where we will remember manually that $X(t) = 0$ if $t < 0$, so the limits are changed from Eq. (65))

$$\begin{aligned} M(t) &= b \int_{-\infty}^{+\infty} X(t - \tau) e^{-i\omega\tau} d\tau \quad \text{chang of var} \\ &= b e^{-i\omega t} \int_{-\infty}^{\infty} X(\tau) e^{i\omega\tau} d\tau \end{aligned}$$

or more compactly

$$\begin{aligned} M(t) &= b e^{-i\omega t} \chi(\omega) \\ \chi(\omega) &= \int_{-\infty}^{\infty} X(\tau) e^{i\omega\tau} dt \end{aligned} \tag{66}$$

Because response is linear, if we split up the frequency domain susceptibility into real and imaginary components

$$\chi(\omega) = \chi'(\omega) + i\chi''(\omega),$$

then the response to

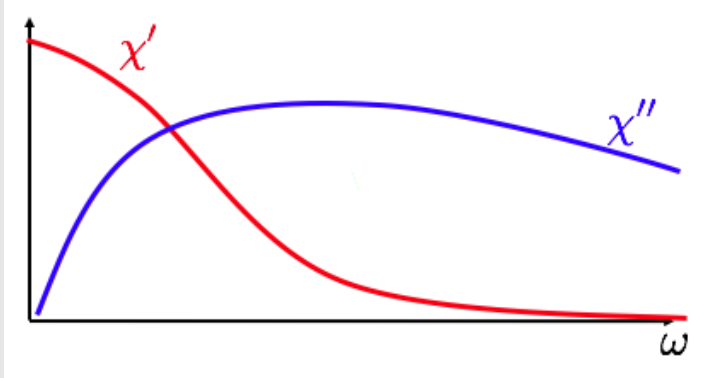
$$b \cos(\omega t) = \Re[b e^{-i\omega t}] = \Re[M(t)] = b [\cos(\omega t) \chi'(\omega) + \sin(\omega t) \chi''(\omega)],$$

with an **in-phase** and **quadrature** components.

Moreso, the unbound limits of Eq. (66) mean that

$$\begin{aligned} \chi(\omega) &= \chi^*(-\omega) \\ \chi'(\omega) &= \chi'(-\omega) \\ \chi''(\omega) &= -\chi''(-\omega) \end{aligned}$$

meaning that the real and imaginary parts of dynamical susceptibility are even and odd respectively.



41.4.2 Frequency representation

For this section we shall use definition of the FT:

$$\begin{aligned} X(t) &= \frac{1}{2\pi} \int X(\omega) e^{-i\omega t} d\omega \\ X(\omega) &= \int X(t) e^{i\omega t} dt \end{aligned}$$

Eq. (66) describes the response to a single sinusoidal excitation. Now let us consider that the excitation is a superposition of such sinusoids :

$$be^{-i\omega t} \Rightarrow B(t) = \frac{1}{2\pi} \int_{-\infty}^{\infty} b(\omega) e^{-i\omega t} d\omega.$$

Defining $m(\omega)e^{i\omega t}$ as the response to one of these sinusoids (in Eq. (66))

$$m(\omega)e^{-i\omega t} = b(\omega)e^{-i\omega t}\chi(\omega) \xrightarrow{\text{integrating over all } \omega + \text{normalising}}$$

$$M(t) = \frac{1}{2\pi} \int_{-\infty}^{\infty} m(\omega)e^{-i\omega t} d\omega = \int_{-\infty}^{\infty} \chi(\omega)b(\omega)e^{-i\omega t} d\omega.$$

Fully this will all read

Given a superposition of forces (expressed by $b(\omega)$ in the frequency range)

$$B(t) = \frac{1}{2\pi} \int_{-\infty}^{\infty} b(\omega)e^{-i\omega t} d\omega, \quad (67)$$

the response can be found by evaluating the response at frequency:

$$m(\omega) = \chi(\omega)b(\omega), \quad (68)$$

and ‘summing’ them up, which is equivalent to taking the fourier transform

$$M(t) = \frac{1}{2\pi} \int_{-\infty}^{\infty} m(\omega) e^{-i\omega t} d\omega.$$

41.4.3 Step excitation

A step excitation is removed from the system at time $t = 0$

$$B(\tau) = b \text{ only for } \tau < 0.$$

Evaluating Eq. (65)

$$\begin{aligned} M_{\text{step}}(t) &\equiv b \int_{-\infty}^0 X(t - \tau) d\tau \\ &= b \int_t^\infty X(\tau) d\tau = b\Phi(t) \end{aligned}$$

$\Phi(t)$ - response of system to step function

41.4.4 Delta exciation

A delta excitation is only switched on at a certain time.

$$B(\tau) = b\delta(\tau)$$

The selection mechanism of this function results in

$$M_\delta(t) = bX(t) \equiv -b \frac{d}{dt}\Phi(t)$$

$X(t)$ - response of system to delta function

41.5 Summary

Table 6: Reference table for responses

Excitation	Response $M(t)$	Special Response for $b = 1$
$b \cos(\omega\tau)$	$b[\cos(\omega t)\chi'(\omega) + \sin(\omega t)\chi''(\omega)]$	
$b\theta_-(\tau)$	$b \int_t^\infty X(\tau) d\tau$	$\Phi(t)$
$b\delta(\tau)$	$bX(t)$	$X(t)$

The delta function is minus the derivative of the step down function

$$\delta(\tau) = -\frac{d}{dt}\theta_-(\tau).$$

Because our system is linear, any relation between the excitation will mirror itself in the response

$$X(t) = -\frac{d}{dt}\Phi(t).$$

41.6 Energy

If we treat $B(t)$ as a force and M as a displacement, then we can in general write that

$$B = \frac{\partial \text{Energy}}{\partial M}, \quad (69)$$

and the power dissipation is then:

$$P = \left\langle \frac{\partial \text{Energy}}{\partial t} \right\rangle = \left\langle B \frac{\partial M}{\partial t} \right\rangle.$$

Using an excitation of the form for the response function $M(t)$ we get

$$\begin{aligned} B &= b \cos(\omega t) \\ M(t) &= b[\cos(\omega t)\chi'(\omega) + \sin(\omega t)\chi''(\omega)] \end{aligned} \Rightarrow P = \omega b^2 \left[-\chi'(\omega) \langle \sin(2\omega t)/2 \rangle + \chi''(\omega) \langle \cos^2(\omega t) \rangle \right]$$

which evaluates to ($\langle \sin(2\omega t)/2 \rangle = 0$ and $\langle \cos^2(\omega t) \rangle = 1/2$)

$$P = \frac{1}{2}b^2\omega\chi''(\omega). \quad (70)$$

Dissipation that occurs is proportional to imaginary part of the susceptibility, $\chi''(\omega)$.

Using the definitions for working out the units of different quantities:

$$\rightarrow [\chi] = [M^2]/[\text{energy}].[M] = [\chi][B] \quad \text{from Eq.(66)}$$

$$[B] = [\text{energy}]/[M] \quad \text{from Eq. (69)}$$

$$\rightarrow [X] = [M^2]/[\text{energy}][\text{time}], [\Phi] = [M^2]/[\text{energy}].[M] = [X][B][\text{time}] \quad \text{from Eq.(65)} \quad (71)$$

$$[B] = [\text{energy}]/[M] \quad \text{from Eq. (69)}$$

$[\chi]$	$[X]$	$[\Phi]$
$[M^2]/[\text{energy}]$	$[M^2]/[\text{energy}][\text{time}]$	$[M^2]/[\text{energy}]$

41.7 Onsager's hypothesis

Let us make an assumption, (that Onsager made), that after a step-like disturbance, a system, $M_{\text{step}}(t)$, regresses to its equilibrium state in the same way as it would under a random fluctuation.

$$\begin{cases} M_{\text{step}}(t) = \beta \langle M(0)M(t) \rangle & \text{according to Onsager, regression same as equilibrium one} \\ M_{\text{step}}(t) = \beta \Phi(t) & \text{when we deal with step excitation as in Table. 6} \\ X(t) = -\frac{d}{dt} \Phi(t) & \text{definition of dynamical susceptibility} \end{cases},$$

where β is a constant, which for classical mechanics, and quantum treatment at high temperatures, reduces to $\frac{1}{kT}$.

The Fourier Transform (only need to do it after the response at $t=0$ has occurred)

$$\begin{aligned} \chi(\omega) &= \int X(t) e^{i\omega t} dt \\ &= -\frac{1}{kT} \int_0^\infty \langle M(0) \dot{M}(t) \rangle e^{i\omega t} dt \\ &= \langle M(0)M(t) \rangle e^{i\omega t} \Big|_0^\infty - \frac{1}{kT} i\omega \int_0^\infty \langle M(0)M(t) \rangle e^{i\omega t} dt \\ &= \chi_0 + \frac{i\omega}{kT} \int_0^\infty \langle M(0)M(t) \rangle e^{i\omega t} dt \end{aligned} \tag{72}$$

For a step like disturbance, the susceptibility function in the frequency domain can be evaluated using

$$\chi(\omega) = \chi_0 + \frac{i\omega}{kT} \int_0^\infty \langle M(0)M(t) \rangle e^{i\omega t} dt$$

Converting to the usage of $\Phi(t)$ instead of $M_{\text{step}}(t)$, we need to add a normalisation factor β to keep the units from Eq. (71)

$$\begin{aligned} \rightarrow X(t) &= -\frac{1}{kT} \langle M(0) \dot{M}(t) \rangle \Phi(t) = \beta \langle M(0)M(t) \rangle \\ \Phi(t) &= -\frac{dX(t)}{dt} \end{aligned}$$

where, without going into too much depth, $\beta = \frac{1}{kT}$ from equipartition (derived in the last chapter of the book). The dynamical susceptibility, evaluated for after the excitation,

$$\chi(\omega) = -\frac{1}{kT} \int_0^\infty \langle M(0)\dot{M}(t) \rangle$$

So if we know the autocorrelation function of a systems response, we can evaluate the dynamic susceptibility,

41.8 Charge and current

Consider the step to be voltage, $B \leftrightarrow V$, and the response a charge, $M \leftrightarrow Q$. **We can monitor the charge Q .** Like Eq.(67),(68):

$$Q(t) = \int X(t-\tau)V(t)d\tau$$

$$q(\omega) = \chi(\omega)v(\omega),$$

$\chi(\omega)$ being the frequency dependent capacitance. As we saw in Eq (70), its imaginary part will lead to dissipation, $P = \langle B \frac{dM}{dt} \rangle = \langle V \frac{dQ}{dt} \rangle = \frac{1}{2}b^2\omega\chi''(\omega)$.

Above in Eq. (72) we have seen how this capacitance susceptibility, $\chi(\omega)$, can be calculated from the response, $Q(t)$

$$\chi(\omega) = -\frac{1}{kT} \int_0^\infty \langle Q(0)\dot{Q}(t) \rangle e^{i\omega t} dt = -\frac{1}{kT} \int_0^\infty \langle Q(0)I(t) \rangle e^{i\omega t} dt$$

not trivial, but you don't need to do it

$$= \frac{i\omega}{kT} \int_0^\infty \langle I(0)I(t) \rangle e^{i\omega t} dt$$

Or in terms of the Impedance $Z = \frac{1}{i\omega\chi(\omega)}$ (equation for capacitive impedance)

$$\frac{1}{Z(\omega)} = \frac{1}{kT} \int_0^\infty \langle I(0)I(t) \rangle e^{i\omega t} dt.$$

The impedance of an object is related to the area under the current autocorrelation graph.

And this is different from the $\frac{1}{R} = \frac{1}{2kT} \int \langle I(0)I(t) \rangle dt$ expression form before, because now we are getting the impedance at a particular frequency, not just the general one. (In fact its just the above intergrated for all the frequencies).

REFERENCES

- [1] A. A. Abdumalikov et al. “Electromagnetically Induced Transparency on a Single Artificial Atom”. In: *Phys. Rev. Lett.* 104 (19 May 2010), p. 193601. DOI: 10.1103/PhysRevLett.104.193601. URL: <https://link.aps.org/doi/10.1103/PhysRevLett.104.193601>.
- [2] O. V. Astafiev et al. “Coherent quantum phase slip”. In: *Nature* 484.7394 (Apr. 2012), pp. 355–358. DOI: 10.1038/nature10930. URL: <https://doi.org/10.1038/nature10930>.
- [3] O. Astafiev et al. “Resonance Fluorescence of a Single Artificial Atom”. In: *Science* 327.5967 (2010), pp. 840–843. ISSN: 00368075, 10959203. URL: <http://www.jstor.org/stable/40509905>.
- [4] Alexandre Blais et al. “Cavity quantum electrodynamics for superconducting electrical circuits: An architecture for quantum computation”. In: *Phys. Rev. A* 69 (6 June 2004), p. 062320. DOI: 10.1103/PhysRevA.69.062320. URL: <https://link.aps.org/doi/10.1103/PhysRevA.69.062320>.
- [5] P. Forn-Diaz et al. “On-Demand Microwave Generator of Shaped Single Photons”. In: *Physical Review Applied* 8.5 (Nov. 2017). DOI: 10.1103/physrevapplied.8.054015. URL: <https://doi.org/10.1103/physrevapplied.8.054015>.
- [6] M. Galli et al. “Light scattering and Fano resonances in high-Q photonic crystal nanocavities”. In: *Applied Physics Letters* 94.7 (Feb. 2009), p. 071101. DOI: 10.1063/1.3080683. URL: <https://doi.org/10.1063/1.3080683>.
- [7] Xiu Gu et al. “Microwave photonics with superconducting quantum circuits”. In: *Physics Reports* 718-719 (2017), pp. 1–102. DOI: <https://doi.org/10.1016/j.physrep.2017.10.002>. URL: <http://www.sciencedirect.com/science/article/pii/S0370157317303290>.
- [8] I.-C. Hoi et al. “Probing the quantum vacuum with an artificial atom in front of a mirror”. In: *Nature Physics* 11.12 (Sept. 2015), pp. 1045–1049. DOI: 10.1038/nphys3484. URL: <https://doi.org/10.1038/nphys3484>.
- [9] Morten Kjaergaard et al. “Superconducting Qubits: Current State of Play”. In: *Annual Review of Condensed Matter Physics* 11.1 (Mar. 2020), pp. 369–395. DOI: 10.1146/annurev-conmatphys-031119-050605. URL: <https://doi.org/10.1146/annurev-conmatphys-031119-050605>.
- [10] Jens Koch et al. “Charge-insensitive qubit design derived from the Cooper pair box”. In: *Physical Review A* 76.4 (Oct. 2007). DOI: 10.1103/physreva.76.042319. URL: <https://doi.org/10.1103/physreva.76.042319>.

- [11] Riccardo Manenti et al. “Circuit quantum acoustodynamics with surface acoustic waves”. In: *Nature Communications* 8.1 (Oct. 2017). DOI: 10.1038/s41467-017-01063-9. URL: <https://doi.org/10.1038/s41467-017-01063-9>.
- [12] Vladimir E. Manucharyan et al. “Evidence for coherent quantum phase slips across a Josephson junction array”. In: *Physical Review B* 85.2 (Jan. 2012). DOI: 10.1103/physrevb.85.024521. URL: <https://doi.org/10.1103/physrevb.85.024521>.
- [13] J. E. Mooij et al. “Josephson Persistent-Current Qubit”. In: *Science* 285.5430 (Aug. 1999), p. 1036. DOI: 10.1126/science.285.5430.1036. URL: <http://science.sciencemag.org/content/285/5430/1036.abstract>.
- [14] J.E. Mooij and Yu.V. Nazarov. “Quantum phase slip junctions”. In: (). eprint: cond-mat/0511535. URL: <https://arxiv.org/pdf/cond-mat/0511535>.
- [15] T.P. Orlando et al. “A Superconducting Persistent Current Qubit”. In: *Science* 285 (1999), p. 1036. eprint: cond-mat/9908283. URL: <https://arxiv.org/pdf/cond-mat/9908283>.
- [16] M. Pechal et al. “Superconducting Switch for Fast On-Chip Routing of Quantum Microwave Fields”. In: *Physical Review Applied* 6.2 (Aug. 2016). DOI: 10.1103/physrevapplied.6.024009. URL: <https://doi.org/10.1103/physrevapplied.6.024009>.
- [17] J. T. Peltonen et al. “Coherent dynamics and decoherence in a superconducting weak link”. In: *Physical Review B* 94.18 (Nov. 2016). DOI: 10.1103/physrevb.94.180508. URL: <https://doi.org/10.1103/2Fphysrevb.94.180508>.
- [18] J. T. Peltonen et al. “Coherent flux tunneling through NbN nanowires”. In: *Physical Review B* 88.22 (Dec. 2013). DOI: 10.1103/physrevb.88.220506. URL: <https://doi.org/10.1103/2Fphysrevb.88.220506>.
- [19] J. T. Peltonen et al. “Hybrid rf SQUID qubit based on high kinetic inductance”. In: *Scientific Reports* 8.1 (July 2018). DOI: 10.1038/s41598-018-27154-1. URL: <https://doi.org/10.1038/s41598-018-27154-1>.
- [20] Yueyin Qiu et al. “Four-junction superconducting circuit”. In: *Scientific Reports* 6 (2016), p. 28622. eprint: 1602.00072. URL: <https://arxiv.org/pdf/1602.00072>.
- [21] Mika A. Sillanpaa et al. “Autler-Townes Effect in a Superconducting Three-Level System”. In: *Phys. Rev. Lett.* 103 (19 Nov. 2009), p. 193601. DOI: 10.1103/PhysRevLett.103.193601. URL: <https://link.aps.org/doi/10.1103/PhysRevLett.103.193601>.
- [22] Xiaobo Zhu et al. “Coherent operation of a gap-tunable flux qubit”. In: *Applied Physics Letters* 97.10 (2019/01/24 2010), p. 102503. DOI: 10.1063/1.3486472. URL: <https://doi.org/10.1063/1.3486472>.